Mathematical Model of Glucose-Insulin Metabolism Considering Meal Absorption Rate and Model-based Blood Glucose Control for Prandial State in Type 1 Diabetes

Claudia Cecilia Yamamoto Noguchi

Mathematical Model of Glucose-Insulin Metabolism Considering Meal Absorption Rate and Model-based Blood Glucose Control for Prandial State in Type 1 Diabetes

Doctoral Dissertation

Claudia Cecilia Yamamoto Noguchi

Department of Electrical Engineering
Kyoto University

July, 2016

To Ken, *in memoriam*.

Acknowledgments

I would like to thank Professor Shinji Doi and all the committee members formed by Professor Tetsuo Kobayashi and Associate Professor Yoshio Ebihara for their constant advice throughout the PhD course, not only for the completion of the present manuscript but also for providing invaluable advice on the treacherous path of research in general. To Associate Professor Eiko Furutani, since the present study and the complete research topic could not have been possible without the continuous guidance through a long journey that started in April 2009 and his invaluable academic advice ever since including his expertise in physiological systems modeling, insight and above it all, patience due to language and cultural barriers.

A very special thanks to Dr. Tomoyuki Kawamura from Osaka City University Hospital for his collaborative work and in particular for his insight on the current treatment of T1DM in children and adolescents as well. It is more than inspiring to see a group of professionals from different areas of expertise working together towards improvements in the care of their patients, especially the youngest ones.

I would also like to thank Associate Professor S. Tanaka and Assistant Professor M. Kimura from the Laboratory of Composite Systems for their advice, and all the fellow students in the aforementioned research group and particularly those related to modeling and control of physiological systems: S. Wu, S. Hashimoto, S. Taniguchi, N. Kunikane, M. Tanimoto and C. Yujing for their support and mutual teaching/learning throughout these years regardless of the hierarchical senior-junior societal Japanese system, and for always providing a cozy environment during the countless days and nights spent inside the lab and out.

On a more personal note, my eternal gratitude to all the people who assumed the responsibility of my emotional and physical well-being—just as important, or even more than the intellectual one—in such a foreign country so far from home. Not only for providing support in a large number of ways, but also a space in their lives like close relatives. For the time, energy and understanding of the tribulations a foreign student has to face for the sake of a better education and the encouragement to continue pursuing my aspirations even though the Monbukagakusho scholarship found an unfortunate end before the start of the Master course. Above

it all, for teaching me to ignore the opinion of those who do not matter regardless of their status, which ended up being priceless not only in academic research but in every single aspect in life, and I believe will continue being so in the future as well. One learns by experience that trust and respect is earned as a result of one's integrity between their words and actions and not just imposed or expected (let alone demanded) from others. If it were not for each and every one of you, I would not be here writing these small words of appreciation and maybe be somewhere else having a few regrets about the past for the rest of my life.

Last, but most importantly, I would like to dedicate this manuscript to Ken for not being able to keep the only promise I ever made to you right before my departure. Even though a written acknowledgment has never ever brought anyone back to life—and never will—, I just wanted to let you know that I never forgot my promise to the last day you were still alive, and thank you for letting me know the day you weren't anymore even from the opposite side of the world. As time passes by I become more and more convinced that it was too high a price to pay for an academic title because the loss feels much heavier than anything all the time. To my family and close friends in my home country, for the long absence that lasted over 7 years, which is more than any of us could have ever imagined. One thing I learned from experience is that the greatest appreciation is for those who sacrifice themselves silently and let go of an essential part of themselves for the sake of somebody or something else. A beautiful example that taking less speaks louder than any give-and-take relationship one might have built through the years or even decades. Of course, a hug(e) thanks to nono and chicchi for their invaluable and constant emotional support throughout these years and for proving once again that animals are, unlike their human counterparts, free from the fetters of society, nationality or ethnicity whatsoever, and being the best example that just 'being there' is exactly the kind of support that is needed the most.

Thank you.

Contents

Acronyms

ADA	American Diabetes Association
AP	Artificial pancreas
ApoB	Apolipoprotein B
AUC	Area-under-the-curve
AvCHO	Available carbohydrate
BG	Blood glucose
BMI	Body mass index
CHO	Carbohydrates
CM	Chylomicron
CM-TG	Chylomicron-triglyceride
DHA	Docosahexaenoic acid
DKA	Diabetes ketoacidosis
EGP	Endogenous glucose production
EPA	Eicosapentaenoic acid
FDA	Food and drug administration (United States)
FII	Food Insulin Index
FFA	Free fatty acids
GI	Glycemic index
GIR	Glucose infusion rate
GLUT-4	Glucose transporter type 4
HbA1c	Glycated hemoglobin
HDL	High-density lipoprotein
HSL	Hormone-sensitive lipase
HTGL	Hepatic triglyceride lipase
IDL	Intermediate-density lipoprotein
iAUC	Incremental area-under-the-curve
IV	Intravenous
IVGTT	Intravenous glucose tolerance test
LDL	Low-density lipoprotein
LPL	Lipoprotein lipase
MPC	Model predictive control
NEFA	Non-esterified fatty acids

Acronyms (continued)

OGTT	Oral glucose tolerance test
PID	Proportion-integral-derivative
PID-IFB	proportional-integral-derivative with insulin feedback
PK	Pharmacokinetics
PD	Pharmacodynamics
RAG	Rapidly available glucose
Ra_{max}	Maximum rate of glucose appearance
RS	Resistant starch
SAG	Slowly available glucose
SC	Subcutaneous
T1DM	Type 1 diabetes mellitus
T2DM	Type 2 diabetes mellitus
TG	Triglycerides
TRL	Triglyceride-rich lipoprotein
VLDL	Very low density lipoprotein

Abstract

Mathematical Model of Glucose-Insulin Metabolism Considering Meal Absorption Rate and Model-based Blood Glucose Control for Prandial State in Type 1 Diabetes

by Claudia Cecilia Yamamoto Noguchi
Kyoto University

Type 1 diabetes mellitus (T1DM) is a specific form of diabetes wherein the immune system attacks insulin-producing cells until complete deterioration and inability to secrete insulin. These patients require intensive insulin therapy based on insulin bolus administration prior to every mealtime, in addition to continuous basal infusion to maintain blood glucose (BG) levels within the range of 70–180 mg/dL (3.9–10 mmol/L) the following two hours after meals and between 70–130 mg/dL (3.9–7.2 mmol/L) during non-feeding periods, although such range is often difficult to achieve. Among the current research on next-generation technologies for the treatment of T1DM, the artificial pancreas (AP) is a conceptual device that maintains BG levels automatically within the normal range by means of a continuous BG monitoring system, an insulin pump and a closed-loop control algorithm. Nevertheless, the difficulty to maintain BG levels within the recommended range during diurnal BG control is arguably one of the main impediments for the development of AP systems, which is also the main motivation in the present study.

Firstly, we propose a novel mathematical model of glucose-insulin metabolism in T1DM based on previous well-known models (Bergman minimal model and Shimoda insulin model), with minimal modification of parameter values for a more accurate representation. In addition to this, we propose a novel model of carbohydrate digestion/absorption for an accurate representation of meal-derived glucose appearance and its impact on BG levels in patients with T1DM based on carbohydrate intake and type, which determines the absorption rate.

Secondly, utilizing the aforementioned model, we assess *in silico* the feasibility of prandial BG control after consumption of carbohydrates with Glycemic Index (GI) values throughout the range. We consider a control strategy that comprises a pre-meal bolus insulin administration 60 min prior to the expected mealtime, which is computed from meal information of carbohydrate intake and the type of food (GI) to be consumed. At mealtime, the control algorithm shifts to Model Predictive Control (MPC) considering its predictive capabilities and ability to consider long delays to stabilize post-meal BG levels at the clinically recommended target value of 100 mg/dL (5.56 mmol/L). The performance of the present control algorithm indicates that maintenance of postprandial BG excursion within levels comparable to that of nondiabetics is feasible

under ideal conditions of mealtime, carbohydrate intake and patient-model match; and within clinical recommendations considering sources of variability for the aforementioned cases.

Lastly, as dietary fat is being increasingly acknowledged as an important contributor to postprandial glycemic excursion and an impediment for appropriate BG control due to the differences in BG excursion from the model-predicted values, an extended 'minimal' compartmental representation from the model of carbohydrates above considers fat metabolism with a novel compartmental representation of triglycerides and non-esterified fatty acids (NEFA) to derive a physiologically meaningful representation of lipid-derived insulin resistance on glucose kinetics. Simulation results of the proposed mixed meal model show an acceptable representation of gastric emptying rate after consumption of a high-fat mixed meal, as well as postprandial BG, triglycerides and NEFA levels in patients with T1DM according to clinical data in the literature. This suggests that the proposed model can be eventually used for successful BG control of mixed meals to overcome the current limitations in diurnal BG control algorithms.

The present study provides *in silico* evidence that prandial BG control within the recommended clinical range is feasible, provided the utilization of an accurate mathematical model of the impact of different types of carbohydrates on postprandial glucose-insulin metabolism in patients with T1DM. Moreover, the extension of a minimal compartmental model approach to represent the indirect impact of dietary fat on glucose-insulin metabolism in patients with T1DM is also feasible, which can be similarly used for BG control purposes in the near future.

Chapter 1

Introduction

1.1 Framework

Diabetes mellitus (henceforth diabetes) is the most common disease of the endocrine system, which specifically affects glucose-insulin metabolism to produce the necessary energy to live. Currently, it has reached epidemic levels affecting 382 million people worldwide, with a projected rise to 592 million by 2035 [1]. Diabetes is characterized by abnormally high blood glucose (BG) levels that need to be treated by either oral medicine or insulin administration several times a day and maintained within the normoglycemic range of 70–130 mg/dL (3.89–7.2 mmol/L). Otherwise, the likeliness to develop several diabetes-related complications increases, including blindness, amputation, kidney dialysis/transplant and cardiovascular diseases. The cost of diabetes treatment in the United States alone is estimated to USD 306 billion, or 23% of the healthcare budget [2], with additional hospitalization costs estimated to USD 2.4 billion [3] basically due to mismanagement of diabetes related to acute—and potentially mortal—severe hypoglycemia or critical hyperglycemia, with the latter being most notably known as diabetes ketoacidosis (DKA). China, one of the largest economies in the world with an even more promising future ahead, is estimated to have the largest number of diabetic patients with currently over 100 million, *i.e.,* one in four diabetic patients worldwide, and a projected health cost of 360 billion RMB (USD 57 billion) by 2030 partly due to its extremely deficient public health system [4, 5]. Although Japan has a considerably lower population than other industrialized nations, there is an increasing pressure on the health care system due to the continuous rise of the ageing population and treatment of chronic diseases (including diabetes). It is estimated that JPY 1077.7 billion or 4–6% of the healthcare budget is being spent on diabetes alone, which including diabetes-related complications—mainly due to dialysis—elevates the total figure to JPY 5000 billion (USD 41 billion) [6].

The incidence of type 1 diabetes mellitus (T1DM) in particular—a specific form of diabetes known as juvenile diabetes—is having a continuous increase of 2–5% worldwide, with an estimated diagnosis (below 18 years old) of 1 in 300 in the United States [7]. The etiology of T1DM is commonly attributed to the destruction of insulin-producing β-cells in the pancreas until complete inability to secrete insulin in a very short period, which reflects on their ever-increasing BG levels. The rapid increase in the number of diagnoses, nonetheless, also suggests that environmental factors such as early infant nutrition, infection and diet also contribute to the development of the disease [8].

Because there is currently no cure that can possibly restore the lost insulin secretion ability, these patients undergo a lifetime of intensive insulin therapy that comprises subcutaneous (SC) insulin boluses immediately before every meal, in addition to a low-dose continuous basal insulin to imitate endogenous insulin secretion from β-cells during postprandial and fasting state, respectively. In the past decades, fasting BG levels were considered to be the main indicator for the diagnosis of diabetes, HbA1c (average BG levels for the previous 2–3 months) and even postprandial BG excursion [9]. Nevertheless, recent studies provide cogent evidence that postprandial BG levels are actually a larger contributor to HbA1c inasmuch as 70% [10], and more detrimental than sustained hyperglycemia for the development of microvascular damage, activation of oxidative stress [11] and increase in the risk of cardiovascular diseases [12]. Since diurnal BG excursion comprises consecutive prandial states, postprandial BG management for patients with T1DM is being increasingly acknowledged as a better predictor of long-term complications than fasting or HbA1c levels—once the gold standard—and hence more important to maintain within the recommended range [13]. However, despite current clinical recommendations by the American Diabetes Association (ADA) to maintain post-meal BG levels within the range of 70–180 mg/dL (3.9–10.0 mmol/L), this is very difficult to achieve in practice [14].

Natural insulin secretion from β-cells in nondiabetics reaches the bloodstream more rapidly in fine-tuned exact doses according not only to variations in BG levels but other enzymes in the stomach and small intestine [15], thus being able to maintain normal BG levels throughout the day. Large plasma insulin concentrations finely timed with meal-derived glucose appearance are necessary for glucose uptake into the cells to be used as energy, or storage in the liver for eventual energy provision. Compared to nondiabetics, diurnal BG management in patients with T1DM requires a large bolus insulin administration immediately before every single mealtime, as the carbohydrate content of a meal is directly digested (broken down) and absorbed as glucose into the bloodstream, which causes a rapid increase in BG levels. However, BG levels in these patients are characterized by a large peak (typically $>$200 mg/dL) between 0.5–2 hours after a meal and followed by a rapid decline afterwards. Such steep glycemic excursion is the

result of a poor coordination between the rapid glucose appearance from carbohydrates and the slow absorption of insulin from SC tissue, whose effect lasts over four hours until complete absorption after bolus insulin administration.

Estimation of the adequate prandial bolus insulin dose is based on the carbohydrate counting method [16], wherein the amount of carbohydrates to be consumed is multiplied by an individual insulin-to-carbohydrate (I:C) ratio, *i.e.*, a patient-specific ratio that depends on their particular sensitivity to insulin, which is usually defined as the required insulin dose after consumption of 10 g of carbohydrates. In this way, patients with T1DM manage their BG levels throughout the day by means of bolus insulin administration prior to every single meal, which not only has a deleterious physiological effect but also psychological burden due to the constant attention required, which affects—directly or indirectly—every aspect of their everyday life. Miscalculation in the bolus insulin dosage leads to post-meal hypoglycemia or hyperglycemia, which are accompanied by acute symptoms—such as trembling, headaches, blurred vision, nausea and fatigue to name but a few—that cause temporary motor and cognitive deterioration [17]. It is estimated that patients with T1DM have an estimated reduction of 20 years in lifespan and over 30 years in reduced quality-of-life with adjusted time for a hypothetical diagnosis at 10 years old [18].

The artificial pancreas (AP) is the next big step forward in the development of new technologies to improve the quality of life of patients with T1DM. Conceptually, the AP is a wearable device that comprises an insulin pump for continuous subcutaneous insulin infusion and a continuous glucose monitoring system (CGMS) for real-time measurement of BG levels. Both are already commercially available devices that, in addition to a control algorithm, can be used together to maintain BG levels automatically within the normal range 24 hours a day without intervention from the patients themselves, thus alleviating the continuous burden of BG management—measurement of BG levels and insulin administration at mealtimes and correction boluses whenever necessary—throughout the day. By using real-time BG information from the CGMS, the exact insulin dose is computed in the control algorithm and infused to the patient via the insulin pump. The same process is done iteratively at several-minute intervals (usually 1–5 min) in a continuous loop process of BG data reading, computation of the necessary insulin to maintain BG levels within the normal range, and respective instantaneous infusion. The control algorithm, in particular, is based on the traditional proportional-integral-derivative approach largely utilized in industrial processes, although a more recent model-based approach is considered most suitable to manage long delays in the hypoglycemic effect of insulin caused by the slow subcutaneous absorption kinetics of insulin formulations.

In the global scenario, the Juvenile Diabetes Research Foundation in the United States,

the co-joint research group from the University of Virginia in the United States and Padova University in Italy (best known for developing the only Food and Drug Administration (FDA)-approved T1DM simulator), the AP project by the University of Cambridge in England, and the Joslin Diabetes Center-Harvard Medical School AP project in the United States are, in no particular order, the most recognized research groups among over 11 artificial pancreas projects worldwide [19] in the pursuit of 'The Artificial Pancreas'. In the past few years, clinical trials of overnight closed-loop BG control have shown that in-development AP systems offer superior BG control compared to conventional insulin pump therapy, with BG fluctuations between 72–144 mg/dL (4–8 mmol/L) in 77–78% of the T1DM test subjects for closed-loop BG control compared to 41–51% for conventional insulin pump therapy. Occurrences of nocturnal hypoglycemia, *i.e.*, BG below 70 mg/dL (3.89 mmol/L), also dropped from 4.1% to 2.1% and from 33% to 20% in children/adolescents and adults, respectively [20].

The benefits of overnight closed-loop BG control in outpatient trials, *i.e.*, utilization of the AP system in everyday life, include reduction of the burden of diabetes, giving a sense of 'freedom' especially in patients suffering from hypoglycemia unawareness, and an improved overall quality of life despite the closed-loop system being effective only during overnight periods [21]. These promising results have started to influence the market of diabetes-related technologies with the release of the first commercially-available Medtronic 670G, an 'all-but-meals' AP system expected to be released by April 2017. Despite these advances, a still inadequate diurnal closed-loop BG control is currently the main impediment for the development of a true AP system. Among the factors that influence in the success of prandial BG control, mathematical models of glucose-insulin metabolism with an accurate representation of the impact of a meal on BG levels is a crucial element, since the continuous iterative computation of the exact bolus insulin relies on BG predictions from such model. Previous clinical implementations of BG control systems have only achieved a limited success in maintaining postprandial BG levels within an acceptable range, perhaps because previous mathematical models consider only carbohydrate amount as model input. Despite their complexity and high level of detail in representing glucose-insulin metabolism, all of them are based on the premise that the impact of a meal on BG levels depends exclusively on the amount of carbohydrates consumed.

Yet another important issue in diurnal BG management is the impact of dietary fat and protein on BG levels in patients with T1DM besides carbohydrates. The carbohydrate counting method is the current gold standard for calculation of bolus insulin doses, which focuses exclusively on the carbohydrate amount of the meal arguably due to early studies on insulin requirements that indicated the irrelevancy of the dietary fat and protein content in mixed meals [22–24]. In the past few years, however, an increasing number of clinical studies have

provided confounding evidence of the impact of dietary protein and fat on BG levels in these patients [25–27], with dietary fat in particular being well-known for causing a sustained state of hyperglycemia several hours after consumption of high-fat meals compared to another with identical carbohydrate composition although with reduced dietary fat content [28]. This effect on BG levels is commonly referred to as the 'pizza meal effect' due to the high amounts of dietary fat and carbohydrate content of this popular meal [29], which is very difficult to manage despite correct application of the carbohydrate counting method. Aware of this, a novel bolus calculation method that includes the three macronutrients has been proposed by Pańkowska *et al.* [30], which consists of an initial single-bolus to cover carbohydrates, and an extended insulin infusion over 6 hours—provided the access to insulin pump technology—whose dose is determined from the fat and protein content of the mixed meal. Alternatively, the Food Insulin Index (FII) [31] provides a quantitative estimation of insulin demands after consumption of different foods including protein and fat. A clinical assessment of bolus calculation using the FII on a mixed meal showed reduction in post-meal BG excursion and normoglycemia three hours after meal consumption in patients with T1DM compared to the carbohydrate counting method [32]. Despite the apparent efficacy of these methods, neither of them has achieved a wide acceptance—considering that they are not included in current guidelines from the ADA regarding the treatment of T1DM—, perhaps because of the increased complexity in the calculation and the necessity of an insulin pump for extended bolusing in Pańkowska method, and the limited information of FII values in commonly consumed foods on an everyday basis.

Moreover, the performance of closed-loop BG control systems in clinical studies [33] is also affected by high-fat mixed meals, which show a prolonged state of hyperglycemia compared to low-fat meals despite requiring a larger insulin infusion. Given these circumstances, some studies of BG control algorithms resort to mathematical models of mixed meals with *ad hoc* model parameter fitting to previous clinical data of meal-derived glucose absorption [34]. Such in hindsight approach, however, does not provide a solid mathematical representation that can be utilized for BG prediction purposes in model-based BG control algorithms. The difficulty in developing an adequate mathematical model of mixed meals is arguably due to the poor current knowledge of the exact metabolic mechanism by which dietary fat affects glucose-insulin metabolism after consumption of a high-fat mixed meal.

1.2 Objective

We hypothesize that an accurate mathematical model of glucose-insulin metabolism can improve the performance of model-based BG control algorithms for prandial state such that clin-

ical recommendations for BG management in patients with T1DM can be satisfied. Due to the crucial role of mathematical modeling in the development of closed-loop BG control algorithms, we aim to develop a more accurate representation of the impact of carbohydrates on BG levels with particular emphasis on model simplicity. Considering the high risk of patient exposure to acute hypoglycemia due to the combination of large prandial insulin bolus doses and minimal safety restrictions to assess the feasibility of strict BG control, the present study opts for an *in silico* approach utilizing computer simulations in MATLAB, prior to clinical evaluation of diurnal BG control systems in actual patients with T1DM. We contemplate the explicit representation of the absorption rate of carbohydrates depending on the food consumed by utilizing an additional model parameter associated with the Glycemic Index (GI) of foods—a quantitative index of the impact of carbohydrates on BG levels—. Moreover, we propose a further extension of mathematical modeling of glucose-insulin metabolism from carbohydrates to a mixed meal model of dietary fat and carbohydrates. This requires a thorough analysis of the metabolic processes involved in postprandial fatty acid metabolism prior to analyze the feasibility to include already existing models or the proposal of a novel compartmental model to represent the impact of dietary fat on glucose-insulin metabolism. In this way, the three main objectives in the present manuscript can be summarized as follows:

- Mathematical modeling of the impact of carbohydrates on postprandial glucose-insulin metabolism in patients with T1DM.
- *In silico* assessment of the feasibility of prandial BG control algorithm within the clinically recommended range of 70–180 mg/dL (3.89–10 mmol/L) within two hours after a meal and 70–130 mg/dL (3.89–7.2 mmol/L) afterwards.
- Mathematical model of the effect of dietary fat on postprandial glucose-insulin metabolism in patients with T1DM.

1.3 Thesis structure

The present manuscript is divided into three main parts (see Figure 1.1) wherein each of them relates to each specific objective in the above. First, in Chapter 2 we provide a brief introduction to the mechanisms involved in glucose-insulin metabolism with emphasis on T1DM and current treatment of the disease. Thence, we describe the most representative mathematical models of glucose-insulin metabolism developed to date, as well as several BG control approaches taken by different research groups used in studies of AP systems.

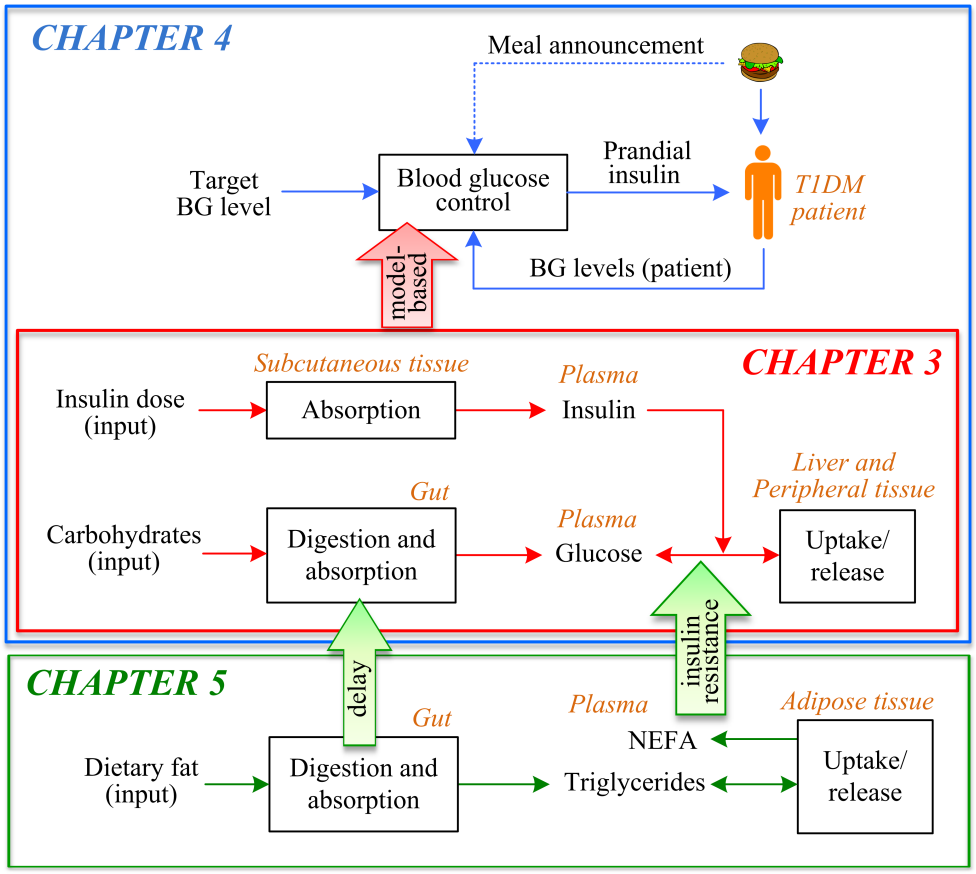

Figure 1.1: Structure of the present manuscript by chapter division. Chapter 3 (red) concerns a mathematical model of glucose-insulin metabolism in T1DM from carbohydrates, Chapter 4 (blue) proposes a BG control algorithm for prandial state based on the aforementioned model, and Chapter 5 (green) involves a mixed meal model of dietary fat and its effect on glucose-insulin metabolism as an extension of the model in Chapter 3.

In Chapter 3 (red) we propose a novel mathematical model of glucose-insulin metabolism in T1DM that considers differences in the absorption rate of carbohydrates to represent the impact on BG levels, which is coupled with existing models of subcutaneous insulin absorption and glucose-insulin metabolism with minimal modifications in parameter values to obtain a more accurate representation. In Chapter 4, based on such model, we evaluate the degree of BG control considering a fixed target value in the controller such that recommended clinical values are satisfied. We consider an *in silico* implementation of the control strategy that includes meal announcement, *i.e.*, information of the intended meal to be consumed should be given to the control algorithm in advance. Because of the high risk of hypoglycemia associated with large bolus insulin doses—as expected from the controller to maintain post-meal normoglycemia—, the actual T1DM patient is replaced by a continuous-time T1DM patient model. Lastly, in

Chapter 5, we propose a mathematical model of the effect of dietary fat on glucose-insulin metabolism (green) as an extension of the model developed in Chapter 3 that reflects in an accurate representation of the impact of dietary fat on BG levels in patients with T1DM. Similar to carbohydrates, we include gut transit of the dietary fat portion of the mixed meal and its delaying effect on gastric emptying of carbohydrates. Moreover, insulin resistance due to fatty acid metabolism from exogenous and endogenous sources is represented by the combined post-meal increase in triglycerides and non-esterified fatty acids (NEFA), respectively, wherein the former in particular is directly affected by dietary fat consumption.

Chapter 2

Type 1 diabetes mellitus (T1DM) and previous studies relevant to diurnal blood glucose (BG) control

2.1 Glucose-insulin metabolism and T1DM

Glucose is the main source of energy in the human body, which needs to be obtained from external sources in the form of food. Among the three macronutrients of a balanced diet, carbohydrates provide a direct source of glucose after break-down of complex chemical structures (see Table 2.1) during digestion and absorption in the stomach and small intestine, respectively. Thence, glucose enters the bloodstream for its delivery and utilization as energy by the body.

Glucose-insulin metabolism after meal consumption is known as postprandial state (see Figure 2.1), which is the period of time wherein carbohydrates are broken down into glucose and

Table 2.1: Classification of carbohydrates according to their chemical composition [35].

Class	Sugar	Oligosaccharides	Polysaccharides
Sugar units	1–2	3–9	≥ 10
Subgroup	monosaccharides, disaccharides	raffinose, stachyose, verbacose	starch, glycogen, dietary fiber
Component	glucose, fructose, galactose	glucose, fructose, galactose	glucose

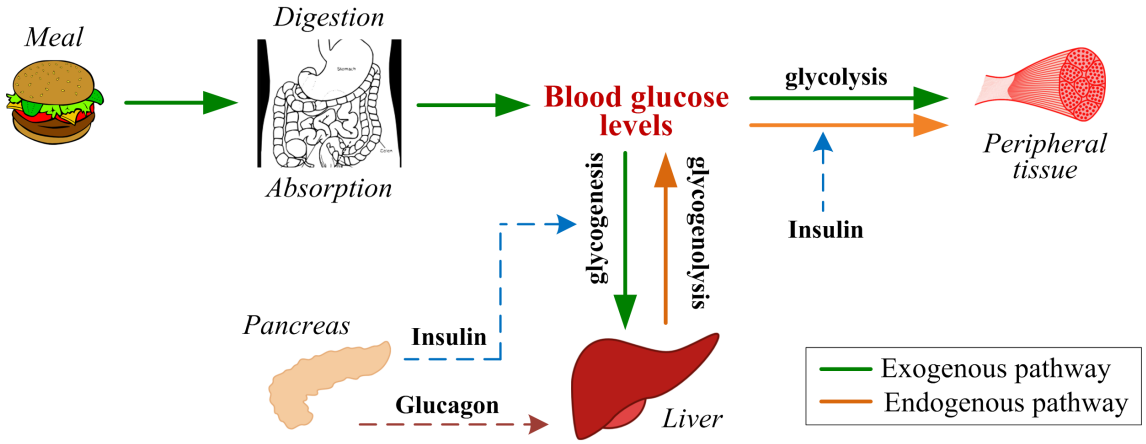

Figure 2.1: Exogenous (green arrows) and endogenous (orange arrows) pathways for glucose-insulin metabolism. Meal-derived glucose requires large insulin secretion from the pancreas for its utilization as energy or storage in the liver. In turn, during fasting state, only small doses of insulin are required for continuous energy provision.

metabolized for its utilization as energy (*glycolysis*). The surplus is stored in the liver as glycogen (*glycogenesis or glycogen synthesis*) for its eventual utilization during non-feeding energy demand periods known as *postabsorptive* or fasting state typically in-between meals and sleep. It is characterized by glucose metabolism from hepatic glucose storage (*endogenous* glucose pathway), wherein glycogen break down from the liver (*glycogenolysis*) is transported towards the peripheral tissue for its glycolysis to satisfy energy requirements. Hence, the liver in particular plays an important role in glucose metabolism, both during exogenous and endogenous pathways, through alternation of *glycogenesis* and *glycogenolysis* depending on insulin concentration.

Insulin—the main gluco-regulatory hormone—is secreted by pancreatic β-cells into the bloodstream to activate glucose transporter type 4 (GLUT-4), which is the most important insulin-sensitive enzyme for glucose uptake. In this way, large plasma insulin levels proportional to the amount of meal-derived glucose appearance are typical during postprandial state, whereas low plasma insulin levels during fasting allows glycogenolysis (endogenous glucose appearance) from the liver. During postprandial state, high insulin levels also inhibit hepatic glucose production, since presence of large amounts of meal-derived glucose does not require additional glycogenolysis. Glucose homeostasis is the result of a delicate balance between plasma glucose appearance (whether exogenous or endogenous) and uptake (either for utilization as energy or storage) such that BG levels are maintained constantly at a very nar-

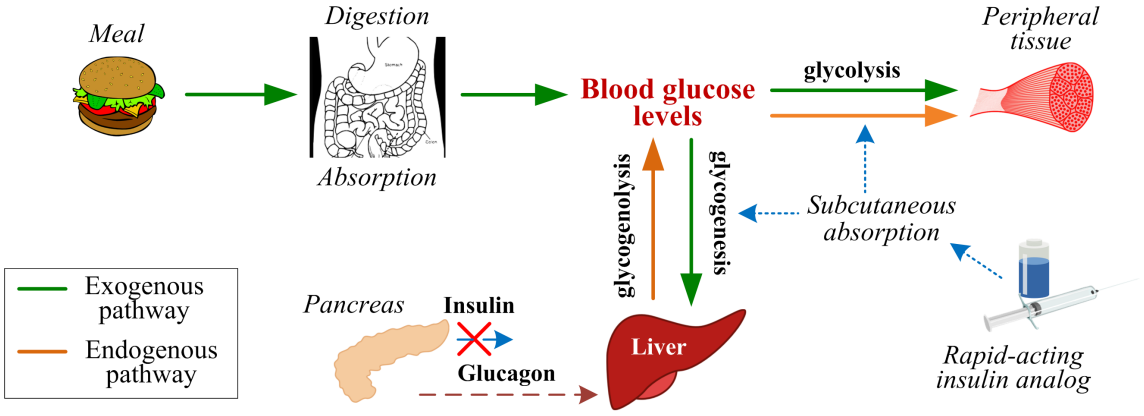

Figure 2.2: Destruction of pancreatic β-cell leads to complete absence of insulin secretion in patients with T1DM. Subcutaneous insulin therapy intends to replace the function of the pancreas to provide insulin for glucose-insulin metabolism and energy utilization.

row range between 80–120 mg/dL (4.4–6.7 mmol/L). In case BG levels drop below 70 mg/dL (3.9 mmol/L), glucagon secretion from pancreatic α-cells is triggered to induce additional glycogenolysis for restoration of normal BG levels. Otherwise, acute hypoglycemia occurs, which is a dangerous condition where excessive insulin-induced glucose uptake by peripheral tissue limits the delivery of glucose to the brain with possible fatal consequences in a matter of hours.

In patients with T1DM, pancreatic β-cell destruction by the immune system causes a complete deficiency in endogenous insulin secretion (see Figure 2.2). To compensate for the lost endogenous insulin secretion ability, patients undergo SC insulin therapy, which is characterized by a slow SC insulin absorption kinetics compared to endogenous insulin secretion in healthy nondiabetics. Moreover, SC insulin delivery route causes insulinization of peripheral tissue prior to that of the liver—the opposite occurs in endogenous insulin secretion—which contributes to an excessive endogenous glucose production (EGP) in these patients [36]. In this way, although exogenous insulin therapy cannot exactly replace endogenous insulin secretion and maintain the same level of homeostasis, it is the only therapy currently available for the treatment of T1DM.

After bolus insulin is administered, it forms a subcutaneous insulin depot from which insulin is gradually degraded. In its original form, insulin is composed by hexamers, *i.e.*, six molecules of insulin bond together, which are gradually broken down into dimers and monomers in the subcutaneous tissue before entering the bloodstream for its utilization by the liver and peripheral tissue for glucose uptake. As shown in Figure 2.3, the insulinization process in T1DM patients

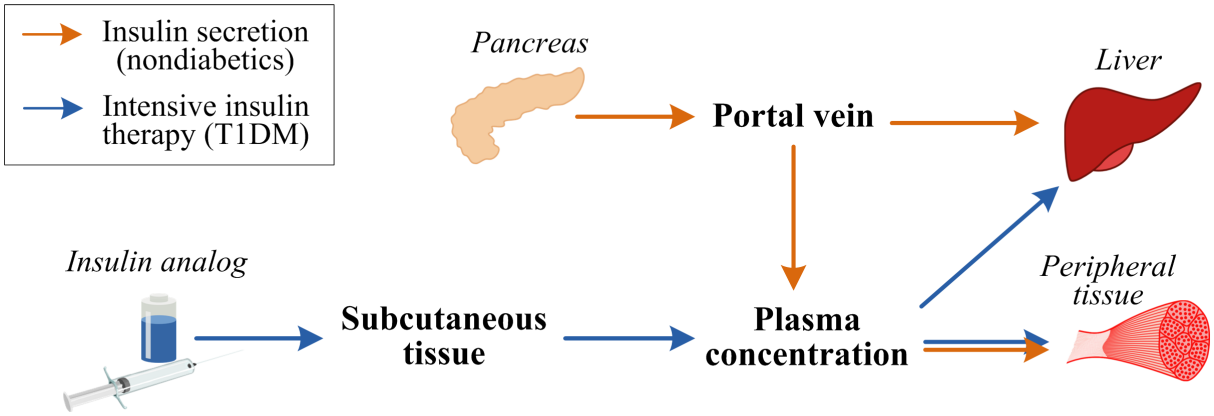

Figure 2.3: Insulinization pathway after subcutaneous insulin administration in patients with T1DM compared to endogenous pancreatic β-cell secretion in nondiabetics. In the latter, insulin reaches directly the liver through the portal vein for direct regulation of hepatic glucose uptake/production. Compared to this, insulin is slowly absorbed into the bloodstream (plasma concentration) after subcutaneous administration for its delivered throughout the body until it eventually reaches the liver thus resulting in an inadequate timing of hepatic glucose regulation.

is clearly different from nondiabetics, which affects the timing in glucose-insulin metabolism and the maintenance of homeostasis. In healthy individuals, pulsatile endogenous insulin secretion enters the portal vein, which is directly connected to the liver where up to 80% of insulin is extracted [37] and thus the portal insulin concentration is several-fold higher than peripheral insulin. In diabetics, absence of β-cell secretion causes an almost absent portal insulin concentration [38].

2.2 Intensive insulin therapy

The current treatment of T1DM comprises a combined administration of bolus and basal insulin. To date, several types of insulin formulations with different action times have been developed (see Table 2.2), with faster insulin formulations attempting to reproduce the same effect as endogenous insulin secretion in nondiabetics. Insulin doses are calculated in international units (IU), wherein each unit has a volume of 0.01 mL.

Basal-bolus insulin therapy consists of insulin administration in two patterns, which require the utilization of two types of insulin for instantaneous single-bolus administration by insulin pen or syringe: a long or very long acting insulin for basal needs administered once a day, in

Table 2.2: Types of insulin formulations in the market divided by their effect [39].

Insulin formulation	Onset	Peak action	Duration	Brand name
Rapid acting	5–15 min	1–2 h	4 h	lispro, aspart, glulisine
Short acting	30–45 min	2–3 h	5–8 h	Regular
Intermediate acting	2–4 h	4–8 h	10–16 h	lente (NPH)
Long acting	3–5 h	8–12 h	16–20 h	ultralente
Very long acting	2–4 h	6–16 h	20–24 h	glargine, detemir

addition to a rapid-acting (or short-acting) bolus insulin administered before every meal via a syringe or insulin pen injection. Since rapid-acting insulin formulations have the shortest onset and peak effect, they are the current standard type utilized for prandial insulin bolusing. State-of-the-art technologies in insulin delivery devices include insulin pumps—which is continuously attached to the subcutaneous tissue of the patient by a cannula—wherein bolus insulin is administered upon indication of bolus dose from the patient, and basal insulin is continuously infused with very low doses of rapid-acting insulin.

The main advantage of insulin pumps over the traditional instantaneous single-bolus administration by insulin syringes or pens—where the total bolus can only by given at once— is that they include additional bolus insulin delivery patterns (see Figure 2.4). Square bolus infuses the total insulin bolus over a determined period of time (usually within 2 hours) at a constant rate, whereas dual-wave bolus splits the total bolus dose into a fractional single-bolus followed by a square bolus. These alternative bolus deliveries require manual input by the patients themselves to specify the time span and fraction of insulin to be delivered under a given mode. Their effectiveness in maintaining desirable BG levels are, however, contradictory. While some studies [40] emphasize the benefits of insulin pumps on diurnal BG management in patients with T1DM, others suggest that these extended boluses result in a larger postprandial BG excursion compared to the traditional single-bolus type [41].

The carbohydrate counting method [16] consists of the estimation of the necessary bolus insulin dose for the carbohydrate content of a given meal such that BG levels are maintained within the recommended range of 70–130 mg/dL (3.9–7.2 mmol/L) two hours after meal consumption [42]. Early studies on prandial insulin estimation for different meals [22–24] show that the total insulin dose requirement is linearly proportional to the amount of carbohydrate consumed regardless of the dietary fat or protein content. In this way, the carbohydrate count-

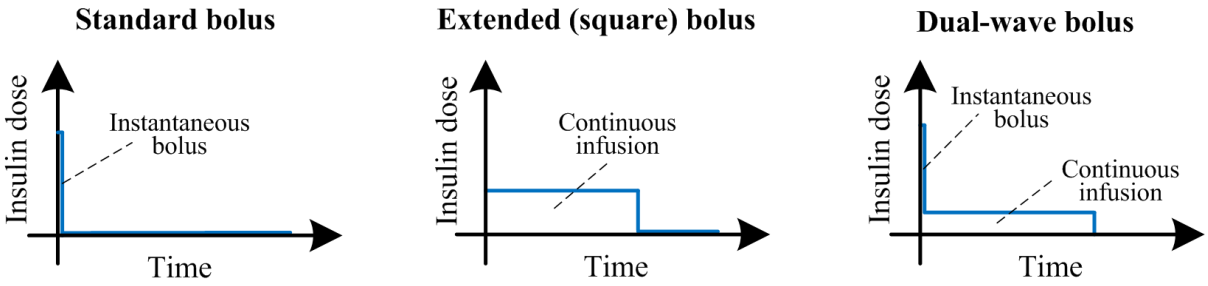

Figure 2.4: Insulin infusion patterns available in current insulin pumps aimed to improve the management of post-meal BG levels in patients with T1DM. Besides standard single-bolus administration (left), alternative bolus infusion types include extended/square insulin (center) and dual-wave bolus (right), although the effectiveness of such extended infusion types have not yet been proved or included in ADA guidelines for the treatment of T1DM [41].

ing method indicates that the required bolus insulin dose is determined by

$$\text{Bolus insulin} = \text{carbohydrate amount} \times \text{I:C ratio} \tag{2.1}$$

where I:C ratio is the insulin-to-carbohydrate ratio, *i.e.*, a patient-specific value that depends on their particular sensitivity to insulin.

2.3 Mathematical modeling of T1DM

Mathematical models of glucose-insulin kinetics can be divided into compartmental models and empirical (data-driven) models. The former describes the kinetics involved in glucose-insulin metabolism as compartments whose physiological interaction are mathematically represented by differential equations, whereas the latter relies on regressive model identification by using prior data to build auto-regressive or auto-regressive moving average models of glucose-insulin dynamics. Compartmental models can be divided into three main parts: (a) Carbohydrate digestion/absorption in the gut and exogenous glucose appearance, (b) Subcutaneous insulin absorption kinetics and (c) glucose-insulin metabolism, as shown in Figure 2.5. In the following, the most relevant mathematical models developed to date are briefly described considering the aforementioned division.

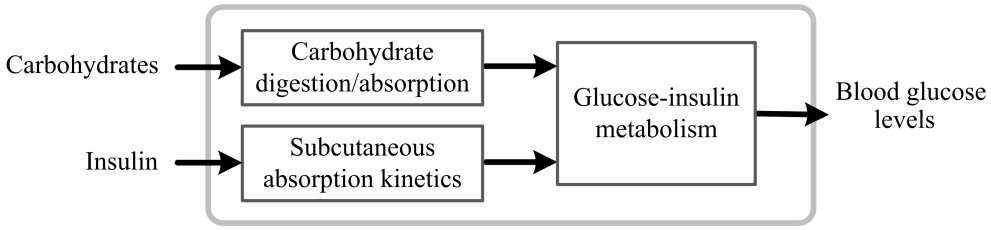

Figure 2.5: Mathematical models of glucose-insulin kinetics for postprandial state can be divided into (a) carbohydrate digestion and absorption to represent the impact of a meal on BG levels, (b) subcutaneous insulin kinetics and the effect of insulin to lower BG levels, and (c) glucose-insulin metabolism. These three main elements determine BG dynamics after meal consumption in patients with T1DM.

Provided the basis on glucose-insulin metabolism and the current treatment of T1DM from intensive insulin therapy, in the following we introduce the most relevant mathematical models in the literature that represent gut absorption from carbohydrates, subcutaneous insulin absorption after administration of bolus insulin doses and glucose-insulin metabolism in nondiabetics and diabetics as well. Some proposals include only one specific division, whereas more elaborated models not only include the complete metabolic representation and the impact of a meal on BG levels but also consider more detailed physiological processes beyond the brief introduction given in the previous section.

2.3.1 Mathematical models of carbohydrate digestion and absorption

Models of gut absorption represent gut transit of carbohydrates as an equivalent of rate of exogenous glucose appearance based on the amount of carbohydrates consumed. The most relevant models are described in the following.

Lehmann model

One of the most well-known models of gut absorption is proposed by Lehman *et al.* [43]. It originally comprises a complete mathematical representation of glucose-insulin metabolism in patients with T1DM using four differential equations with twelve auxiliary equations. Meal-derived glucose appearance is represented by a trapezoidal function as detailed in the Appendix A.2 (page 152).

Elashoff model of gastric emptying

A model of gastric emptying as a power exponential gastric retention model is proposed by Elashoff *et al.* [44] as

$$y(t) = 2^{-(t/T_{1/2})^{\beta}} \tag{2.2}$$

where $y(t)$ is the meal retention at time t, $T_{1/2}$ is the half-emptying time and β is a constant of gastric emptying determined by the food consumed.

Siegel model of gastric retention

A derivation of Elashoff model is proposed by Siegel *et al.* [45], who additionally considers the lag phase in gastric emptying as given by

$$y(t) = 1 - (1 - e^{-kt})^{\beta} \tag{2.3}$$

where k is gastric emptying rate and β is the extrapolated intercept of the curve with $\beta > 1$ indicating a slow gastric emptying typical in solid foods and $\beta < 1$ a rapid gastric emptying for liquids. The lag time t_{lag} is obtained by assuming $\mathrm{d}^2y(t)/\mathrm{d}t^2 = 0$ in Eq. (2.3), from which $t_{\text{lag}} = 1/k$, whereas the half-emptying time is calculated with $y(t) = 0.5$ and solving for t as

$$t_{1/2} = -\frac{1}{k}\ln(1 - 0.5^{1/\beta}). \tag{2.4}$$

2.3.2 Minimal compartmental models

Minimal models provide a simple and clear representation of the dynamics involved in glucose-insulin metabolism utilizing compartments to describe the most important interactions, with a reduced number of parameters that provide a simplified model identification. In particular, we consider two minimal models of subcutaneous insulin kinetics and glucose-insulin metabolism, as both of them are utilized in the present study.

Shimoda Insulin model

Shimoda insulin model represents SC insulin kinetics with compartments x_1 and x_2, in addition to a plasma insulin compartment I with model parameters validated for both *monomeric* and

soluble insulin pharmacokinetics. The model is given by

$$\frac{\mathrm{d}x_1(t)}{\mathrm{d}t} = -k_{21}x_1(t) + u_{\mathrm{s}}(t), \tag{2.5}$$

$$\frac{\mathrm{d}x_2(t)}{\mathrm{d}t} = k_{21}x_1(t) - (k_{\mathrm{d}} + k_{\mathrm{a}})x_2(t), \tag{2.6}$$

$$\frac{\mathrm{d}I(t)}{\mathrm{d}t} = \frac{k_{\mathrm{a}}}{V_{\mathrm{d}}}x_2(t) - k_{\mathrm{e}}I(t), \tag{2.7}$$

where $x_1(t)$ and $x_2(t)$ are insulin mass at the SC depot and compartment proximal to plasma respectively, $I(t)$ is plasma insulin concentration, V_{d} is plasma distribution volume, k_{21} is the insulin diffusion parameter, k_{a} is the insulin transition rate, k_{d} is the degradation rate constant in SC tissue, k_{e} is the degradation rate constant in plasma, and $u_{\mathrm{s}}(t)$ is the input for SC insulin administration.

Bergman minimal model

Bergman minimal model [46] is arguably the most attractive model of glucose-insulin dynamics in terms of simplicity. It comprises only two compartments to represent glucose and 'remote' insulin dynamics, where the rate of change in glucose is given by the difference in net hepatic glucose balance and glucose disappearance into peripheral tissue as

$$\frac{\mathrm{d}G(t)}{\mathrm{d}t} = -X(t)G(t) + p_1\left(G_{\mathrm{b}} - G(t)\right) + \frac{F_{\mathrm{G}}(t)}{V_{\mathrm{G}}}, \tag{2.8}$$

$$\frac{\mathrm{d}X(t)}{\mathrm{d}t} = -p_2X(t) + p_3I(t), \tag{2.9}$$

where $G(t)$ is plasma glucose concentration, $X(t)$ is a 'remote' insulin compartment that represents interstitial insulin concentration, p_2 is the rate of decrease in tissue glucose uptake ability and p_3 is the rate of insulin-dependent tissue glucose uptake ability. Although not originally considered in the minimal model, a representation of exogenous glucose infusion $F_{\mathrm{G}}(t)$ was eventually added by Furler *et al.* [47]. Intrinsically, the minimal model also considers:

- **Net hepatic glucose balance *B(t)***, which describes glucose uptake and production in the liver as:

  $$B(t) = B_0 - \left(k_5 + k_6X(t)\right)G(t) \tag{2.10}$$

  where B_0 is a constant that represents hepatic net balance at hypothetical zero plasma glucose, and constants k_5 and k_6 are insulin-independent and insulin-dependent glucose

uptake constants. Eq. (2.10) has a double interpretation of net hepatic glucose balance, with $B > 0$ denoting net hepatic glucose balanced towards glucose production while $B < 0$ indicates predominance of glucose uptake.

- **Glucose disappearance into peripheral tissue $U_p(t)$**, which is given by:

$$U_p(t) = (k_1 + k_4 X(t))\, G(t) \tag{2.11}$$

where k_1 represents insulin-independent glucose uptake and k_4 represents insulin-dependent glucose uptake.

- **Glucose effectiveness S_G**, a parameter that measures the ability of glucose to favor its own disposal and inhibits its own production at basal insulin secretion given by

$$S_G = p_1 \tag{2.12}$$

where $p_1 = -(k_1 + k_5)$ represents total insulin-independent glucose uptake.

- **Insulin sensitivity** represents the ability of insulin to induce glucose uptake as

$$S_I = -\frac{p_3}{p_2} \tag{2.13}$$

where S_I has a good independency from errors in S_G estimation [48] and the negative sign in parameter p_2 is added for consistency in the physiological representation since $p_2 < 0$ represents rate of increase in insulin proportional to glucose uptake.

2.3.3 Large-scale compartmental models

Compared to minimal models, large-scale mathematical models of glucose regulation include a complete mathematical description of the three main components given in Figure 2.5. These models represent not only glucose-insulin dynamics but also the complete regulatory mechanisms involved in glucose homeostasis, with the action of insulin and other detailed mechanisms depending on the complexity of the model proposed. Thence they are extended to represent T1DM state by adjustment of model parameters according to the pathology of the disease. In the following we consider the two most important mathematical models as they are widely utilized for model-based BG control purposes for the development of AP systems.

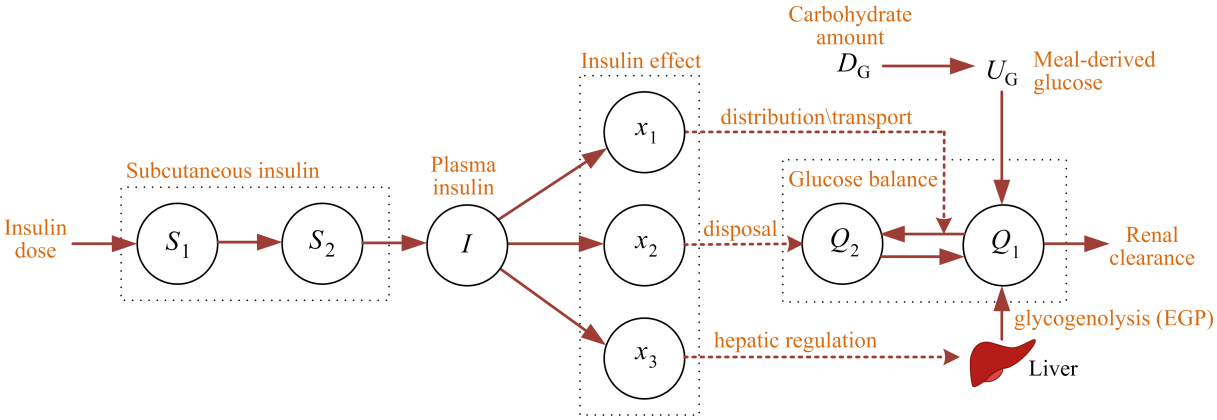

Figure 2.6: Compartmental diagram of Hovorka model [49]. Detailed mathematical repesentation is given in Appendix A.3 (page 153).

Hovorka model

Hovorka model [49] comprises a compartmental model representation (see Figure 2.6) of subcutaneous insulin absorption into plasma, from which it is divided into three 'remote' compartments to include the effect of insulin on glucose distribution/transport, disposal and hepatic regulation. Meal consumption is represented by an exponential function according to the amount of carbohydrates D_G, which enters the glucose compartment Q_1. For a complete mthematical description of Hovorka model, see Appendix A.3 (page 153).

Dalla Man model

Dalla Man and colleagues [50] propose a very complete mathematical model of glucose-insulin metabolism, which is currently the only FDA-approved model for simulation purposes and officially developed as an interactive simulation software implemented on MATLAB [51]. Dalla Man model consider two-compartmental representations for both subcutaneous insulin absorption and insulin kinetics, followed by a single compartment for insulin effect X. Provided the amount of carbohydrates, gut transit of carbohydrates is represented by a three-compartmental model for solids and liquids, with an additional representation of glucose absorption in the small intestine from which meal-derived glucose enters plasma glucose compartment G_p. The detailed mathematical description of Dalla Man model is included in the Appendix A.4 on page 156.

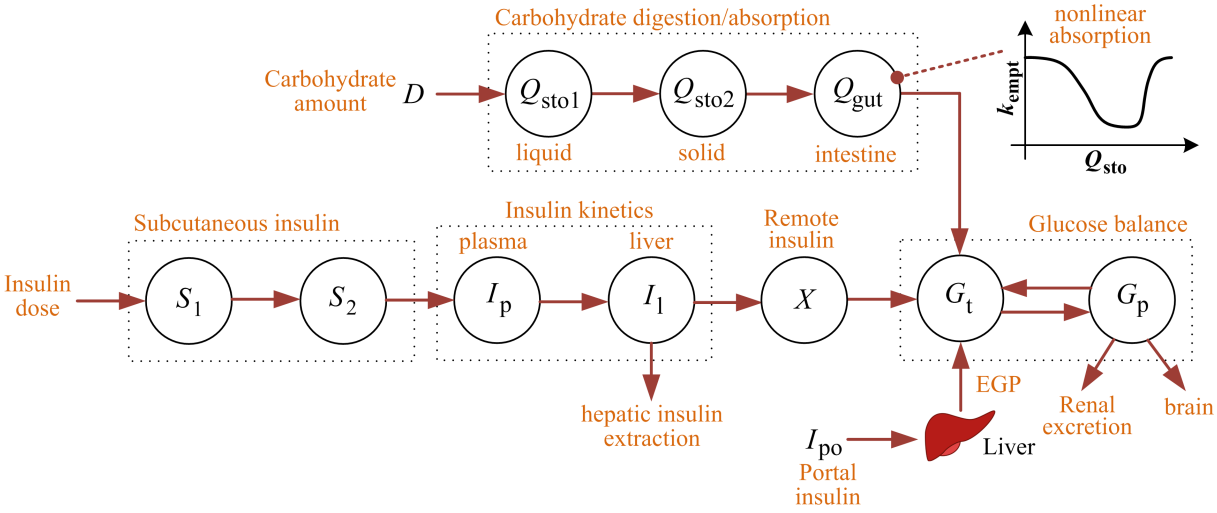

Figure 2.7: Compartmental diagram of Dalla Man model [50]. The mathematical description of Dalla Man model is given in the Appendix A.4 (page 156).

One of the main difficulties in the validation of mathematical models of glucose-insulin dynamics is the difficulty to measure *in vivo* glucose and insulin dynamics accurately, especially meal-derived glucose appearance and endogenous glucose production. For this reason, the same research group developed a triple tracer method for a more accurate estimation of glucose fluxes during postprandial state due to the underestimation of glucose fluxed of the double-tracer method [52]. Such method is explicitly utilized for the validation of model parameter values in Dalla-Man model.

2.4 Dietary fat metabolism

Dietary fat is an alternative energy substrate that is ultimately metabolized as fatty acids by the body, and provides inasmuch as over twofold the amount of calories compared to carbohydrates or protein. Energy homeostasis is the result of the tight regulation of glucose and fatty acids metabolism that essentially involves the liver, muscle and adipose tissue, both during postprandial and fasting states. The former, which refers to the *exogenous pathway* of fatty acid metabolism (see Figure 2.8), begins with dietary fat consumption from a meal, followed by break-down of triglycerides and cholesterol into monoglycerides and free fatty acids by several gastric enzymes in the stomach, and absorption by enterocytes in the small intestine. Gut transit of dietary fat involves several re-assembling processes with activation of several enzymes in a

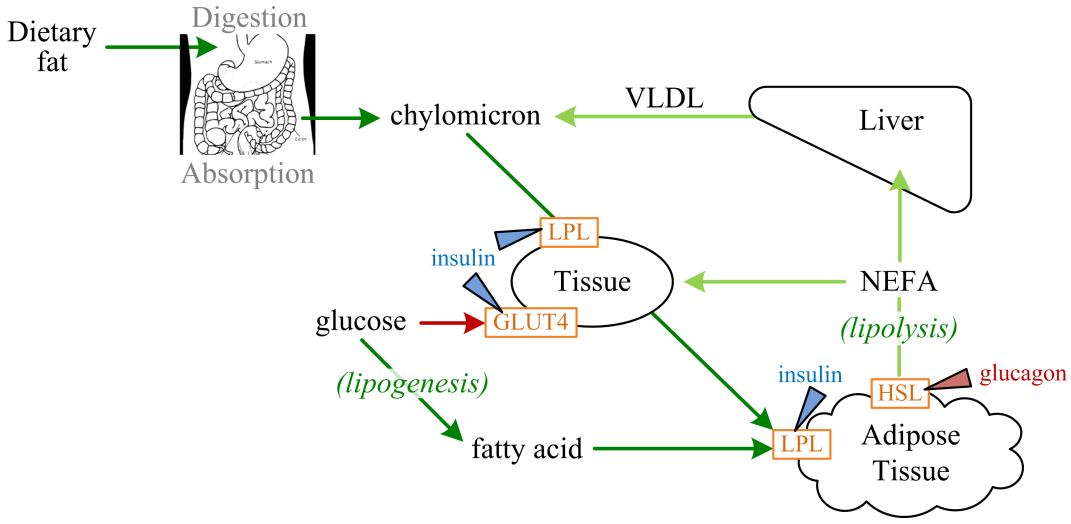

Figure 2.8: Dietary fat metabolism is divided into exogenous pathway (green lines) where fat is obtained from mixed meals after digestion and absorption in the gut during postprandial state. Endogenous pathway (light green lines) includes fat metabolism in the liver and adipose tissue for its utilization as energy substrate during fasting state.

far more complex process than that of carbohydrates, although further details are irrelevant for the mathematical modeling purposes in the present study. They are ultimately assembled into a protein-rich coating knows as chylomicron (CM) for the transportation of meal-derived triglycerides (TG) through the bloodstream because of the water-insoluble nature of fats. Chemically, TG are composed of three fatty acid molecules attached to a molecule of glycerol, which are transported as triglyceride-rich lipoprotein (TRL) through the bloodstream for its utilization by peripheral tissue for energy, or storage in fat cells (adipocytes) for eventual utilization as energy substrate.

During fasting state, the *endogenous pathway* of fatty acid metabolism involves utilization of lipids previously stored in adipose tissue for its utilization as energy. Lipids stored in the adipose tissue as TG are broken down and released as NEFA into the bloodstream for uptake by peripheral tissue or liver. The latter in particular, metabolizes NEFA to produce very-low density lipoprotein (VLDL) for its utilization as energy by peripheral tissue. In particular NEFA, also known as free fatty acids (FFA), plays a central role in fatty acid metabolism, whose dynamics is briefly described in Figure 2.9. Fatty acid metabolism involves an intricate hormone signaling that release fatty acid from adipocytes to provide energy after glucose sources are depleted. Lipolysis is induced by the action of hormone-sensitive lipase (HSL)—a glucagon-

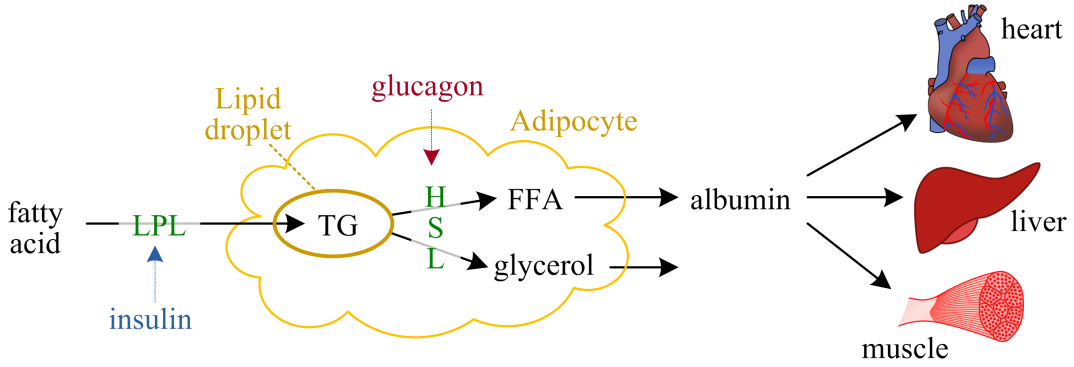

Figure 2.9: Simplified diagram of NEFA dynamics. High insulin levels activate LPL to promote lipid uptake and storage in adipocytes. During fasting state, high glucagon levels activate HSL to promote lipolysis for the utilization of lipids as energy by peripheral tissue.

sensitive hormone—and other secondary non-HSL-mediated enzymes such as triglyceride hydrolase (TGH) [53, 54], glucagon, epinephrine and norepinephrine. Together, they induce several complex intracellular processes that leads to lipolysis and a resulting increase in plasma NEFA levels. Conversely, lipoprotein lipase (LPL)—an insulin-sensitive hormone—induces lipid uptake and storage as TG prior esterification. Furthermore, high plasma NEFA levels, typical during postprandial state, promote TG production as VLDL and blocks lipolysis at the same time. Hence, a delicate balance between exogenous and endogenous fatty acid metabolism can be achieved by the action of insulin, which is the major regulatory hormone not only for glucose but also lipid metabolism for both exogenous and endogenous pathways.

2.5 Mathematical models of fatty acid metabolism

In the following we briefly introduce a few mathematical models of NEFA dynamics that have been developed to date, in addition to the only one mixed meal model in the literature to the best of our knowledge.

Boston model of NEFA kinetics

Boston minimal model [55] is a compartmental model of NEFA kinetics after intravenous glucose tolerance tests (IVGTT) or oral glucose tolerance tests (OGTT). Compared to other models of NEFA kinetics, it explicitly considers the initial latency, nadir and late rebound characteristics of postprandial NEFA levels [56]. The detailed mathematical representation of Boston model

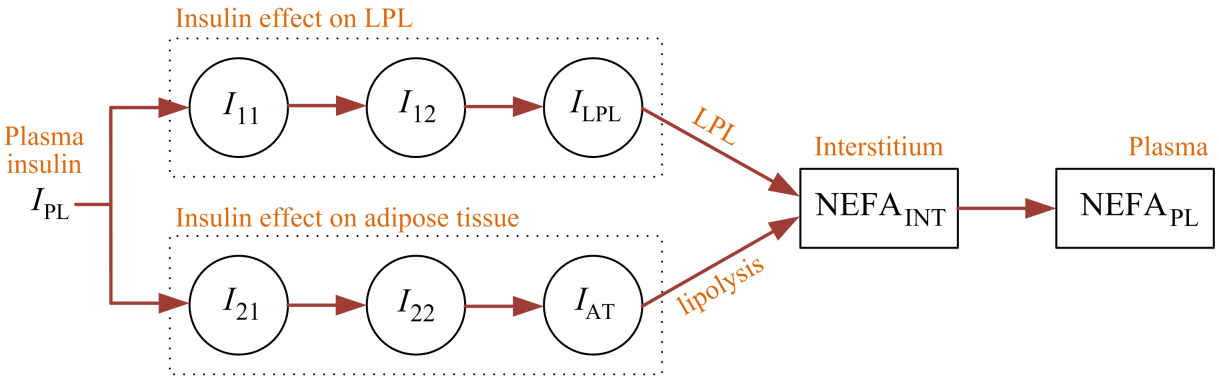

Figure 2.10: Compartmental diagram of Jelic model [57] (see A.6 on page 159 for details).

is given in Appendix A.5 (page 158).

Jelic model of postprandial NEFA kinetics

A model of NEFA dynamics specifically for postprandial state is proposed by Jelic *et al.* [57], as shown in Figure 2.10, which is validated from OGTT and mixed meal consumption. It includes two compartments for plasma and interstitial NEFA concentration, in addition to three-compartmental models for the effect of insulin on LPL-activated fatty acid uptake and lipolysis from adipose tissue. A more detailed mathematical description of Jelic model is included in Appendix A.6 (see page 159).

Roy model of dietary fat metabolism

A mixed meal model by Roy *et al.* [58,59] is arguably the only mathematical model developed to date that gives a complete mathematical representation of mixed meal absorption in the gut and the effect of fat on postprandial glucose-insulin metabolism, as shown in Figure 2.11. Gut transit is represented by Lehmann model [43], with each macronutrient portion being represented by separate variables. The dietary fat portion enters the free fatty acid compartment F by the action of plasma insulin I over a remote compartment Y. The effect on BG levels is represented from compartment F through another remote compartment Z. Roy model is described in more detailed in Appendix A.7 on page 160.

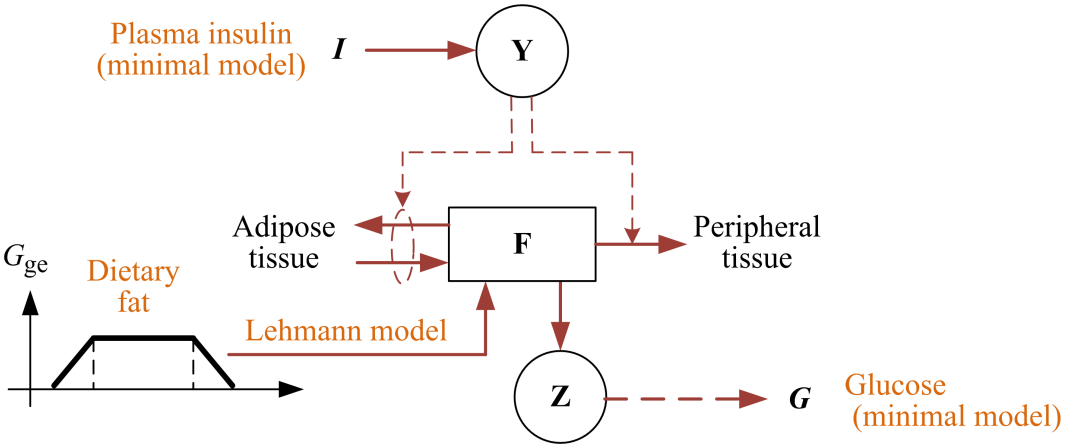

Figure 2.11: Compartmental diagram of fat metabolism in Roy model [58, 59] (see A.7 on page 160 for details)

2.6 BG control algorithms for prandial state

In-development AP systems basically have three components: A CGMS, an insulin pump and a control algorithm applied to BG control purposes (see Figure 2.12). The CGMS provides real-time measurement of BG levels which, along with a mathematical model of glucose-insulin metabolism, is utilized by an insulin optimization algorithm for the iterative computation of the appropriate insulin at several-minute intervals by the controller. The variable continuous insulin dose is respectively infused to the patient via an insulin pump for the maintenance of BG levels at the target value. Diurnal BG control algorithms are basically divided into fully closed-loop and closed-loop with meal announcement. While the former follows the conceptual definition of AP systems for complete automatic insulin delivery, the latter requires patient input to indicate an intended meal and thus has an overall performance above fully closed-loop BG control systems.

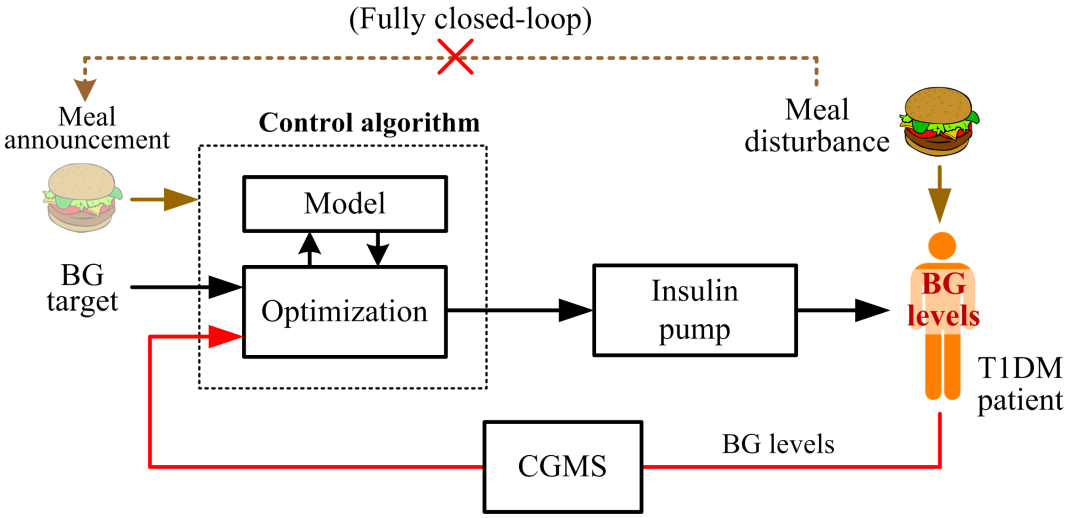

Figure 2.12: Closed-loop BG control systems maintain BG levels automatically at a given target value (normoglycemia) by computation of the optimal insulin using information from real-time BG levels measured with a CGMS and a mathematical model of glucose-insulin metabolism for BG prediction, and insulin delivery via an insulin pump. BG control algorithms for prandial state are divided into fully closed-loop and closed-loop with meal announcement. The former utilizes an automatic meal detection algorithm whereas the latter requires the patient to specify the carbohydrate amount of the intended meal to the controller in advance.

The majority of closed-loop BG control algorithms are based on proportional-integral-derivative (PID) and model predictive control (MPC), with other alternative approaches including fuzzy logic and adaptive control. These control approaches are described concisely as follows.

Proportional-integral-derivative (PID) control

The research group led by F. Doyle III and colleagues from the University of Santa Barbara is arguably one of the most representative supporters of PID control algorithms for BG control [60]. The three basic components of PID algorithms applied to BG control are (a) insulin delivery *proportional* to the difference between measured and target BG levels, (b) an *integral* element that provides basal insulin needs to maintain target BG values during steady state, and (c) a *derivative* component that increases/decreases the insulin infusion rate according to the variation in BG levels. To reduce hypoglycemic events, insulin feedback [61] is typically included in the PID control algorithm, and referred to as proportional-integral-derivative with insulin feedback (PID-IFB) that utilizes a two-compartment model of SC insulin kinetics to estimate plasma insulin concentration [62]. After the implementation of the control algorithm, the authors also acknowledged an increased risk of hypoglycemia due to reset windup for large carbohydrate loads (100 g). After consideration of several alternatives such as removal of the integral component, addition of constraints or re-tuning of the integral term, the authors weighted the benefits and disadvantages of each approach and resolved to include an anti-reset windup based on fuzzy logic. The system was tested *in silico* using the FDA-approved Dalla Man model with 10 subjects, with resulting BG control between 93$\pm$7.3 (5.17$\pm$0.41 mmol/L) and 196$\pm$14 mg/dL (10.89$\pm$0.78 mmol/L) for a carbohydrate load of 100 g. Additionally, a manual insulin bolus of 2 IU at mealtime contributed to a reduction in postprandial BG peak to 175$\pm$8 mg/dL (9.72$\pm$0.44 mmol/L) [63].

Model Predictive Control (MPC)

Because of the long delay associated with subcutaneous insulin absorption, MPC is considered to be one of the most suitable control approaches for BG control purposes. It heavily relies on a mathematical model of glucose-insulin dynamics to compute the prospective control moves considering restrictions in any of the model variables. Fully closed-loop BG control algorithms using MPC have been continuously improved through the years by including a limitation in bolus insulin delivery as a percentage of the nominal bolus, constraint in insulin delivery for negative insulin doses, and saturation of the control variable (insulin) for prandial state [64].

In spite of this, clinical trials show that a narrower BG excursion than fully closed-loop algorithms can be achieved with hybrid BG control, which consists of a combination of manual bolus insulin administration (a fraction of the total bolus) accompanied by fully closed-loop basal BG control. Expansion of hybrid control includes a multiple model probabilistic predictive controller with prior information of daily insulin dose and basal profile, BG prediction for future meals, endogenous insulin production and insulin sensitivity from a bank of mathematical models. During inpatient clinical trials, it achieved a performance in BG control of 78% within the normoglycemic range of 70–180 mg/dL (3.89–10.0 mmol/L) for unannounced meals of approximately 1 g/kg weight [65].

Fuzzy Logic

An alternative approach in BG control algorithms considers fuzzy logic, whose main advantage is perhaps that it does not require a mathematical model of glucose-insulin metabolism. Still, due to occurrences of late postpradial hypoglycemia in simulation environments of early fuzzy logic control algorithms, it has been extended to include insulin-on-board and a personalization factor—a tuning parameter based on the individual daily insulin dose of the patient—which resulted in an improved BG control performance [66]. Clinical implementation in a 24-hour control with unannounced carbohydrate loads of 30 g and 60 g resulted in average blood glucose values of 165 mg/dL (9.17 mmol/L) and BG excursion between 70–200 mg/dL (3.89–11.11 mmol/L) during 76% of the time [67].

Supplementary algorithms

Due to the limited success of diurnal BG control systems in maintaining postprandial normoglycemia, additional algorithms are being continuously developed and utilized with one of the control approaches above. The most relevant advances are:

- **Meal detection algorithms**
  Fully closed-loop BG control algorithms require meal detection algorithms in order to regulate BG levels during prandial state. An automatic meal-detection algorithm from CGMS has been proposed by the group led by F. J. Doyle III (University of California, USA) [68], wherein calculation of glucose rate change is based on two methods: three-point BG measurements from the current value and the two previous ones (backward difference), and Kalman filter estimation from actual BG change considering measurement noise. For an average 56 g of carbohydrates (22–105 g used), time of meal detection and increase in BG levels are 29 min with 13 mg/dL (0.72 mmol/L) for backward difference,

35 min with 30 mg/dL (1.67 mmol/L) for Kalman filter, and 31 min with 18 mg/dL (1 mmol/L) for combined backward difference and Kalman filter.

- **Insulin-on-board**
  The slow subcutaneous insulin absorption and remnant hypoglycemic effect several hours after its administration increases the risk of late postprandial hypoglycemia, especially for large insulin doses. Because of this, recent BG control algorithms include constrains for insulin-on-board such as Safety Auxiliary Feedback Element (SAFE) [69]. For insulin-on-board estimation, usually two-compartmental models for insulin absorption are considered, along with several tuning parameters that need to be determined by an additional meal test. *In silico* tests of the SAFE layer on a classical and insulin-feedback PID algorithms, in addition to linear MPC algorithm, all of which are implemented in Dalla Man model, result in a considerable reduction of hypoglycemic events with no considerable negative effect on postprandial BG excursion [70]. In particular, MPC-based BG control resulted in a reduction of hypoglycemic episodes from 6 to 0 (out of 18 BG control simulations) for a given patient after consumption of mixed meals with different carbohydrate loads between 50–78.5 g.

- **Fully-integrated AP system**
  Arguably the most advanced fully closed-loop BG control system developed to date [71, 72] has a modular architecture based on two interacting blocks: Range correction module and Safety supervisor module. The former is responsible for the detection of possible hyper- and hypoglycemic deviations and appropriate insulin infusion to maintain BG levels at the target range, whereas the latter exclusively analyses the risk of hypoglycemia and might also include constraint algorithms for insulin-on-board. Clinical results in multi-center studies [73] show that the average postprandial BG control range is 159 mg/dL (8.83 mmol/L) in adults and 166 mg/dL (9.22 mmol/L) in adolescents, although individual BG excursions reach BG levels as high as 350 mg/dL (19.44 mmol/L).

- **Parameter auto-tuning**
  Other closed-loop BG control systems involve an adaptive meal-priming bolus delivery [74] to eliminate the necessity to repeatedly re-tune the control algorithm due to considerable changes in insulin requirements caused by hormonal imbalances, since insulin requirements increase inasmuch as four times throughout the transition from childhood to adolescence and eventually to adulthood. This fully-automated BG control system utilizes a bi-hormonal control approach that adapts to the patient in less than twenty four hours using only information of body weight as initialization parameter. It demonstrated

the ability to maintain postprandial BG levels below 250 mg/dL (13.89 mmol/L), although postprandial normoglycemia is currently unfeasible. Meal detection algorithms are capable of detecting meal consumption within 30 min after meal ingestion, which is not sufficient to prevent postprandial hyperglycemia.

Chapter 3

Mathematical model of postprandial glucose-insulin metabolism in T1DM

Mathematical models of glucose-insulin metabolism serve several purposes including fault detection algorithms for next-generation CGMS and insulin pumps [75], decision support systems for prandial bolus estimation, diabetes diagnostics/prognosis and a better understanding of the disease [76]. They also provide simulation environments for the evaluation of closed-loop BG control systems [77, 78] to facilitate costly, time-consuming and perhaps even ethically-questionable clinical trials. As briefly introduced in Chapter 2, several mathematical models of glucose-insulin metabolism have been proposed to date in order to represent the impact of carbohydrates on BG levels Among them, Hovorka and Dalla Man models are predominantly utilized in model-based BG control algorithms since the exactitude of the mathematical model utilized influences to a considerable extent the control performance. In spite of the high level of detail in the physiological representation of gut absorption, such as in Dalla Man model (see Eq. (A.27) and Figure A.2 on page 157), these models consider only the amount of carbohydrates in order to represent the impact of a meal on BG levels. Other limitations include the lack of authentication of subcutaneous insulin effect instead of only their absorption kinetics and plasma levels.

In the present study, we propose a minimal model of glucose-insulin metabolism in T1DM that includes a more accurate mathematical presentation of the impact of carbohydrates on BG levels by considering the differences in gut absorption rate according to the specific food consumed. Beyond the traditional classification of carbohydrates according to their chemical structure (see Table 2.1 on page 9), an alternative classification based exclusively on its absorption rate is given by the Glycemic index (GI) of foods. Pioneering clinical studies [79] demonstrate that the post-meal increase in BG levels after consumption of 62 commonly eaten

carbohydrate-rich foods differs inasmuch as sixfold for the same amount of 50 g. Moreover, for an authentic representation of the hypoglycemic effect of rapid-acting insulin, we contemplate a thorough validation of model parameters from clinical data to represent the glucose-lowering effect of insulin as glucose-equivalent. In this way, postprandial BG excursion in T1DM can be accurately represented by the impact of meal-derived glucose and the opposing hypoglycemic effect of insulin. Because of the emphasis on model simplicity in the present study, we consider the representation of glucose-insulin metabolism in T1DM and its disrupted homeostasis as an extension of the minimal model. Therefore, in the present chapter we propose a novel mathematical model of glucose-insulin metabolism from carbohydrates in T1DM that provides a more accurate representation of the impact of food-specific carbohydrates on BG levels using a minimal—yet accurate—compartmental approach compared to more complex models in the literature.

First, we introduce several concepts related to the rate of carbohydrate absorption of meals, which serve as the theoretical base from which we propose a novel representation of carbohydrate digestion and absorption. To represent the hypoglycemic effect of insulin, parameters of subcutaneous insulin kinetics in Shimoda insulin model are re-validated using a simple three-step method using pertinent clinical data. The representation of glucose-insulin metabolism in T1DM considers a minimal parameter modification of Bergman model provided a thorough consideration of the physiological representation. To demonstrate the accuracy of the present model, we include simulation results and comparison with clinical data of post-meal BG excursion for different foods and provide an extensive discussion of our findings.

3.1 Proposed model of carbohydrate digestion/absorption

In the present study, we propose a novel mathematical representation of carbohydrate digestion and absorption in the gut. To represent the glycemic impact of carbohydrates on postprandial BG levels, we first consider the calculation of a total glucose-equivalent of carbohydrates (GR), as shown in Figure 3.1, which depends on the carbohydrate amount and GI value of the meal. Thence, it is further divided into rapidly and slowly available glucose (RAG and SAG) proportions, according to the amount of glucose release from carbohydrates between two specific time period defined by the classification of carbohydrate bioavailability by Englyst *et al.* [80]. Thence, we consider the physiologically-relevant representation of maximum rate of glucose appearance $\mathrm{Ra}_{\mathrm{max}}$ to limit the absorption rate of exogenous glucose, in addition to a first-order delay in gastric emptying to represent the impact of carbohydrates as meal-derived glucose appearance $G_{\mathrm{ext}}(t)$.

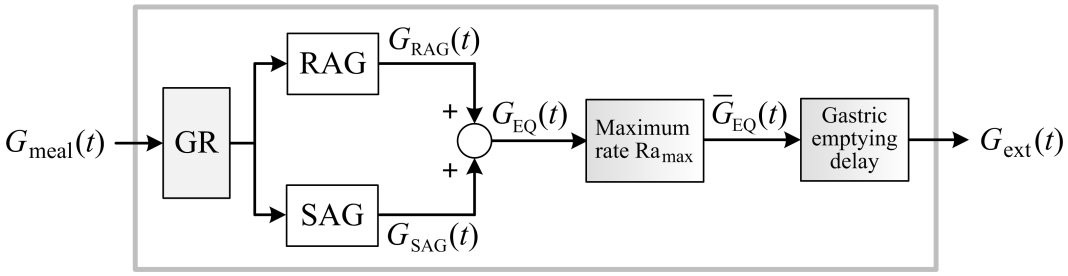

Figure 3.1: Mathematical model of carbohydrate digestion/absorption proposed in the present study. GR represents the total glucose-equivalent of carbohydrates according to the amount and GI value of the meal. It is further divided into its rapidly and slowly available glucose components (RAG and SAG), and followed by a maximum rate of glucose appearance Ra_{max} in addition to a first-order gastric emptying delay to represent meal-derived exogenous rate of glucose appearance $G_{\text{ext}}(t)$.

The concept of GI, RAG and SAG absorption are introduced in the following subsection prior to the explanation of the present model proposal.

3.1.1 The Glycemic Index (GI) of foods

The glycemic index (GI) of foods [79] provides a quantitative estimation of the impact of different types of carbohydrates on BG levels *in vivo*. It is calculated from the 2-hour incremental area-under-the curve (iAUC) of BG excursion after consumption of 50 grams of a test food divided by that of a reference food—usually glucose, although some studies use white break because of palatability issues—with the same amount, and multiplied by 100 to obtain an integer value. By definition, the GI value is given as

$$\text{GI} = \frac{\text{iAUC}_{\text{test food}}}{\text{iAUC}_{\text{REF}}} \times 100 \tag{3.1}$$

where $\text{iAUC}_{\text{test food}}$ is the iAUC of the foods whose GI is to be determined, and iAUC_{REF} is the iAUC of glucose as reference food[1]. In this way, the GI value provides an index of the impact of different types of carbohydrates on BG levels independent of the amount consumed (constant).

Previous studies by Wolever *et al.* [81] present a quantitative assessment of the glycemic impact of carbohydrate-rich foods in healthy patients by considering varying amounts (25 g, 50

[1] A few studies utilize white bread instead of glucose due to palatability and tolerance issues, which affects the GI value of a food. For instance, white bread has a GI value of 100 or 71 depending on whether the reference food considered in the test is white bread or glucose, respectively.

g, 75 g and 100 g) and GI values (48, 71, 100 and 129 considering white bread as reference); and developed a formula to predict the impact of carbohydrates as percentage related to 50 g of white bread. We propose a mathematical representation of meal consumption indicated with the input $G_{\text{meal}}(t)$ and GR based on the aforementioned formula as

$$\text{AvCHO} = \int_0^{t_{\text{food}}} G_{\text{meal}}(t)\text{d}t, \tag{3.2}$$

$$\text{GR} = 1.5\frac{\text{GI}}{100}\left(1 - \text{e}^{-k_{\text{GR}}\cdot\text{AvCHO}}\right) + 0.13\, k_{\text{w2g}}, \tag{3.3}$$

where $k_{\text{GR}} = 0.018\ \text{g}^{-1}$ is a parameter from the original model obtained from curve fitting analysis, $k_{\text{w2g}} = 71/100$ adjusts the GI value with glucose as reference (instead of white bread) and AvCHO is the total amount of available carbohydrates ingested over the time span from 0 to t_{food}. In particular, a single-meal is represented by a unitary impulse with carbohydrate intake given by $G_{\text{meal}}(t) = \text{AvCHO} \cdot \delta(t)$.

Moreover, since GR in Eq. (3.3) expresses the total glucose-equivalent as a percentage relative to 50 g of glucose, its equivalent as glucose amount is calculated by

$$\text{GR}_{\text{EQg}}(t) = \left(\frac{50\ \text{g} \cdot \text{GR}}{\text{AvCHO}}\right) \cdot G_{\text{meal}}(t). \tag{3.4}$$

3.1.2 Carbohydrate Bioavailability

An alternative classification of the type of carbohydrate depends on the digestion/absorption of glycaemic and non-glycaemic carbohydrates as carbohydrate bioavailability from *in vitro* studies [82, 83], which considers biomolecular properties of carbohydrates including chemical identity (linkage type of saccharide, size), food matrix (degree of processing), meal factor (macronutrient composition) and gastrointestinal handling. According to Englyst *et al.*, dietary carbohydrates are divided into available carbohydrates and resistant carbohydrates (see Figure 3.2). The former includes all types of sugar and starch including glucose, fructose, galactose, maltose, sucrose and lactose; and starch previously hydrolyzed *in vitro* to glucose to represent enzymatic digestion. The latter includes resistant starch, non-starch polysaccharides commonly known as dietary fiber, resistant short-chain carbohydrates and sugar alcohols.

In particular, we consider the two main classifications of starch as (a) Rapidly Available Glucose (RAG), which is defined as the amount of glucose released from carbohydrates between 0–20 min after incubation with gastric enzymes [84], and (b) Slowly Available Glucose (SAG), which refers to the amount of glucose release from carbohydrates between 20–120 min

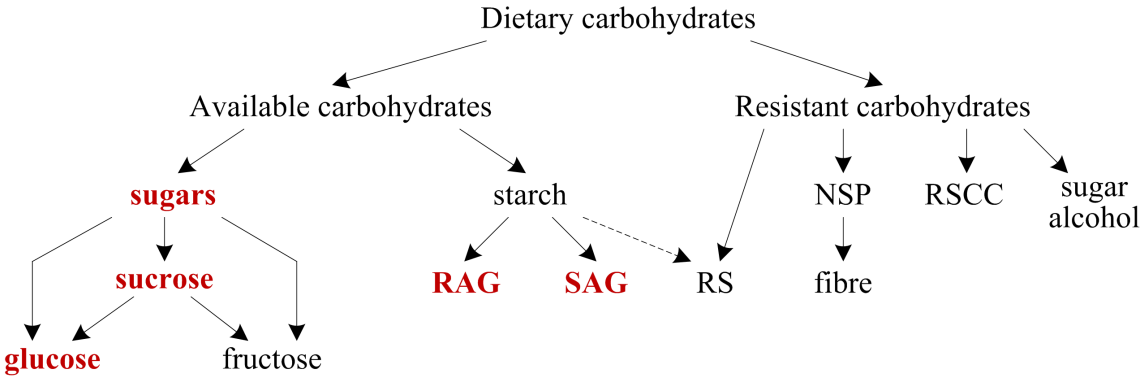

Figure 3.2: Classification of carbohydrates according to Englyst *et al.* [83]. RS: Resistant starch, NSP: Non-starch polysaccharides, RSCC: resistant short-chain carbohydrates. In the present study, we include RAG and SAG classifications of carbohydrate bioavailability for the representation of carbohydrate digestion/absorption as glucose.

following the same procedure. A third classification as Resistant Starch (RS) is defined as the product of starch degradation left unabsorbed by the small intestine and is further divided into four subgroups (RS1–RS4) depending on the enzyme resistance characteristics, although is not currently considered in the present model.

Following the definition of RAG and SAG, the absorption dynamics of $G_{\text{RAG}}(t)$ and $G_{\text{SAG}}(t)$ are represented by critically-damped second-order systems (blocks RAG and SAG in Figure 3.1) considering the total glucose-equivalent of carbohydrates in Eq. (3.4) as input. The matrix representation is thus given by

$$\frac{\mathrm{d}x_{\text{RAG}}(t)}{\mathrm{d}t} = \begin{bmatrix} 0 & 1 \\ -\dfrac{1}{T_{\text{RAG}}^2} & -\dfrac{2}{T_{\text{RAG}}} \end{bmatrix} x_{\text{RAG}}(t) + \begin{bmatrix} 0 \\ \dfrac{K_{\text{RAG}}}{T_{\text{RAG}}^2} \end{bmatrix} \text{GR}_{\text{EQg}}(t), \tag{3.5}$$

$$\frac{\mathrm{d}x_{\text{SAG}}(t)}{\mathrm{d}t} = \begin{bmatrix} 0 & 1 \\ -\dfrac{1}{T_{\text{SAG}}^2} & -\dfrac{2}{T_{\text{SAG}}} \end{bmatrix} x_{\text{SAG}}(t) + \begin{bmatrix} 0 \\ \dfrac{K_{\text{SAG}}}{T_{\text{SAG}}^2} \end{bmatrix} \text{GR}_{\text{EQg}}(t - \tau_{\text{SAG}}), \tag{3.6}$$

$$G_{\text{RAG}}(t) = \begin{bmatrix} 1 & 0 \end{bmatrix} x_{\text{RAG}}(t), \tag{3.7}$$

$$G_{\text{SAG}}(t) = \begin{bmatrix} 1 & 0 \end{bmatrix} x_{\text{SAG}}(t), \tag{3.8}$$

Table 3.1: Values of GI [85], RAG, SAG and RS [80] for four representative staple foods (solids) and a sugary drink (liquid). (*) grams as 100 g of food eaten.

FOOD	**GI**	**RAG***	**SAG***	**RS***
Instant potato	83	12.0	1.1	0.8
White bread	71	42.0	3.7	0.6
Pineapple juice	46	10.0	0.0	0.0
Spaghetti	41	15.0	9.0	1.0
Pearled barley	25	9.0	7.0	2.1

with variables $x_{\text{RAG}}(t)$ and $x_{\text{SAG}}(t)$ for representation of RAG and SAG absorption respectively, with time-constant parameters T_{RAG} and T_{SAG}, and gains $K_{\text{RAG}} = \text{RAG}/(\text{RAG} + \text{SAG})$ and $K_{\text{SAG}} = \text{SAG}/(\text{RAG} + \text{SAG})$ considering the proportion of RAG ans SAG according to food-specific values [80], in addition to $\tau_{\text{SAG}} = 20$ min by definition of SAG. In the present study we consider four staple foods represented by instant potato, white bread, spaghetti and pearled barley whose parameters values of GI, RAG and SAG are specified in Table 3.1.

Assuming a unit impulse in $G_{\text{meal}}(t)$ to represent single-meal consumption, we determine the values of T_{RAG} and T_{SAG} considering that RAG absorption should satisfy (i) complete glucose absorption before 20 min and (ii) area-under-the-curve (AUC) of $G_{\text{RAG}}(t)$ be equivalent to that of $K_{\text{RAG}} \cdot \text{GR}_{\text{EQg}}(t)$. Likewise, for SAG absorption, (iii) glucose absorption between 20–120 min and (iv) AUC for $G_{\text{SAG}}(t)$ be equal to that of $K_{\text{SAG}} \cdot \text{GR}_{\text{EQg}}(t)$. Nonetheless, due to the nature of second-order critically-damped systems, it is not feasible to have a rigorous compliance with the stipulated time span for RAG and SAG absorption in (i) and (iii), respectively, and thus we assume a small error margin of 5%. Under these conditions, time-constant parameters for RAG and SAG are calculated to $T_{\text{RAG}} = 4.22$ min and $T_{\text{SAG}} = 21.1$ min, respectively, and the absorption rate of total glucose-equivalent of carbohydrates is the sum of RAG ans SAG absorption as

$$G_{\text{EQ}}(t) = G_{\text{RAG}}(t) + G_{\text{SAG}}(t). \tag{3.9}$$

3.1.3 Maximum rate of glucose appearance

By considering the GI value, RAG and SAG of the specific meal, not only the amount but also its absorption rate provides a more accurate representation of meal-derived glucose appearance and the impact of a meal on BG levels. In some clinical studies in nondiabetics, however, there

appears to be a particular plateau after consumption of very large carbohydrates test meals (5 g/kg weight) [86], which suggests the existence of a maximum rate of meal-derived glucose appearance thought to be regulated by the caloric gastric emptying rate with an estimated maximum of 1–3 kcal/min in nondiabetics [87]. Although neither the rate of gastric emptying nor exogenous glucose appearance are usually measured in clinical studies, insulin secretion and BG excursion implicitly indicate that the impact of very large carbohydrate meals (111 ± 1.9 g) on glucose-insulin metabolism continues as long as 5 hours post-meal, especially for high GI foods (value of 89) [88]. Such response suggests that exogenous glucose is still being metabolized during late postprandial state, although the exact mechanism is yet to be elucidated. To our knowledge, only one study to this date [89] investigated the glycemic response in T1DM to different carbohydrate loads up to 150 g. The resulting BG excursion is characterized by a rebound in hyperglycemia that lasts over 6 hours, which also suggests the existence of a sustained exogenous glucose appearance proportional to the amount of carbohydrates consumed.

Because of these evidences, we include a maximum rate of glucose appearance Ra_{max} in the glucose-equivalent $G_{\text{EQ}}(t)$, which is re-defined as $\overline{G}_{\text{EQ}}(t)$ in our model (see Figure 3.3). Parameters t_1 and t_2 indicate the instants at which RAG absorption reaches Ra_{max} upwards and downwards, respectively, whereas t_3 in $\overline{G}_{\text{EQ}}(t)$ is the start in the decay from Ra_{max}. It is also assumed that $t_1 < \tau_{\text{SAG}}$ regardless of the food consumed.

The respective analysis and parameter calculation assumes a single-meal input signal considering that

a) The total AUC of $\overline{G}_{\text{EQ}}(t)$ must be equal to the total glucose-equivalent $G_{\text{EQ}}(t)$, *i.e.*, the sum of $G_{\text{RAG}}(t)$ and $G_{\text{SAG}}(t)$.

b) SAG absorption remains unaltered regardless of the addition of Ra_{max}.

c) Glucose absorption profile of $\overline{G}_{\text{RAG}}(t)$ for $t > t_3$ is the same as $G_{\text{RAG}}(t)$ for $t > t_4$ (see Figure 3.3, top and bottom).

Regarding c), we acknowledge that the total glucose-equivalent $\overline{G}_{\text{EQ}}(t)$ as the sum of RAG absorption (whose decay follows Eq. (3.7) for $t \geq t_4$) and SAG absorption surpasses the maximum rate Ra_{max} for a transient time at $t \geq t_3$. To prevent this, we consider an additional parameter t_4 (see Figure 3.3) in RAG absorption. Provided that Ra_{max} is known, t_1 and t_2 can be directly obtained from $G_{\text{RAG}}(t)$, and the remaining parameters t_3 and t_4 being calculated as

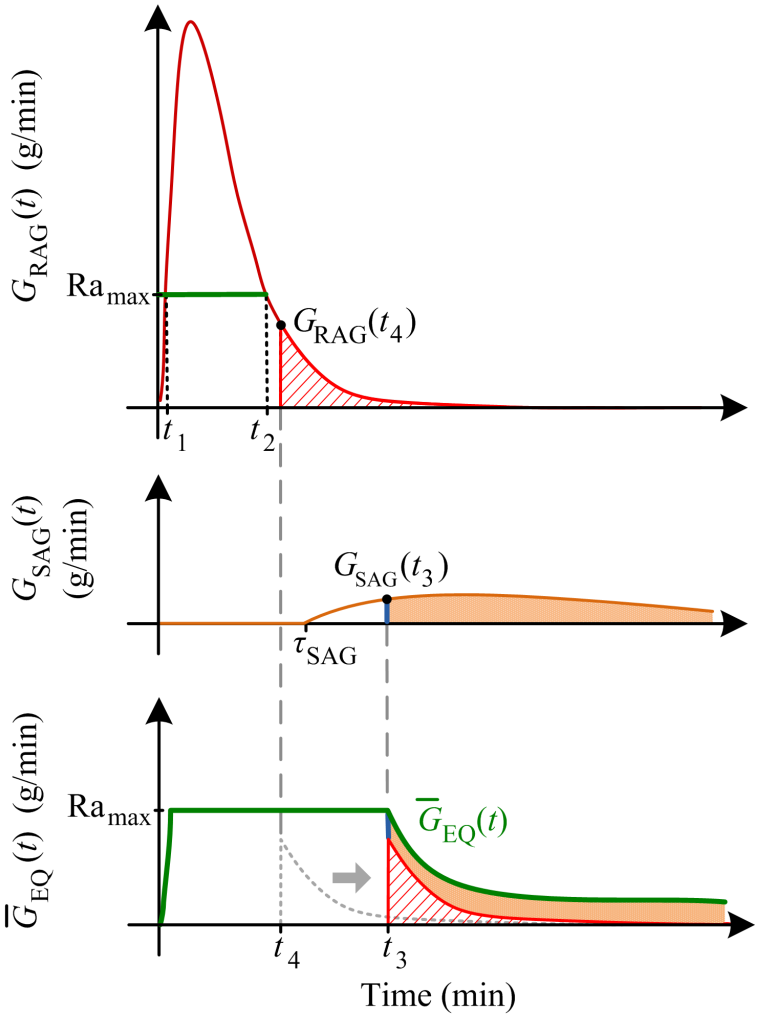

Figure 3.3: Illustration of RAG, SAG absorption and total glucose-equivalent $\overline{G}_{\mathrm{EQ}}(t)$ considering maximum rate of glucose appearance $\mathrm{Ra}_{\mathrm{max}}$ with specification of parameters t_1, t_2, t_3 and t_4.

follows. From a),

$$\int_{t_1}^{\infty} \overline{G}_{\text{EQ}}(t)\mathrm{d}t = \int_{t_1}^{\infty} G_{\text{EQ}}(t)\mathrm{d}t, \tag{3.10}$$

$$(t_3 - t_1) \cdot \text{Ra}_{\text{max}} + \int_{t_3}^{\infty} \overline{G}_{\text{EQ}}(t)\mathrm{d}t = \int_{t_1}^{\infty} G_{\text{RAG}}(t)\mathrm{d}t + \int_{\tau_{\text{SAG}}}^{\infty} G_{\text{SAG}}(t)\mathrm{d}t. \tag{3.11}$$

From b), since SAG absorption is unaltered, it can be removed as

$$\int_{t_3}^{\infty} \left(\overline{G}_{\text{EQ}}(t) - G_{\text{SAG}}(t)\right) \mathrm{d}t = \int_{t_4}^{\infty} G_{\text{RAG}}(t)\mathrm{d}t, \tag{3.12}$$

which is replaced in Eq. (3.11) as

$$(t_3 - t_1) \cdot \text{Ra}_{\text{max}} + \int_{t_4}^{\infty} G_{\text{RAG}}(t)\mathrm{d}t = \int_{t_1}^{\infty} G_{\text{RAG}}(t)\mathrm{d}t + \int_{\tau_{\text{SAG}}}^{t_3} G_{\text{SAG}}(t)\mathrm{d}t, \tag{3.13}$$

$$(t_3 - t_1) \cdot \text{Ra}_{\text{max}} = \int_{t_1}^{t_4} G_{\text{RAG}}(t)\mathrm{d}t + \int_{\tau_{\text{SAG}}}^{t_3} G_{\text{SAG}}(t)\mathrm{d}t, \tag{3.14}$$

$$A_3 = A_1 + A_2, \tag{3.15}$$

where A_1, A_2 and A_3 are the AUC as illustrated in Figure 3.4.
Lastly, $\overline{G}_{\text{EQ}}(t)$ from c) is given by

$$\overline{G}_{\text{EQ}}(t) = G_{\text{RAG}}(t - t_3 + t_4) + G_{\text{SAG}}(t - \tau_{\text{SAG}}), \tag{3.16}$$

which at $t = t_3$ we have

$$\text{Ra}_{\text{max}} = G_{\text{RAG}}(t_4) + G_{\text{SAG}}(t_3). \tag{3.17}$$

For a single-meal, RAG and SAG absorption in Eqs. (3.11)–(3.17) are represented by second-

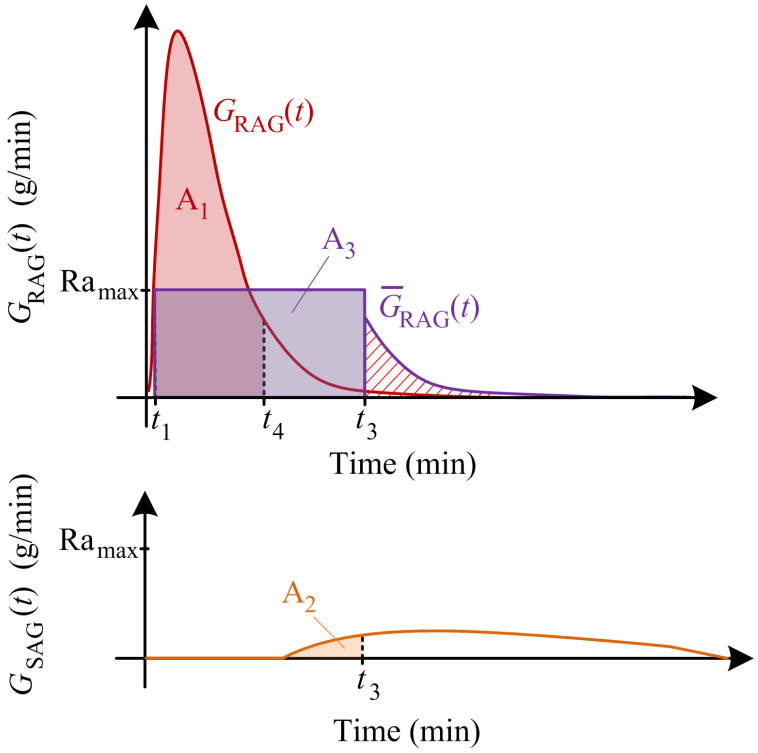

Figure 3.4: Calculation of parameters t_3 and t_4 by considering the equivalent area-under-the-curve in RAG absorption (top) including the portion of SAG absorption $t \leq t_3$ such that $A_3 = A_1 + A_2$.

order critically-damped impulse response systems. Thus,

$$\int_{t_1}^{t_4} G_{\text{RAG}}(t)\mathrm{d}t = K_{\text{RAG}}\left(1+\frac{t_1}{T_{\text{RAG}}}\right)\cdot\exp\left(-t_1/T_{\text{RAG}}\right) - K_{\text{RAG}}\left(1+\frac{t_4}{T_{\text{RAG}}}\right)\cdot\exp\left(-t_4/T_{\text{RAG}}\right), \tag{3.18}$$

$$\int_{\tau_{\text{SAG}}}^{t_3} G_{\text{SAG}}(t)\mathrm{d}t = K_{\text{SAG}} - K_{\text{SAG}}\left(1+\frac{t_3-\tau_{\text{SAG}}}{T_{\text{SAG}}}\right)\cdot\exp\left(-(t_3-\tau_{\text{SAG}})/T_{\text{SAG}}\right), \tag{3.19}$$

$$G_{\text{RAG}}(t_4) = \frac{K_{\text{RAG}}}{T_{\text{RAG}}^2}\cdot t_4\cdot\exp\left(-t_4/T_{\text{RAG}}\right), \tag{3.20}$$

$$G_{\text{SAG}}(t_3) = \frac{K_{\text{SAG}}}{T_{\text{SAG}}^2}\cdot t_3\cdot\exp\left(-t_3/T_{\text{SAG}}\right), \tag{3.21}$$

where the equations formulated above from Eqs. (3.14) and (3.17) with values of t_3, t_4 can be solved by any solution method for nonlinear equations such as the the Newton-Rhapson method.

The mathematical representation of gut absorption from carbohydrates $\overline{G}_{\text{EQ}}(t)$ considering maximum rate of exogenous glucose appearance Ra_{max} for the specific case of a single-meal (impulse response) is thus given by

$$\overline{G}_{\text{EQ}}(t) = \begin{cases} \dfrac{G_{\text{EQg}}\cdot K_{\text{RAG}}}{T_{\text{RAG}}^2}\cdot t\mathrm{e}^{-t/T_{\text{RAG}}}, & t < t_1 \\ \text{Ra}_{\text{max}}, & t_1 \le t \le t_3 \\ \dfrac{G_{\text{EQg}}\cdot K_{\text{RAG}}}{T_{\text{RAG}}^2}\cdot(t-t_5)\mathrm{e}^{-(t-t_5)/T_{\text{RAG}}} & \\ \quad + \dfrac{G_{\text{EQg}}\cdot K_{\text{SAG}}}{T_{\text{SAG}}^2}\cdot(t-\tau_{\text{SAG}})\mathrm{e}^{-(t-\tau_{\text{SAG}})/T_{\text{SAG}}}, & t > t_3 \end{cases}, \tag{3.22}$$

where t_3 and $t_5 = t_3 - t_4$ are time-constant parameters specific to the food (see Table 3.2) and the remaining parameters are the same as in Eqs. (3.7) and (3.8).

Although parameter Ra_{max} physiologically reflects the maximum rate of glucose appearance and thus must be determined from actual clinical studies, there is none which explicitly aims to determine such value. Therefore, to determine a physiologically-relevant value of Ra_{max}, we consider studies from human biology and sport nutrition due to the particular interest in the effect of carbohydrate ingestion and absorption during athletic performance. In one study [90],

during exercise at 50% of maximal oxygen consumption, a maximum glucose appearance of 0.41–0.42 g/min after a low carbohydrate load[2] was observed with an almost complete metabolization of exogenous glucose. However, for a high carbohydrate load[3], the glucose appearance rose to 0.96–1.04 g/min suggesting this to be the maximum rate of digestion/absorption of exogenous glucose.

It can be argued that gastric emptying and glucose absorption might be affected by exercise, especially in continuous workload conditions as 120 min of cycling in the aforementioned study. Even though exercise causes gastrointestinal distress resulting in lower gastric emptying/absorption of carbohydrates, several studies suggest that it only occurs during strenuous exercise above 70–80% of maximal oxygen consumption [91, 92]. Considering that exercise mainly affects muscle glycogen oxidation and is independent of exogenous carbohydrate-derived digestion/absorption, the maximum rate of glucose appearance in such study might be applied to resting conditions as well.

3.1.4 Gastric emptying delay

Typical postprandial hyperglycemia in patients with T1DM is usually accompanied with a delay in gastric emptying [93, 94], and even extends to chronic gastroparesis in critical cases. Some studies suggest that hyperglycemia is the cause of delayed gastric emptying in patients with T1DM by means of the gastrointestinal motor mechanism [93], hyperglycemia delays gastric emptying in both nondiabetics and T1D patients equally [94], while others rather opt for an inconclusive cause-effect relationship [95]. On the contrary, other studies indicate that meal-derived glucose appearance in these patients does not differ from their healthy counterparts at either normoglycemia or hyperglycemia over 400 mg/dL [96], which indicates no association between postprandial hyperglycemia and delayed gastric emptying. Explanations on the differences in gastric emptying include fasting BG levels, the meal composition (proportion of the macronutrient content), size and energy content, with the latter in particular having a strong correlation and low inter-individual variability [97]. In nondiabetics, there seems to be a strong relationship between the GI value and rate of gastric emptying [98] which seems to indicate that the differences in gastric emptying is not caused by BG levels but the food composition *per se*.

To represent delay in gastric emptying and meal-derived glucose appearance, we consider a

[2] total of 70 g of glucose solution throughout 120 min of exercise
[3] 3 g per minute with a total of 350 g glucose

Table 3.2: Time-constant parameters of carbohydrate digestion/absorption in the present model for representative staple foods with varying GI values and a sugary drink, with their respective time-constant delay τ_{dg}.

FOOD	**GI**	t_1	t_2	t_3	t_4	τ_{dg}
Instant potato	83	0.99	15.1	38.0	15.4	34.5
White bread	71	1.07	14.6	32.3	14.6	54.5
Pineapple juice	46	1.30	12.8	22.5	12.6	0.5
Spaghetti	41	2.28	8.7	12.2	9.8	95.6
Pearled barley	25	–	–	–	–	142.4

first-order delay function as

$$\frac{\mathrm{d}G_{\text{ext}}(t)}{\mathrm{d}t} = \frac{1}{\tau_{\text{dg}}}\left(\overline{G}_{\text{EQ}}(t) - G_{\text{ext}}(t)\right), \tag{3.23}$$

where $G_{\text{ext}}(t)$ is the output of the carbohydrate metabolism subsystem, $\overline{G}_{\text{EQ}}(t) = \overline{G}_{\text{RAG}}(t) + \overline{G}_{\text{SAG}}(t)$ is total glucose equivalent from carbohydrates and τ_{dg} is the food-specific time delay of carbohydrate digestion in T1D patients. The physiological representation of gastric emptying delay in Eq. (3.23) refers to the additional time required for the chyme to mobilize from the stomach to the duodenum, and thus should rather be considered before the division into its RAG and SAG components. Nevertheless, we first build RAG and SAG absorptions and thence add a gastric emptying delay to maintain the clarity in the definition of RAG and SAG and facilitate the calculation of parameters related to Ra_{max}.

The food-specific value of τ_{dg} is determined by minimizing

$$Q_1[\max(G(t_i)) - \max(\hat{G}(t_i))]^2 + Q_2 \sum_{i=1}^{n} E^2(i), \tag{3.24}$$

where $E(i) = G(t_i) - \hat{G}(t_i)$ is the difference between BG in the present model $G(t_i)$ and clinical data $\hat{G}(t_i)$ from [85] measured at t_i from 0 to 240 min at 30-min intervals ($n = 9$). The value of τ_{dg} for each food and sugary drink is calculated with $Q_1 = 1$ and $Q_2 = 1$ and given in Table 3.2.

3.2 Modified model of subcutaneous rapid-acting insulin effect

Some models are thoroughly validated with clinical data from nondiabetic subjects, which is arguably one of the principal causes of inaccuracy in the mathematical representation of their hypoglycemic effect. In active pancreatic β-cell function, endogenous insulin is rapidly mobilized through the portal vein towards the liver before reaching peripheral tissue for GLUT-4 activation and glucose uptake. In contrast to this, exogenous insulin is distributed throughout peripheral tissues before reaching the liver for insulin clearance (although also occurs in muscle and adipose tissue in a lesser degree). The clearly difference in insulin pathways between endogenous and exogenous insulin have thus to be considered for an appropriate representation of the effect of SC insulin on BG levels in patients with T1DM in particular.

3.2.1 Insulin pharmacokinetics (PK) and pharmacodynamics (PD)

For an accurate representation of the effect of exogenous insulin on BG levels, it is first important to differentiate insulin pharmacokinetics (PK) and pharmacodynamics (PD). The pharmacokinetics of insulin comprise the absorption process, the distribution (including binding) and its ultimate degradation and excretion. For instance, after a SC bolus administration, an insulin depot is formed below the SC tissue from which insulin is slowly degraded by action of SC enzymes until its distribution as free plasma insulin, which is directly measurable from plasma insulin concentration. The complexity in the representation of insulin kinetics includes the presence of circulating insulin-binding antibodies [99] among other factors. In this way, insulin pharmacokinetics describe the time-course of insulin absorption kinetics, including a large number of complex biochemical reactions in the process in inaccessible (non-measurable) conditions.

Compared to this, insulin pharmacodynamics describe the physiological effect of insulin on glucose metabolism, *i.e.,* activation of the receptor GLUT-4 for glucose uptake, in addition to its relationship with plasma insulin concentration. Although direct measurement is not possible due to inaccessibility to tissues and membranes, the effect *per se* is quantified by its biopotency. Therefore, although insulin PK and PD are closely related, they essentially seek to represent different characteristics of insulin.

3.2.2 Glucose Infusion Rate (GIR) as insulin PD

Due to our particular interest in an accurate mathematical representation of the actual hypoglycemic effect of rapid-acting insulin on BG levels, we contemplate the utilization of clinical data of glucose infusion rate (GIR) for such purpose. In this method, a single insulin bolus administration at $t = 0$ is accompanied with a continuous variable IV glucose infusion such that BG levels are maintained at normoglycemia until complete bolus insulin absorption several hours afterwards. In this way, GIR represents the insulin time-action profile, *i.e.,* a time-course of the BG lowering effect of insulin. Clinical data of insulin pharmacokinetics and GIR for a variety of types of insulin formulations including rapid-acting insulin [100] clearly shows the existence of a delay and extended effect in time-action profile compared to plasma insulin levels for all types of insulin formulations.

In previous mathematical models of glucose-insulin metabolism in T1DM, accurate models of SC insulin kinetics, *i.e.*, representation of insulin PK, are coupled with models of glucose kinetics without further consideration and validation of the actual hypoglycemic effect of insulin, *i.e.*, insulin PD. In the present study, we consider Shimoda insulin model for the sake of simplicity, and re-validate its original model parameters to represent insulin PD instead while maintaining the original structure.

3.2.3 Shimoda insulin model adapted to insulin PD

In the present subsection we consider Shimoda insulin model which comprises compartments x_1, x_2 and I, and the remote-insulin compartment of Bergman minimal model X for parameter adjustment of rapid-acting insulin PK/PD with consideration of a provisional input $u_{\mathrm{i}}(t)$ in plasma insulin compartment given by Eq. (2.7) to represent IV insulin administration. The purpose of model re-identification is to obtain an authentic representation of insulin PD, *i.e.*, the hypoglycemic effect of subcutaneous rapid-acting insulin on BG levels. For a genuine representation of insulin kinetics from subcutaneous insulin absorption to plasma insulin appearance and its ultimate hypoglycemic effect through the aforementioned compartments, the identification of model parameters is divided into three steps as follows (see Figure 3.5):

1. *IV insulin PK and PD:* Parameters of I and X are identified from IV data of GIR [101] for an input in the provisional IV input $u_{\mathrm{i}}(t)$ to obtain a more accurate representation of IV insulin PD compared to the original Shimoda and minimal model parameters (see Figure 3.6).

2. *SC insulin PK:* With fixed parameters of compartment I and X, subcutaneous insulin PK

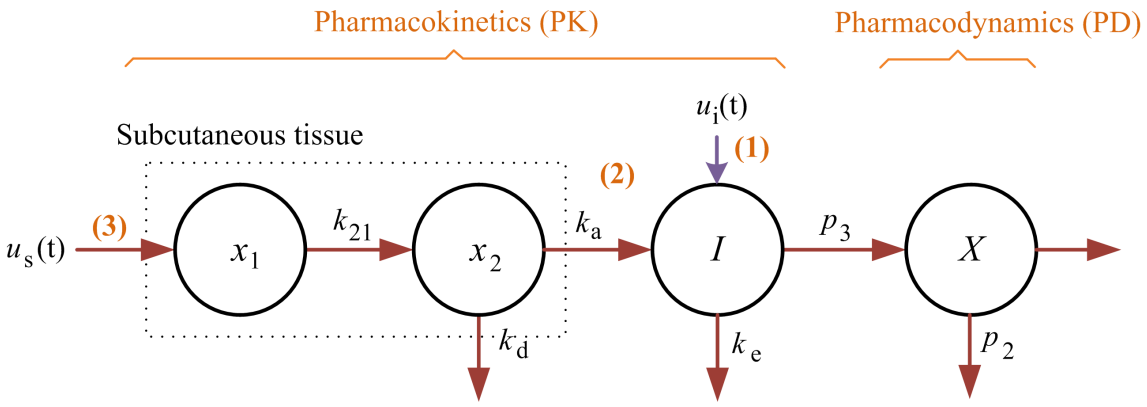

Figure 3.5: Parameter identification of Shimoda SC insulin model and remote insulin compartment of Bergman minimal model using clinical data of (1) IV insulin PK+PD, (2) SC insulin PK, and (3) SC insulin PK+PD.

in compartments x_1 and x_2 are identified from clinical data [102] for an insulin bolus input in $u_s(t)$. Compared to the original Shimoda model parameters (see Figure 3.7), the parameters of the present study for rapid-acting insulin resembles clinical data more accurately.

3. *SC insulin PK+PD:* Although having a complete identification of model parameters, we verify the accuracy to represent subcutaneus insulin PD for an input in $u_s(t)$ with GIR data for SC insulin [103]. Compared to the original Shimoda and minimal model parameters (see Figure 3.8), the present study effectively represents the hypoglycemic effect of SC insulin administration.

Therefore, SC rapid-acting insulin absorption kinetics from Shimoda *et al.* [104] maintains the original structure given in Eqs. (2.5)−(2.6), although parameters are modified as given in Table 3.3 for an accurate representation of rapid-acting insulin PK/PD validated from clinical data.

Rapid-acting insulin is the standard insulin type for prandial insulin bolusing due to its fast PK/PD, with the three commercially available brands being insulin lispro or Humalog (Eli Lilly, USA), insulin aspart or Novolog (Novo Nordisk, Denmark) and insulin glulisine or Apidra (Sanofi, France). Even though each of these rapid-acting insulin formulations have different DNA-recombinant modifications to the molecular structure of human insulin, all of them share similar PK/PD profiles [105] and thus can be used interchangeably in the present model.

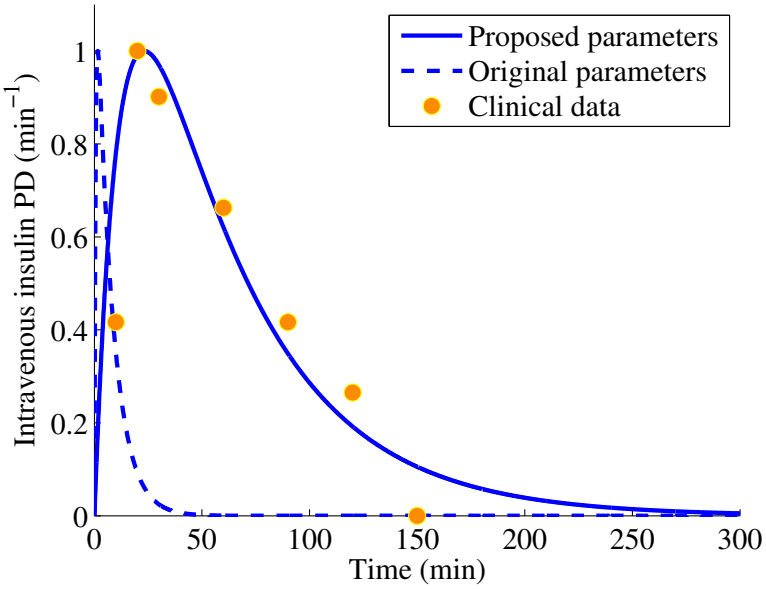

Figure 3.6: Comparison of the proposed model parameters for IV insulin PK+PD with corresponding clinical IV data of GIR from Sekigami *et al.* [101].

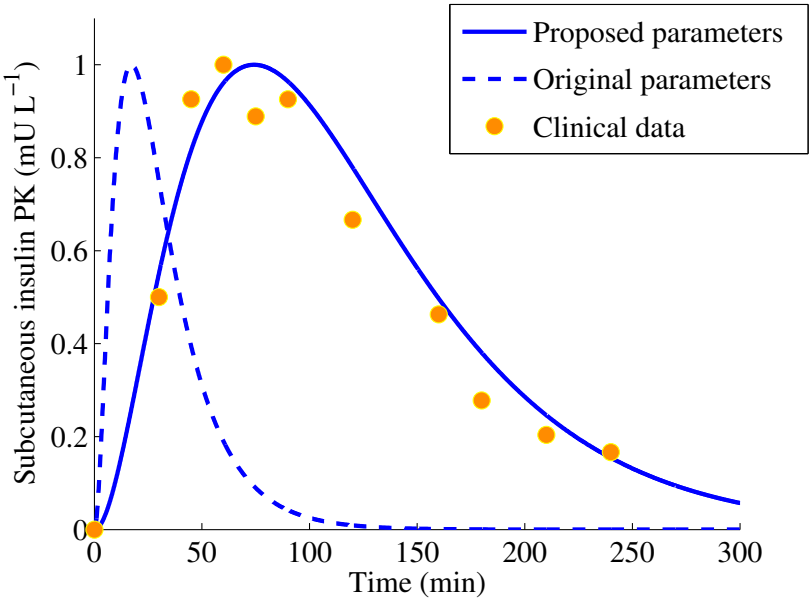

Figure 3.7: Comparison of the proposed model parameters for SC insulin PK with corresponding clinical data from Heinemann *et al.* [102].

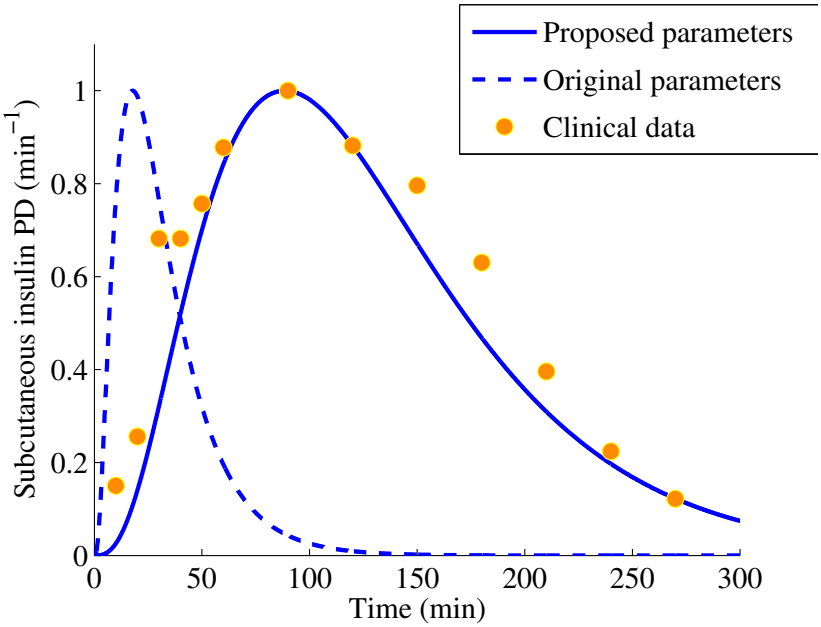

Figure 3.8: Comparison of the proposed model parameters for SC insulin PK+PD with corresponding clinical data from Swan *et al.* [103].

Table 3.3: Proposed model parameters in Bergman minimal model and Shimoda insulin model for an accurate representation of subcutaneous insulin PK/PD in patients with T1DM.

$p_2 = 8 \times 10^{-2}$ min^{-1}	$p_3 = 10 \times 10^{-6}$ L min^{-2}
$k_{21} = 4.5 \times 10^{-2}$ min^{-1}	$k_\mathrm{a} = 2.0 \times 10^{-2}$ min^{-1}
$k_\mathrm{e} = 2.0 \times 10^{-2}$ min^{-1}	$k_\mathrm{d} = 2.1 \times 10^{-3}$ min^{-1}
$V_\mathrm{d} = 4.5 \times 10^{-2}$ L	

3.3 Proposed model of postprandial glucose-insulin metabolism

Among several mathematical models developed to date, the main advantage of Bergman minimal model is arguably its simplicity in the representation of plasma glucose-insulin dynamics with the fewest number of parameters for model identification. To have a valid extension of the minimal model to T1DM, it is necessary to consider several physiological similarities and differences, and their mathematical representation as detailed as follows.

3.3.1 Bergman model adapted to T1DM

The main characteristic of T1DM is the absence of endogenous insulin secretion, which causes an abnormal elevation of BG levels to hyperglycemia. In the minimal model, however, such state cannot be adequately represented by simple inspection in Eq. (3.25) under absence of insulin from the interstitial compartment $X(t) = 0$. Thus, the purpose is to represent T1DM in the minimal model with minimal alteration—and yet maintaining the physiological interpretation—of the original model reproduced as follows

$$\frac{\mathrm{d}G(t)}{\mathrm{d}t} = -X(t)G(t) + p_1\left(G_\mathrm{b} - G(t)\right) + \frac{G_\mathrm{ext}(t)}{V_1}, \tag{3.25}$$

where $G_\mathrm{ext}(t)$ is the meal-derived exogenous rate of glucose appearance as proposed in the first part of the present chapter.

3.3.2 Glucose effectiveness

Glucose effectiveness in the minimal model as developed by Bergman *et al.* represents the ability of glucose *per se* to perform glucose disposal and suppress endogenous glucose production under basal conditions. Although insulin-mediated glucose uptake is considered the main metabolic pathway for glucose removal, it is estimated that up to 50% of the glucose disposal after an oral glucose tolerance test (OGTT) is due to glucose effectiveness [106]. The minimal model, in particular, has been criticized for the overestimation of post-meal glucose effectiveness after glucose or meal tolerance tests [107, 108].

Studies on the minimal model and its accuracy to represent glucose metabolism in patients with T1DM using the Biostator showed that parameter estimation was in excellent agreement with clinical data, whereas only basal insulin infusion in the same patients with T1DM resulted in an overestimation of glucose effectiveness [109]. Similarly, other studies [110] using an IVGTT without incremental insulin (only basal insulin according to the strict definition of S_G)

showed that clinical data of glucose effectiveness was poorly predicted by the minimal model even though minimal model parameters for patients with T1DM are lower than their nondiabetics counterparts with values of 0.013 ± 0.004 min^{-1} vs 0.021 ± 0.002 min^{-1}, respectively.

It is thus clear that the minimal model does not accurately reflect glucose kinetics in patients with T1DM under the same parameter evaluation as in nondiabetics. Glucose effectiveness is defined in the minimal model (nondiabetics) as a 'measure of the capacity of glucose to mediate its own disposal at basal insulin levels', which is the case of patients with T1DM is gradually deteriorated with the progression of the disease, although some detectable β-cell activity in long-standing patients is also present [111]. Although artificial infusion of basal insulin is included for the estimation of S_{G} by definition, the inability to represent glucose effectiveness appropriately is evident by the results in the aforementioned clinical studies.

We consider that other factors particularly specific to patients with T1DM are not being considered, such that the fact that these patients have increased EGP during basal conditions with secretion rates depending on the quality of their management [112]. During postprandial state, also, there seems to be an over-production of glucagon (hyperglucagonemia) after a meal load [113]. In this way, to represent T1DM state using the minimal model, we propose a minor conceptual modification of parameter G_{b} to represent basal glucose levels with no exogenous basal insulin infusion conditions. By doing so, the physiological representation of glucose effectiveness S_{G} is no different to that of the original minimal model for $G(t) > G_{\mathrm{b}}$, while the enhanced hepatic glucose production—due to absent endogenous insulin secretion—is also represented for $G(t) < G_{\mathrm{b}}$. The nonlinear component $X(t)G(t)$ for insulin-dependent glucose uptake remains unaltered.

In the glucose compartment of the minimal model, the non-insulin mediated glucose balance (assuming absence of exogenous insulin $X(t) = 0$) is given by

$$G(t) = (G(0) - G_{\mathrm{b}})\, e^{-S_{\mathrm{G}} t} + G_{\mathrm{b}}, \tag{3.26}$$

where glucose dynamics depends on the values of G_{b} and S_{G}. Because of the difficulty to assess G_{b} under insulin absence conditions, we rather consider steady-state conditions as

$$S_{\mathrm{G}} = \frac{X_{\mathrm{ss}} \cdot G_{\mathrm{ss}}}{G_{\mathrm{b}} - G_{\mathrm{ss}}}, \tag{3.27}$$

$$= \frac{p_2 \cdot V_{\mathrm{d}} \cdot k_{\mathrm{e}} \cdot (G_{\mathrm{b}} - G_{\mathrm{ss}}) \cdot (k_{\mathrm{d}} + k_{\mathrm{a}})}{G_{\mathrm{ss}} \cdot p_3 \cdot k_{\mathrm{a}} \cdot u_{\mathrm{b}}(t)}, \tag{3.28}$$

from which S_{G} can be determined from G_{b} and a continuous basal insulin infusion $u_{\mathrm{b}}(t)$.

3.4 Simulation

In the present section, we simulate the model of glucose-insulin metabolism from carbohydrates in T1DM proposed in the present chapter and validate it with clinical data of postprandial BG excursion after consumption of carbohydrate-rich foods with GI values throughout the range as represented by instant potato, white bread, spaghetti and pearled barley, in addition to pineapple juice to represent a sugary drink as well.

3.4.1 Simulation settings

We simulate a single-meal with AvCHO $=$ 50 grams of carbohydrates as $G_{\text{meal}}(t) = 50 \cdot \delta(t)$ for each representative carbohydrate-rich food with respective parameters of GI, RAG and SAG specified in Table 3.1, in addition to Table 3.2 for time-constant parameters considering a constant maximum rate of meal-derived glucose appearance $\text{Ra}_{\text{max}} = 0.9$ g/min regardless of the specific food to be consumed. Considering parameters in Table 3.3 for subcutaneous insulin PK and PD as proposed in the present model, a prandial single-bolus dose of $u_{\text{s}}(0) = 7$ IU/min is administered simultaneous with meal at $t = 0$ considering a continuous basal insulin infusion $u_{\text{s}}(t) = 0.0186$ IU/min to maintain fasting BG levels at 90 mg/dL, which is similar to the basal insulin regimen of 1.2 IU/h in the only patient under insulin pump therapy in [114]. Parameters to represent T1DM in the glucose compartment of the minimal model in Eq. (3.25) are $p_1 = 0.001$ min^{-1} and $G_{\text{b}} = 300$ mg/dL (16.67 mmol/L).

3.4.2 Maximum rate of exogenous glucose appearance

Simulation of glucose-equivalent digestion/absorption from carbohydrates considering maximum rate of glucose appearance Ra_{max} is shown in Figure 3.9 for a very high GI food (instant potato). The large RAG content in instant potato causes a maximum glucose-equivalent absorption of $>$3 g/min in $G_{\text{EQ}}(t)$, which is restrained to 0.9 g/min by considering Ra_{max}. To maintain the total glucose equivalent (AUC of $G_{\text{EQ}}(t)$) effectively constant, the maximum absorption Ra_{max} is maintained until t_3 according to Eq. (3.22).

3.4.3 Postprandial BG excursion for varying GI values

Simulation of postprandial BG excursion after ingestion of several types of foods with constant carbohydrate amount AvCHO $=$ 50 g and insulin bolus is shown in Figure 3.10 considering clinical data from 8 patients with T1DM (3 male and 5 female, 36.7$\pm$7.1 years old, body mass

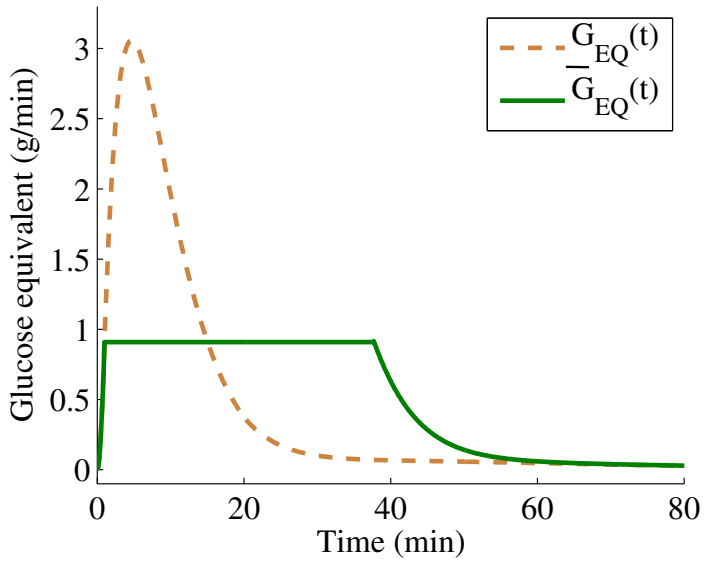

Figure 3.9: Glucose-equivalent of carbohydrates $\overline{G}_{\text{EQ}}(t)$ and $G_{\text{EQ}}(t)$ with and without maximum rate of glucose appearance $\text{Ra}_{\text{max}} = 0.9$ g/min, respectively.

index (BMI) 23.8±1.4 kg/m^2 and HbA1c 7.2±0.5%) [85]. The postprandial BG peak typical in high GI foods (instant potato and white bread) are accurately represented as well as BG excursion during late postprandial state. Medium and low GI foods (spaghetti and pearled barley, respectively) are also accurately represented for late postprandial BG excursion, although the modest peak at $t = 30$ min cannot be properly replicated. Furthermore, simulation of a sugary drink is shown in Figure 3.11 for 50 g of pineapple juice and comparison with clinical data from patients with T1DM. The postprandial BG peak has a legitimate representation, even though the excursion for $t > 100$ min starts to diverge increasingly until late postprandial state.

3.5 Discussion

In the present study we propose a mathematical model of glucose-insulin metabolism from carbohydrates in patients with T1DM, which is built from already existing models of SC insulin kinetics and glucose-insulin metabolism, in addition to an original proposal for carbohydrate digestion/absorption. Model parameters are adjusted to increase the accuracy of the compartmental model without altering their original structure. Further discussion is elaborated in the following.

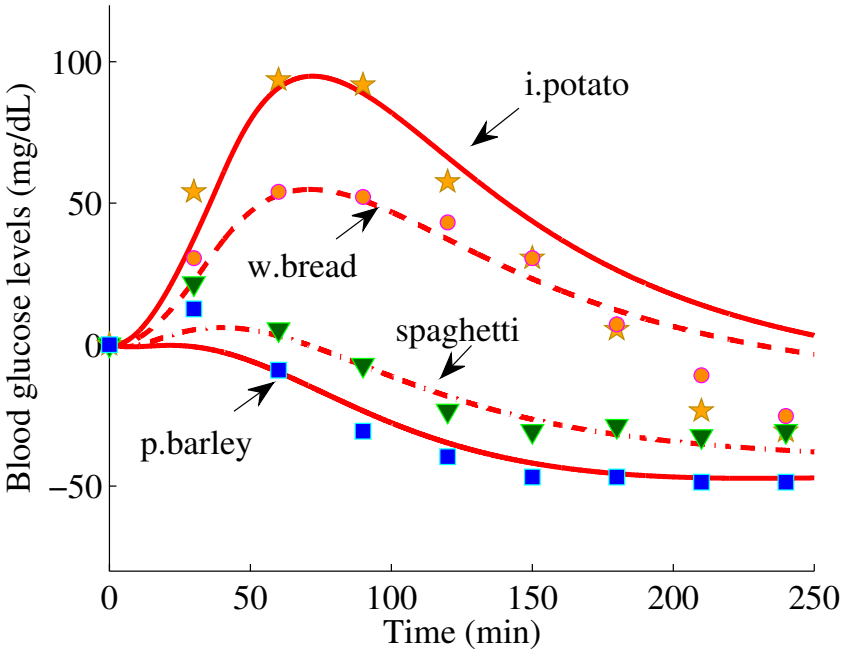

Figure 3.10: Simulation of postprandial BG excursion after consumption of 50 grams of carbohydrate-rich foods with varying GI values considering a SC single-bolus of $u_{\mathrm{s}}(0) = 7$ IU and constant basal insulin infusion $u_{\mathrm{s}}(t) = 0.0186$ IU/min. Comparison with clinical data from 8 T1DM patients (3 male and 5 female, 36.7±7.1 years old, BMI 23.8±1.4 kg/m^2, HbA1c 7.2±0.5%) from Mohammed *et al.* [85].

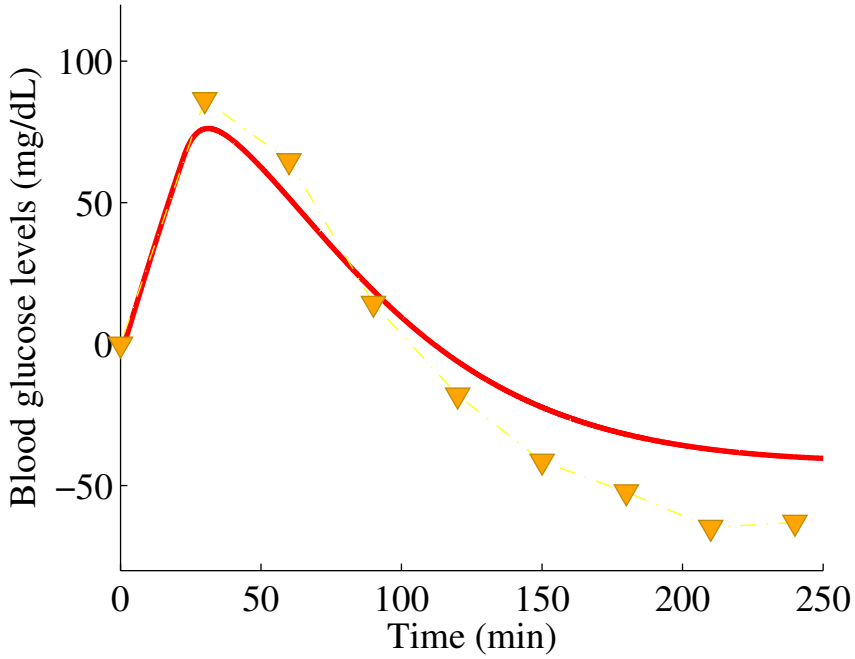

Figure 3.11: Simulation of postprandial BG excursion after consumption of a sugary drink with equivalent 50 grams of starch (sucrose) and SC single-bolus of $u_s(0) = 7$ IU with constant basal insulin infusion $u_s(t) = 0.0186$ IU/min. Comparison with clinical data from 8 T1DM patients (3 male and 5 female, 36.7±7.1 years old, BMI 23.8±1.4 kg/m^2, HbA1c 7.2±0.5%) from Mohammed *et al.* [85].

- *Utilization of GI, RAG and SAG as model parameters*
  To our knowledge, this is the first mathematical model of carbohydrate digestion and absorption that includes food-specific model parameters for GI and carbohydrate availability to obtain an accurate representation of the glycemic impact of a meal. These concepts were developed independently from one another in the research areas of clinical nutrition and food chemistry, respectively, and as such, are conceptually different. The former is an *in vivo* methodology that quantifies the impact of different types of carbohydrates on BG levels and inherently includes all physiological factors—both known and unknown—associated with gut transit, whereas the latter relies on *in vitro* conditions to quantify the amount of glucose release from carbohydrates according to its biochemical properties. Even though there seems to be a close relationship between the GI and RAG values of carbohydrate-rich foods [84, 115], both methodologies have different approaches that are equally employed as model parameters in the present study. Compared to previous mathematical models with a notorious nonlinear complexity (see Figure A.2), in the present model RAG and SAG absorption are represented as two second-order linear differential equations whose sum has an interestingly 'nonlinear' shape. In this way, we demonstrate the feasibility to develop an accurate yet simple representation of exogenous glucose absorption from carbohydrates as observed in clinical studies [116].

- *Gastric emptying delay τ_{dg}*
  In addition to parameters for GI, RAG and SAG, a first-order delay with time constant τ_{dg} is also included in the model of carbohydrate digestion/absorption. It could be argued that because of the specific time span for RAG and SAG absorption by definition and the *in vivo* assessment of the GI value, additional delays need not be considered. However, RAG and SAG parameters represent *in vitro* glucose release in the gut, which excludes additional delays due to carbohydrate break-down by gastric enzymes and glucose delivery from the lower stomach to the small intestine such as glucose transport across the epithelium. Indeed, previous studies [117] that compared the Englyst method with actual *in vivo* gastric emptying and portal glucose appearance show a strong correlation with *in vivo* gastric emptying provided an additional time-delay adjustment for *in vitro* values, which in our model is represented by the time constant τ_{dg}.

- *Gastric emptying and hyperglycemia*
  Previous studies suggest an association between gastric emptying and BG levels, with a marked delay in gastric emptying at even mild hyperglycemia of 144 mg/dL (8 mmol/L) in both diabetics and healthy subjects [94]. As an explanation, the gastric motor mech-

anism involved in hyperglycemia-induced gastric emptying delay is associated with a reduction of antral pressure and duodenal motility [93], although the magnitude and gastric emptying rate is yet to be elucidated. These studies suggest that τ_{dg} should be a function that includes BG levels instead of a food-specific parameter. Nevertheless, patients with T1DM seem to suffer from an impaired hyperglycemia-induced delay in gastric emptying [118], which might be restored to rates comparable to that of nondiabetics after *pramlintide* administration. Some others report an inverse relationship between gastric emptying and postprandial BG increments in T1DM between 0–180 mg/dL (0–10 mmol/L) [119]. These mixed results prevent the development of a mathematical association between BG levels and gastric emptying delay in the present study.

- *Effectiveness in combining GI, RAG and SAG to represent gut absorption*
  An additional advantages of including both GI and RAG/SAG for the representation of meal-derived exogenous glucose appearance in the present model is the ability to compute the different impact of foods with the same GI value but different RAG/SAG proportion. Such difference can be observed in clinical studies with nondiabetics [120], although it could not be properly validated in our model due to absence of clinical data for similar test meals in patients with T1DM. Even though the present model provides such advantage, the utilization of several parameters (for GI, RAG and RAG) also increases the number of sources of model errors. For instance, in the simulation of the present model we consider the GI value of 41 for spaghetti provided by Mohammed *et al.* [85] coupled with values of 15/9 for RAG/SAG obtained from Englyst *et al.* [80] Compared to this, a study by Jenkins *et al.* [121] indicates that the GI value for white spaghetti and wholemeal spaghetti are 51 and 42, respectively, with RAG/SAG parameters for wholemeal spaghetti of 18.1/9.4 [83]. Hence, it might be difficult to determine the exact combination of parameter values for the GI values and RAG/SAG as they usually have to be determined from different studies and might be considered as a source of model error in carbohydrate absorption parameters.

- *Maximum rate of glucose appearance Ra_{max}*
  Although the consideration of a maximum rate of glucose appearance $\mathrm{Ra}_{\mathrm{max}}$ increases the complexity of the present model, we determined it to be indispensable due to its direct effect on the impact of carbohydrates on postprandial BG levels, especially for high GI food and/or large carbohydrate amounts. The present model is validated with foods with only regular carbohydrate amount of 50 g that result in a glucose appearance rate fairly above $\mathrm{Ra}_{\mathrm{max}} = 0.9$ g/min. However, we contemplate that very large carbohydrate loads with high and even medium GI values lead to prolonged exogenous glucose appearances and

rebound in BG levels several hours after meal consumption as observed in clinical tests. Very high carbohydrate loads are then expected to further validate the utility of Ra_{max} in the present model. Furthermore, we also contemplate the possibility that actual exogenous rate of glucose appearance be food-specific instead of a constant value of Ra_{max} as proposed in the present study. In nondiabetics, maximum rate of glucose appearance reaches a different plateau value with approximately 2.5 mg/kg·min and 4 mg/kg·min, respectively, after consumption of 50 g of white bread and pasta [122]. Although the same differences still need to be elucidated for T1DM patients in particular, the significance of parameter Ra_{max}, at least for the representative foods in the present model for a regular amount, is demonstrated.

- *Representation of liquids (sugary drink)*
  The present model is not only able to simulate solids but also the impact of liquids (pineapple juice) as well without requiring additional compartments or parameters as in previous mathematical models. Different from starchy foods, the carbohydrate content of pineapple juice mainly consists of sucrose, which in turn is composed of glucose and fructose in an approximately equal ratio between 0.84–1.1 whether *in vitro* [123] or *in vivo* [124]. Since fructose is well known for not eliciting insulin secretion, among other metabolic differences from glucose [125], a carbohydrate intake of 25 g is considered appropriate in the simulation. Because of the increasing amount of foods with added natural/artificial sweeteners in the western diet, further consideration of Pg (proportion of carbohydrate absorbed as glucose), as considered by Mohammed *et al.* [85], can be eventually included in the present model.

- *Shimoda model and representation of subcutaneous insulin effect*
  The sole purpose of the representation of SC insulin kinetics in the present model is to provide an accurate representation of the time-action profile of rapid-acting insulin. For this reason, the simplicity of Shimoda insulin model is more appealing than more detailed and complex mathematical representations such as Wilinska model, which considers the differences in absorption kinetics between single bolus and continuous insulin infusion [126]. Contemplating the continuous development of novel insulin formulations in the market, parameter identification is also an important issue that needs special consideration with the advent of ultra-rapid acting insulin formulations in the upcoming years [127]. Because of the simplicity of Shimoda model, we could also propose a simple procedure for identification of model parameters from clinical data of insulin PK/PD from IV and SC bolus insulin administration.

- *Variability in insulin absorption*
  Sources of variation in SC insulin absorption—and consequently its hypoglycemic effect—include ambient temperature, injection site, dosage [128] and increased insulin sensitivity due to acute exercise [129]. Although these factors should ideally be considered, they not only increase the complexity of the model but also require additional input parameters to indicate each specific conditions. Furthermore, since model parameters of the present model are validated with a set of clinical data—from both i.v. and s.c. insulin administration routes—, re-validation of model parameters would require data for each of the aforementioned sources of insulin variability. As a future research topic, however, the SC insulin compartment of the present model might eventually include methods for model validation considering variability sources for an improved accuracy in the representation of insulin time-action profile under a number of circumstances.

- *Bergman minimal model and glucose-insulin metabolism in T1DM*
  The glucose compartment in Eq. (3.25) remains intact since the maintenance of the original model structure is one of the main priorities for the specific representation of glucose-insulin metabolism in patients with T1DM. Although more complex multi-compartmental glucose models include specific physiological processes such as EGP and renal glucose disposal, the main factors that influence glucose dynamics are arguably meal-derived exogenous glucose appearance and hepatic glucose production. Both of them, in addition to insulin-mediated glucose uptake, are neatly considered in Bergman model. In this way, given the advantages of a minimal approach for model-based BG control purposes, simulation results show that the minimal model provides an accurate representation provided the modification of parameter G_{b} as in our proposal.

3.6 Concluding remarks

In the present chapter we proposed a novel model of glucose-insulin metabolism from carbohydrates in patients with T1DM. Differences in absorption rate of carbohydrates are represented by considering food-specific parameters based on absorption rate indices GI, RAG and SAG, in addition to a single gastric emptying delay. The present model not only demonstrates that an accurate representation of the impact of carbohydrate-rich meals on BG levels in patients with T1DM is possible, but it can be achieved utilizing a simple representation using previously developed minimal model with adequate parameter settings for a legitimate physiological representation of carbohydrate gut transit, as well as glucose and insulin metabolism specifically in these patients.

Chapter 4

Semi closed-loop BG control algorithm in T1DM for prandial state

The inherent difficulty to maintain postprandial normoglycemia is a strong drive for the development of diurnal AP systems considering their previous success in overnight closed-loop BG control [130, 131]. Although most in-development AP systems utilize either Hovorka or Dalla Man models, in addition to an ever-increasing level of complexity in the control algorithm, clinical results show only acceptable results [132] that do not satisfy current recommendations for BG management in T1DM from the ADA (see Table 4.1). In the previous chapter, we proposed a novel mathematical model of glucose-insulin metabolism in T1DM for prandial BG control purposes because of its ability to represent the impact of carbohydrates with different absorption rates on BG levels with a minimal model representation which is particularly advantageous

Table 4.1: Recommendations for BG management in T1DM by the ADA [42], including the most strict BG management for pregnancy.

Period	**BG range mg/dL (mmol/L)**
Fasting plasma BG	70–130 (3.9–7.2)
Peak postprandial BG	<180 (<10.0)
Premeal/overnight (pregnancy)	60–99 (3.3–5.4)
Peak postprandial glucose (pregnancy)	100–129 (5.4–7.1)

to minimize the computational burden of BG control algorithms.

Because of the apparent inability of current BG control systems in the literature—whether *in silico* testing or clinical trials—to deal with rapid meal-derived glucose appearance after meal consumption, in the present chapter we will determine *in silico* the feasibility of tight prandial BG control. For simplicity, first only ideal conditions and minimal safety restrictions for the patient are considered, and then the most important sources of variability and model error are considered to assess the performance of the control algorithm under a number of scenarios. Despite continuous improvements in BG control algorithms, some studies point out that one of the main difficulties that prevent a truly tight prandial BG control is the absence of a reliable mathematical model of the impact of meals on BG levels [133]. Hence, the model-based control algorithm proposed in the present chapter utilizes the mathematical model of glucose-insulin metabolism in T1DM developed in the previous one, which provides an accurate representation of the impact of representative carbohydrate-rich foods with different absorption rates. Moreover, since we believe the slow absorption kinetics of subcutaneous insulin administration route is one of the main impediments to achieve tight diurnal BG control, we consider a control strategy based on meal announcement and pre-meal insulin administration (as either continuous infusion or single-bolus) with unrestricted dosage and start in insulin infusion. The *in silico* assessment in the present study concedes us the opportunity to determine the feasibility of tight prandial BG control without additional concern for patient safety, especially due to the extremely elevated risk of severe hypoglycemia—as observed in previous studies in the literature—due to the aggressive control approach necessary to maintain postprandial normoglycemia. Depending on the degree of success in the present *in silico* study, we contemplate an eventual clinical implementation of the present control in actual patients with T1DM in clinical trials.

In the present chapter we first introduce some issues related to prandial BG control from previous studies in the literature, which are taken into consideration to delineate the structure of the control strategy utilized. Thence, we provide a detailed explanation of the preprandial insulin optimization algorithm considering either continuous insulin infusion or single-bolus administration. Since we utilize MPC for maintenance of postprandial BG levels at the target value, we include a concise description of its theoretical scheme prior its application in the present study. *In silico* assessment of the present control algorithm includes computer simulations for the nominal case considering both continuous and single-bolus preprandial insulin administration for the ideal case, in addition to sources of variability due to patient-model mismatch and meal consumption related to intake and actual mealtime. Lastly, we include further discussions and concluding remarks at the end of the present chapter.

4.1 Proposed BG control algorithm with meal announcement (intake and GI)

First we consider some issues related to prandial BG management and previous control approaches in the literature, which are briefly summarized as follows.

4.1.1 Considerations for prandial BG control

Different from overnight control, prandial BG control algorithms require a prompt response of the actuator (insulin infusion system) to rapid fluctuations in BG levels due to a large meal-derived glucose appearance. Nevertheless, they are still unattainable by current in-development AP system, whose performance does not comply with clinical recommendations from the ADA (see Table 4.1 on page 58). To strictly satisfy these clinical recommendations for postprandial BG levels in patients with T1DM, we first examine previous control strategies in the literature, the obstacles encountered and a number of relevant issues as carefully considered in the following.

- **Start of prandial insulin infusion**
  Current medical recommendations from the ADA advise administration of prandial insulin immediate before meal consumption or within 15 min in advance in order to prevent hypoglycemia due to the rapid absorption of insulin [134]. Recent clinical studies on bolus insulin timing, however, suggest that 15 min [135] and even 20 min [136] prior to mealtime contribute to a relative reduction in postprandial BG levels. In fact, clinical evaluation of recent prandial closed-loop BG control algorithms [137] consider a manual bolus 15 min prior to mealtime among different bolus administrations types, wherein such hybrid control showed no sign of postprandial hypoglycemia despite the early bolus administration, although large peaks in postprandial BG levels were still present.

  We hypothesize that the optimal start in preprandial insulin infusion depends on the absorption rate of the food to be consumed, with higher GI values in particular requiring an earlier start in insulin infusion to curb the rapid increase in BG levels, whereas low GI foods need not a preprandial insulin infusion as early as high GI counterparts because of its slow meal-derived glucose appearance. Although it might be highly debatable from a medical vantage point due to the elevated risk of severe hypoglycemia, we contemplate a start of preprandial insulin infusion as early as necessary in order to satisfy ADA recommendations. Moreover, the start time in prandial BG control should ideally remain

fixed at the same time regardless of the type of food to be consumed for consistency in the control strategy utilized.

- **Exogenous insulin administration routes**
  Although subcutaneous insulin administration route is most widely utilized in closed-loop BG control systems, alternative routes have been also proposed and implemented, including IV and intraperitoneal routes [60]. In terms of insulin absorption velocity, IV route presents the shortest delay, followed by intraperitoneal and SC insulin routes. Regarding safety and practicability, IV insulin route presents the least reliability for an eventual wearable AP and intraperitoneal route requires a surgical procedure for its initial implant and eventual re-operation within a few years due to complications or battery end-of-life [138]. In this way, SC administration route is the least invasive of all, even though its slow subcutaneous absorption kinetics is arguably the principal reason for the current inadequate performance of closed-loop prandial BG control algorithms.

- **Single/Dual hormonal infusion (insulin/glucagon)**
  Besides insulin infusion, an alternative approach considers the utilization of both insulin and glucagon, where the latter is only instantaneously infused in cases of impending hypoglycemia. Compared to open-loop insulin pump treatment, bi-hormonal AP systems show a reduction of BG levels from 159±30 mg/dL (8.83±1.67 mmol/L) to 133±13 (7.39±0.72 mmol/L) in adults and 157±27 mg/dL (8.72±1.5 mmol/L) to 138±18 mg/dL (7.67±1 mol/L) in adolescents [139]. However, disadvantages of glucagon utilization include solution instability, some side-effects including nausea and constipation, and reported general discomfort during clinical trials of bi-hormonal AP systems [140]. Even though glucagon is explicitly dismissed as the cause by the authors of the study, to our knowledge no similar symptoms have been reported in single-hormone AP systems in the literature. In fact, the very same symptoms are commonly found in clinical studies utilizing glucagon doses over 1 g in nondiabetics [141]. Considering the commercial development of AP systems in the future, a double infusion kit for insulin and glucagon sensors and respective pumps (see Figure 1 in [142]) not only would increase the burden to the patient but also the additional cost of the system. Because there seems to be no substantial difference in the time spent in the normoglycemic range for dual- and single-hormone AP systems [143] or overnight hypoglycemic events [144], the present study considers only a single-hormone control approach.

- **Meal announcement or automatic meal detection**
  Theoretically, an AP system should be able to detect meal ingestion automatically and

infuse the appropriate bolus insulin without any interference from the patient. For this, the control algorithm relies on meal detection algorithms, although none of them is able to achieve tight prandial BG control. Another alternative often utilized is hybrid control, wherein a manual 15-min insulin bolus prior to mealtime with a carbohydrate load of 1 g/kg body weight (58–75 g) was able to maintain postprandial BG levels below 400 mg/dL (22.22 mmol/L) [137]. However, it was not sufficient to meet the goals of the ADA to mantain postprandial BG levels below 180 mg/dL for over 75% of the cases. Still, both meal announcement and hybrid control approaches undoubtedly result in more time being spent in range than fully automated closed-loop control systems [145]. Other non-algorithmic approaches to reduce glycemic excursion in BG control algorithms include infusion of pramlintide prior to each meal [146], which together with a fully closed-loop BG control strategy, postprandial BG levels >220 mg/dL for breakfast and >180 mg/dL for lunch and dinner were achieved. Recently, the effect of pramlintide on postprandial glucose metabolism in patients with T1DM specifically include gastric emptying delay and inhibition of glucagon without noticeable alteration in total nor hepatic insulin sensitivity [147].

- **Target BG levels**
  Previous BG control algorithms with meal announcement include target BG levels of 180 mg/dL [148] in order to prevent hypoglycemic episodes due to infusion of large bolus doses, whereas bi-hormonal BG control algorithms with automatic meal detection consider target BG levels of 100 mg/dL due to the availability of a glucagon infusion system to recover from imminent hypoglycemia [149]. In accordance to the objectives of the present study, the target value to aim for is, according to clinical recommendations in Table 4.1, 100 mg/dL (5.56 mmol/L) independently of the control strategy utilized.

- **Performance assessment**
  Regardless of the fact that the number of closed-loop BG control algorithms for *in silico* and clinical trials have increased considerably in recent years, standardized methods for performance assessment of BG control algorithms have not been established. This includes the BG range defined as 'normoglycemia' and the specific meal intake or glucose challenge upon which the definition of 'successful' prandial BG control is determined. BG values at which hypoglycemia is defined are also arbitrarily determined among different studies, ranging from $\leq$70 mg/dL (3.89 mmol/L) to $\leq$50 mg/dL (2.78 mmol/L). Recently, a control-variability grid analysis was proposed as a tool to interpret large data in an easy-to-identify manner [150] as a graphical assessment of the performance of BG

control systems. In such proposal, BG levels are divided in 9 zones with ranges of minimum and maximum BG levels between 50–100 mg/dL and 110–140 mg/dL respectively. Alternatively, another study [151] proposes a grading system divided in 6 ranges (from A to F) depending on the level of control achieved for the assessment of its efficacy and safety. As the objective of the present study is to assess the degree of tight postprandial BG control, *i.e.*, maintenance of post-meal BG levels within the recommended range 100% of the time, the aforementioned performance assessment based exclusively on BG excursion are temporarily excluded.

4.1.2 Prandial insulin infusion strategy

Considering the above issues related to prandial BG control and the recommendations for BG management in patients with T1DM from the ADA (see Table 4.1 on page 58), we contemplate that preprandial insulin administration for the insulin infusion strategy is inevitably necessary, and it can be only achieved by a BG control algorithm with meal announcement. Therefore, in the present study, mealtime is defined at 0 (see Figure 4.1) for reference purposes, from which prandial state is defined from an initial time (defined as <0) before mealtime in order to include preprandial insulin administration, until a final time several hours afterwards wherein postprandial BG excursion is expected to be completely stabilized at the target BG value. In this way, the prandial BG control strategy proposed in our study comprises (1) computation of the adequate continuous subcutaneous insulin throughout the prandial state provided meal information (carbohydrate amount and specific food) to be consumed at mealtime, which is therefore effectively infused until mealtime at 0, and immediately followed by an (2) automatic switch to closed-loop MPC until the final time, wherein BG levels are completely stabilized at the target BG value. Alternatively to continuous subcutaneous insulin infusion, we consider the case of preprandial single-bolus administration (see Figure 4.2) in order to assess the advantages of preprandial insulin bolusing under the current insulin therapy for T1DM. Such instantaneous bolus is given at a specific instant between the *initial* time and 0, even earlier than 20 min pre-meal—as suggested by clinical studies—if necessary, as determined by the optimization algorithm. For either preprandial bolus type, the same postprandial MPC-based BG control is used to provide for basal insulin needs. In the following subsections, we elaborate on the insulin optimization computed in (1) and postprandial MPC control strategy in (2).

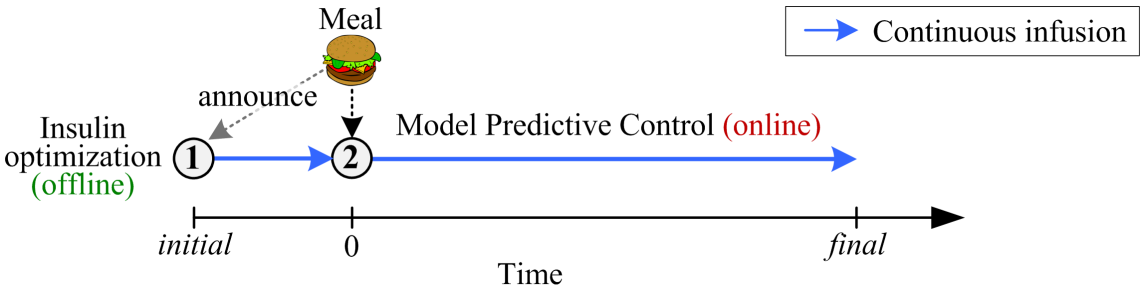

Figure 4.1: Insulin infusion strategy for the prandial BG control algorithm in the present study. (1) At the initial time, an insulin optimization algorithm is computed offline using the mathematical model proposed in the previous chapter provided information of carbohydrate amount and specific food to be consumed at mealtime, and effectively infused until 0. (2) At mealtime, the control algorithm switches to closed-loop MPC for the remaining of the prandial state to guarantee complete stabilization of BG levels at the target value.

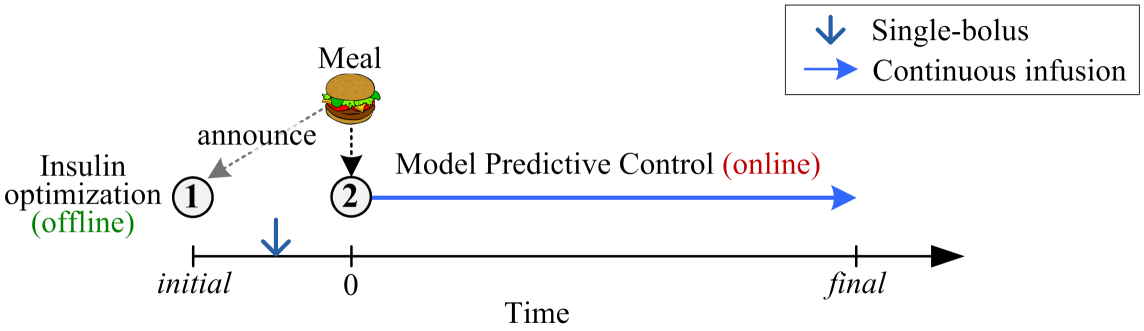

Figure 4.2: A preprandial single-bolus administration as a substitute of variable preprandial bolus insulin infusion in Figure 4.1 is considered to assess the benefits of preprandial bolus insulin.

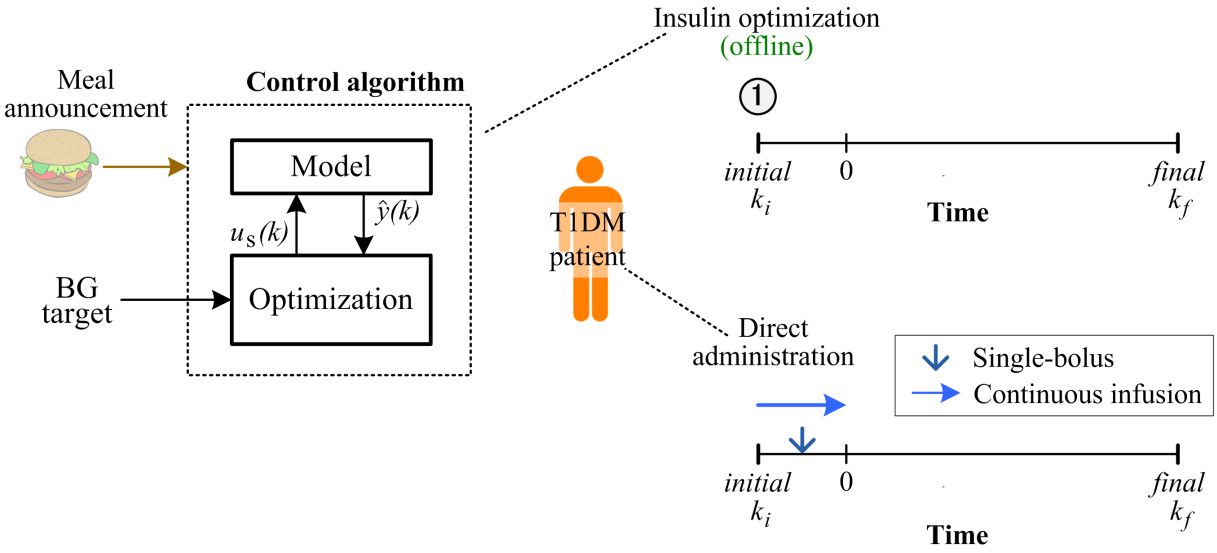

Figure 4.3: Preprandial insulin optimization is computed at the start of the prandial state (top right) utilizing the mathematical model developed in the previous chapter (left) for either continuous preprandial insulin infusion or single-bolus (independently from one another). Only after the optimization problem is solved, it is effectively administered by single-bolus or continuous infusion until mealtime at 0 (bottom right).

4.1.3 Preprandial bolus insulin optimization: continuous/single-bolus

As shown in Figure 4.3, preprandial insulin infusion is determined from an optimization problem at the start of the prandial state utilizing the mathematical model of glucose-insulin metabolism in T1DM from carbohydrates detailed in the previous chapter for prediction of postprandial BG excursion. For the mathematical connotation in the present BG control algorithm, we consider time-steps in discrete time intervals $t = k\Delta t$ with $k = k_i, k_i - 1, ..., 0, ..., k_f - 1, k_f$. From this we define the start and final instants that delimit prandial state by k_i and k_f, respectively, and predicted BG levels in discrete-time from the model given by $\hat{y}(k)$ as utilized by the optimization algorithm. After the optimization problem is solved, it is effectively infused to the patient (see Figure 4.3, bottom right) until mealtime at $k = 0$.

The optimization problem to solve is given in Eq. (4.1) as

$$\begin{aligned} \underset{\{u_{\mathrm{s}}(k)\}}{\text{minimize}} \quad & J_{\text{opt}} \\ \text{subject to} \quad & 0 \leq u_{\mathrm{s}}(k) \leq U_{\text{pre}}, \qquad k < 0 \\ & 0 \leq u_{\mathrm{s}}(k) \leq U_{\text{post}}, \qquad k \geq 0, \end{aligned} \tag{4.1}$$

considering U_{pre} and U_{post} as the maximum preprandial and postprandial insulin infusions, respectively, and the cost function J_{opt} given by

$$J_{\text{opt}} = \sum_{i=0}^{k_f - k_i} Q(E(k_i + i \mid k_i)) \cdot E^2(k_i + i \mid k_i) + \sum_{i=k_i}^{k_f} R\, \Delta u_{\mathrm{s}}^2(i), \tag{4.2}$$

where $E(k_i + i \mid k_i) = \hat{y}(k_i + i \mid k_i) - W_{\text{REF}}$ is the deviation of the estimated output $\hat{y}(k_i + i \mid k_i)$ from the target BG value W_{REF}, $\Delta u_{\mathrm{s}}(i) = u_{\mathrm{s}}(i) - u_{\mathrm{s}}(i-1)$ is insulin rate of change and Q, R are weighting matrices for BG deviation and insulin rate of change, respectively. To differentiate the instants at which the predicted variables are computed with respect to the referential step, the connotation $\hat{y}(k + i \mid k)$ is utilized to refer to the predicted BG value at $k + i$ in the future calculated at the instant k. In particular, the estimated output $\hat{y}(k_i + i \mid k_i)$ utilizes the mathematical model developed in the previous chapter according to the amount of carbohydrates and GI value of the meal to be consumed, and the value of the weight gain Q also depends on the difference between predicted BG levels and the target W_{REF} as

$$Q(E) = \begin{cases} Q, & E \geq 0 \\ Q_{\text{LO}}, & E < 0 \end{cases}, \tag{4.3}$$

where $Q_{\text{LO}} > Q$ to prevent postprandial hypoglycemia.

For the calculation of single-bolus preprandial administration, we consider the cost function J_{1b} instead, given by

$$J_{\text{1b}} = \sum_{i=0}^{k_{f\text{1b}} - k_i} Q(E(k_i + i \mid k_i)) \cdot E^2(k_i + i \mid k_i), \tag{4.4}$$

where bolus administration can be effective from $k = k_i$ to 0 (mealtime) with only positive

insulin bolus doses being allowed and that single-bolus insulin administration is by definition:

$$u_{\mathrm{s}}(t) = \begin{cases} U_{\mathrm{B}}, & k = k_{\mathrm{bolus}} \\ 0, & \text{otherwise.} \end{cases} \tag{4.5}$$

The optimization problem for preprandial single-bolus administration is given by

$$\begin{aligned} \underset{\{u_{\mathrm{s}}(k)\}}{\text{minimize}} \quad & J_{1\mathrm{b}} \\ \text{subject to} \quad & U_{\mathrm{B}}(k) \geq 0, \\ & \text{Eq. (4.5).} \end{aligned} \tag{4.6}$$

from which the single-bolus dose U_{B} and instant $k = k_{\mathrm{bolus}}$ are determined.

4.1.4 Postprandial BG control with Model Predictive Control (MPC)

Along with the stat of meal consumption at $k = 0$, the present control algorithm automatically switches to closed-loop BG control based on MPC (see Figure 4.4). This control strategy basically utilizes real-time information of current BG levels from the patient at k-intervals for an iterative computation of insulin by the control algorithm—which in turn utilizes an optimization algorithm that relies on a mathematical model for prediction of BG levels—and respective infusion to maintain BG levels at the target value indicated to the controller. The predictive capabilities of MPC are briefly described as follows.

At a given instant k (see Figure 4.5), the optimization algorithm first computes the future BG excursion $\hat{y}(k)$ using a mathematical model of glucose-insulin metabolism in T1DM. Considering also a dynamic reference trajectory $w(k)$, the cost function of the optimization problem calculates the difference between $\hat{y}(k)$ and $w(k)$ over a predetermined 'Prediction horizon' within a span defined by N_1 and N_2. Each candidate insulin dose over a range from 0 to a maximum U_{post} is evaluated at ΔU increments to determine the optimal insulin dose that minimizes the cost function of the optimization problem. Furthermore, the control horizon N_{u} specifies the number of time-steps ahead in the prospective continuous variable insulin dose until $k + N_{\mathrm{u}}$, considering that a larger value resulting in a smoother control at the expense of increased computational cost.

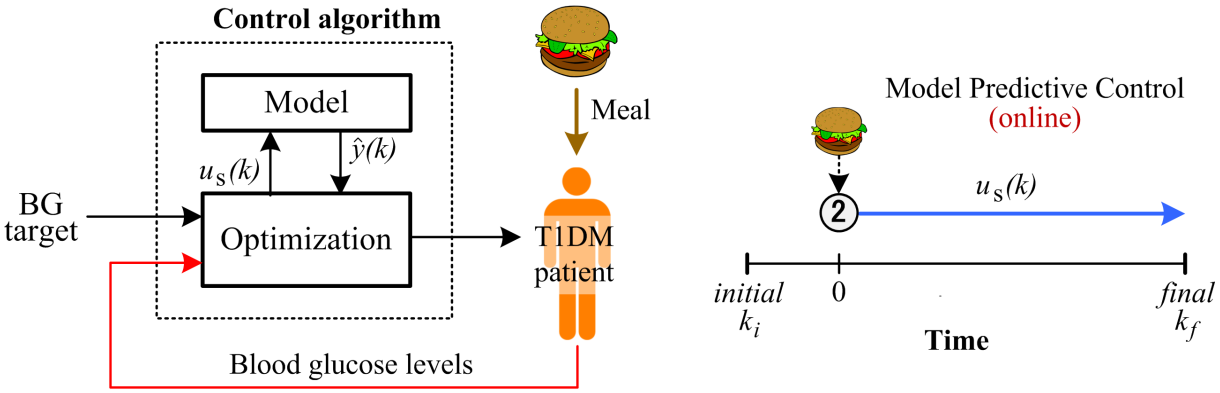

Figure 4.4: At $k = 0$ (mealtime), the control algorithm switches to closed-loop MPC to stabilize postprandial BG levels towards the normoglycemic target BG value indicated to the controller.

After infusion of the optimal insulin $u_s(k)$, the next step $k + 1$ becomes the 'new' k and control variables including real-time BG levels from the T1DM patient are updated to repeat the same optimization algorithm. The same process is iteratively computed for the subsequent steps until k_f according to the concept of receding horizon control.

The cost function of the MPC algorithm is given by

$$J_{\text{MPC}} = \sum_{i=N_1}^{N_2} Q(e) \cdot e^2(k+i \mid k) + \sum_{i=0}^{N_u-1} R\, \Delta u_s^2(k+i), \tag{4.7}$$

where the weight matrix $Q(e)$ also follows Eq. (4.3), N_1 and N_2 are the prediction horizon, N_u is the control horizon and $e(k+i \mid k) = \hat{y}(k+i \mid k) - w(k+i \mid k)$ is the deviation of the predicted BG levels $\hat{y}(k+i \mid k)$ from the dynamic reference trajectory $w(k+i \mid k)$, which in turn is given by

$$w(k+i \mid k) = \alpha^i w(k \mid k) + (1-\alpha^i) W_{\text{REF}}, \qquad i = N_1, ..., N_2 \tag{4.8}$$

considering $w(k \mid k) = G(k)$ as the initial value of the reference trajectory and convergence rate constant $0 < \alpha < 1$.

The optimization of the postprandial MPC control is given by

$$\begin{aligned} &\underset{\{u_s(i)\}}{\text{minimize}} \quad J_{\text{MPC}}(k) \\ &\text{subject to} \quad 0 \le u_s(i) \le U_{\text{post}}, \qquad k \le i \le k + N_u \end{aligned} \tag{4.9}$$

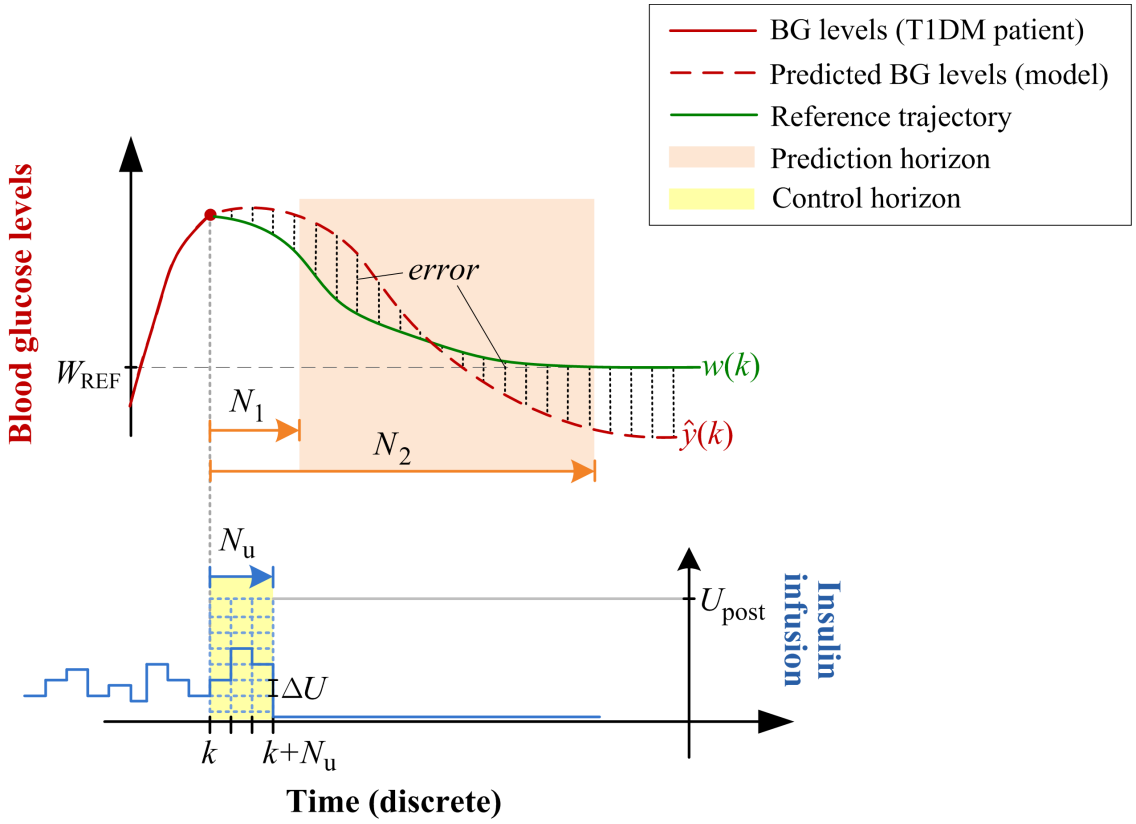

Figure 4.5: Illustrative representation of the MPC strategy for postprandial closed-loop BG control in the present study. At the current time k, each candidate insulin dose from $u_s = 0$ to U_{post} is evaluated using the cost function in Eq. (4.7) wherein the difference (error) between the model-predicted BG levels $\hat{y}(k)$ and the reference trajectory $w(k)$ are computed from $k = N_1$ to $k = N_2$ at k-intervals. For a control horizon $N_u > 1$, not only the current $u_s(k)$ but also future moves up to $u_s(k + N_u)$ are considered in the computation of the total cost.

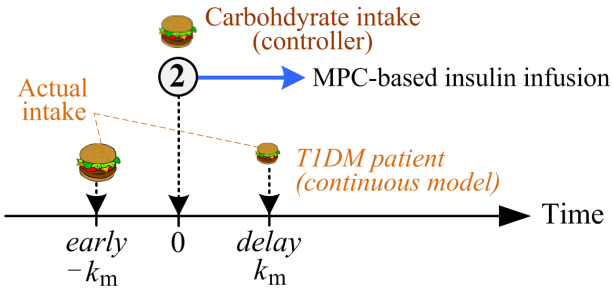

Figure 4.6: To assess the performance of the present BG control algorithm under food-related uncertainties, we consider deviations in the actual mealtime k_m in combination with miscalculation of carbohydrate intake AvCHO in the T1DM patient (continuous model) with respect to the meal announcement information given to the controller at k_i. Advanced and delayed mealtime in the patient are represented by $k_m < 0$ and $k_m > 0$, respectively, whereas the originally expected mealtime is maintained at $k = 0$ in the controller.

from which the online optimal insulin is obtained iteratively from the solution of Eq. (4.9) and administered to the patient at Δt intervals from $k = 0$ to k_f.

4.1.5 Intra-individual variability and meal-related uncertainty

The nominal case represents the ideal scenario wherein the mathematical model of the controller and the actual patient—represented by a continuous-time T1DM patient model in our study—have an exact patient-model match. Additionally, the same meal information of carbohydrate amount and GI value given to the control algorithm at k_i is effectively consumed at $k = 0$. Nevertheless, since there exists a diurnal variation in the glucose-insulin metabolism in the patients themselves that introduce small differences in the mathematical representation, we consider intra-patient variability of insulin sensitivity due to continuous same-tissue utilization [103] with variation in parameter p_3 of the minimal model for the continuous-time patient model. Additionally, we include food-related uncertainties due to differences in reproducibility of the GI value [152, 153] and miscalculations in the total carbohydrate amount (AvCHO) in Eq. (3.3), as well as the exact mealtime in the input $G_{\text{meal}}(t)$ for the patient model (continuous time) represented by $t < 0$ or $t > 0$ for advanced or delayed mealtime (see Figure 4.6) while maintaining mealtime at $k = 0$ in the controller.

4.1.6 Clinically-relevant parameters

Parameter values of the present control algorithm must have a delicate balance between aggressiveness and safety such that the control algorithm not only has an adequate performance but also guarantees patient safety against hypoglycemia. First, the rapid BG variation throughout the prandial state requires a short interval between BG measurements, and thus we consider $\Delta t = 1$ min adequate as often utilized in BG control systems for prandial state [68, 154]. Initial time for the prandial BG control strategy in the present study is $k_i = -60$ considering that the time-to-maximum biopotency of rapid-acting insulin is 1–2 hours and thus the computation of preprandial insulin and respective infusion 60 min prior to mealtime provides sufficient time margin to contain post-meal hyperglycemia. For the final time, we estimate that $k_f = 440$ is an adequate value for complete stabilization of BG levels. Target BG is set to $W_{\text{REF}} = 100$ mg/dL (5.56 mmol/L) according to clinical recommendations from the ADA (see Table 4.1 on page 4.1), even though patient safety due to hypoglycemia becomes of particular concern because of such ambitious target. Considering that the I:C ratio in non-obese T1DM adults is between 1:7 and 1:12 [155], from which instantaneous insulin bolus requirements for a regular meal of 50 g are estimated to be 4.17–7.14 IU, and thus the maximum preprandial insulin infusion rate is set to $U_{\text{pre}} = 2$ IU/min. In this way, insulin overdosing is not only prevented but a regular carbohydrate load is also guaranteed to be covered in fewer than 8 min of continuous insulin infusion at such maximum rate. For maximum postprandial closed-loop insulin infusion rate, $U_{\text{post}} = 0.05$ IU/min might be considerably above typical basal profiles [156], although such value is necessary not only to provide basal insulin but also supplementary prandial insulin for $k > 0$ particularly for low GI foods because of their characteristic slow gut absorption.

4.2 Simulation results

In this section we present simulation results of the proposed prandial BG control algorithm for four carbohydrate-rich foods with representative GI values throughout the range. We consider two bolusing patterns as (a) continuous preprandial bolus infusion coupled with postprandial MPC, and (b) preprandial single-bolus administration coupled with postprandial MPC, first for the nominal case with carbohydrate loads of 50 g and 100 g, exact patient-model matching (no model error) and effective mealtime in the T1DM patient model exactly at 0 as in the controller, in addition to intra-individual variability and food-related uncertainties as detailed in subsection 4.1.5 for a regular carbohydrate intake of 50 g. In the following, we specify simulation parameters and provide simulation results using MATLAB® R215b for each of the aforementioned cases to determine the compliance of the present semi closed-loop control algorithm with

clinical recommendations given by the ADA as specified in Table 4.1 (see page 58).

4.2.1 Simulation settings

Simulations setting for the control strategy proposed in the present study, as well as meal-related uncertainties in the T1DM patient model are detailed as follows.

- *Preprandial continuous insulin optimization*
  Parameters for the continuous preprandial insulin optimization problem in Eqs. (4.1)—(4.3) are $Q = 1$ mmol^2 L^{-2}, $Q_{\text{LO}} = 10$ mmol^2 L^{-2}, $R = 111$ mg^2 min^2 dL^2 IU^2.

- *Preprandial single-bolus optimization*
  Parameters for the single-bolus insulin optimization in Eq. (4.6) includes and unrestricted maximum dose U_{B} given at the instant k_{bolus} between k_i and 0 (limited to preprandial bolus) in Eq. (4.5), in addition to matrix weight gains of $Q = 1$ mmol^2 L^{-2} and $Q_{\text{LO}} = 10$ mmol^2 L^{-2} in the cost function in Eq. (4.4) with final time $k_{f1\text{b}} = 240$ min as an approximation of the total lasting hypoglycemic effect after a single-bolus insulin administration.

- *Postprandial MPC*
  Tuning parameters for the postprandial MPC algorithm in Eqs. (4.7)–(4.9) are $Q = 1$ mmol^2 L^{-2}, $Q_{\text{LO}} = 10$ mmol^2 L^{-2}, $R = 111$ mg^2 min^2 dL^2 IU^2, $N_1 = 30$ steps, $N_2 = 140$ steps, $N_{\text{u}} = 1$, $\Delta U = 0.005$ IU and $\alpha = 0.995$ such that the control algorithm satisfies clinical recommendations of prandial BG levels as detailed in Table 4.1. In particular, the prediction horizon defined by N_1 and N_2 is determined considering subcutaneous rapid-acting insulin PD with time-to-maximum-effect being most relevant between 30–150 min (see Figure 3.8 on page 47).

- *Mathematical model of T1DM and variability/uncertainty parameters*
  Using the mathematical model developed in Chapter 3, meal consumption is represented with an impulse signal with specific carbohydrate intake given by $G_{\text{meal}}(t) = \text{AvCHO}\,\delta(t)$ for a single meal. Model parameters for a representative patient with T1DM and carbohydrate digestion/absorption parameters for 50 g of carbohydrate intake are the same as in Chapter 3, whereas for the specific simulation of 100 g carbohydrate, model parameters for each staple food are specified in Table 4.2. Initial parameter values for the T1DM patient model at k_i for all the simulations are set to represent fasting state under basal insulin infusion such that BG levels in the patient model are maintained at 100 mg/dL (5.56

mmol/L). For intra-individual variability we consider a variation of parameter $p_3 \pm$ 20% in the continuous-time patient model, whereas for meal-related uncertainties, an early ($k_{\mathrm{m}} = -15$ min) or delayed ($k_{\mathrm{m}} = 15$ min) mealtime is indicated by $G_{\mathrm{meal}}(t) = 50 \cdot \delta(k_{\mathrm{m}})$ in Eq. (3.4) for the patient model.

4.2.2 Nominal case

For the combined preprandial continuous insulin infusion with postprandial MPC, the performance of the present BG control algorithm for nominal intake of 50 g and 100 g with GI values throughout a wide range (value in parenthesis) represented by instant potato (83), white bread (71), spaghetti (41) and pearled barley (25) is shown in Figures 4.7 and 4.8, respectively, with Table 4.3 additionally showing the total continuous preprandial insulin bolus and the start in infusion for each meal. It can be seen that BG levels are satisfactorily maintained within the narrow range of 80–140 mg/dL (4.44–7.78 mmol/L) for a carbohydrate intake of 50 g, although for 100 g of instant potato, BG levels reach the maximum limit by ADA recommendations of 130 mg/dL (7.22 mmol/L) at $t = 120$ min. For medium and low GI foods, the control strategy achieves an almost complete flat response in both 50 g and 100 g. The preprandial continuous insulin infusion pattern for the different types of foods and carbohydrate intakes seems to indicate that the start in preprandial insulin infusion is independent of the specific meal consumed.

Alternative to continuous preprandial insulin infusion, the case of a preprandial single-bolus administration calculated from the optimization problem given by Eqs. (4.4)–(4.6) coupled with the same postprandial closed-loop MPC. As shown in Figures 4.9 and 4.10 for consumption of 50 g and 100 g, respectively, preprandial single-bolus administration also satisfies clinical recommendations from the ADA. For 50 g, BG levels are maintained within the narrow range of 80–150 mg/dL (4.44–7.78 mmol/L), whereas for 100 g, BG excursion for even the highest GI food (instant potato) adheres to the recommended values from the ADA throughout the prandial state compared to the case of continuous preprandial insulin infusion. According to the solution of the optimization algorithm given by Eqs. (4.4)–(4.6), the insulin bolus necessary for each specific food, as well as the specific instant k_{bolus} has a strong dependence on the GI value beyond the total carbohydrate intake, as shown in Table 4.4 for both 50 g and 100 g.

4.2.3 Intra-individual variability

Simulation of the present BG control strategy for intra-individual variability in subcutaneous insulin absorption p_3 of 20% its nominal value for a carbohydrate intake of 50 g consumed

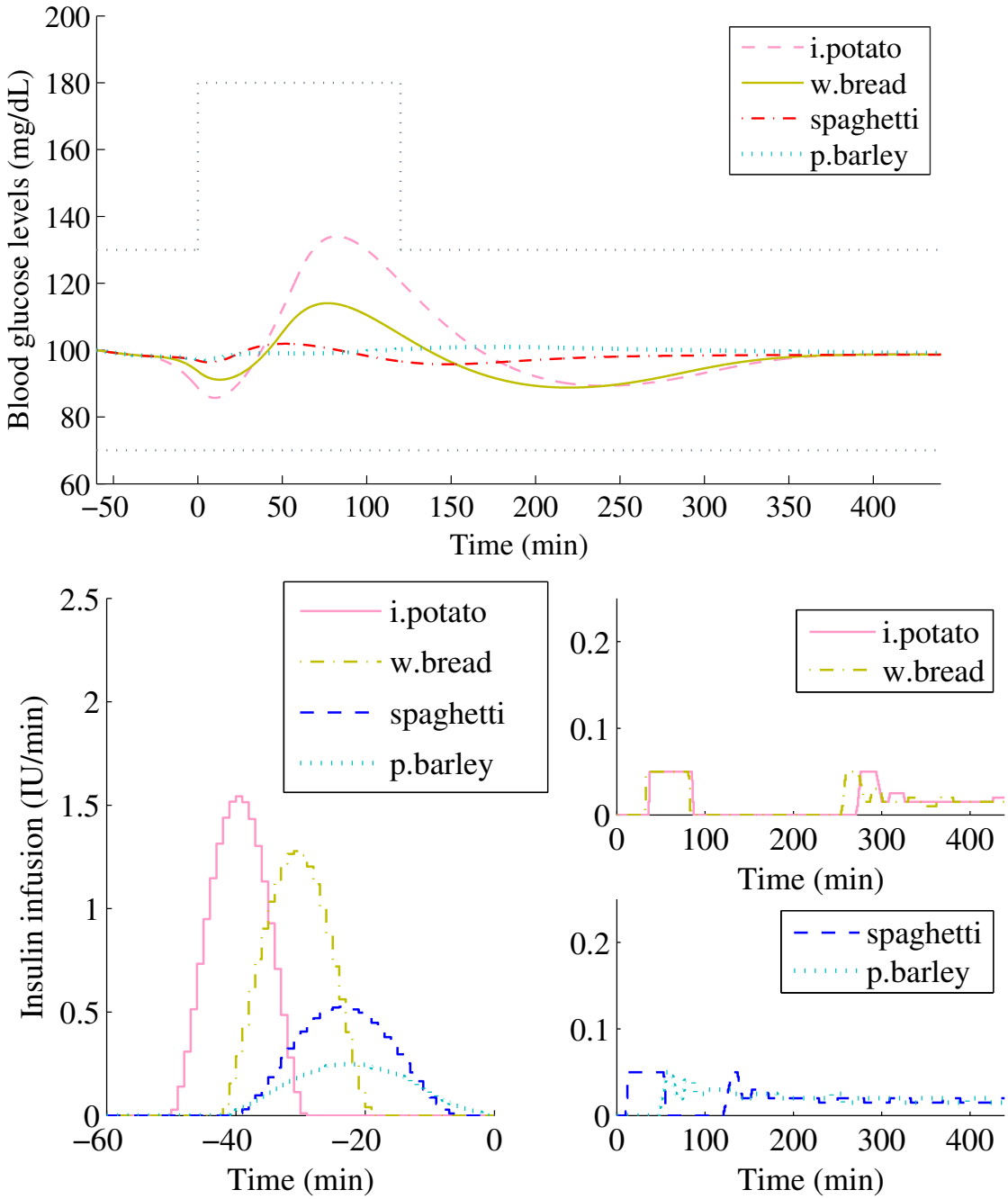

Figure 4.7: (Top) Prandial BG control response using continuous variable preprandial insulin bolus combined with postprandial MPC for the nominal case of carbohydrate intake of 50 g varying GI values (in parenthesis) represented by instant potato (83), white bread (71), spaghetti (41) and pearled barley (25) consumed at 0. Dotted lines delineate clinical recommendations of BG levels for patients with T1DM from the ADA (see Table 4.1 on page 58). (Bottom) Continuous insulin infusion from $k_i = -60$ to 0 (left) and postprandial MPC-based insulin infusion from 0 to $k_f = 440$ for high GI foods (top right), and medium/low GI foods (bottom right).

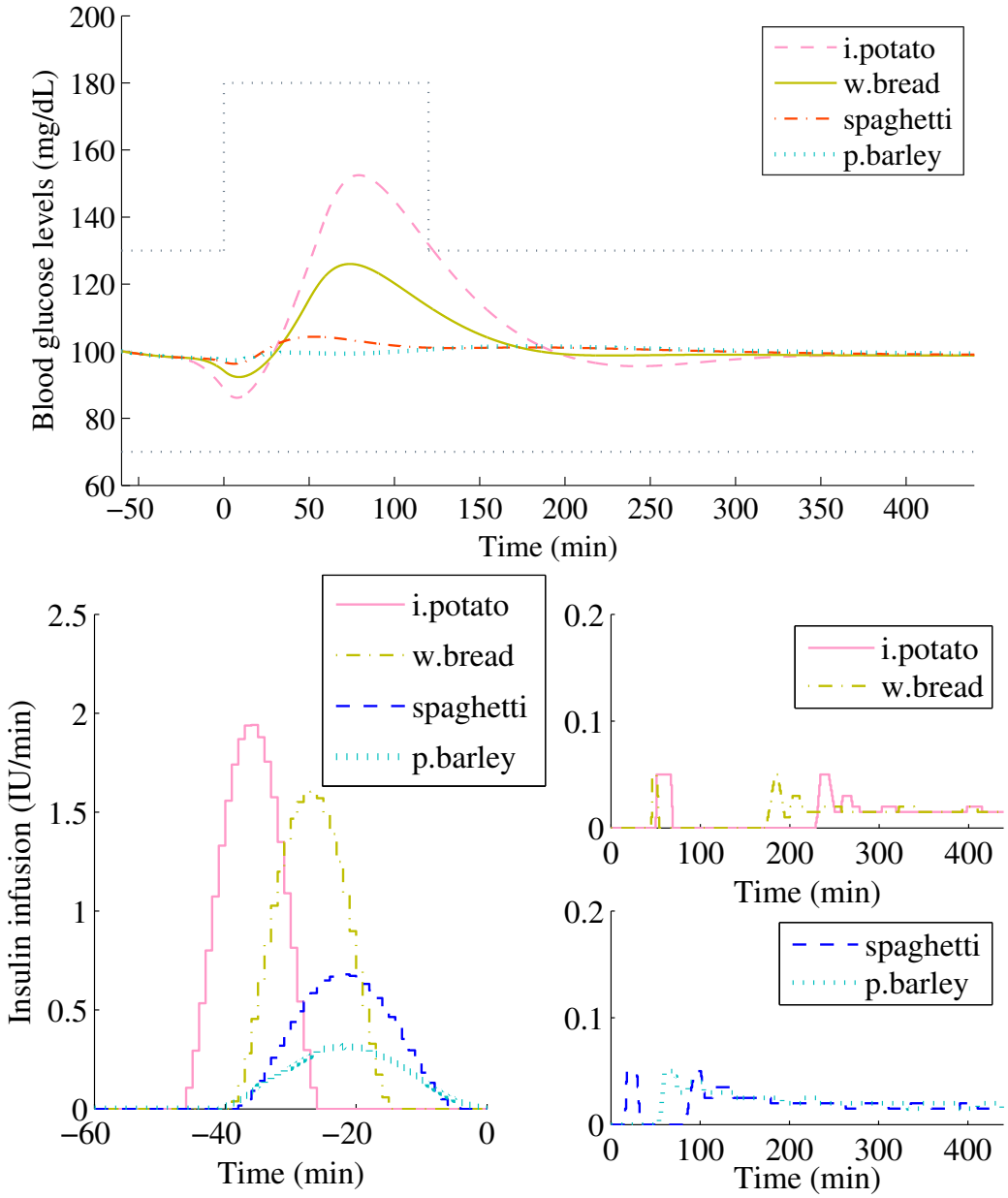

Figure 4.8: (Top) Prandial BG control response using a continuous variable preprandial insulin bolus combined with postprandial MPC for a nominal carbohydrate intake of 100 g in four meals with different GI values (in parenthesis) represented by instant potato (83), white bread (71), spaghetti (41) and pearled barley (25) consumed at 0. Dotted lines delineate clinical recommendations of BG levels for patients with T1DM from the ADA (see Table 4.1 on page 58). (Bottom) Prandial insulin infusion from $k_i = -60$ to 0 (left) and postprandial MPC-based insulin infusion from 0 to $k_f = 440$ for high GI foods (top right), and medium/low GI foods (bottom right).

Table 4.2: Time-constant parameters of carbohydrate digestion/absorption for 100 g used in the simulation of prandial BG control for a high carbohydrate load.

FOOD	**GI**	t_1	t_3	t_4
Instant potato	83	0.84	55.0	17.2
White bread	71	0.91	46.6	16.4
Spaghetti	41	1.66	17.1	12.3
Pearled barley	25	–	–	–

Table 4.3: Start in preprandial insulin infusion for 50 g and 100 g of foods with varying GI values as a solution of the optimization problem in Eq. (4.2) under nominal conditions.

		50 g		**100 g**	
FOOD	**GI**	u_s **(IU)**	**Start**	u_s **(IU)**	**Start**
Instant potato	83	17.44	−51	22.44	−54
White bread	71	16.70	−42	21.67	−46
Spaghetti	41	7.75	−40	9.88	−43
Pearled barley	25	4.79	−44	5.85	−46

Table 4.4: Preprandial single-bolus dose and administration instant k_{bolus} as the solution of the optimization algorithm given in Eq. (4.6) for the nominal case of carbohydrate loads of 50 g and 100 g with exact patient-model match and mealtime at 0.

		50 g		**100 g**	
FOOD	**GI**	U_B **(IU)**	k_{bolus}	U_B **(IU)**	k_{bolus}
Instant potato	83	16.8	−41	21.9	−37
White bread	71	15.8	−33	20.4	−29
Spaghetti	41	10.8	−18	15.0	−18
Pearled barley	25	8.0	− 1	13.1	−10

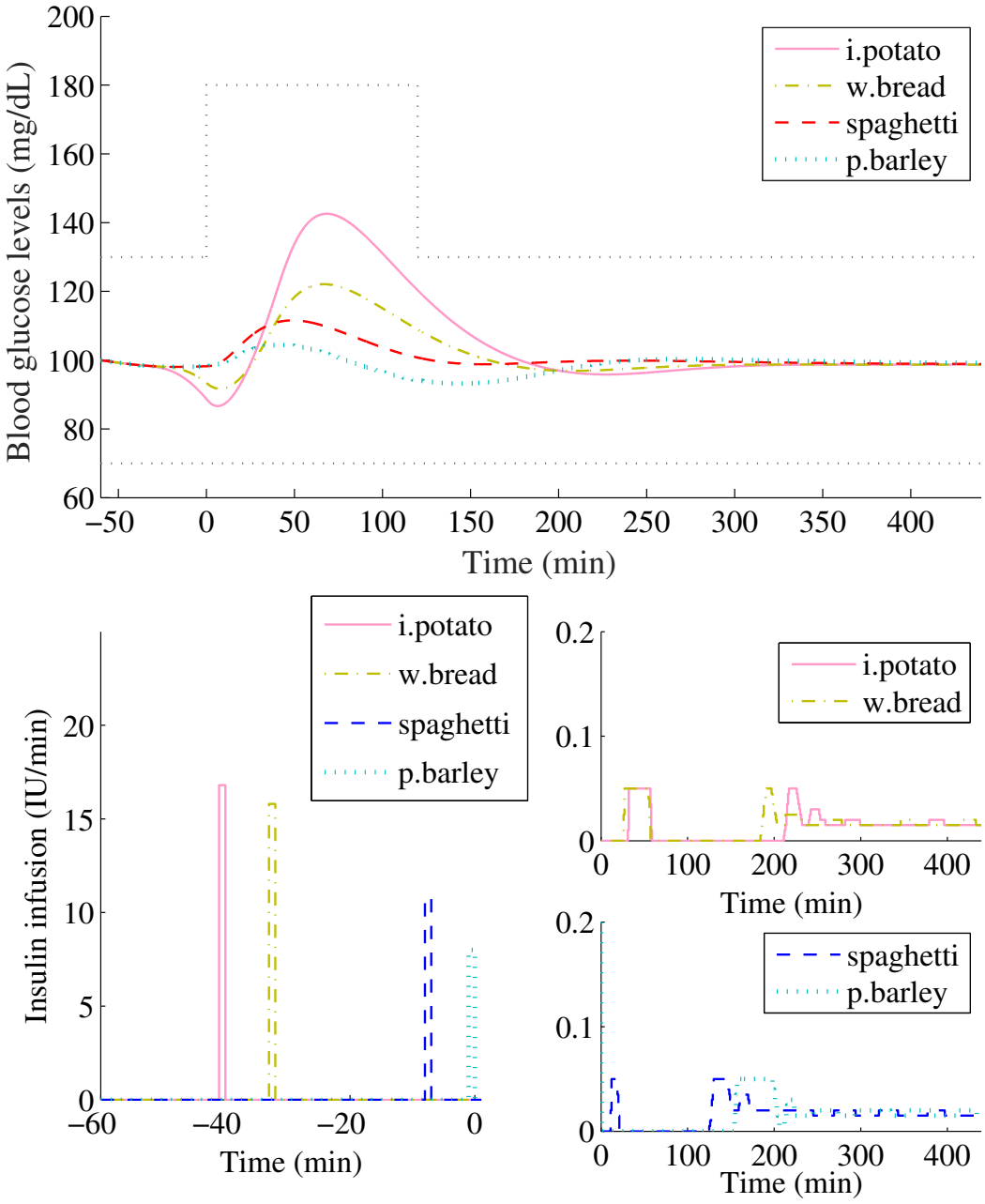

Figure 4.9: Prandial BG control response using a preprandial single-bolus insulin administration combined with postprandial MPC in the nominal case of carbohydrate intake of 50 g with varying GI values (in parenthesis) represented by instant potato (83), white bread (71), spaghetti (41) and pearled barley (25) consumed at 0. Dotted lines delineate clinical recommendations of BG levels for patients with T1DM from the ADA (see Table 4.1 on page 58). (Bottom) Preprandial single-bolus for each food according to Table 4.4. (left) and postprandial MPC-based insulin infusion from 0 to $k_f = 440$ for high GI foods (top right), and medium/low GI foods (bottom right).

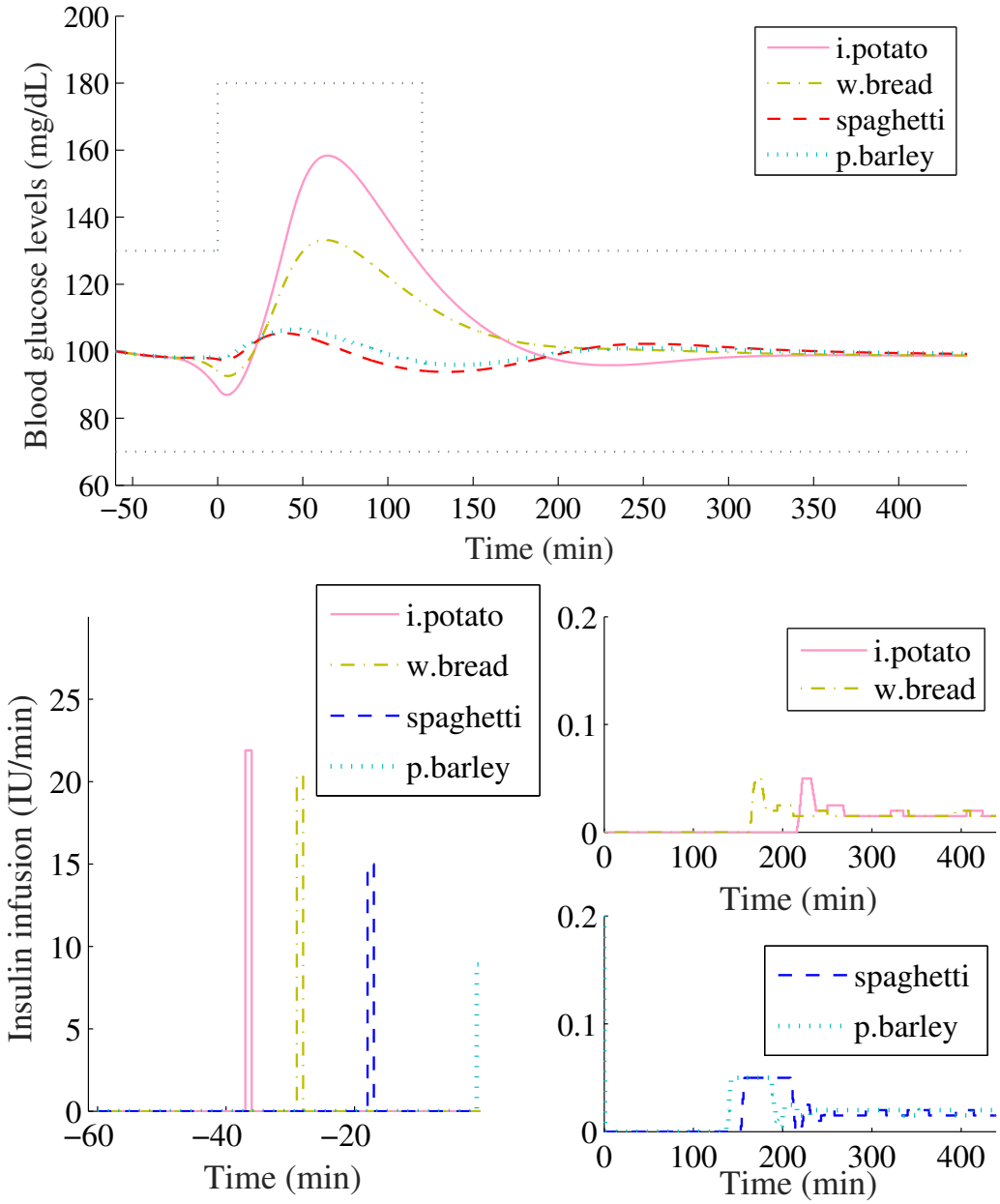

Figure 4.10: (Top) Prandial BG control response using a preprandial single-bolus insulin administration combined with postprandial MPC in the nominal case with carbohydrate intake of 100 g and varying GI values (in parenthesis) represented by instant potato (83), white bread (71), spaghetti (41) and pearled barley (25) consumed at 0. Dotted lines delineate clinical recommendations of BG levels for patients with T1DM from the ADA (see Table 4.1 on page 58). (Bottom) Preprandial single-bolus for each food according to Table 4.4 (left) and postprandial closed-loop insulin infusion from 0 to $k_f = 440$ for high GI foods represented by instant potato and white bread (top right), and medium/low GI foods represented by spaghetti and pearled barley (bottom right).

exactly at 0 is shown in Figure 4.11 for the highest and lowest GI meals represented by instant potato and pearled barley, respectively. For instant potato, BG excursion can be maintained within 81–158 mg/dL (4.5–8.78 mmol/L), whereas for low GI foods there is an almost flat response of ± 10 mg/dL (0.56 mmol/L) from the target value of 100 mg/dL (5.56 mmol/L).

The case of preprandial single-bolus insulin is shown in Figure 4.12, wherein for a high GI meal (instant potato), the glycemic excursion slightly exceeds the recommended ADA values between 120–150 min. For the low GI food, the 2-hour postprandial BG recommendation is effectively maintained within the normoglycemic range, although the BG control is not as narrow as for the case of continuous preprandial insulin infusion. None of the simulation results show any risk of hypoglycemia whatsoever with all the BG excursions being constantly above 80 mg/dL (4.44 mmol/L).

4.2.4 Food-related uncertainties

We also assess the response of the BG control algorithm for uncertainties of 20% in the GI value of the meal, in addition to miscalculations of the actual carbohydrate intake of ± 10 g in the continuous-time T1DM patient model—from an originally assumed nominal 50 g in the controller—in combination with deviations in mealtime of ± 15 min considering nominal values for the remaining model parameters. For continuous preprandial insulin infusion, the BG excursions are shown in Figures 4.13 and 4.15. Differences in the GI value result in a postprandial peak as high as 158 mg/dL (8.78 mmol/L) for high GI values, whereas is has almost no effect on low GI foods. Moreover, a reduced consumption of -10 g in high GI foods causes a reduced glycemic excursion below 80 mg/dL (4.44 mmol/L) either between 0–50 min and 150–250 depending on the mealtime deviation, although BG levels can effectively be maintained within the desirable range. For low GI foods, the BG control algorithm maintains the glycemic excursion within ± 10 mg/dL (± 0.56 mmol/L) from the target value.

For preprandial single-bolus, the response of the present control algorithm against uncertainty in the GI value of the meal is shown in Figure 4.14 and the response to miscalculations in carbohydrate intake and actual mealtime are given in Figure 4.16. Differences in the GI value cause a high postprandial BG excursion for high GI foods above clinical recommendations at $t = 120$ min, although only temporarily, whereas low GI foods are barely affected. Furthermore, a 15-min delay in meal consumption for high GI foods results in a drop in BG levels below 80 mg/dL (4.44 mmol/L) between 0–50 min, although BG excursion is still maintained above the minimum of 70 mg/dL (3.89 mmol/L). Compared to this, the glycemic excursion for the lowest GI food (pearled barley) is maintained within a narrow range within ± 10 mg/dL

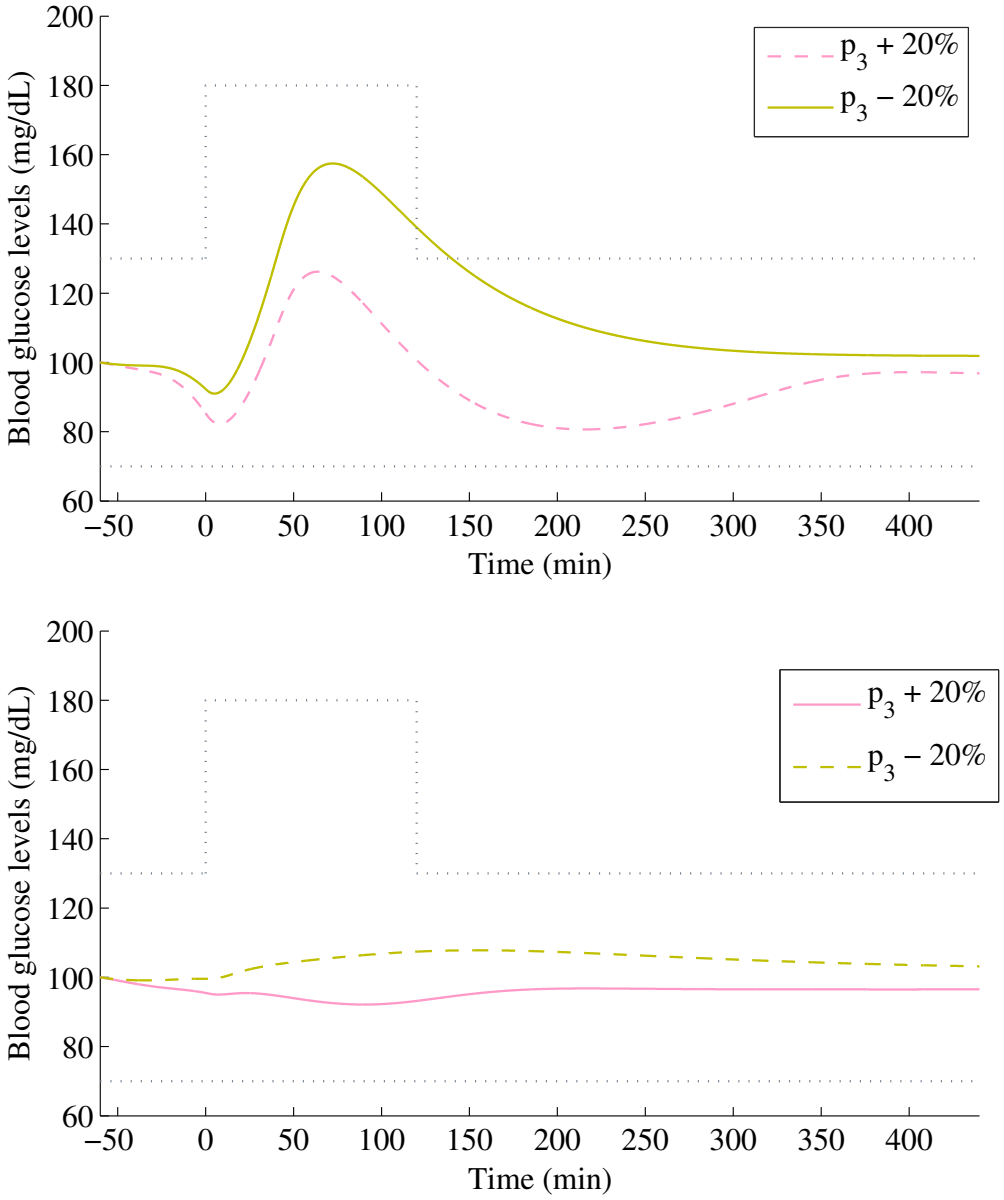

Figure 4.11: Simulation of the prandial BG control response using a continuous variable preprandial insulin infusion combined with postprandial MPC against intra-individual variability in subcutaneous insulin effect p_3 of $\pm 20\%$ for a high GI food represented by instant potato (top) and low GI food as pearled barley (bottom) considering a nominal carbohydrate load of 50 g. Dotted lines delineate clinical recommendations of BG levels for patients with T1DM from the ADA (see Table 4.1 on page 58).

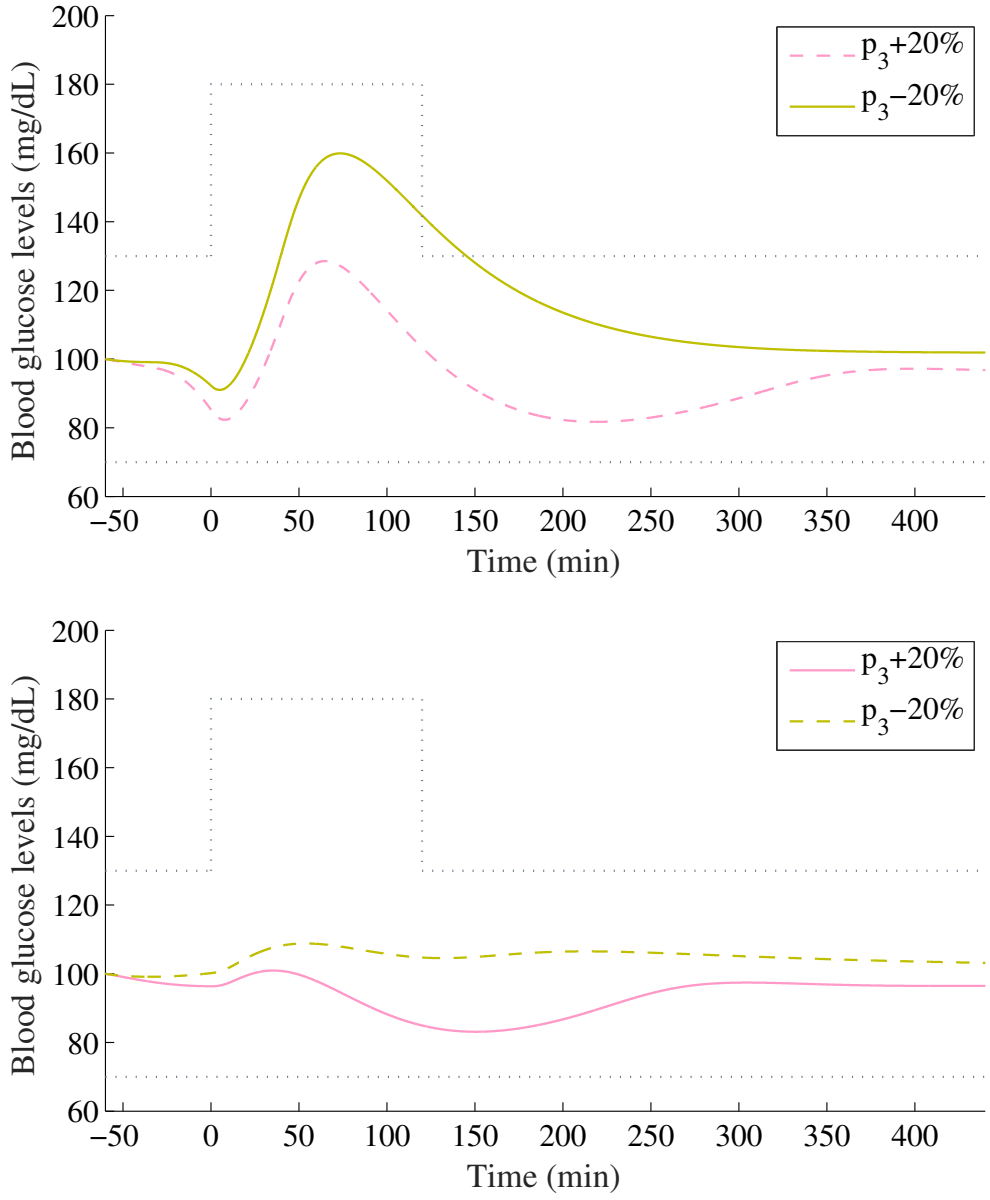

Figure 4.12: Prandial BG control response using a preprandial single-bolus insulin administration combined with postprandial MPC against intra-individual variability of $\pm 20\%$ in parameter p_3 for a high (top) and low (bottom) GI food represented by instant potato and pearled barley, respectively, with a nominal carbohydrate load of 50 g. Dotted lines delineate clinical recommendations of BG levels for patients with T1DM from the ADA (see Table 4.1 on page 58).

(±0.56 mmol/L) close to the target value of 100 mg/dL (5.56 mmol/L) throughout the prandial state.

In Table 4.5 we include the prandial BG excursion of each representative meal considering each of the above conditions for the combined continuous preprandial bolus insulin and postprandial MPC. Similarly, BG excursion for the case of preprandial single-bolus administration combined with postprandial MPC is shown in Table 4.6.

4.3 Discussion

In the present chapter we propose a semi closed-loop BG control algorithm to assess the feasibility to maintain prandial BG excursion in T1DM within clinical recommendations from the ADA. It comprises an optimization algorithm for preprandial insulin (continuous variable insulin infusion or single-bolus at a given instant) computed 60 min prior to the intended mealtime, and directly administered to the T1DM patient model until mealtime, wherein a closed-loop postprandial BG control using MPC provides basal insulin to stabilize BG levels at 100 mg/dL (5.56 mg/dL). Several pertinent issues related to the present control algorithm are further discussed in the following.

- *Assessment of the degree of tight BG control (nominal case)*
  In this study we demonstrate that prandial BG excursion using our semi closed-loop BG control algorithm for regular and high carbohydrate loads of 50 g and 100 g not only comply with ADA recommendations but the control strategy implemented *in silico* is capable of maintaining normoglycemia for high GI foods (value in parenthesis) such as white bread (71) and instant potato (83). Despite having the same carbohydrate amount, the total continuous preprandial insulin infusion or single-bolus dose for each meal is proportional to their respective GI value, which is in accordance with previous clinical studies that suggest consumption of lower GI foods results in a reduced glycemic excursion compared to high GI foods for an identical carbohydrate intake [157]. Other studies have started to realize the necessity to include the GI in the assessment of bolus insulin doses and thus suggest, albeit arbitrarily, an increase of 30% to the insulin bolus for high GI meals [158]. Moreover, the postprandial BG excursion for the four representative foods considered in the present study are unexpectedly similar to that of nondiabetics, who maintain a modest BG excursion of 40 mg/dL (2.22 mmol/L) above basal levels after consumption of high GI foods and a completely flat response to low GI foods [159].

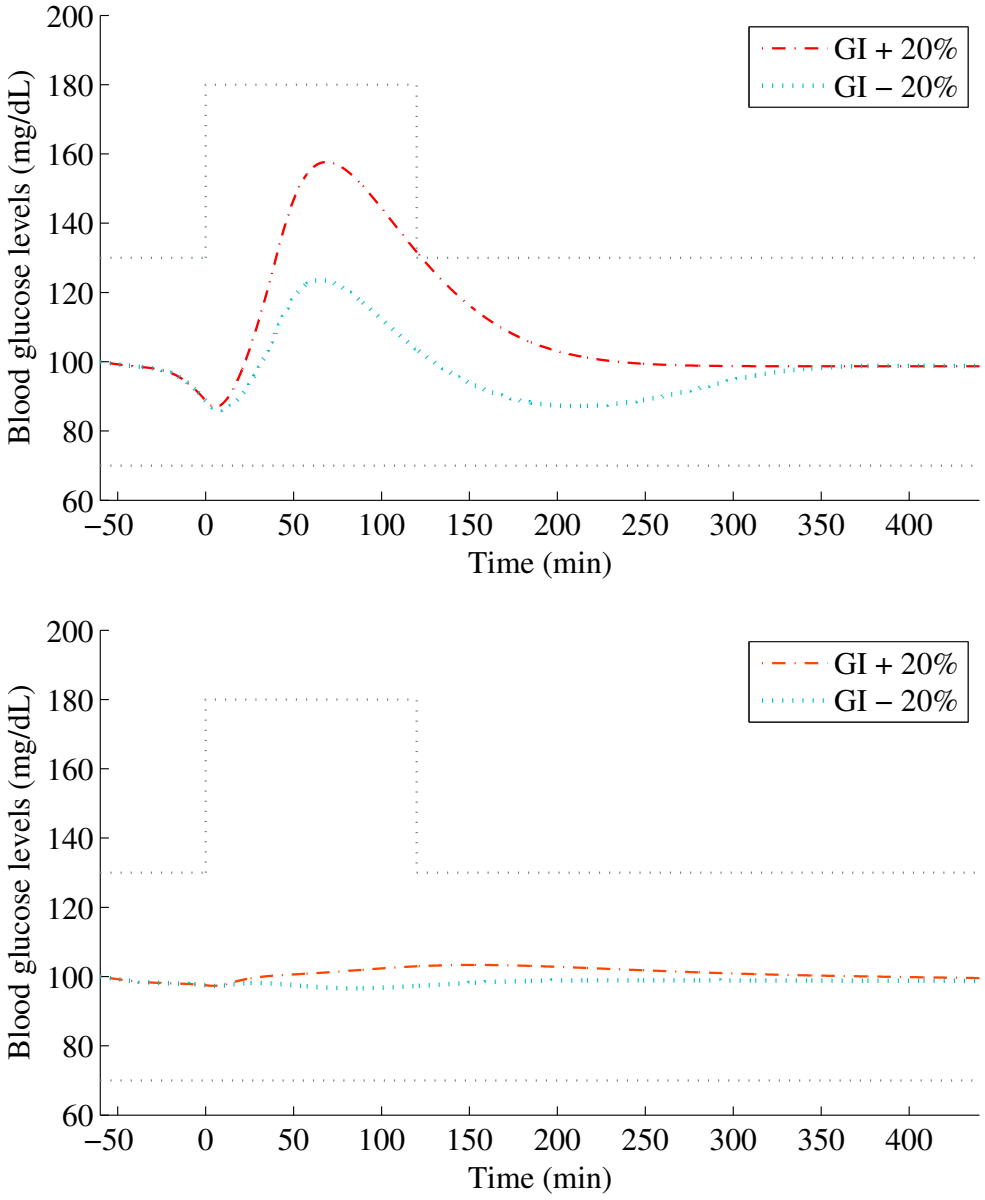

Figure 4.13: Prandial BG control response using a continuous variable preprandial insulin infusion combined with postprandial MPC against food-related variation of ±20% in the GI value of the meal for a high (top) and low (bottom) GI food represented by instant potato and pearled barley, respectively, with nominal carbohydrate load of 50 g. Dotted lines delineate clinical recommendations of BG levels for patients with T1DM from the ADA (see Table 4.1 on page 58).

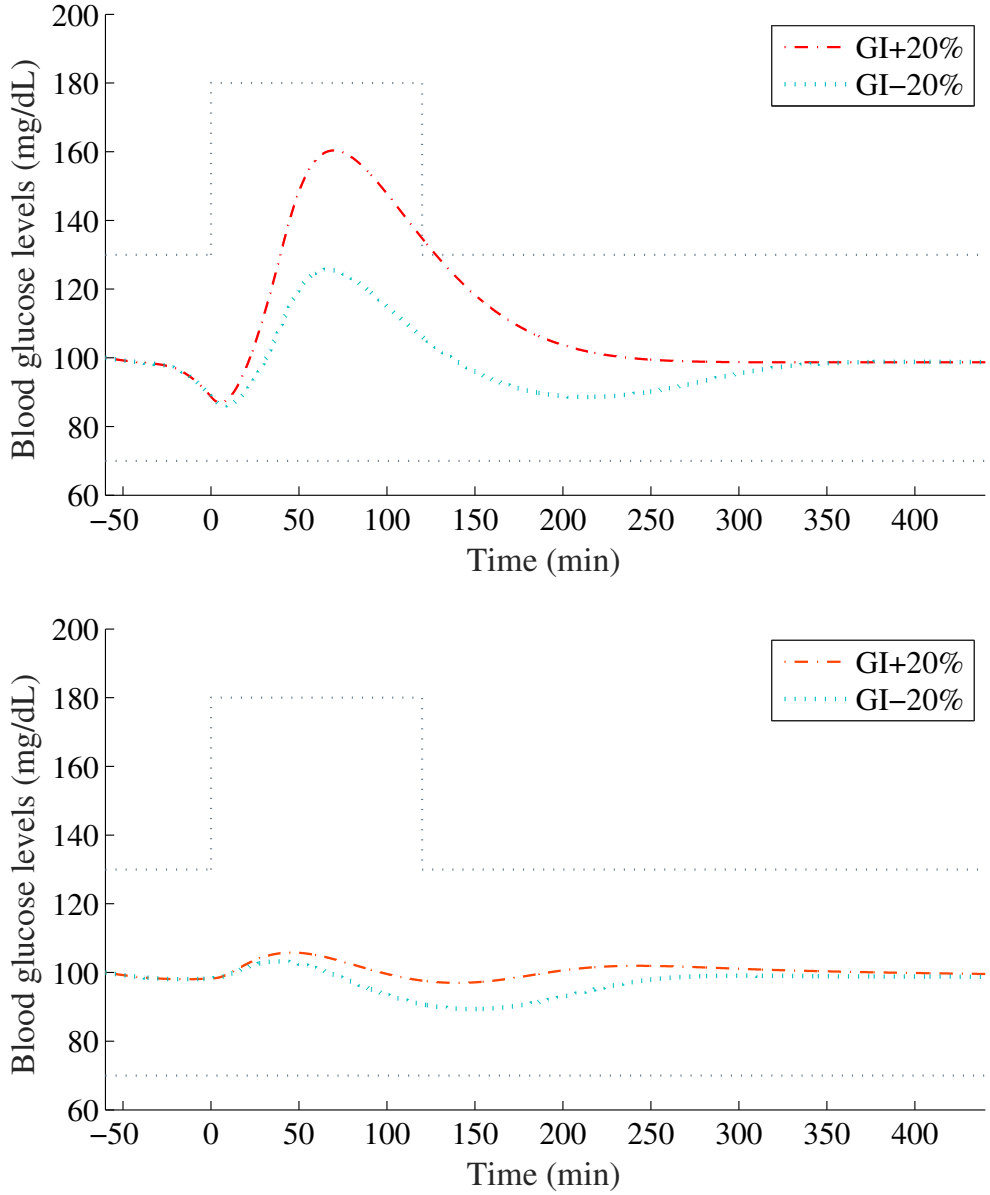

Figure 4.14: Simulation of prandial BG control response using a preprandial single-bolus insulin administration combined with postprandial MPC against variation of ±20% in the GI value for a high (top) and low (bottom) GI food represented by instant potato and pearled barley, respectively, with a nominal carbohydrate load of 50 g. Dotted lines delineate clinical recommendations of BG levels for patients with T1DM from the ADA (see Table 4.1 on page 58).

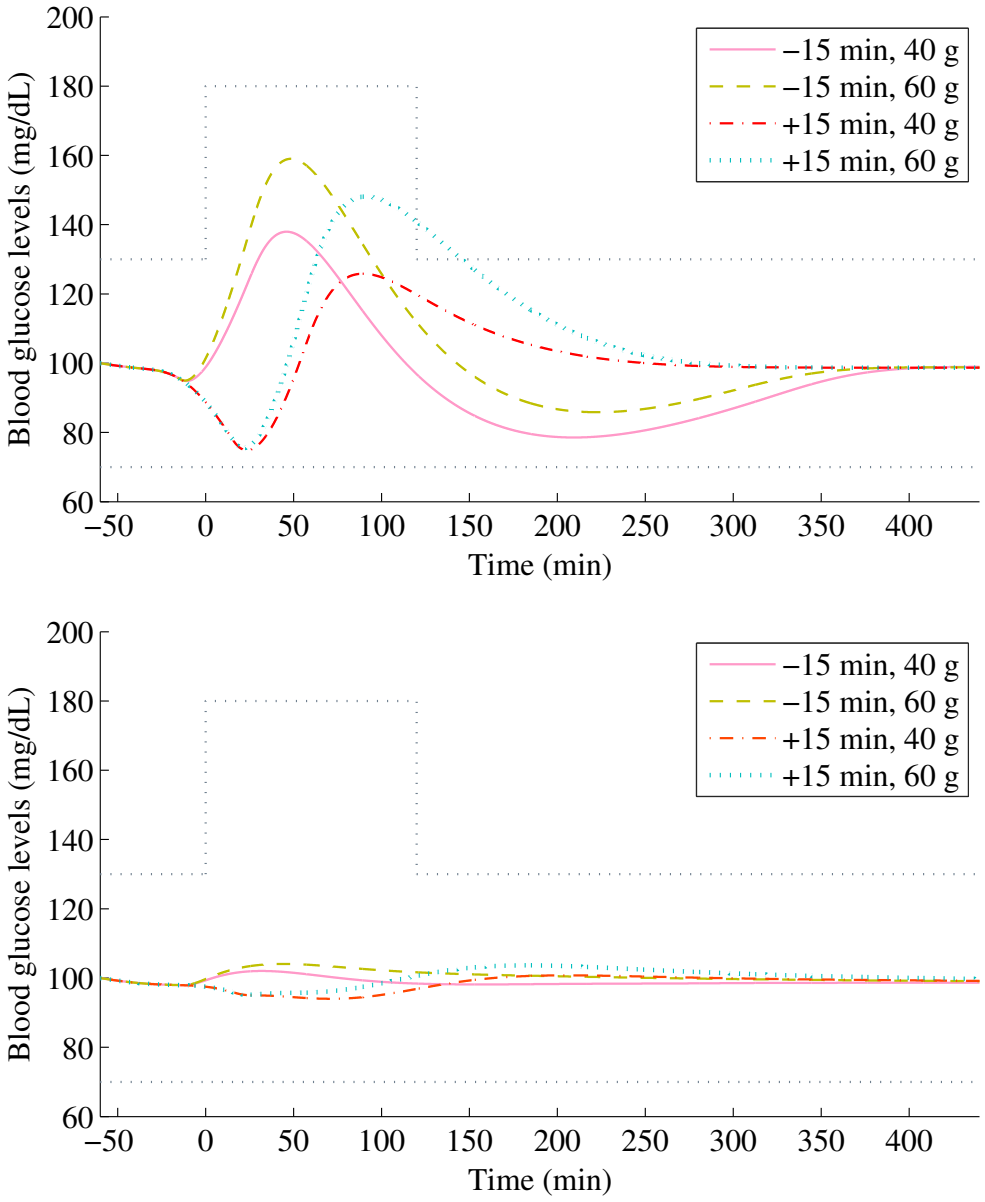

Figure 4.15: Simulation of continuous variable preprandial insulin bolus combined with postprandial MPC against food-related uncertainties for a carbohydrate load of 50 g in a high (top) and low (bottom) GI food represented by instant potato and pearled barley, respectively, considering miscalculations of ± 10 g in carbohydrate intake and deviation in mealtime of $k_{\mathrm{m}} = \pm\ 15$ min in the T1DM patient model for the four possible combined scenarios. Dotted lines delineate clinical recommendations of BG levels for patients with T1DM from the ADA (see Table 4.1 on page 58).

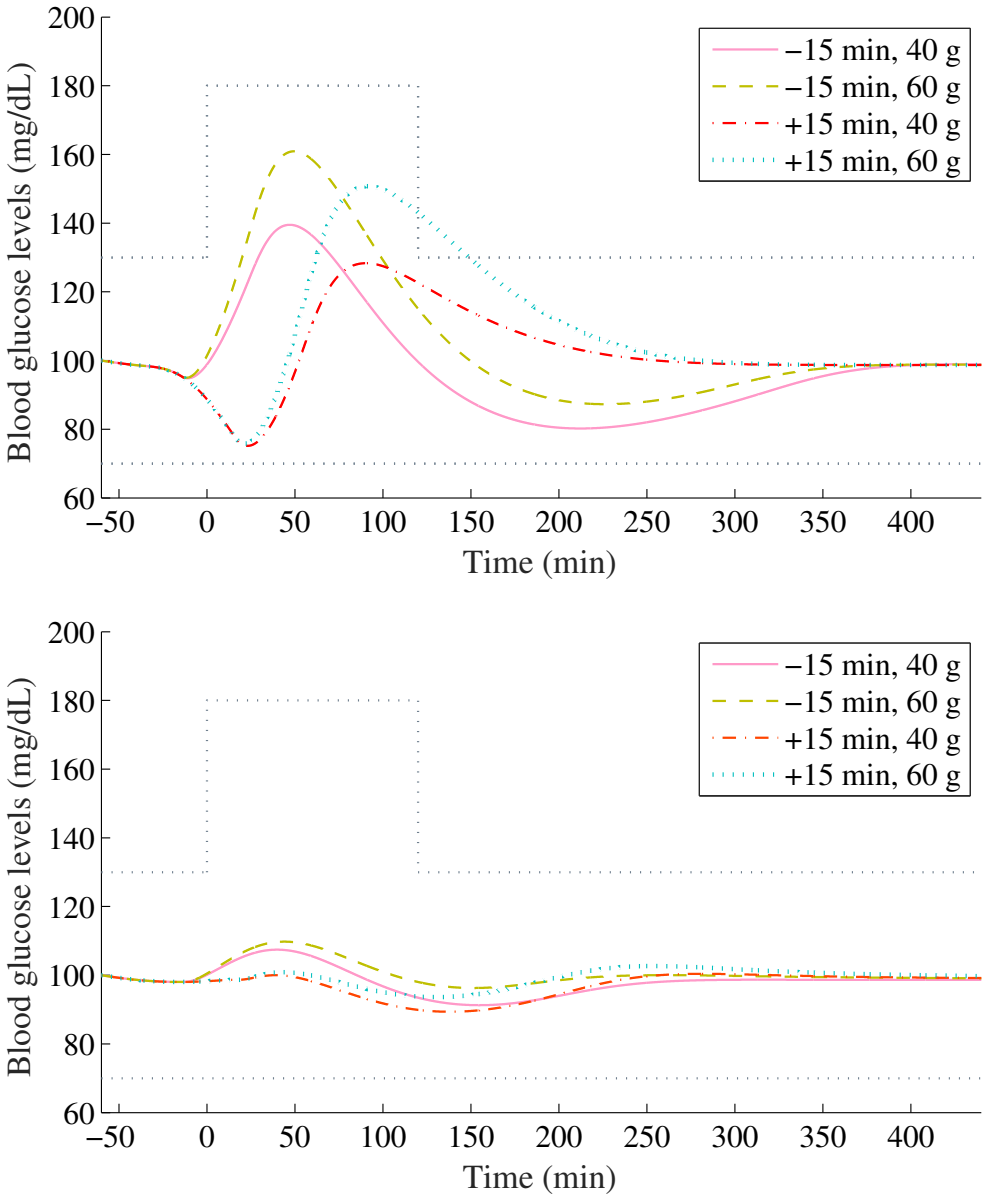

Figure 4.16: Simulation of prandial BG control using a preprandial single-bolus insulin administration combined with postprandial MPC for a carbohydrate load of 50 g in a high (top) and low (bottom) GI food represented by instant potato and pearled barley, respectively, considering miscalculations of ± 10 g in carbohydrate intake and deviation in mealtime of $k_{\mathrm{m}} = \pm 15$ min in the T1DM patient model considering all four possible combined scenarios. Dotted lines delineate clinical recommendations of BG levels for patients with T1DM from the ADA (see Table 4.1 on page 58).

Table 4.5: BG excursion in the present control algorithm for continuous preprandial insulin infusion combined with postprandial MPC. For the nominal case, meal announcement information of the controller is exactly the same as for the continuous-time T1DM patient model considering carbohydrate loads of 50 g and 100 g in four representative foods with varying GI values. Intra-individual variability due to subcutaneous insulin effect p_3, in addition to food-related uncertainties in the GI value and combined miscalculation of carbohydrate intake with mealtime deviations in the T1DM patient model are also considered.

Controller	**Patient (actual)**	**GI**	**BG excursion mg/dL (mmol/L)**
50 g (nominal)	50 g 0 min	83	86–134 (4.78–7.44)
		71	91–114 (5.06–6.33)
		41	96–102 (5.33–5.67)
		25	97–101 (5.39–5.61)
100 g (nominal)	100 g 0 min	83	86–152 (4.78–8.44)
		71	92–126 (5.11–7.00)
		41	96–104 (5.33–5.78)
		25	97–101 (5.39–5.61)
50 g	$p_3\pm$ 20% 0 min	83	81–157 (4.50–8.72)
		71	82–135 (4.56–7.50)
		41	89–112 (4.94–6.22)
		25	92–108 (5.11–6.00)
50 g	GI $\pm$ 20% 0 min	83	86–158 (4.78–8.78)
		71	87–132 (4.83–7.33)
		41	93–108 (5.17–6.00)
		25	97–103 (5.39–5.72)
50 g	$\pm$10 g $-$15 min	83	79–159 (4.39–8.83)
		71	81–139 (4.50–7.72)
		41	93–114 (5.17–6.33)
		25	98–104 (5.44–5.78)
50 g	$\pm$10 g $+$15 min	83	75–148 (4.17–8.22)
		71	82–122 (4.56–6.78)
		41	92–106 (5.11–5.89)
		25	94–103 (5.22–5.72)

Table 4.6: Simulation results of BG excursion in the present control algorithm for preprandial single-bolus according to Table 4.4 in combination with postprandial MPC. For the nominal case, meal announcement in the controller is exactly the same as in the continuous-time T1DM patient model for carbohydrate loads of 50 g and 100 g in four representative foods with varying GI values. Intra-individual variability due to subcutaneous insulin effect p_3, in addition to food-related uncertainties of the GI value and combined miscalculations of carbohydrate intake with mealtime deviation in the T1DM patient model are also considered.

Controller	**Patient (actual)**	**GI**	**BG excursion mg/dL (mmol/L)**
50 g (nominal)	50 g 0 min	83	87–143 (4.83–7.94)
		71	92–122 (5.11–6.78)
		41	98–112 (5.44–6.22)
		25	93–104 (5.17–7.78)
100 g (nominal)	100 g 0 min	83	87–158 (4.83–8.78)
		71	93–133 (5.17–7.39)
		41	94–105 (5.22–5.83)
		25	96–107 (5.33–5.94)
50 g	$p_3 \pm 20\%$ 0 min	83	82–160 (4.56–8.89)
		71	84–137 (4.67–7.61)
		41	87–118 (4.83–6.56)
		25	83–109 (4.61–6.06)
50 g	GI $\pm 20\%$ 0 min	83	86–160 (4.78–8.89)
		71	88-134 (4.89–7.44)
		41	92–116 (5.11–6.44)
		25	89–106 (4.94–5.89)
50 g	± 10 g -15 min	83	80–161 (4.44–8.94)
		71	83–139 (4.61–7.72)
		41	91–123 (5.06–6.83)
		25	91–110 (5.06–6.11)
50 g	± 10 g $+15$ min	83	80–151 (4.44–8.39)
		71	81–125 (4.50–6.94)
		41	95–105 (5.28–5.83)
		25	89–103 (4.94–5.72)

In this way, even though compliance with ADA recommendations might be an indicator of the degree of success in the performance of prandial BG control algorithms to a certain extent, we consider the postprandial glycemic response in nondiabetics to be a superior—if not the ideal—reference.

- *Response against intra-patient variability*
  Performance assessment of the present BG control algorithm against the most essential source of intra-individual variability due to subcutaneous insulin effect in the T1DM patient model is also included. Studies of the diurnal pattern of insulin action in nondiabetics show that insulin sensitivity reduces from breakfast to dinner [160]. Interestingly, the opposite seems to occur in T1DM wherein insulin sensitivity improves throughout the day [161], whereas other studies have also found similar or opposite patterns in postprandial glucose-insulin dynamics [162, 163]. As the mathematical model of glucose-insulin metabolism developed in Chapter 3 does not include such circadian variation of carbohydrate tolerance, variability in insulin effect in the present study is limited to an arbitrary variation of 20% in parameter p_3.

- *Response against food-related uncertainties*
  The GI has perhaps the highest intra-individual variability with half of the total test subjects having at least 10 units away from the mean value [153]. This is represented by a variation of 20% in the GI value for the T1DM patient model to assess the control performance in our study, with satisfactory results. Another typical source of uncertainty is the poor estimation of the carbohydrate content of the meal in an everyday basis, which is not the exception but the norm. In fact, studies on the ability to calculate carbohydrates accurately indicate that only 23% of adolescents with T1DM seem to predict the amount within ± 10 grams/day even with the availability of nutritional labels [164]. Other studies show that poor carbohydrate estimation has clearly a deleterious effect on postprandial BG levels [165]. Besides carbohydrate amount, the exact mealtime is also difficult to predict, especially one hour in advance as the exact meal information is required for the control algorithm to initiate the computation of preprandial insulin. Hence, the performance of the proposed control algorithm against carbohydrate miscalculations of 20%, in combination with a deviation in mealtime of ± 15 min is thus also evaluated. Simulation results show that BG excursions are within recommended clinical values for both high and low GI foods (see Figures 4.15 and 4.16 for continuous variable infusion and single-bolus, respectively), although they also suggest that mealtime deviations beyond 15 min—both before and after the intended mealtime—have a potential risk of post-meal

hypoglycemia for high GI foods when combined with overestimation of the carbohydrate content of the meal, *i.e.*, less amount consumed than the information initially given to the controller. Even though we contemplated the addition of an input to indicate the actual mealtime to the controller (since the present control strategy assumes mealtime is always given at 0), this would have required a additional manual operation and thus decrease the level of automatization of the present control algorithm.

- *Control strategy 1: Start in preprandial insulin infusion*
  One of the main impediments of fully closed-loop AP systems to maintain postprandial normoglycemia is arguably the slow absorption kinetics of subcutaneous insulin administration route. For this reason, in the present study we assess the feasibility to achieve tight BG control for nominal carbohydrate loads of 50 g and 100 g by considering administration of preprandial insulin infusion as early as 60 min prior to mealtime, which seems to be the only feasible strategy given the PD of the so-called rapid-acting insulin formulations (see Figure 3.8 on page 47). Even though some recent studies [135, 166] suggest that prandial insulin administration 15–20 min prior to the meal contributes to a relative reduction in postprandial glycemic excursion, it still does not prevent postprandial hyperglycemia. Hence, the appropriate insulin administration timing to prevent the typical BG peak after meal consumption is also an important point of discussion in the present study. Results from the optimization problem for preprandial single-meal bolus insulin given at a specific instant between k_i and 0 (see Table 4.4) suggests that both the bolus insulin amount and timing depend on the GI value of the meal, which is beyond the current gold standard in bolus insulin estimation according to the carbohydrate counting method. For continuous subcutaneous insulin infusion (see Table 4.3), the start in preprandial insulin infusion is between 39–54 min prior to mealtime regardless of the type of food or amount, which indicates the adequacy of the value of $k_i = -60$, with total pre-meal bolus insulin required for each meal being also proportional to their respective GI value. Knowing the optimal bolus insulin infusion pattern (as in Figure 4.7) necessary to maintain tight BG control from *in silico* results in our study, it is now comprehensible that current AP systems in the literature cannot maintain tight BG control after a carbohydrate load.

- *Control strategy 2: Hypoglycemia prevention*
  Hypoglycemia prevention is arguably the main concern in BG control algorithms for prandial state, since daytime hypoglycemia has a direct impact on the quality of life and healthcare costs of patients with T1DM, even for mild episodes [167, 168]. To prevent a large preprandial bolus from causing post-meal hypoglycemia, we consider a penalty

term Q_{LO} exclusively for hypoglycemia in Eq. (4.3) for the solution of the optimization problem in Eq. (4.1) (continuous preprandial infusion) and Eq. (4.6) (single-bolus). Additionally, we include maximum rates of preprandial and postprandial insulin infusion U_{pre} and U_{post}, respectively, for patient safety reasons.

- *Single hormone/bihormonal BG control*
  Among the different BG control strategies for prandial state, one of them opts for bihormonal *i.e.* insulin and glucagon, closed-loop BG control systems [169, 170] to avoid the risk of hypoglycemia caused by the lagging effect of subcutaneous insulin infusion. Such approach, though effective, adds a considerable degree of complexity to the control system, not to mention the burden to the patient by including a glucagon infusion set. In the present approach, a mathematical model of glucose-insulin metabolism in T1D that considers the absorption rate of different types of carbohydrates is used to predict the optimal preprandial insulin instead. Hence, our study dispense with an additional infusion algorithm for glucagon and still have no critical postprandial hypoglycemic episodes. More specific real-life scenarios wherein glucagon infusion can have a decisive role, however, is the case of meal omission after preprandial insulin bolus has been infused, or actual meal consumption being considerably less than expected due to a number of reasons including illness, fullness or mindlessness.

- *Future direction: Clinical implementation*
  With the development and commercialization of even faster insulin formulations such as ultra-rapid insulin in the near future, further improvements in the performance of closed-loop BG control algorithms can be expected. Despite such positive forecast, there is still much work to be done before a commercially available AP system can be developed. Patient variability is arguably one of the most difficult problems to tackle in BG control systems, especially during prandial state. Differences in glucose-insulin metabolism among patients and day-to-day or same-day variations within the same subject, known as inter-individual and intra-individual variability, respectively [171], introduce errors to the mathematical model utilized that reflects negatively on the performance of the BG control algorithm. It is also noteworthy that ADA recommendations for pregnancy with pre-existing diabetes—not to be confused with gestational diabetes—are even more rigorous than the conventional treatment for T1DM (see Table 4.1 on page 58) perhaps due to the high risk of pregnancy complications such as miscarriage/stillbirth, delivery complications and birth defects.

4.4 Concluding remarks

In the present chapter we demonstrated the feasibility of tight BG control for prandial state in patients with T1DM using a semi closed-loop control strategy based on meal announcement of the food to be consumed as early as 60 min before mealtime. Prandial insulin strategy consists of either a preprandial continuous variable insulin infusion or instantaneous single-bolus, which is followed by postprandial closed-loop basal insulin infusion based on MPC for automatic stabilization and maintenance of BG levels at the target value of 100 mg/dL (5.56 mmol/L). *In silico* assessment of the present control algorithm indicates that prandial BG excursion not only complies with clinical recommendations from the ADA but also that a tight BG control comparable to nondiabetics is actually feasible. The control performance, however, is slightly attenuated when considering realistic sources of variability such as model-patient mismatch and uncertainties related to the meal content. Interestingly, the preprandial insulin required for each food suggests that both the total bolus dose and timing varies considerably depending on the type of food to be consumed, which defies the current clinical guidelines based on the carbohydrate-counting method in the treatment of T1DM.

Chapter 5

Mixed meal model in T1DM

Mixed meals with a considerable fat content have been recently acknowledged to cause an aberrant post-meal glycemic excursion that—besides affecting negatively BG management in patients with T1DM—reduces the performance of closed-loop BG systems [33]. Due to the difficulty to develop an accurate mathematical model of the impact of mixed meals on glucose-insulin metabolism in patients with T1DM, some closed-loop BG control algorithms [172] have resorted to arbitrary parameter adjustment from clinical data of nondiabetics after consumption of a mixed meal using the triple-tracer meal protocol to fit parameters k_{min}, k_{max}, k_{abs}, b and d of Dalla Man model for insulin and carbohydrate absorption of mixed meals, while others [173] have proposed an alternative simplified measurement method of rate of glucose appearance from mixed meals without relying on the triple tracer method for modeling purposes. Other studies [174] have fitted model parameters of plasma insulin and glucose from a combined model from Sherwin, Bergman and Wilinska models for insulin PK/PD, glucose uptake/EGP and meal glucose appearance, respectively, and assume that subcutaneous insulin depot, plasma insulin and remote interstitial fluid surrounding insulin-sensitive tissue are unaltered by high-fat mixed meals. Interestingly, interpretation of parameter values in such study for low and high fat mixed meals quantitatively indicate that the effect of dietary fat on postprandial glucose-insulin metabolism are delay in gastric emptying and decrease in insulin sensitivity, as has been usually suggested by previous clinical studies on the effect of dietary fat on posprandial BG levels in patients with T1DM, although only qualitatively [27, 28].

As model-based control algorithms have a strong dependency on model accuracy, the absence of a reliable mathematical model of the impact of dietary fat on postprandial BG levels prevents further development of diurnal BG control algorithms for mixed meals. Arbitrary parameter adjustment to clinical data cannot be regarded as a valid approach for model-based BG control systems, since they require *a priori* estimation of model parameters. For this reason,

in the present chapter we propose a novel mathematical model of mixed meals with a quantitative representation of the effect of dietary fat and carbohydrates on postprandial glucose-insulin metabolism in patients with T1DM. It considers a relevant physiological representation of lipid metabolism that follows the same minimal compartmental representation as in the mathematical model of carbohydrates proposed in Chapter 3.

In the following sections, we first give a general description of the mixed meal model proposed, which is divided into a model of gut absorption of dietary fat and its delaying effect on gastric emptying of carbohydrates, in addition to meal-derived lipid metabolism in patients with T1DM as a new compartmental model proposal for plasma TG and NEFA levels as well. For the physiologically-relevant representation of lipid-derived insulin resistance, we first provide an exhaustive review on the literature concerning the etiology of insulin resistance and the significance of the glucose-fatty acid cycle—the most accepted theoretical explanation of insulin resistance—to propose a novel representation of insulin resistance based on the aforementioned compartments. Simulation of the present model and parameter identification using clinical data from patients with T1DM are presented along with further discussion of the model proposed and its most relevant points.

5.1 Proposed minimal mixed meal model

A physiologically-relevant mathematical model of the effect of dietary fat on glucose-insulin metabolism is to represent not only its ultimate impact on postprandial BG levels but also the complete gut transit from mixed meal ingestion, absorption and metabolism. Moreover, such model must represent the metabolic state of T1DM patients in particular. In the present section we give a brief general introduction of the model proposed, with further description of each part with complete support from clinical studies.

5.1.1 General description

As shown in Figure 5.1, the present mixed meal model (carbohydrates and dietary fat) is an extension of the model of postprandial glucose-insulin metabolism from carbohydrates developed in Chapter 3. It includes digestion/absorption of dietary fat, and the delaying effect on gastric emptying of carbohydrates [28] separately. The mathematical representation of postprandial fatty acid metabolism considers plasma NEFA and triglyceride levels in order to further include lipid-induced acute insulin resistance, as elaborated in the respective subsection of the present chapter.

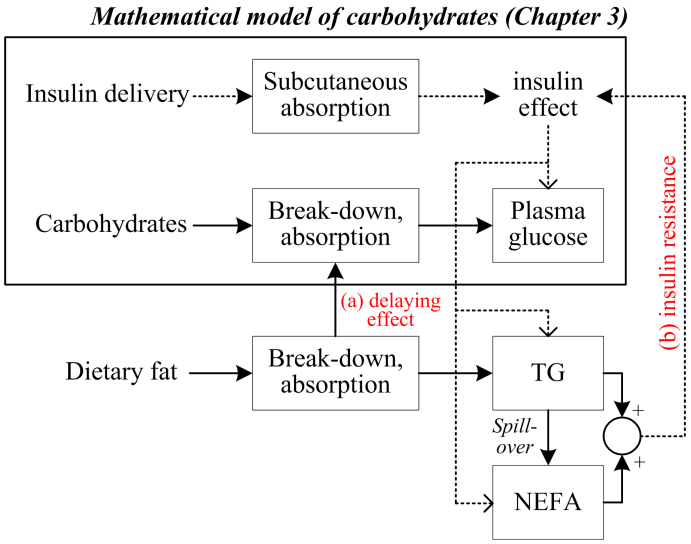

Figure 5.1: Extension of the mathematical model of glucose-insulin metabolism in T1DM from carbohydrates to a mixed meal model that includes dietary fat digestion/absorption and fatty acid metabolism from triglycerides (TG) and non-esterified fatty acids (NEFA) to represent the two main effects on glucose-insulin metabolism as (a) delay in gastric emptying of the meal and (b) lipid-derived acute insulin resistance.

5.1.2 Model of carbohydrate digestion/absorption (mixed meal)

After a mixed meal enters the gastrointestinal tract, the digestion process begins with the break-down of large food particles in an extremely complex process. As shown in Figure 5.2, the stomach is anatomically divided into fundus, corpus (body), antrum and pylorus, whereas it is functionally divided into distal and proximal stomach although they belong to the same single chamber. The proximal and distal stomach are associated with gastric emptying of solids and liquids, respectively [175]. Solids are first distributed in the fundus for the initial grinding (lag phase), and later redistributed in the distal stomach for linear gastric emptying at an almost constant rate [176]. Increase in the caloric content of a solid meal—as easily attained by a high dietary fat content—prolongs food retention in the proximal stomach, and thence redistributed to the distal stomach for a linear gastric emptying.

In this way, the proximal and distal stomach seem to play a determinant role in the gastric emptying of mixed meals, with a characteristic biphasic gastric emptying pattern [177]. For the mathematical representation of gut transit of mixed meals, the original model of carbohydrate digestion/absorption given by Eq. (3.23) (see page 42) in Chapter 3 can be either replaced by a more complex model with explicit representation of the distal and proximal stomach [178], or

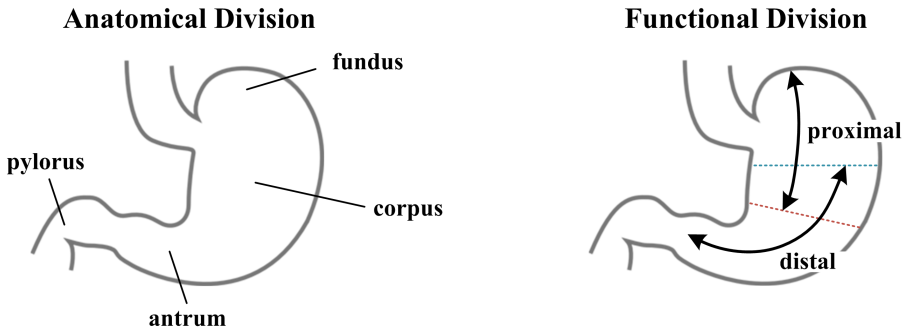

Figure 5.2: Division of the stomach according to its anatomical (left) and functional (right) function.

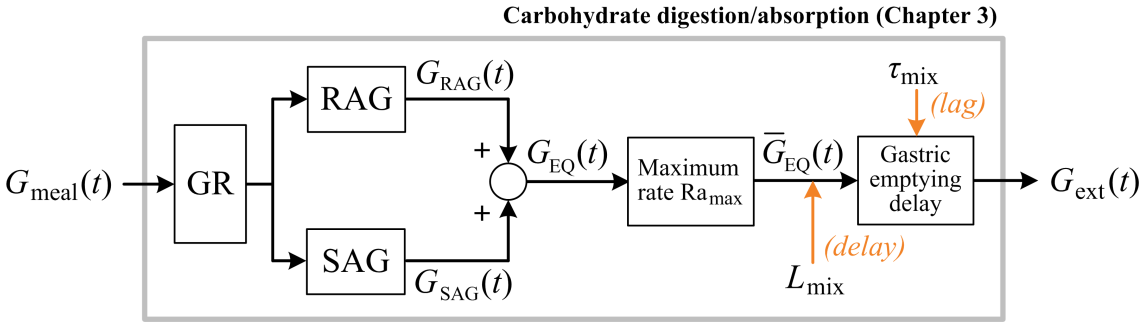

Figure 5.3: The biphasic nature of gut transit of carbohydrates due to the presence of dietary fat is represented by the addition of an emptying delay L_{mix} and lag τ_{mix} to the previous model of carbohydrates in Chapter 3.

be modified accordingly. To maintain a minimal principle, we include a lag and offset in our original model (see Figure 5.3) to represent the biphasic nature of gastric emptying of mixed meals as

$$\frac{\mathrm{d}G_{\text{ext}}(t)}{\mathrm{d}t} = \frac{1}{\tau_{\text{dg}} + \tau_{\text{mix}}} \left(-G_{\text{ext}}(t) + \overline{G}_{\text{EQ}}(t - L_{\text{mix}})\right), \tag{5.1}$$

where τ_{mix} is the fat-induced lag added to the food-specific lag in carbohydrate digestion τ_{dg} with emptying delay L_{mix} of the mixed meal to represent chyme retention in the proximal stomach.

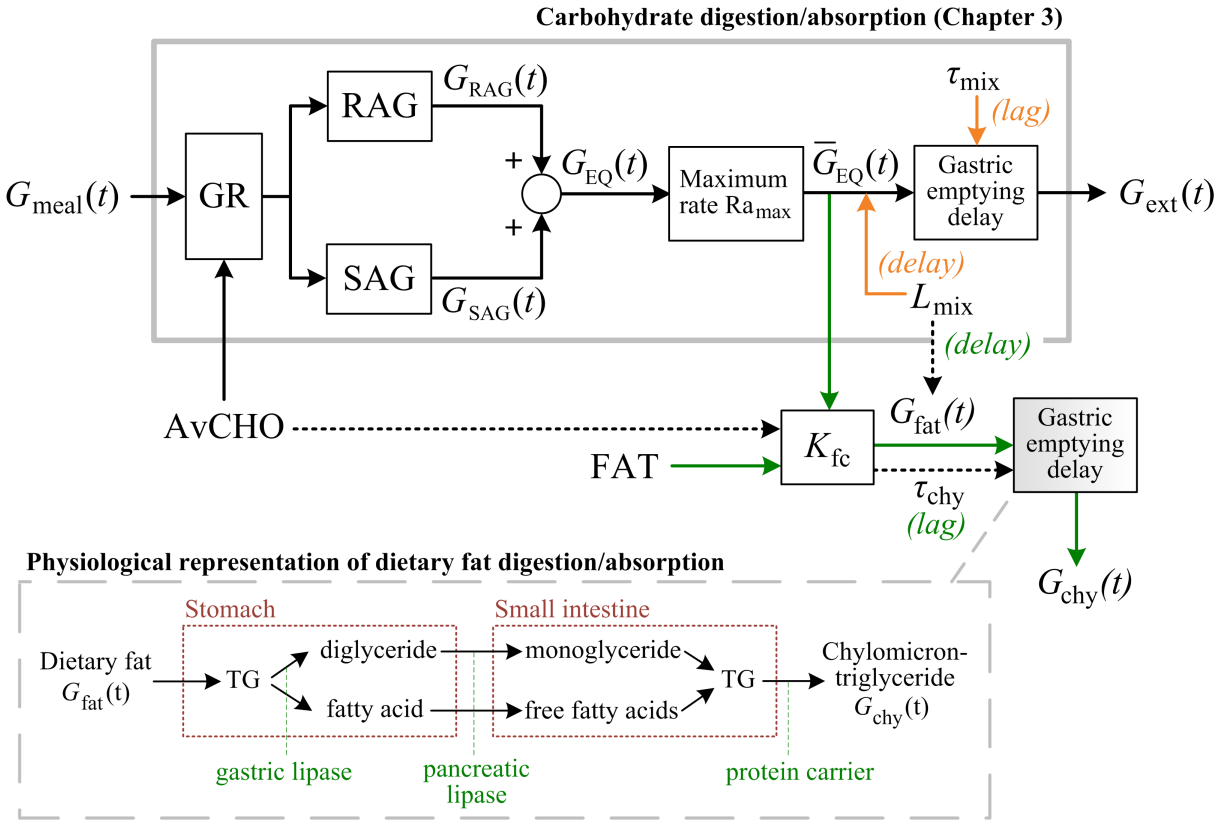

Figure 5.4: Mathematical representation of gut transit of dietary fat dietary fat (in green) proposed in the present study. According to the the physiological mechanism of fat break-down (bottom), total fatty acid remains constant and thus we simplify it with a biphasic gut absorption model with emptying delay L_{mix} (same parameter for carbohydrates) and lag τ_{chy}.

5.1.3 Model of dietary fat digestion/absorption

After consumption of a mixed meal, the dietary fat portion—which mainly consist of triglycerides and cholesterol—is broken down into monoglycerides and fatty acids into the stomach by several enzymes including gastric lipase. After that, it is sent to the small intestine where extremely complex biochemical processes take place[1]. Nascent TG is used for CM assembly, which together with cholesterol and phospholipids form CM prior to its absorption into the bloodstream through the lymphatic system [179].

[1]Chyme enters the small intestine where bile acts as an emulsifier of monoglycerides and fatty acids for their combination with water-based fluids to form micelles. Fatty acids are taken from the intestinal lumen into the enterocytes, where further hydrolysis takes place before reaching the endoplasmic reticulum for further complex lipid synthesis (triglyceride synthesis)

As briefly described in the above, the process of fat digestion and absorption is anything but simple. However, the triglycerides and cholesterol content of the meal seems to remain constant throughout the aforementioned break-down and reassembly process. Thus, different from the relative glucose-equivalent of carbohydrates given in Eq. (3.3), dietary fat metabolism seems to be directly proportional to the amount consumed. Moreover, the digestion of dietary fat seems to be considerably slower than that of carbohydrates. For instance, previous studies [180] indicate a mean gastric emptying rate (as percentage per hour) of 17.4±2.4%/h for the dietary fat and 22.8±1.8%/h for the carbohydrate portion of a mixed meal despite having no apparent intragastric separation for different macronutrients. Hence, we represent the dietary fat portion of a mixed meal separately from carbohydrates by $G_{\text{fat}}(t)$, which is given by

$$G_{\text{fat}}(t) = K_{\text{fc}} \cdot \overline{G}_{\text{EQ}}(t), \tag{5.2}$$

$$K_{\text{fc}} = \frac{\text{FAT}}{\text{AvCHO}}, \tag{5.3}$$

where $\overline{G}_{\text{EQ}}(t)$ is carbohydrate digestion/absorption with maximum rate of glucose appearance which dietary fat digestion is associated with, and fat-to-carbohydrate ratio K_{fc} represents the fat-to-carbohydrate ratio given the amounts (in grams) of dietary fat and carbohydrate consumed as FAT and AvCHO, respectively.

Digestion and absorption of lipids is also represented by a biphasic nature as

$$\frac{\mathrm{d}G_{\text{chy}}(t)}{\mathrm{d}t} = \frac{1}{\tau_{\text{chy}}} \left(-G_{\text{chy}}(t) + G_{\text{fat}}(t - L_{\text{mix}})\right), \tag{5.4}$$

$$\tau_{\text{chy}} = \left(\frac{c_1}{1 + e^{-c_2 K_{\text{fc}}}} - c_3\right) \tau_{\text{fat}}, \tag{5.5}$$

where $G_{\text{chy}}(t)$ represents chylomicron-triglyceride (CM-TG) appearance in the bloodstream, τ_{chy} is the time-constant of dietary fat absorption delay represented as a sigmoid function with constant parameters c_1, c_2 and c_3 and fat-to-carbohydrate proportion K_{fc}.

5.1.4 Plasma triglyceride (TG) compartmental model

Although NEFA is mostly considered for fatty acid metabolism as represented by several mathematical models in the literature, the representation of lipid-derived insulin resistance in the present model depends on the combination of postprandial TG and NEFA dynamics (see Figure 5.1 on page 95). First, for a mathematical representation of TG metabolism as a minimal compartmental model it is necessary to consider lipoprotein metabolism, as it is the most rele-

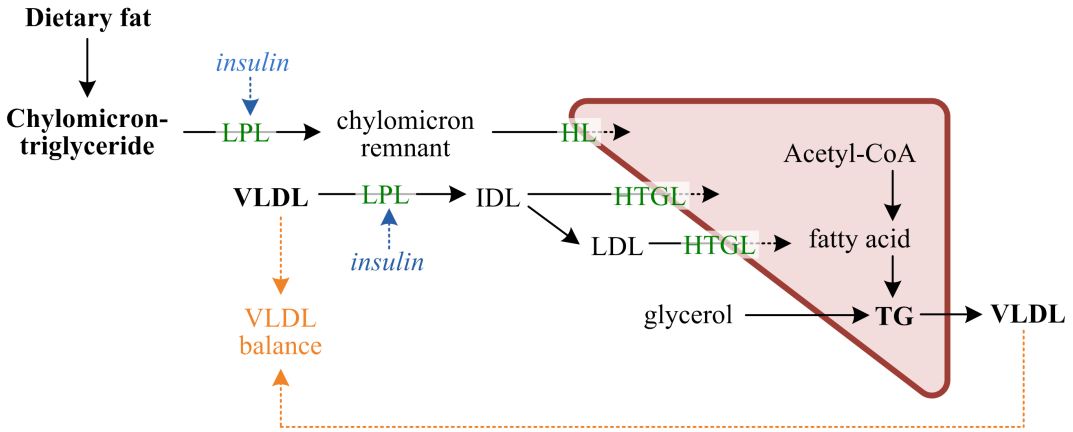

Figure 5.5: Regulation of lipoprotein metabolism in the liver. Postprandial lipid metabolism in particular present high levels of CM-TG and VLDL, which are considered in the present study for the minimal compartmental representation of plasma TG dynamics.

vant process involved and thus briefly described in the following.

Lipoproteins are lipid carriers for the transportation of insoluble lipids to/from the liver, muscles and adipose tissue. It is composed of TG and cholesteryl esters at the core and covered by phospholipids, free cholesterol and proteins in small amounts. Lipoproteins are divided into very-low-density lipoprotein (VLDL), low-density lipoprotein (LDL), intermediate-density lipoprotein (IDL), high-density lipoprotein (HDL) and chylomicron (CM). As shown in Figure 5.5, CM remnant is the by-product of CM after their TG content has been delivered. Similarly, VLDL also carries large quantities of TG and cholesterol to the body prior assembly (synthesis) in the liver as nascent VLDL, which after their TG content is delivered, VLDL remnants or IDL are either cleared or degraded into LDL by hepatic triglyceride lipase (HTGL). Although not directly considered in the compartmental model proposed in the present study, HDL is responsible for removal of excess cholesterol (packed in the other forms of lipoproteins) to the liver, which is commonly known as ‘reverse cholesterol transport’.

Among the different types of liproproteins, VLDL and CM not only follow a similar metabolic mechanism but are together known as triglyceride-rich lipoproteins (TRL) since they play a principal role in endogenous and exogenous TG metabolism, respectively. The remaining types of lipoprotein are not directly associated with postprandial lipid metabolism in particular and thus not further considered in the present study.

In this way, we propose a novel compartmental representation of plasma TG dynamics as

$$\frac{\mathrm{d}T(t)}{\mathrm{d}t} = -p_4 X(t) T(t) + p_5 \left(T_\mathrm{b} - T(t)\right) + \frac{G_\mathrm{chy}(t)}{V_\mathrm{T}}, \qquad T(0) = T_0 \tag{5.6}$$

where $-p_4 X(t) T(t)$ is plasma CM-TG clearance by LPL-induced hydrolysis, $p_5 \left(T_\mathrm{b} - T(t)\right)$ is hepatic VLDL balance, V_T is plasma distribution volume and $G_\mathrm{chy}(t)$ is exogenous plasma CM-TG appearance from the dietary fat content of a mixed meal.

By no coincidence postprandial TG dynamics in Eq. (5.6) is analogous to the glucose compartment of Bergman minimal model in Eq. (3.25). Plasma TG concentration is the result of exogenous and endogenous lipid metabolism, as given by meal-derived CM-TG appearance (ApoB-48) and endogenous hepatic VLDL production (ApoB-100), respectively. Moreover, as occurs with glucose uptake, insulin exerts a regulatory role in TG clearance by means of activation of a number of hepatic receptors, with an apparent preference for CM-TG uptake over VLDL-TG [181].

5.1.5 Plasma non-esterified fatty acid (NEFA) compartment model

As briefly summarized in section 2.5, several mathematical models of NEFA dynamics have been proposed in the past, including one specifically for postprandial state. Nevertheless, the large number of variables and parameters of these models do not adhere to the minimal compartmental approach of the mathematical model developed in Chapter 3. Therefore, we propose a novel compartmental representation of plasma NEFA levels given by

$$\frac{\mathrm{d}F(t)}{\mathrm{d}t} = -p_6 X(t) F(t) + p_7 \left(F_\mathrm{b} - F(t)\right) + \frac{F_\mathrm{sp}(t)}{V_\mathrm{sp}}, \qquad F(0) = F_0 \tag{5.7}$$

where $p_6 X(t) F(t)$ is NEFA uptake by insulin-mediated LPL activity, $p_7 \left(F_\mathrm{b} - F(t)\right)$ is fatty acid balance in adipose tissue including lipolysis and $F_\mathrm{sp}(t)$ is fatty acid spillover with distribution space V_sp. In particular, fatty acid spillover is represented as a first-order delay given by

$$\frac{\mathrm{d}T_\mathrm{sp}(t)}{\mathrm{d}t} = \frac{1}{\tau_\mathrm{sp}} \left(T(t) - T_\mathrm{sp}\right), \qquad T_\mathrm{sp}(0) = T_\mathrm{b} \tag{5.8}$$

$$F_\mathrm{sp}(t) = T_\mathrm{sp}(t) - T_\mathrm{b}, \tag{5.9}$$

where $T(t) - T_\mathrm{sp}$ is CM-TG from which fatty acid spillover due to LPL activity occurs, τ_sp is the time-constant delay to represent spillover during late postprandial state and $F_\mathrm{sp}(t)$ is spillover-

derived NEFA appearance from the splanchnic bed.

The physiological interpretation of the minimal NEFA model given by Eqs. (5.7)–(5.9) is as follows. During postprandial state (see Figure 5.6, left), high insulin levels simultaneously induce CM-TG uptake and suppress lipolysis. After reaching a plateau in systemic NEFA levels, reduction in plasma insulin levels reactivates lipolysis and thereby the gradual restoration of basal plasma NEFA levels. In addition to this, the increased LPL activity during postprandial CM-TG metabolism leads to a spin-off referred to as fatty acid 'spillover' [182], which apparently contributes to postprandial NEFA levels as typically observed as a rebound above basal levels during late postprandial state. During fasting state (see Figure 5.6, right), systemic NEFA levels are the result of the balance between β-oxidation in peripheral tissue and lipolysis in adipocytes (fat tissue), which are respectively regulated by insulin-mediated enzymes LPL and HSL considering basal insulin conditions. In this way, NEFA kinetics during both postprandial and fasting state depend largely on insulin for uptake and storage according to insulin-sensitive LPL receptors in an analogous way to GLUT-4 receptor for glucose regulation. Similarly, lipolysis has also an analogous dynamics to that of hepatic glucose balance depending on plasma insulin concentrations. Based on the above premise, we propose an original representation of NEFA dynamics in Eq. (5.7) identical to that of glucose considering their strong analogy during both postprandial and fasting state, and the main regulatory role of insulin for that matter.

5.1.6 Mathematical representation of insulin resistance

Besides the delaying effect of dietary fat on gut absorption of carbohydrates as detailed in the previous subsection, the present model also represents the indirect effect of lipid-derived insulin resistance on glucose-insulin metabolism. In general terms, insulin resistance state is a permanent metabolic condition wherein the ability of insulin to remove glucose from plasma is reduced and thus requires higher insulin concentrations to maintain glucose homeostasis. Although a high-fat diet is known to increase insulin resistance as short as in a five-day period [183], the mechanism involved in acute insulin resistance, *i.e.*, temporary insulin resistance in a several-hour span as in postprandial state, are largely unknown. Given these circumstances, we provide a brief summary of the current knowledge, the specific case of patients with T1DM, and some proposed mechanisms by which dietary fat induces acute insulin resistance in order to provide a physiologically-meaningful mathematical representation of lipid-derived insulin resistance in patients with T1DM.

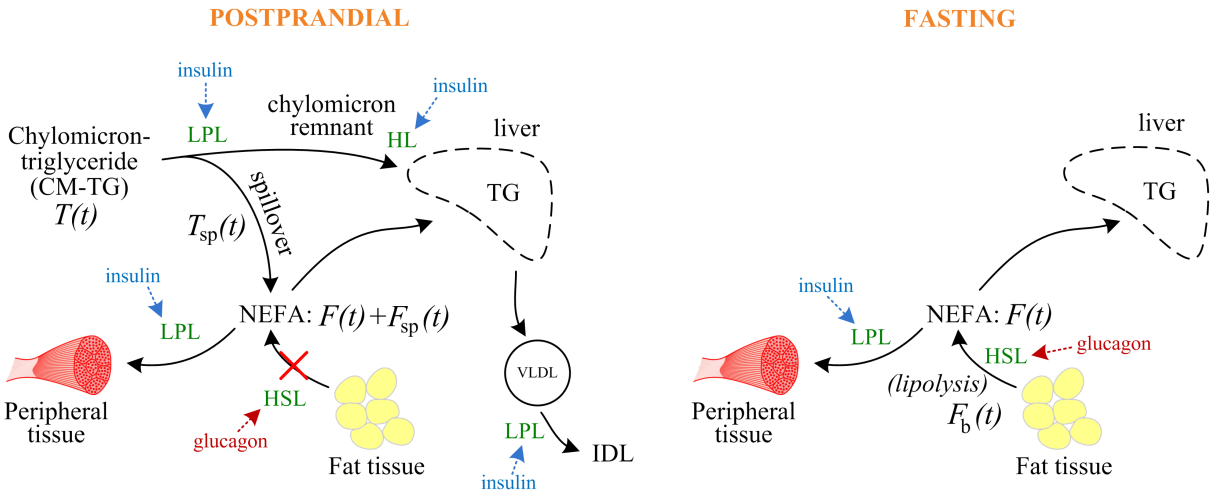

Figure 5.6: Simplified physiological representation of NEFA dynamics by the novel compartmental model proposed in Eq. (5.7). (Left) NEFA dynamics during postprandial state includes fatty acid uptake via insulin-activated LPL and inhibition of lipolysis by the regulatory action of insulin. (Right) During fasting state, NEFA dynamics is characterized by the balance between lipolysis and fatty acid uptake by the liver and peripheral tissue by the action of basal insulin levels on HSL and LPL, respectively.

Causes of insulin resistance

Insulin resistance is typically observed in—but not limited to—the metabolic syndrome, insulin-deficient T1DM and type 2 diabetes (T2DM). Since insulin is the principal signaling hormone for both glucose and fatty acid metabolism, insulin resistance is not only associated with dysglycemia but also dyslipidemia (see Figure 5.7). The latter is characterized by enhanced VLDL secretion, hypertriglyceridemia, increase in plasma cholesterol levels and reduction in HDL [184]. Others present increased VLDL-cholesterol levels due to an abnormal cholesterol synthesis, in addition to higher TG and VLDL-TG despite having normal plasma NEFA levels [185]. An abnormal increase in hepatic HTGL during insulin resistance is also observed [186] when it normally should decrease due to the effect of hepatic insulin. The molecular mechanisms involved in insulin resistance include interference of insulin signaling in the liver, suppression of glycogenolysis and lipolysis, impaired suppression of EGP and overestimulation of β-cell insulin secretion [187, 188], in addition to reduction in carbohydrate oxidation and inhibition of insulin-mediated glucose uptake, glycogen synthesis and glycolysis due to elevated NEFA levels [189]. These studies suggest that high NEFA levels affect every single component associated with glucose-insulin metabolism ranging from hepatic synthesis

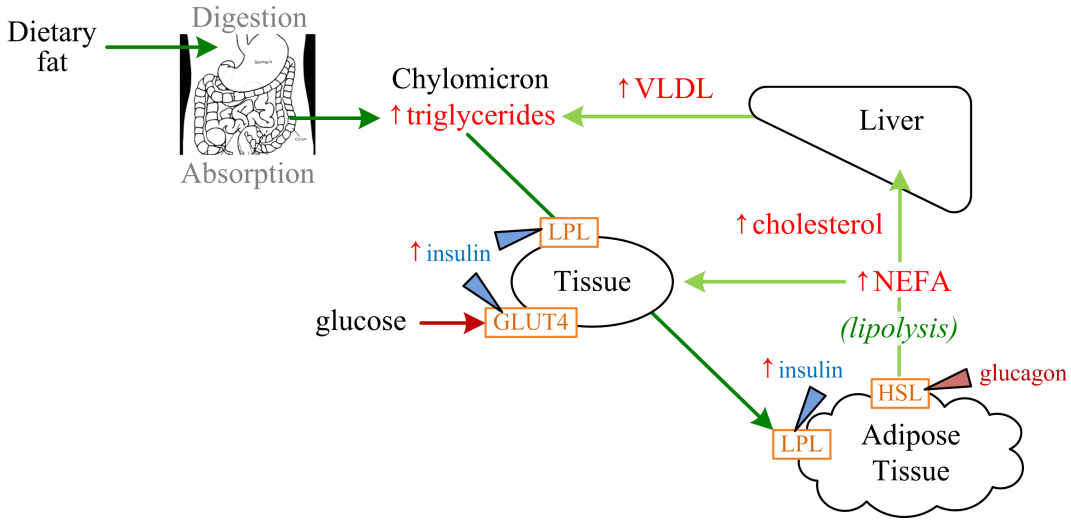

Figure 5.7: Pathology of insulin resistance in exogenous and endogenous lipid metabolism. Insulin resistance is characterized by an abnormal lipid profile (dyslipidemia) commonly seen in healthy subjects suffering from the metabolic syndrome, T2DM and insulin-deficient T1DM. Although insulin resistance is commonly associated with increased NEFA levels, the pathogenesis of postprandial insulin resistance due to dietary fat consumption is currently unknown.

to glucose uptake and insulin-mediated enzymes in favor of β-oxidation of NEFA, as confirmed by infusion of large doses of fat and heparin [190].

As briefly described in the above, the complexity of lipid metabolism and the number of possible mechanisms by which insulin resistance develops might explain the absence of consensus on its etiology, despite extensive research on the subject from chemical to systemic level [191]. One certain fact is that there exists a strong association between fat metabolism and insulin, both during normal conditions and dislipidemia [192]. Nevertheless, insulin-regulatory hormones, better known as incretins, seem to be unrelated to lipid-induced insulin resistance according to studies that indicate an extremely large increase in gastric inhibitory polypeptide after consumption of a fat-added meal, although the insulin response remained unaltered [193].

Arguably one determinant factor is the difficulty to measure insulin sensitivity during postprandial state. Among the different types of glucose/insulin infusion protocols in clinical settings, the hyperinsulinemic-euglycemic clamp technique[2] [194] is used for a quantitative as-

[2]Clinical method to quantify insulin sensitivity by infusion and maintenance of plasma insulin levels at 100μU/mL (hyperinsulinemic) and variable infusion of glucose to maintain BG levels at normoglycemia (euglycemic). Hence, the glucose infusion rate is a measure of glucose uptake ability (insulin sensitivity) at steady-state conditions.

sessment of insulin sensitivity. This method cannot measure continuously the degree of insulin resistance, as after digestion of a high-fat meal.

Insulin resistance in T1DM

In patients with T1DM, insulin resistance is identified by larger basal and bolus insulin needs [195] or present at the time of diagnosis and reversed shortly after the start of insulin therapy [196]. Lipid-derived insulin resistance in these patients is even less understood since it is only limited to the comparison of BG excursion after consumption of test meals with and without added fat [25, 33], whereas others suggest that insulin resistant state might be eliminated after a few months following a low-fat diet [197].

The etiology of insulin resistance specifically in patients with T1DM, the absence of endogenous insulin secretion not only affects BG levels but also lipid metabolism because of the role of insulin-mediated LPL enzyme [198]. Furthermore, patients with poor BG management suffer from a high lipid profile as well, including hypertriglyceridemia at the onset of the disease [199] and marked DKA [200, 201]. Even though these abnormalities are shortly reversed by appropriate insulin therapy, there seems to be a particular difference in postprandial lipoprotein particles in patients with T1DM and nondiabetics, such as accumulation of macrophages after fat ingestion for at least 7 hours [202], and increased postprandial lipid peroxidation after high-fat meals including increase in plasma TG from 1.0 mmol/L fasting to a maximum of 1.6 mmol/L [203]. In particular, poorly-controlled T1DM patients seem to have a reduced peripheral glucose uptake caused by the inability to suppress lipolysis, as observed by increased NEFA levels [204]. Hence, the etiology of insulin resistant state in T1DM is similarly attributed to increased fatty acids as observed in their nondiabetic counterparts.

For a physiologically-meaningful mathematical representation of insulin resistance in our model proposal, we consider a theoretical explanation of the mechanisms by which fatty acids affect glucose uptake in the following.

Glucose-fatty acid cycle (Randle cycle)

In 1963, Randle *et al.* [205] proposed a theoretical explanation for an apparent fuel selection mechanism between the two main energy substrates: glucose and fatty acids, and as such the Randle cycle is alternatively known as 'glucose-fatty acid cycle'. Clinical studies at the time showed that IV lipid infusion intriguingly led to a reduction in glucose uptake, and thus the authors proposed a hypothesis wherein the utilization of one substrate inhibits the use of another. Basically, it is proposed that glucose and fatty acids compete as energy substrates due

to increased β-oxidation of NEFA while decreasing glucose oxidation altogether due to a large increment in acetyl-CoA in skeletal muscle [206]. More recently, fatty acid oxidation over glucose has been demonstrated to effectively occur during mitochondrial respiration process at a cell-level [207].

Glucose-fatty acid cycle reversed

The glucose-fatty acid cycle states that NEFA is preferred over glucose as energy substrate based on the assumption that glucose oxidation equals glucose uptake, *i.e.*, the totality of glucose uptake is oxidized. However, the 'glucose-fatty acid cycle reversed' [208] proposes a strong opposite stance with equally valid arguments to refute the Randle cycle theory utilizing accurate measurement methods not available at the time.

For instance, in one study [209], healthy nondiabetic subjects were given (a) a very large glucose infusion (8 mg·kg^{-1}·min^{-1}) to ensure glycolysis in all tissues[3], followed by (b) a constant intravenous infusion of fat emulsion and heparin to stimulate LPL activity and hydrolysis of TG[4]. As a result, there was no effect of NEFA on plasma glucose oxidation even though a 20-fold increase in FFA concentration was observed, even though the considerable reduction in total glucose oxidation was found to be due to a similar reduction in glycogen oxidation. Following a similar procedure, other studies [210] confirmed the inhibition of EGP considering different doses of NEFA infusion (50, 550 and 750 μmol), in addition to a dose-dependent decrease of glycogen synthesis[5]. More recent studies reached a similar conclusion on NEFA-induced insulin resistance and its effect on insulin-dependent glucose uptake and glycogenolysis [211], whereas some others [212] include inhibition of muscle glycogen synthesis to account for the reduced intravenous glucose infusion typically observed in the Randle cycle.

In this way, glucose-fatty acid cycle reversed states that it is actually the reduction in glucose uptake—mainly from the liver—, that stimulates fatty acid uptake. In fact, reduction in LPL activity—additionally verified at a cell-level—was observed after consumption of a standardized low-fat meal in insulin-sensitive and resistant nondiabetic subjects [213], which confirms that insulin resistance is the cause—not the effect—of reduced glucose and fatty acid uptake.

[3] in addition to a large carbohydrate meal the night before, and verification of maximum rate of oxidation with a respiration quotient of 0.97±0.07.

[4] fat infusion given at a rate of 1 ml/min, and initial heparin bolus of 500 U followed by a continuous infusion of 500 U/h for the following 2 hours.

[5] glycogenesis, or storage of plasma glucose in the liver as glycogen.

Chylomicron-triglyceride effect

Even though the etiology of insulin resistance is commonly attributed to NEFA levels, a clinical study in nondiabetics [214] suggests that increase in TG levels is actually the cause of lipid-derived insulin resistance after consumption of two isocaloric test meals with dietary fat composition such that induced elevation of only TG or both TG and NEFA levels. The resulting decrease in insulin sensitivity—as directly measured by IVGTT before and after the test meals—for both test meals demonstrated that increase in TG levels induce postprandial insulin resistance regardless of NEFA levels. Although a similar study has not been verified for T1DM patients in the literature, to the best of our knowledge, clinical studies [215] that include postprandial TG excursion in these patients also indicate the same impact of a lipid load independent of large variations in postprandial NEFA levels. Furthermore, other studies on lipid-derived insulin resistance indicate that high Apo-48 levels (a type of apolipoprotein present in CM-TG) have been observed in insulin resistant state of animal models [216,217]. In humans, also, Apo-48 has the closest relationship with the metabolic syndrome above other types of lipids [218] and thus the ratio of ApoB-to-ApoA (apolipoprotein present in HDL) has also been proposed as an alternative diagnosis criterion of insulin resistance that can be eventually implemented in clinical guidelines [219].

In this way, despite the common association of insulin resistance with increase in plasma NEFA levels, the studies above provide cogent evidence that lipid-derived insulin resistance is directly associated with elevation in plasma TG levels, as can be easily inferred from large CM-TG absorption from the gut after consumption of mixed meals with considerable dietary fat content.

Mathematical representation of postprandial insulin resistance

Since the mathematical model of glucose-insulin metabolism in patients with T1DM originally developed in Chapter 3 is based on Bergman model, we examine the representation of insulin sensitivity according to its compartmental structure (see Figure 5.8) beyond its general definition as 'the quantitative influence of insulin to increase the enhancement of glucose disappearance' [46]. The physiological representation of insulin sensitivity in the minimal model comprises insulin-dependent glucose uptake in the liver and peripheral tissue as given by Eqs. (2.10) and (2.11) (see page 17), respectively, from which insulin sensitivity is explicitly defined as

$$S_{\mathrm{I}} = -\frac{k_2}{k_3}(k_4 + k_6), \tag{5.10}$$

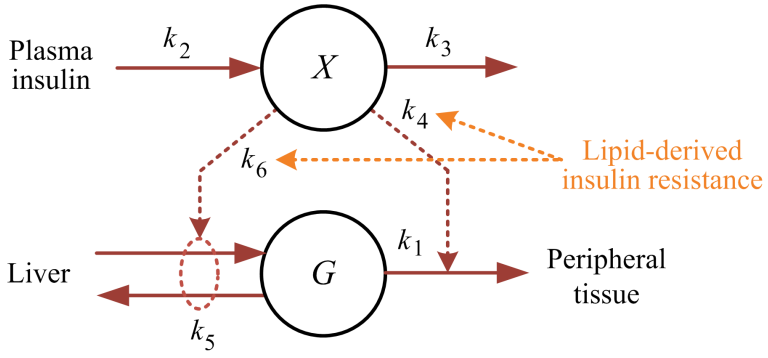

Figure 5.8: Representation of lipid-induced postprandial insulin resistance in the present study by alteration of insulin-dependent glucose uptake parameters of the minimal model according to the original definition of insulin sensitivity by Bergman *et al.* [46].

where k_2 is rate of decrease in insulin-dependent glucose uptake ability, k_3 is insulin disappearance (insulin dissociation constant) in the interstitial fluid, k_4 is insulin-dependent glucose uptake into peripheral tissue and k_6 is insulin-dependent hepatic glucose uptake. Considering explicit parameters of the minimal model, insulin sensitivity parameters are given by $p_3 = k_2(k_4 + k_6)$ and $p_2 = -k_3$, where the negative sign implies that increase in insulin increases glucose uptake.

Considering the exhaustive analysis of lipid-derived insulin resistance in the literature, we utilize the compartmental models of TG and NEFA dynamics given by Eqs. (5.6) and (5.7), respectively, to represent meal-derived insulin resistance as a combination of (a) postprandial increase in TG levels as a result of dietary fat consumption and (b) NEFA-derived insulin resistance. For the latter in particular, we propose a novel interpretation of insulin resistance whose physiological representation includes the combined effect of increased NEFA levels from fatty acid spillover according to the Randle cycle, in addition to the reduced ability to suppress glycogenolysis according to the glucose-fatty acid cycle reversed (see Figure 5.9). In this way, since parameter p_3 of the minimal model represents insulin-dependent glucose uptake in hepatic and peripheral tissue, we propose an extension of such parameter to a variable that includes postprandial CM-TG increase from basal levels as the principal cause of lipid-derived acute insulin resistance and late postprandial fatty acid spillover for the representation of lipid-derived

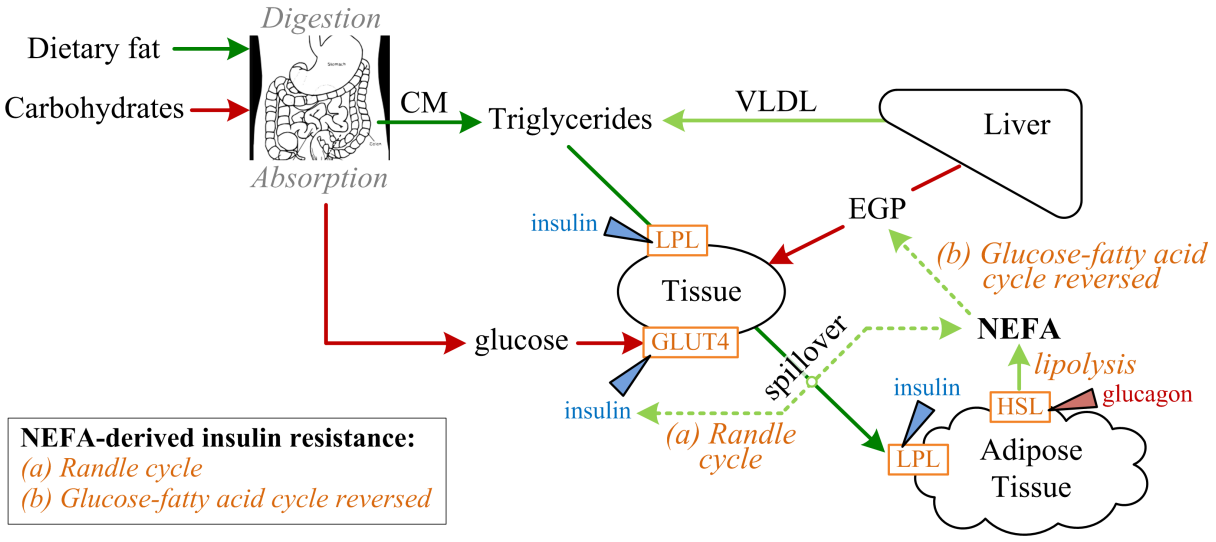

Figure 5.9: Novel interpretation of NEFA-derived insulin resistance proposed in the present study by considering both the Randle cycle and reversed glucose-fatty acid cycle in spite of their apparently contrasting viewpoints. The former provides a theoretical explanation of the effect of increased NEFA levels on reduction of insulin sensitivity, which is caused by fatty acid spillover from TG metabolism during postprandial state. The latter refers to the inability of insulin to suppress EGP due to high NEFA levels, thereby affecting the regulation of glucose.

insulin resistance as

$$p_3'(t) = p_3 - p_8 \mathrm{IR_T}(t) - p_9 \mathrm{IR_F}(t), \tag{5.11}$$

$$\mathrm{IR_T}(t) = T(t) - T_\mathrm{b}, \qquad 0 \le \mathrm{IR_T}(t) \le \mathrm{IR_{T,max}} \tag{5.12}$$

$$\mathrm{IR_F}(t) = \frac{c_4}{1 + e^{-c_5 F(t)}} - c_6, \qquad 0 \le \mathrm{IR_F}(t) \le \mathrm{IR_{F,max}} \tag{5.13}$$

where $\mathrm{IR_T}$ is decrease in insulin-dependent glucose uptake with maximum value $\mathrm{IR_{T,max}}$ and parameter p_8; and $\mathrm{IR_F}$ is decrease in insulin-dependent glucose uptake due to fatty acid spillover with maximum value $\mathrm{IR_{F,max}}$ and parameter p_9.

Although high VLDL1 ApoB-100 (a type of apolipoprotein metabolized in the liver) levels are characteristic of insulin-resistant subjects [220], there is an absence of correlation with dietary fat consumption and BG levels, thus only CM-TG as given by $T(t) - T_\mathrm{b}$ is considered.

Physiologically-relevant parameter settings

For parameters in the present model with a clear physiological representation we consider clinical studies of gut transit of mixed meals and the effect of TG and NEFA on lipid-derived insulin resistance as follows:

- *Gut transit of mixed meals*: The biphasic gastric emptying of carbohydrates in Eq. (5.1) is represented with $L_{\text{mix}} = 4$ min and $\tau_{\text{mix}} = 20$ min. For the gut transit of dietary fat in Eq. (5.4), we consider the same value for L_{mix} whereas parameters of the sigmoid function in Eq. (5.5) are set to $\tau_{\text{fat}} = 170$ min, $c_1 = 0.4625$, $c_2 = 1.7527$ and $c_3 = 0.0845$ such that for fat-to-carbohydrate proportions $K_{\text{fc}} > 1$, the delay constant τ_{chy} has values close to τ_{fat}.

- *Insulin resistance due to postprandial TG increase:* Considering that the maximum decrease in insulin sensitivity is half its fasting state value after consumption of a high-fat meal [214], we replace $p_3' = 0.5 \cdot p_3$ in Eq. (5.11) considering $\text{IR}_{\text{T,max}} = 1$ mmol/L for the maximum increase in postprandial TG levels in patients with T1DM after consumption of a mixed meal with 100 g fat [215] and thus we obtain parameter $p_8 = 0.5 \cdot p_3$ from

$$\frac{p_3'}{2} = p_3 - p_8 \cdot \text{IR}_{\text{T,max}}. \tag{5.14}$$

- *Insulin resistance due to late postprandial fatty acid spillover:* A clinical study by Belfort *et al.* [221] indicates a dose-response effect of NEFA on insulin resistance, wherein exogenous fatty acid infusions of 30 ml/h, 60 ml/h and 90 ml/h with respective plasma NEFA levels of 695 μmol/L, 1251 μmol/L and 1688 μmol/L lead to a corresponding decrease in glucose uptake of 22% (6 male and 3 female, 31$\pm$4 years old and BMI 24$\pm$1), 30% (3 male and 3 female, 25$\pm$1 years old and BMI 24$\pm$1) and 34% (4 male and 2 female, 26$\pm$2 years old and BMI 24$\pm$1). Hence, provided that $p_9 = p_3$, model parameters in Eq. (5.13) are set to $c_4 = 0.479$, $c_5 = 1.353$ and $c_6 = 0.0706$ to represent insulin resistance due to increased NEFA levels (see Figure 5.10) considering a maximum reduction $\text{IR}_{\text{F,max}} = 34\%$.

Model parameter setting

Model parameters of TG and NEFA compartments in Eqs. (5.6) and (5.7), respectively, are fitted with clinical data from different clinical studies in patients with T1DM as detailed in the following.

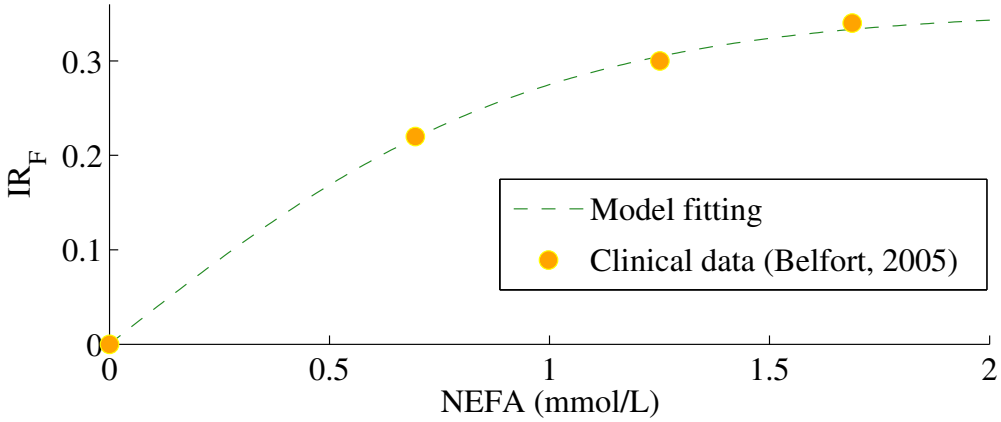

Figure 5.10: Sigmoid function with parameters $c_4 = 0.708$, $c_5 = 2.069$ and $c_6 = 0.354$ in Eq. (5.13) to represent NEFA-induced insulin resistance IR_F.

1. We consider TG excursion after a mixed meal with fat content of 100 g and basal insulin infusion at a reduced dose of $u_\text{s}(t) = 6.7 \times 10^{-3}$ IU/min (0.4 IU/h) from a study by Lewis *et al.* in patients with T1DM [215], from which we determine parameters $p_4 = 0.1$ min^{-1}, $p_5 = 5.4 \times 10^{-3}$ min^{-1} and $V_\text{T} = 12$ L for the TG compartmental model given in Eq. (5.6).

2. Non-insulin dependent parameter p_7 is identified from NEFA excursion in insulin-deprived T1DM patients using clinical data from Burge *et al.* [222]. In such study, normoglycemia is initially maintained at 6.3±0.5 mmol/L by means of IV regular human insulin infusion and withdrawn at $t = 0$. To reproduce the same scenario, we consider similar initial parameters in the mathematical model of glucose-insulin metabolism, including $G_\text{meal}(t) = 0$ for model parameter estimation of non-insulin dependent glucose uptake $p_1 = 0.009$ min^{-1} and non-insulin-dependent lipid uptake $p_7 = 0.025$ min^{-1} and lipolysis given by $F_\text{b} = 1.5$ mmol/L.

3. Postprandial NEFA excursion including fatty acid spillover after consumption of a mixed meal with 60 g pasta, 80 g veal, 200 g vegetables dressed with 20 g olive oil, 50 g white bread and 150 g apple (with presumably carbohydrate and dietary fat intakes of 65 g and 28 g, respectively) according to a study by Pampanelli *et al.* [223]. For an insulin bolus given 5 min prior to mealtime according to such study, we consider an insulin bolus of $u_\text{s}(-5) = 9$ IU for parameter identification of insulin-mediated NEFA uptake to $p_6 = 114.7$ min^{-1}, $\tau_\text{sp} = 460$ min and $V_\text{sp} = 6.1$ L.

5.1.7 Compartmental representation of the proposed model

The minimal model of mixed meal effect on glucose and fat metabolism proposed in the present chapter is shown in Figure 5.11, where the mathematical model of gluocose-insulin metabolism developed in Chapter 3 is extended to include gut absorption of dietary fat and the delaying effect on carbohydrate digestion. Moreover, two additional single-compartments for plasma TG (T) and NEFA (F) are included to represent lipid metabolism and their explicit utilization to represent the effect of lipid-derived postprandial insulin resistance.

5.2 Simulation

In this section, we present simulation results implemented on MATLAB® of parameter fitting from previous clinical data. Nevertheless, due to the extremely limited clinical data in the literature for patients with T1DM in particular, model fitting is done separately for the gastric emptying of mixed meals, as well as each compartment of TG and NEFA dynamics.

5.2.1 Simulation settings

Simulation of gastric emptying in the present model considers the sum of carbohydrates and dietary fat as a chyme given by $G_{\text{ext}}(t) + G_{\text{chy}}(t)$ considering a mixed meal input of 4.6 g carbohydrates and 26.3 g fat (9.1 g protein content is not considered) for a total 260 kcal content according to a study [224]. Clinical data of gastric emptying retention in patients with T1DM in such study is used for model-fitting parameters of emptying rate -0.0089 and $\beta = 1.21$ from Siegel model [45], in addition to nondibetic subjects with parameters of emptying rate -0.015 and $\beta = 1.25$ for reference of normal gastric emptying. Parameters of the model of glucose-insulin metabolism in T1DM are as detailed in Chapter 3 in all the simulation results of the present section, unless otherwise specified.

5.2.2 Simulation of gastric retention of a high-fat food

Rate of gastric emptying in the present model is compared with clinical data from 41 patients with T1DM (20 male and 21 female, 33.1$\pm$11.6 years old, 69.7$\pm$9.7 kg weight) using Siegel model-fitted parameters after consumption of a high-fat mixed meal as shown in Figure 5.12, where the rate is expressed as gastric retention. The present model presents a slightly slower gastric emptying constant throughout the postprandial state, although the total gastric emptying time is comparable to Siegel model.

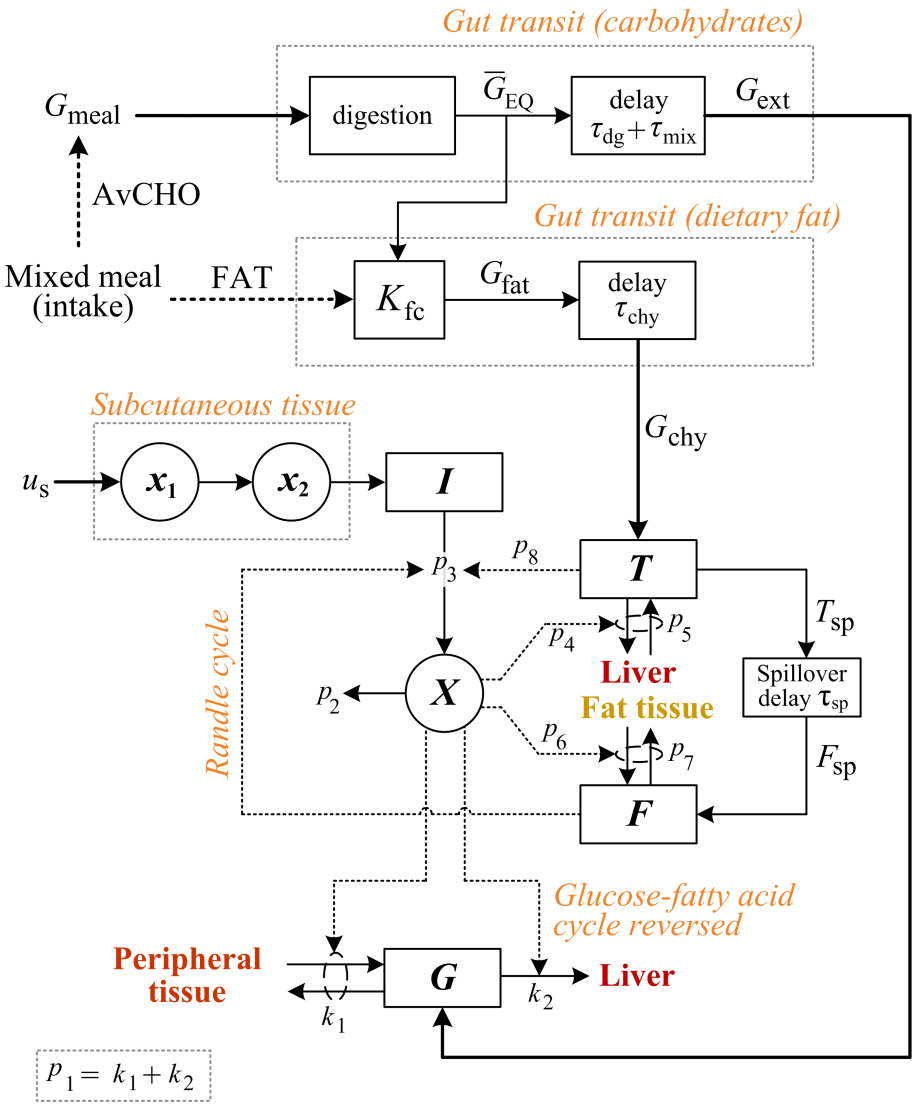

Figure 5.11: Proposed mixed meal model as an extension of the model developed in Chapter 3 to include the effect of dietary fat on glucose-insulin metabolism in patients with T1DM as (a) gut transit of mixed meals and the delaying effect of dietary fat on gastric emptying of carbohydrates, and (b) lipid-derived insulin resistance according to variation in insulin-dependent glucose uptake parameter p_3 of the minimal model, which in turn is affected by postprandial increase in plasma TG and NEFA levels according to a novel compartmental representation proposed in the present study.

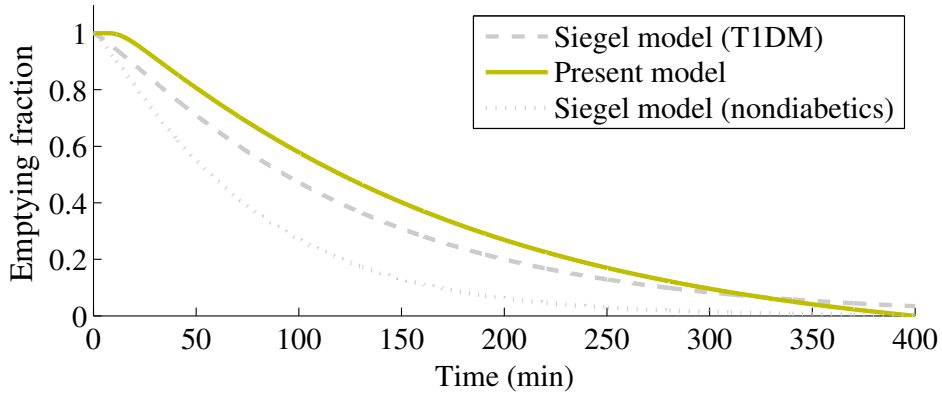

Figure 5.12: Gastric emptying retention proposed in the present study after ingestion of a high-fat meal composed of 4.6 g carbohydrate and 26.3 g fat, compared to fitted parameters from clinical data in 41 patients with T1DM (20 male and 21 female, 33.1±11.6 years old, 69.7±9.7 kg weight) using Siegel model of gastric retention with parameters of emptying rate -0.0089 and $\beta = 1.21$. For reference, we also consider control (nondiabetics) subjects with emptying rate -0.015 and $\beta = 1.25$ [224].

5.2.3 Simulation of postprandial TG excursion

Simulation results for postprandial TG excursion in 7 patients with T1DM (6 female and 1 male, 30.3±2.0 years old, BMI 23.9±0.8 kg/m^2) after a fat load of 100 g is given in Figure 5.13, where parameters of the TG compartmental model in Eq. (5.6) are fitted to clinical data from Lewis *et al.* [215].

5.2.4 Simulation of insulin-deprived lipolysis

The exaggerated lipolysis in patients with T1DM [222] during insulin-deprived state, as represented with parameter F_{b} in the present model, is shown by simulation of NEFA excursion in 10 T1DM patients (3 male and 7 female, 38 years old average, 68.5 kg and BMI 23.7 kg/m^2) as shown in Figure 5.14, wherein maximum lipolysis reaches a maximum of $F_{\mathrm{b}} = 1.5$ mmol/L at the rate specified by parameter p_7.

5.2.5 Simulation of postprandial response to a high-fat mixed meal

Simulation of postprandial BG and NEFA excursion of the mathematical model proposed in the present study is compared to clinical data from 6 patients with T1DM (3 male and 3 female,

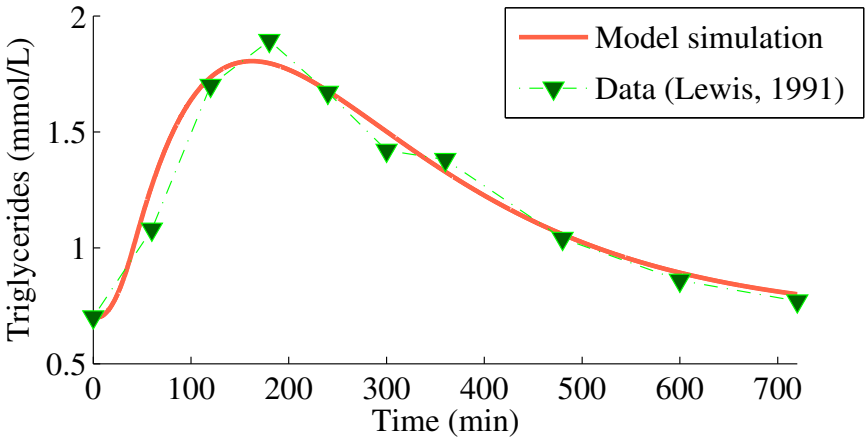

Figure 5.13: Parameter fitting of the TG compartmental model proposed in Eq. (5.6) using clinical data of postprandial TG excursion after consumption of 100 g fat from 7 subjects with T1DM (6 female and 1 male, 30.3±2.0 years old, BMI 23.9±0.8 kg/m^2) from Lewis *et al.* [215].

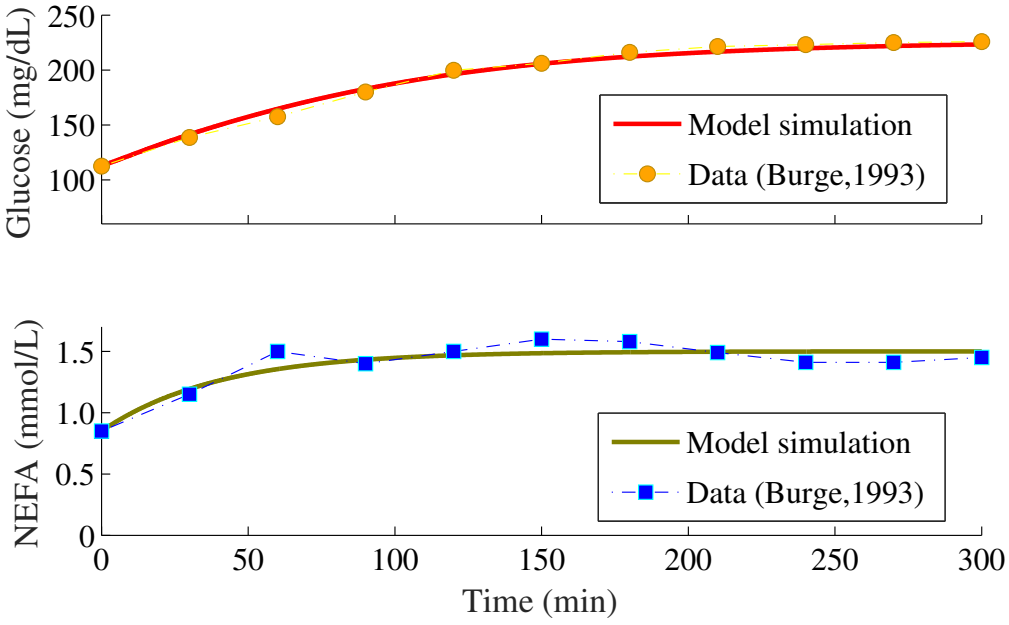

Figure 5.14: Postprandial BG (top) and NEFA (bottom) excursions during fasting state with no exogenous insulin infusion, from which non-insulin mediated NEFA balance is set to $p_7 = 0.025$ min^{-1}. Comparison with clinical data from 10 subjects with T1DM (3 male and 7 female, 38 years old average, 68.5 kg and BMI 23.7 kg/m^2) from Burge *et al.* [222].

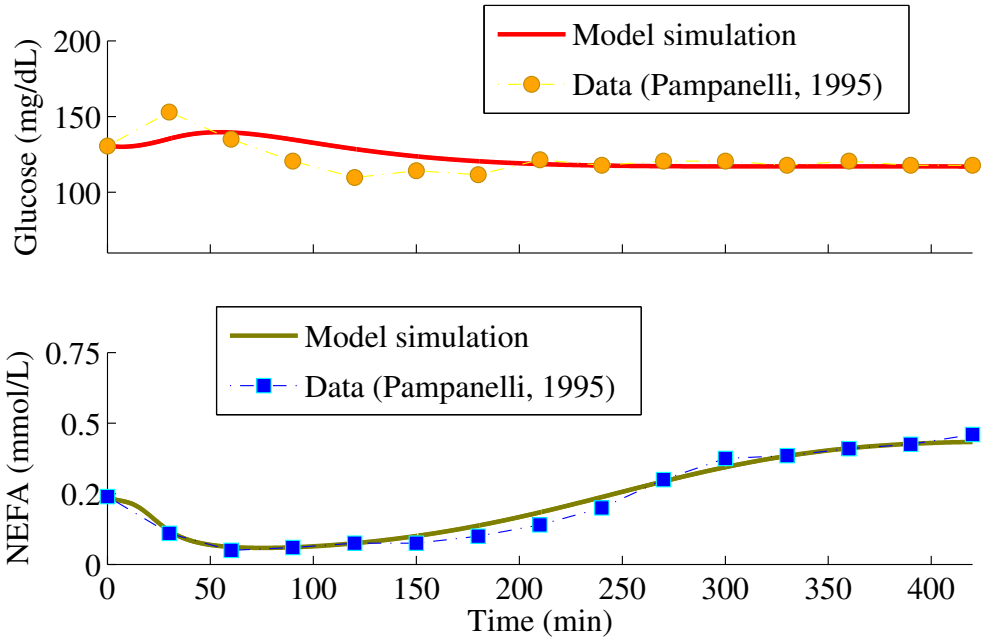

Figure 5.15: Simulation of postprandial BG and NEFA levels after a high-fat mixed meal consisting of 65 g carbohydrates and 28 g dietary fat, along with a bolus of $u_s(-5) = 9$ IU. Comparison with clinical data from 6 subjects with T1DM (3 male and 3 female, 25±2 years old, BMI 21.8±0.5 kg/m^2) from Pampanelli *et al.* [223].

25±2 years old, BMI 21.8±0.5 kg/m^2) according to the same research design described by Pampanelli *et al.* [223], with results shown in Figure 5.15. Postprandial BG excursion in the present model has a considerable difference with clinical data for the first 200 min, although stabilization during late postprandial state is similarly represented. Postprandial NEFA excursion throughout the postprandial state resembles clinical data very closely, including fatty acid spillover at $t > 300$ min.

5.3 Discussion

In the present chapter we propose a mathematical model of mixed meals that represents the effect of dietary fat on postprandial glucose-insulin metabolism using a minimal compartmental approach. Dietary fat affects indirectly glucose metabolism by reducing the gastric emptying of the mixed meal and insulin metabolism by causing lipid-derived increase in insulin resistance. Specific points related to the current model proposal are further discussed in the following.

- *Model overview*
  The present mixed meal model has a thorough consideration of the most relevant physiological processes involved in both exogenous and endogenous lipid metabolism beyond the sole impact on BG levels on patients with T1DM. It is also particularly important to provide a minimal representation of glucose, lipids and insulin metabolism for its intended utilization in model-based BG control purposes. Because of the complexity involved in previous models of gastric emptying and NEFA dynamics in the literature, we coupled the model of glucose-insulin metabolism from carbohydrates developed in Chapter 3 to a new compartmental representation of plasma TG and NEFA concentration to represent their combined effect on acute insulin resistance as a result of dietary fat consumption.

- *Comparison to Roy model*
  The present model is comparable to a previous mixed meal model proposed by Roy *et al.* (see Appendix A.7 on page 160) since both include a minimal representation of glucose dynamics based on Bergman model and a minimal compartmental representation of lipid metabolism. Nonetheless, Roy model considers a compartment F to represent plasma FFA levels, which is utilized to extend the glucose compartment of the minimal model to include the lipolytic effect of hyperglycemia and FFA-induced impairment of glucose uptake. Two additional remote-insulin compartments Y and Z are also considered to represent the effect of insulin on plasma FFA levels and the effect of FFA on glucose uptake, respectively. In particular, they assume an explicit association of lipolysis with hyperglycemia based on studies in rats. However, studies in humans [225] actually suggest an inverse relationship, whereas studies in nondiabetics and T1DM patients s well [226] indicate an absence of correlation between hyperglycemia and fatty acid turnover. Compared to Roy model, the present study considers two single-compartments for plasma TG and NEFA dynamics, given by T and F, respectively. While the former is directly affected by dietary fat consumption, the latter represents not only lipolysis but also fatty acid spillover. Different from Roy model, BG levels are not included in the minimal compartmental representation proposed in our study due to the absence of evidence in clinical studies between hyperglycemia and lipolysis.

- *Biphasic gastric emptying model*
  Remarkably accurate models of gastric retention such as Elashoff and Siegel models have been proposed in the past to represent the biphasic nature of gastric emptying of mixed meals. Their utilization in our model, however, would require their modification from

gastric retention to emptying rate, including the increased complexity due to the necessity to include the variable τ_{chy} as given in Eq. (5.5). In this way, we extend the single-delay model of gut absorption of carbohydrates in Eq. (3.23) to include the biphasic gastric emptying nature of high-fat mixed meals as given by Eq. (5.1). Simulation results for a high-fat mixed meal in Figure 5.12 show an acceptable representation of the gastric emptying rate of mixed meals without having to resort to considerable modifications to the original model of carbohydrates digestion/absorption in Chapter 3.

- *Model identifiability from clinical data (parameter estimation)*
  Simulations of the present model with clinical data show that the minimal compartmental representation of lipid metabolism from dietary fat consumption provides an accurate representation of lipid metabolism. However, the present study only provides a theoretical framework that needs a solid methodology for model parameter validation in clinical settings. In keeping with a minimal representation of exogenous and endogenous lipid metabolism, we consider only four parameters in total, which can be identified with clinical methods currently available such as oral [U-^{13}C] palmitic acid for meal-derived fatty acids and intravenous [$^{2}H_2$] palmitate to distinguish between CM-TG and VLDL-TG [227] and the standardization of oral lipid tolerance tests [228], as occurs with OGTT. In this way, the compartmental representation of TG and NEFA dynamic proposed is not only accurate, but also provides a feasible methodology for model parameter identification.

- *Compartmental representation of plasma TG and NEFA levels*
  In the present study, plasma TG levels are represented by the combined balance between exogenous meal-derived dietary fat appearance fro CM-TG and endogenous fat metabolism from VLDL-TG, where the former contributes to increases in postprandial TG levels in a considerably larger extent [181]. Plasma NEFA dynamics not only include the representation of lipolysis but also fatty acid spillover, although the limited amount of studies in the literature does not currently provide a quantitative estimation relative to the amount of dietary fat consumed [229]. Both plasma TG and NEFA compartments in Eqs. (5.6) and (5.7), respectively, have a strong resemblance to that of plasma glucose in the minimal model in Eq. (3.25). Besides their similar dynamics and interaction with peripheral tissue and the liver according to the regulatory role of insulin, their biochemical reactions have an interesting resemblance, such as long-chain fatty acid uptake being regulated by translocation of insulin-sensitive fatty acid transporters as occurs with glucose, among others [230].

- *Mathematical representation of insulin resistance*
  To the best of our knowledge, lipid-derived insulin resistance in Eq. (5.11) provides a unique interpretation of the different findings in the areas of endocrinology, nutritional sciences and biochemistry to represent its etiology as postprandial CM-TG excursion and increased NEFA levels during late postprandial state due to fatty acid spillover. While high NEFA levels are commonly accepted to be the cause of insulin resistance, dietary fat consumption is not directly associated to NEFA metabolism. It is thus comprehensible that a study [214] suggests TG to be the actual cause of meal-derived insulin resistance, which also reveals the extremely poor understanding of acute insulin resistance in present medicine and nutrition sciences. The proposal of the Randle cycle several decades ago might have deviated the attention from other alternative causes, including TG metabolism, since it seems to be an appealing hypothesis on substrate competition between glucose and fatty acids. Because of the validity of clinical studies that support the existence of the Randle cycle, we include a mathematical representation of NEFA-derived insulin resistance to a maximum of 34% [221] (see Figure 5.10) as a result of increased NEFA levels. Furthermore, glucose-fatty acid reversed also provides an interesting vantage point originally interpreted as 'opposed' to that of the Randle cycle. By personal interpretation, instead of selecting only one viewpoint—which implies denying the other—to represent insulin resistance in our model, we consider both stances as valid to propose a complementary mathematical representation of the glucose-fatty acid cycle and its reversed counterpart (see Figure 5.9) as a spiral between increased NEFA levels $F(t)$ and reduction in insulin effect $X(t)$ by means of $p_3'(t)$ as given in Eqs. (5.7) and (5.11).

- *Future direction: Second-meal effect*
  The present mixed meal model provides the postprandial metabolic response to a single meal, which might be extended to a mathematical model of diurnal glucose-insulin metabolism by sequential meal inputs in $G_{\text{meal}}(t)$. However, consumption of high-fat meals have particular metabolic effects such as the existence of the 'second-meal effect', which is characterized by an exaggerated rise in postprandial TG levels despite consumption of a low-fat meal [231, 232]. Such intriguing response is believed to be due to the existence of a hypothetical 'lipid storage pool' caused by a previous high-fat meal that has only recently [233] been clarified to be located in the enterocytes (small intestine) as indicated by an increase in ApoB-48 concentration and TG levels, which in turn contribute to postprandial insulin resistance and the impact on an 'apparently' low-fat meal on BG excursion. Hence, the mathematical representation of such lipid storage, in addition to a short-term history of prior meals might be necessary to consider for the eventual

extension to a diurnal model of mixed meals. Besides the second-meal effect, a large carbohydrate intake also impacts postprandial TG through *de novo* lipogenesis levels by increasing CM ApoB-48 concentration [234]. Several independent studies also show an association between a high-carbohydrate intake with surplus carbohydrate lipogenesis despite the low—or absent—dietary fat content [235, 236]. These particular cases illustrate the inherent complexity in the mathematical representation of the impact of mixed meals on glucose-insulin metabolism during postprandial state.

- *Future direction: BG control for mixed meals*
  Because of the difficulty for T1DM patients to maintain BG levels within the recommended range after consumption of high-fat mixed meals, some studies support the use of extended bolusing methods (square/dual-wave) [237]. Nevertheless, others [238] show no definite improvement compared to single-bolus and some [239] even suggest a 15 min pre-meal bolus for high-fat meals to compensate for the typical sustained hyperglycemia. Because of these contradictory results, the establishment of adequate bolus dosing guidelines for high-fat mixed meals has not been attained [240]. Given these circumstances, an accurate mathematical model of mixed meals as given in the present proposal, and its implementation in the BG control algorithm proposed in Chapter 4—with possible modifications to the control algorithm parameters if necessary—can be expected to eliminate the aberrant postprandial BG excursion after consumption of high-fat mixed meals and contribute to the development of diurnal AP systems in the near future. Even though postprandial BG control based on present mixed meal model is beyond the scope of the present manuscript, the reduced impact of high-fat mixed meals on BG levels suggest that the prandial BG control algorithm developed in the previous chapter should theoretically be able to maintain postprandial normoglycemia similar to carbohydrate-only meals.

5.4 Concluding remarks

In the present chapter we proposed a novel model of postprandial fatty acid metabolism in patients with T1DM as an extension of the glucose-insulin metabolism from carbohydrates proposed in Chapter 3 of the present manuscript. According to the well-known effects of dietary fat on glucose-insulin metabolism, *i.e.*, delaying effect on gastric emptying and an acute increase in insulin resistance, we considered a thorough physiological representation using a minimal compartmental approach. We include the delaying effect of dietary fat on carbohydrate digestion/absorption using the mathematical model proposed in Chapter 3, and propose two single-compartments to represents TG and NEFA dynamics, which in turn serve for the

representation of lipid-derived acute insulin resistance according to their post-meal elevation above basal levels. All the model parameters are validated from clinical data specifically from patients with T1DM. Simulation results of the present model effectively show a reduction in the initial impact of a mixed meal on BG levels, in addition to the extended hyperglycemia during late postprandial state caused by increased insulin resistance. The present model provides a valid mathematical representation of glucose and fatty acid metabolism from a mixed meal using a minimal compartmental approach.

Chapter 6

Conclusions

In patients with T1DM, the inherent difficulty to maintain adequate BG management has encouraged the development of new technologies to reduce the burden of the disease. Among them, studies on AP systems and the positive results obtained in the past years expect to bring a close alternative to a cure. Despite their success in overnight BG control in actual clinical settings, the performance of in-development AP systems during diurnal BG control does not currently comply with clinical recommendations from the ADA despite continuous improvements—accompanied with increasing complexity—in the control algorithm. This is arguably due to limitations in current mathematical models of glucose-insulin metabolism and the representation of the impact of a meal on BG levels. For this reason, the main purpose of the present study was to examine the feasibility of prandial BG control within the range of 70–180 mg/dL (3.89–10 mmol/L) within two hours after meals and 70–130 mg/dL (3.89–7.22 mmol/L) afterwards, as specified by the ADA for management of BG levels in T1DM. To achieve this, the present study is divided into three main chapters that include (a) a novel mathematical model of glucose-insulin metabolism in T1DM with an accurate impact of carbohydrates with different absorption rates for its utilization in (b) a novel semi closed-loop BG control for prandial state that complies with the aforementioned ADA recommendations, and (c) extension to a mixed meal model to include the effect of dietary fat on postprandial glucose-insulin metabolism and its impact on BG levels. The conclusions for each chapter are detailed in the following.

In Chapter 3, we proposed a mathematical model of glucose-insulin metabolism in T1DM with an accurate representation of the impact of carbohydrate-rich foods on BG levels. It includes a meticulous consideration of the physiology involved for the mathematical representation of (a) the impact of carbohydrate-derived glucose on BG levels according to its amount and food-specific absorption rate, (b) subcutaneous insulin absorption and hypoglycemic ef-

fect of rapid-acting insulin on BG levels using Shimoda insulin model, and (c) glucose-insulin metabolism in T1DM considering basal hyperglycemia as a result of absent insulin secretion from β-cells in these patients using Bergman minimal model. A novel representation of carbohydrate digestion and absorption with input parameters for the amount and GI value of the meal—instead of only amount as in previous models—was proposed, which includes additional food-specific parameters of rapidly and slowly available glucose (using published data from *in vitro* studies on the subject) to represent glucose release from carbohydrates during digestion. We also considered a maximum rate of glucose appearance and delay in gastric emptying for a physiologically-relevant representation of a glucose-equivalent model of gut absorption of carbohydrates. Subcutaneous insulin absorption and glucose-insulin metabolism in the present model are adapted from existing models originally proposed by Shimoda and Bergman, respectively, with only a minimal modification of parameter values thus leaving their compartmental structure intact. Thereby, the present mathematical model is, to our knowledge, the first in the literature that provides an accurate representation of postprandial BG excursion for different types of carbohydrates validated from clinical data of postprandial BG excursion in T1DM patients. Despite the accurate representation of postprandial BG excursion, one of the major limitations of the present model is arguably the utilization of average-valued parameters as a result of validation with similarly average clinical data, and the absence of clinical validation for different carbohydrate amounts in combination with representative GI values. Both of them require further validation to fully demonstrate the accuracy of the mathematical model proposed.

In Chapter 4, we contemplated the most adequate strategy to satisfy clinical recommendations for prandial BG management in patients with T1DM from the ADA by implementing a semi closed-loop BG control approach. An insulin optimization algorithm is computed using the mathematical model of glucose-insulin metabolism in T1DM proposed in the previous chapter as early as 60 min prior to the expected mealtime, provided meal announcement of carbohydrate intake and GI value of the meal to be consumed, and administered to the patient to curb postprandial hyperglycemia. Preprandial insulin bolus is alternatively given as continuous variable insulin infusion until mealtime, as would be expected from an AP system, or single-bolus at a given instant—with bolusing dose and timing calculated from the optimization algorithm—in accordance to the current limitations of intensive insulin therapy. Thence, the control strategy automatically switches to MPC at mealtime for closed-loop BG control with automatic basal insulin infusion until complete stabilization of BG levels at the target value of 100 mg/dL (5.56 mmol/L). For the nominal case of 50 g and 100 g of carbohydrate intake in four representative meals with varying GI values under exact patient-model match and mealtime, the present *in silico* control algorithm not only demonstrated that clinical recommendations for postprandial

BG management could be attained but also that the BG control achieved a normoglycemic response similar to nondiabetics, with the degree of 'flatness' being inversely proportional to the GI value of the meal. For more realistic scenarios, we included intra-individual variability due to subcutaneous insulin effect of $\pm 20\%$, in addition to uncertainty in the GI value of the meal of $\pm 20\%$ and combined miscalculations in mealtime of ± 15 min and carbohydrate amount of ± 10 g. Although the consideration of intra-individual variability and meal-related uncertainties undermined the performance of the BG control algorithm, the resulting BG excursion still complied with clinical recommendations from the ADA. We acknowledge, though, that the present control algorithm has several limitations such as the necessity of a start in preprandial insulin infusion inasmuch as 60-min prior to mealtime. This is not only impractical in real-life scenarios but is also accompanied by an extremely high risk of severe hypoglycemia in case meal is delayed over 15 min or even worse, completely forgotten. Furthermore, meal announcement is a common approach in prandial BG control already used in previous studies that requires input from the patient and thus the same repetitive task of carbohydrate counting as in the traditional insulin therapy, which in the present study additional information of the GI value of the meal is additionally necessary.

In Chapter 5, the indisputable evidence of the impact of dietary fat on postprandial BG levels and the performance of previous BG control algorithms in the literature motivated the extension of the original carbohydrate-only model from Chapter 3 to a mixed meal model. Essentially, the model proposed aimed to represent delay in gastric emptying and acute postprandial insulin resistance, as both factors are known to affect post-meal BG excursion in patients with T1DM. The original model developed in Chapter 3 is extended to represent digestion/absorption of carbohydrates and dietary fat as a mixed meal, in addition to a minimal compartmental representation of fat metabolism. In particular, we propose a novel representation of lipid-derived insulin resistance directly associated with post-meal TG and NEFA increase above basal levels. This is arguably one of the most compelling results of the present manuscript since it is based on an exhaustive analysis of the etiology and interpretation of related scientific findings from different areas of research related to insulin resistance. Simulation results showed that it has a considerable accuracy in representing the fat-induced delay in gastric emptying, as well as postprandial BG, TG and NEFA excursions with a minimal compartmental approach. Nevertheless, some issues that require further improvement include a thorough model validation for mixed meals with different carbohydrate-to-fat ratios, not to mention patient variability as well. Due to the nonexistence of a technique that could possibly provide continuous measurement of postprandial insulin sensitivity, proper validation of time variability in lipid-derived postprandial insulin resistance in the present model with clinical studies is currently unfeasible, which

also hinders further extension of the present proposal to represent apparent differences in acute insulin resistance depending on the degree of saturation of dietary fat. Hence, further consideration of such dietary factors—provided their effect on postprandial BG excursion in patients with T1DM—need further evaluation and respective inclusion in the present model if necessary.

The results obtained in the present study also provide substantial material for future investigation. The mathematical model of glucose-insulin metabolism in T1DM proposed in Chapter 3 considers only a single meal and thus can eventually be extended to a complete diurnal model with consecutive prandial states—basically three—by considering metabolic processes such as the circadian regulation of glucose metabolism and the second-meal effect, *i.e.*, the influence of a previous meal on glucose-insulin metabolism of the current one. In Chapter 4, the semi closed-loop BG control proposed in the present study requires clinical implementation on actual patients with T1DM to fully demonstrate its capabilities. The BG control algorithm, also, might also include further prevention of hypoglycemia for the safety of the patient by considering additional algorithms to detect both algorithmic and mechanical problems such as pump occlusion and errors in real-time BG measurement from the patient to name but a few. In Chapter 5, although an essential representation of the indirect impact of dietary fat on glucose-insulin metabolism has been adapted to the minimal model, a number of other additional factors—both known and unknown—also appear to influence glucose-fatty acid metabolism, which requires an extensive investigation in several areas of research including, but perhaps not only limited to, medicine and clinical nutrition in order to propose an accurate mathematical representation with valid representation of the physiological mechanisms involved. Moreover, the mixed meal model proposed in the present study can eventually be extended to include the effect of dietary protein on glucose-insulin metabolism, since a balanced meal often includes all three macronutrients as well. Similar to the models of carbohydrate and dietary fat proposed in the present manuscript, a minimal compartmental representation with a physiologically-relevant description of the most important metabolic processes involved should be one of the main priorities, if not the utmost.

The present study thereby provides solid evidence, though *in silico* assessment, that prandial BG control within the recommended clinical range by the ADA is feasible, provided the utilization of an accurate mathematical model of the impact of different types of carbohydrates on postprandial glucose-insulin metabolism in patients with T1DM. Because of the slow subcutaneous absorption and hypoglycemic effect of current insulin formulations, a semi closed-loop control strategy that includes a considerably early preprandial insulin administration—by either continuous infusion or instantaneous single-bolus—was deemed necessary. Moreover, we

also demonstrate that the development of mathematical models of mixed meals that satisfy both a minimal compartmental approach and a physiologically-meaningful representation of lipid metabolism including the ultimate indirect effect on BG levels is also possible. Such mixed meal model can be expected to serve not only in model-based BG control for an enhanced performance after mixed meal consumption but also to provide further insight to the currently unknown metabolic effect of dietary fat on glucose-insulin metabolism as well.

List of Publications

Journal Publications

1. **Chapter 3:**
   C. C. Yamamoto Noguchi, E. Furutani, and S. Sumi, Mathematical model of glucose-insulin metabolism in type 1 diabetes including digestion and absorption of carbohydrates, *SICE Journal of Control, Measurement, and System Integration*, Vol. 7, No. 6, (2014), pp. 314–320.

2. **Chapter 3:**
   C. C. Yamamoto Noguchi, S. Hashimoto, E. Furutani, and S. Sumi, Mathematical model of carbohydrate digestion/absorption with maximum rate of exogenous glucose appearance, *SICE Journal of Control, Measurement, and System Integration* (Accepted)

3. **Chapter 4:**
   C. C. Yamamoto Noguchi, S. Hashimoto, and E. Furutani, *In Silico* Blood glucose control in type 1 diabetes with meal announcement of carbohydrate amount and glycemic index, *Advanced Biomedical Engineering* (Conditionally accepted)

4. **Chapter 5:**
   C. C. Yamamoto Noguchi, and E. Furutani, Mixed meal model of dietary fat effect on postprandial glucose-insulin metabolism in type 1 diabetes. (To be submitted)

International Conferences

1. C. Yamamoto, E. Furutani, and S. Sumi, Mathematical model of postprandial glucose-insulin metabolism in insulin-dependent diabetics with subcutaneous and intravenous insulin administration routes, SICE Annual Conference 2011, Tokyo, (2011), pp. 2648–2653.

2. C. Yamamoto, E. Furutani, and S. Sumi, Enhanced mathematical model of postprandial glycemic excursion in diabetics using rapid-acting insulin, SICE Annual Conference 2012, Akita, (2012), pp. 566–571.

3. C. C. Yamamoto Noguchi, E. Furutani, and S. Sumi, Mathematical model of glucose-insulin metabolism from carbohydrates in type 1 diabetes during postprandial and postabsorptive states, SICE Annual Conference 2013, Nagoya, (2013), pp. 170–175.

4. S. Hashimoto, C. C. Yamamoto Noguchi, and E. Furutani, Postprandial blood glucose control in type 1 diabetes for carbohydrates with varying glycemic index foods, The 36th Annual International Conference of the IEEE Engineering in Medicine and Biology Society (EMBC14), Chicago, Illinois, USA, (2014), pp. 4835–4838.

5. C. C. Yamamoto Noguchi, N. Kunikane, S. Hashimoto, and E. Furutani, Mixed Model of dietary fat effect on postprandial glucose-insulin metabolism from carbohydrates in type 1 diabetes, The 37th Annual International Conference of the IEEE Engineering in Medicine and Biology Society (EMBC15), Milan, Italy, (2015), pp. 8058–8061.

Domestic Conferences

1. C. C. Yamamoto Noguchi, E. Furutani, and S. Sumi, Mathematical model of carbohydrate-based postprandial glucose excursion in type 1 diabetic patients under rapid-acting insulin therapy, *The 55th Japan Joint Automatic Control Conference Proceedings*, Kyoto, (2012), pp. 345–349.

2. C. C. Yamamoto Noguchi, E. Furutani, and S. Sumi, Mathematical model of postprandial glycemia in type 1 diabetes—consideration of fat and protein metabolism, *The 56th Japan Joint Automatic Control Conference Proceedings*, Niigata (2013), pp. 1196–1200.

3. C. C. Yamamoto Noguchi, S. Hashimoto, and E. Furutani, Feedback-feedforward blood glucose control considering the glycemic index of foods, *The 57th Japan Joint Automatic Control Conference Proceedings*, Shibukawa (2014), pp. 1130–1133.

4. N. Kunikane, C. C. Yamamoto Noguchi, and E. Furutani, Modeling of the effect of fat and protein on blood glucose excursion in patients with type 1 diabetes (In Japanese), *Proceedings of the 59th Institute of Systems, Control and Information Engineers Conference*, Osaka, (2015), 5 pages.

5. S. Hashimoto, C. C. Yamamoto Noguchi, and E. Furutani, Prandial blood glucose control in type 1 diabetes considering model predictive control with two-degree-of-freedom (In Japanese), *Proceedings of the 59th Institute of Systems, Control and Information Engineers Conference*, Osaka, (2016), 5 pages.

6. S. Hashimoto, C. C. Yamamoto Noguchi, and E. Furutani, Effect of patient variability on prandial blood glucose control in patients with type 1 diabetes (In Japanese), *Proceedings of the 59th Institute of Systems, Control and Information Engineers Conference*, Osaka, (2016), pp. 170–174.

Bibliography

[1] L. Guariguata, D. R. Whiting, I. Hambleton, J. Beagley, U. Linnenkamp, and J. E. Shaw, Global estimates of diabetes prevalence for 2013 and projections for 2035, *Diabetes Research and Clinical Practice*, Vol. 103, No. 2, (2014), pp. 137–149.

[2] W. Yang, T. M. Dall, P. Halder, P. Gallo, S. L. Kowal, and P. F. Hogan, Economic costs of diabetes in the U.S. in 2012, *Diabetes Care*, Vol. 36, No. 4, (2013), pp. 1033–1046.

[3] A. E. Kitabchi, G. E. Umpierrez, J. M. Miles, and J. N. Fisher, Hyperglycemic crises in adult patients with diabetes, *Diabetes Care*, Vol. 32, No. 7, (2009), pp. 1335–1343.

[4] No authors listed, Diabetes in China: mapping the road ahead, *The Lancet Diabetes & Endocrinology*, Vol. 2, No. 12, (2014), p. 923.

[5] J. C. Chan, Y. Zhang, and G. Ning, Diabetes in China: a societal solution for a personal challenge, *The Lancet Diabetes & Endocrinology*, Vol. 2, No. 12, (2014), pp. 969–979.

[6] S. E. Neville, K. S. Boye, W. S. Montgomery, K. Iwamoto, M. Okamura, and R. P. Hayes, Diabetes in Japan: a review of disease burden and approaches to treatment, *Diabetes/Metabolism Research and Reviews*, Vol. 25, No. 8, (2009), pp. 705–716.

[7] D. M. Maahs, N. A. West, J. M. Lawrence, and E. J. Mayer-Davis, Epidemiology of type 1 diabetes, *Endocrinology Metabolism Clinics of North America*, Vol. 39, No. 3, (2010), pp. 481–497.

[8] G. P. Forlenza and M. Rewers, The epidemic of type 1 diabetes: what is it telling us?, *Current Opinion in Endocrinology, Diabetes and Obesity*, Vol. 18, No. 4, (2011), pp. 248–251.

[9] R. J. Schrot, Targeting plasma glucose: Preprandial versus postprandial, *Clinical Diabetes*, Vol. 22, No. 4, (2004), pp. 169–172.

[10] E. B. Ketema and K. T. Kibret, Correlation of fasting and postprandial plasma glucose with HbA1c in assessing glycemic control; systematic review and meta-analysis, *Archives of Public Health*, Vol. 73, (2015), p. 43.

[11] L. Monnier, C. Colette, and D. R. Owens, Glycemic variability: the third component of the dysglycemia in diabetes. Is it important? How to measure it?, *Journal of Diabetes Science and Technology*, Vol. 2, No. 6, (2008), pp. 1094–1100.

[12] D. Giugliano, A. Ceriello, and K. Esposito, Glucose metabolism and hyperglycemia, *The American Journal of Clinical Nutrition*, Vol. 87, No. 1, (2008), pp. 217S–222S.

[13] M. S. Rendell and L. Jovanovic, Targeting postprandial hyperglycemia, *Metabolism Clinical and Experimental*, Vol. 55, No. 9, (2006), pp. 1263–1281.

[14] B. Manuel-y Keenoy, J. Vertommen, P. Abrams, L. Van Gaal, I. De Leeuw, D. Messeri, and A. Poscia, Postprandial glucose monitoring in type 1 diabetes mellitus: use of a continuous subcutaneous monitoring device, *Diabetes/Metabolism Research and Reviews*, Vol. 20 Suppl 2, (2004), pp. 24–31.

[15] D. J. Drucker, The role of gut hormones in glucose homeostasis, *The Journal of Clinical Investigation*, Vol. 117, No. 1, (2007), pp. 24–32.

[16] T. Kawamura, The importance of carbohydrate counting in the treatment of children with diabetes, *Pediatric Diabetes*, Vol. 8 Suppl 6, (2007), pp. 57–62.

[17] L. A. Gonder-Frederick, J. F. Zrebiec, A. U. Bauchowitz, L. M. Ritterband, J. C. Magee, D. J. Cox, and W. L. Clarke, Cognitive function is disrupted by both hypo- and hyperglycemia in school-aged children with type 1 diabetes: a field study, *Diabetes Care*, Vol. 32, No. 6, (2009), pp. 1001–1006.

[18] K. M. Narayan, J. P. Boyle, T. J. Thompson, S. W. Sorensen, and D. F. Williamson, Lifetime risk for diabetes mellitus in the United States, *Journal of the American Medical Association*, Vol. 290, No. 14, (2003), pp. 1884–1890.

[19] J. Kropff and J. H. DeVries, Continuous glucose monitoring, future products, and update on worldwide artificial pancreas projects, *Diabetes Technology & Therapeutics*, Vol. 18 Suppl 2, (2016), pp. S253–263.

[20] K. Kumareswaran, D. Elleri, J. M. Allen, J. Harris, D. Xing, C. Kollman, M. Nodale, H. R. Murphy, S. A. Amiel, S. R. Heller, M. E. Wilinska, C. L. Acerini, M. L. Evans, D. B. Dunger, and R. Hovorka, Meta-analysis of overnight closed-loop randomized studies in children and adults with type 1 diabetes: the Cambridge cohort, *Journal of Diabetes Science and Technology*, Vol. 5, No. 6, (2011), pp. 1352–1362.

[21] A. J. Young, H. Thabit, S. R. Heller, M. L. Evans, S. A. Amiel, R. Hovorka, and K. D. Barnard, Holistic impact of closed-loop technology on people with type 1 diabetes, *Journal of Diabetes Science and Technology*, Vol. 9, No. 4, (2015), pp. 932–933.

[22] G. Slama, J. C. Klein, A. Delage, E. Ardila, H. Lemaignen, L. Papoz, and G. Tchobroutsky, Correlation between the nature and amount of carbohydrate in meal intake and

insulin delivery by the artificial pancreas in 24 insulin-dependent diabetics, *Diabetes*, Vol. 30, No. 2, (1981), pp. 101–105.

[23] P. Halfon, J. Belkhadir, and G. Slama, Correlation between amount of carbohydrate in mixed meals and insulin delivery by artificial pancreas in seven IDDM subjects, *Diabetes Care*, Vol. 12, No. 6, (1989), pp. 427–429.

[24] A. L. Peters and M. B. Davidson, Protein and fat effects on glucose responses and insulin requirements in subjects with insulin-dependent diabetes mellitus, *The American Journal of Clinical Nutrition*, Vol. 58, No. 4, (1993), pp. 555–560.

[25] C. E. Smart, M. Evans, S. M. O'Connell, P. McElduff, P. E. Lopez, T. W. Jones, E. A. Davis, and B. R. King, Both dietary protein and fat increase postprandial glucose excursions in children with type 1 diabetes, and the effect is additive, *Diabetes Care*, Vol. 36, No. 12, (2013), pp. 3897–3902.

[26] A. Neu, F. Behret, R. Braun, S. Herrlich, F. Liebrich, M. Loesch-Binder, A. Schneider, and R. Schweizer, Higher glucose concentrations following protein- and fat-rich meals — the Tuebingen Grill Study: a pilot study in adolescents with type 1 diabetes, *Pediatric Diabetes*, Vol. 16, No. 8, (2015), pp. 587–591.

[27] K. J. Bell, C. E. Smart, G. M. Steil, J. C. Brand-Miller, B. King, and H. A. Wolpert, Impact of fat, protein, and glycemic index on postprandial glucose control in type 1 diabetes: implications for intensive diabetes management in the continuous glucose monitoring era, *Diabetes Care*, Vol. 38, No. 6, (2015), pp. 1008–1015.

[28] M. Lodefalk, J. Aman, and P. Bang, Effects of fat supplementation on glycaemic response and gastric emptying in adolescents with type 1 diabetes, *Diabetic Medicine*, Vol. 25, No. 9, (2008), pp. 1030–1035.

[29] J. A. Ahern, P. M. Gatcomb, N. A. Held, W. A. Petit, and W. V. Tamborlane, Exaggerated hyperglycemia after a pizza meal in well-controlled diabetes, *Diabetes Care*, Vol. 16, No. 4, (1993), pp. 578–580.

[30] E. Pańkowska and M. Blazik, Bolus calculator with nutrition database software, a new concept of prandial insulin programming for pump users, *Journal of Diabetes Science and Technology*, Vol. 4, No. 3, (2010), pp. 571–576.

[31] J. Bao, F. Atkinson, P. Petocz, W. C. Willett, and J. C. Brand-Miller, Prediction of postprandial glycemia and insulinemia in lean, young, healthy adults: glycemic load compared with carbohydrate content alone, *The American Journal of Clinical Nutrition*, Vol. 93, No. 5, (2011), pp. 984–996.

[32] J. Bao, H. R. Gilbertson, R. Gray, D. Munns, G. Howard, P. Petocz, S. Colagiuri, and J. C. Brand-Miller, Improving the estimation of mealtime insulin dose in adults with type

1 diabetes: the Normal Insulin Demand for Dose Adjustment (NIDDA) study, *Diabetes Care*, Vol. 34, No. 10, (2011), pp. 2146–2151.

[33] H. A. Wolpert, A. Atakov-Castillo, S. A. Smith, and G. M. Steil, Dietary fat acutely increases glucose concentrations and insulin requirements in patients with type 1 diabetes: implications for carbohydrate-based bolus dose calculation and intensive diabetes management, *Diabetes Care*, Vol. 36, No. 4, (2013), pp. 810–816.

[34] A. Srinivasan, J. B. Lee, E. Dassau, and F. J. Doyle, Novel insulin delivery profiles for mixed meals for sensor-augmented pump and closed-loop artificial pancreas therapy for type 1 diabetes mellitus, *Journal of Diabetes Science and Technology*, Vol. 8, No. 5, (2014), pp. 957–968.

[35] J. H. Cummings and A. M. Stephen, Carbohydrate terminology and classification, *European Journal of Clinical Nutrition*, Vol. 61 Suppl 1, (2007), pp. 5–18.

[36] K. J. Hare, T. Vilsbøll, J. J. Holst, and F. K. Knop, Inappropriate glucagon response after oral compared with isoglycemic intravenous glucose administration in patients with type 1 diabetes, *American journal of physiology. Endocrinology and metabolism*, Vol. 298, No. 4, (2010), pp. E832–837.

[37] J. J. Meier, J. D. Veldhuis, and P. C. Butler, Pulsatile insulin secretion dictates systemic insulin delivery by regulating hepatic insulin extraction in humans, *Diabetes*, Vol. 54, No. 6, (2005), pp. 1649–1656.

[38] W. G. Blackard and N. C. Nelson, Portal vein insulin concentrations in diabetic subjects, *Diabetes*, Vol. 20, No. 5, (1971), pp. 286–288.

[39] E. D. Lehmann, C. Tarín, J. Bondia, E. Teufel, and T. Deutsch, Incorporating a generic model of subcutaneous insulin absorption into the AIDA v4 diabetes simulator. 3. Early plasma insulin determinations, *Journal of Diabetes Science and Technology*, Vol. 3, No. 1, (2009), pp. 190–201.

[40] J. C. Pickup and D. Phil, Insulin-pump therapy for type 1 diabetes mellitus, *The New England Journal of Medicine*, Vol. 366, No. 17, (2012), pp. 1616–1624.

[41] P. Lopez, C. Smart, C. Morbey, P. McElduff, M. Paterson, and B. R. King, Extended insulin boluses cannot control postprandial glycemia as well as a standard bolus in children and adults using insulin pump therapy, *BMJ Open Diabetes Research & Care*, Vol. 2, No. 1, (2014), p. e000050.

[42] No authors listed, Standards of medical care in diabetes—2014, *Diabetes Care*, Vol. 37 Suppl 1, (2014), pp. 14–80.

[43] E. D. Lehmann and T. Deutsch, A physiological model of glucose-insulin interaction in type 1 diabetes mellitus, *Journal of Biomedical Engineering*, Vol. 14, No. 3, (1992), pp. 235–242.

[44] J. D. Elashoff, T. J. Reedy, and J. H. Meyer, Analysis of gastric emptying data, *Gastroenterology*, Vol. 83, No. 6, (1982), pp. 1306–1312.

[45] J. A. Siegel, J. L. Urbain, L. P. Adler, N. D. Charkes, A. H. Maurer, B. Krevsky, L. C. Knight, R. S. Fisher, and L. S. Malmud, Biphasic nature of gastric emptying, *Gut*, Vol. 29, No. 1, (1988), pp. 85–89.

[46] R. N. Bergman, Y. Z. Ider, C. R. Bowden, and C. Cobelli, Quantitative estimation of insulin sensitivity, *American Journal of Physiology*, Vol. 236, No. 6, (1979), pp. E667–677.

[47] S. M. Furler, E. W. Kraegen, R. H. Smallwood, and D. J. Chisholm, Blood glucose control by intermittent loop closure in the basal mode: computer simulation studies with a diabetic model, *Diabetes Care*, Vol. 8, No. 6, (1985), pp. 553–561.

[48] C. McDonald, A. Dunaif, and D. T. Finegood, Minimal-model estimates of insulin sensitivity are insensitive to errors in glucose effectiveness, *The Journal of Clinical Endocrinology and Metabolism*, Vol. 85, No. 7, (2000), pp. 2504–2508.

[49] R. Hovorka, V. Canonico, L. J. Chassin, U. Haueter, M. Massi-Benedetti, M. Orsini Federici, T. R. Pieber, H. C. Schaller, L. Schaupp, T. Vering, and M. E. Wilinska, Nonlinear model predictive control of glucose concentration in subjects with type 1 diabetes, *Physiological Measurement*, Vol. 25, No. 4, (2004), pp. 905–920.

[50] C. Dalla Man, M. Camilleri, and C. Cobelli, A system model of oral glucose absorption: validation on gold standard data, *IEEE Transactions on Biomedical Engineering*, Vol. 53, No. 12 Pt 1, (2006), pp. 2472–2478.

[51] C. Dalla Man, D. M. Raimondo, R. A. Rizza, and C. Cobelli, GIM, simulation software of meal glucose-insulin model, *Journal of Diabetes Science and Technology*, Vol. 1, No. 3, (2007), pp. 323–330.

[52] R. Basu, B. Di Camillo, G. Toffolo, A. Basu, P. Shah, A. Vella, R. Rizza, and C. Cobelli, Use of a novel triple-tracer approach to assess postprandial glucose metabolism, *American journal of physiology. Endocrinology and metabolism*, Vol. 284, No. 1, (2003), pp. 55–69.

[53] H. Okazaki, J. Osuga, Y. Tamura, N. Yahagi, S. Tomita, F. Shionoiri, Y. Iizuka, K. Ohashi, K. Harada, S. Kimura, T. Gotoda, H. Shimano, N. Yamada, and S. Ishibashi, Lipolysis in the absence of hormone-sensitive lipase: evidence for a common mechanism regulating distinct lipases, *Diabetes*, Vol. 51, No. 12, (2002), pp. 3368–3375.

[54] R. E. Duncan, M. Ahmadian, K. Jaworski, E. Sarkadi-Nagy, and H. S. Sul, Regulation of lipolysis in adipocytes, *Annual Review of Nutrition*, Vol. 27, (2007), pp. 79–101.

[55] R. C. Boston and P. J. Moate, A novel minimal model to describe NEFA kinetics following an intravenous glucose challenge, *American Journal of Physiology. Regulatory, integrative and comparative physiology*, Vol. 294, No. 4, (2008), pp. R1140–1147.

[56] A. E. Sumner, R. N. Bergman, G. L. Vega, D. J. Genovese, C. S. Cochran, K. Pacak, R. M. Watanabe, and R. C. Boston, The multiphasic profile of free fatty acids during the intravenous glucose tolerance test is unresponsive to exogenous insulin, *Metabolism, Clinical and Experimental*, Vol. 53, No. 9, (2004), pp. 1202–1207.

[57] K. Jelic, C. E. Hallgreen, and M. Colding-Jørgensen, A model of NEFA dynamics with focus on the postprandial state, *Annals of Biomedical Engineering*, Vol. 37, No. 9, (2009), pp. 1897–1909.

[58] A. Roy and R. S. Parker, Dynamic modeling of free fatty acid, glucose, and insulin: an extended "minimal model", *Diabetes Technology & Therapeutics*, Vol. 8, No. 6, (2006), pp. 617–626.

[59] A. Roy and R. S. Parker, Mixed meal modeling and disturbance rejection in type I diabetic patients, *Conference Proceedings of the Annual International Conference of the IEEE Engineering in Medicine and Biology Society*, Vol. 1, (2006), pp. 323–326.

[60] H. C. Zisser L. M. Huyett, E. Dassau and F. J. Doyle III, Design and evaluation of a robust PID controller for a fully implantable artificial pancreas, *Industrial & Engineering Chemistry Research*, (2015), pp. A–K.

[61] J. L. Ruiz, J. L. Sherr, E. Cengiz, L. Carria, A. Roy, G. Voskanyan, W. V. Tamborlane, and S. A. Weinzimer, Effect of insulin feedback on closed-loop glucose control: a crossover study, *Journal of Diabetes Science and Technology*, Vol. 6, No. 5, (2012), pp. 1123–1130.

[62] G. M. Steil, K. Rebrin, C. Darwin, F. Hariri, and M. F. Saad, Feasibility of automating insulin delivery for the treatment of type 1 diabetes, *Diabetes*, Vol. 55, No. 12, (2006), pp. 3344–3350.

[63] G. M. Steil, C. C. Palerm, N. Kurtz, G. Voskanyan, A. Roy, S. Paz, and F. R. Kandeel, The effect of insulin feedback on closed loop glucose control, *The Journal of Clinical Endocrinology and Metabolism*, Vol. 96, No. 5, (2011), pp. 1402–1408.

[64] C. Toffanin, M. Messori, F. Di Palma, G. De Nicolao, C. Cobelli, and L. Magni, Artificial pancreas: model predictive control design from clinical experience, *Journal of Diabetes Science and Technology*, Vol. 7, No. 6, (2013), pp. 1470–1483.

[65] F. Cameron, G. Niemeyer, D. M. Wilson, B. W. Bequette, K. S. Benassi, P. Clinton, and B. A. Buckingham, Inpatient trial of an artificial pancreas based on multiple model probabilistic predictive control with repeated large unannounced meals, *Diabetes Technology & Therapeutics*, Vol. 16, No. 11, (2014), pp. 728–734.

[66] R. Mauseth, Y. Wang, E. Dassau, R. Kircher, D. Matheson, H. Zisser, L. Jovanovič, and F. J. Doyle, Proposed clinical application for tuning fuzzy logic controller of artificial pancreas utilizing a personalization factor, *Journal of Diabetes Science and Technology*, Vol. 4, No. 4, (2010), pp. 913–922.

[67] R. Mauseth, I. B. Hirsch, J. Bollyky, R. Kircher, D. Matheson, S. Sanda, and C. Greenbaum, Use of a "fuzzy logic" controller in a closed-loop artificial pancreas, *Diabetes Technology & Therapeutics*, Vol. 15, No. 8, (2013), pp. 628–633.

[68] E. Dassau, B. W. Bequette, B. A. Buckingham, and F. J. Doyle, Detection of a meal using continuous glucose monitoring: implications for an artificial beta-cell, *Diabetes Care*, Vol. 31, No. 2, (2008), pp. 295–300.

[69] C. Ellingsen, E. Dassau, H. Zisser, B. Grosman, M. W. Percival, L. Jovanovič, and F. J. Doyle, Safety constraints in an artificial pancreatic beta cell: an implementation of model predictive control with insulin on board, *Journal of Diabetes Science and Technology*, Vol. 3, No. 3, (2009), pp. 536–544.

[70] F. León-Vargas, F. Garelli, H. De Battista, and J. Vehí, Postprandial response improvement via safety layer in closed-loop blood glucose controllers, *Biomedical Signal Processing and Control*, Vol. 16, (2015), pp. 80–87.

[71] B. Kovatchev, S. Patek, E. Dassau, F. J. Doyle, L. Magni, G. De Nicolao, and C. Cobelli, Control to range for diabetes: functionality and modular architecture, *Journal of Diabetes Science and Technology*, Vol. 3, No. 5, (2009), pp. 1058–1065.

[72] M. Breton, A. Farret, D. Bruttomesso, S. Anderson, L. Magni, S. Patek, C. Dalla Man, J. Place, S. Demartini, S. Del Favero, C. Toffanin, C. Hughes-Karvetski, E. Dassau, H. Zisser, F. J. Doyle, G. De Nicolao, A. Avogaro, C. Cobelli, E. Renard, and B. Kovatchev, Fully integrated artificial pancreas in type 1 diabetes: modular closed-loop glucose control maintains near normoglycemia, *Diabetes*, Vol. 61, No. 9, (2012), pp. 2230–2237.

[73] H. Zisser, E. Renard, B. Kovatchev, C. Cobelli, A. Avogaro, R. Nimri, L. Magni, B. A. Buckingham, H. P. Chase, F. J. Doyle, et al., Multicenter closed-loop insulin delivery study points to challenges for keeping blood glucose in a safe range by a control algorithm in adults and adolescents with type 1 diabetes from various sites, *Diabetes Technology & Therapeutics*, Vol. 16, No. 10, (2014), pp. 613–622.

[74] F. H. El-Khatib, S. J. Russell, K. L. Magyar, M. Sinha, K. McKeon, D. M. Nathan, and E. R. Damiano, Autonomous and continuous adaptation of a bihormonal bionic pancreas in adults and adolescents with type 1 diabetes, *The Journal of Clinical Endocrinology and Metabolism*, Vol. 99, No. 5, (2014), pp. 1701–1711.

[75] P. Herrero, R. Calm, J. Vehí, J. Armengol, P. Georgiou, N. Oliver, and C. Tomazou, Robust fault detection system for insulin pump therapy using continuous glucose monitoring, *Journal of Diabetes Science and Technology*, Vol. 6, No. 5, (2012), pp. 1131–1141.

[76] I. Ajmera, M. Swat, C. Laibe, N. L. Novère, and V. Chelliah, The impact of mathematical modeling on the understanding of diabetes and related complications, *CPT Pharmacometrics & Systems Pharmacology*, Vol. 2, (2013), p. e54.

[77] B. P. Kovatchev, M. Breton, C. D. Man, and C. Cobelli, In silico preclinical trials: a proof of concept in closed-loop control of type 1 diabetes, *Journal of Diabetes Science and Technology*, Vol. 3, No. 1, (2009), pp. 44–55.

[78] M. E. Wilinska, L. J. Chassin, C. L. Acerini, J. M. Allen, D. B. Dunger, and R. Hovorka, Simulation environment to evaluate closed-loop insulin delivery systems in type 1 diabetes, *Journal of Diabetes Science and Technology*, Vol. 4, No. 1, (2010), pp. 132–144.

[79] D. J. Jenkins, T. M. Wolever, R. H. Taylor, H. Barker, H. Fielden, J. M. Baldwin, A. C. Bowling, H. C. Newman, A. L. Jenkins, and D. V. Goff, Glycemic index of foods: a physiological basis for carbohydrate exchange, *The American Journal of Clinical Nutrition*, Vol. 34, No. 3, (1981), pp. 362–366.

[80] H. Englyst and G. J. Hudson, The classification and measurement of dietary carbohydrates, *Food Chemistry*, Vol. 57, No. 1, (1996), pp. 15–21.

[81] T. M. Wolever and C. Bolognesi, Source and amount of carbohydrate affect postprandial glucose and insulin in normal subjects, *Journal of Nutrition*, Vol. 126, No. 11, (1996), pp. 2798–2806.

[82] K. N. Englyst and H. N. Englyst, Carbohydrate bioavailability, *British Journal of Nutrition*, Vol. 94, No. 1, (2005), pp. 1–11.

[83] K. N. Englyst, S. Liu, and H. N. Englyst, Nutritional characterization and measurement of dietary carbohydrates, *European Journal of Clinical Nutrition*, Vol. 61 Suppl 1, (2007), pp. 19–39.

[84] H. N. Englyst, J. Veenstra, and G. J. Hudson, Measurement of rapidly available glucose (RAG) in plant foods: a potential in vitro predictor of the glycaemic response, *British Journal of Nutrition*, Vol. 75, No. 3, (1996), pp. 327–337.

[85] N. H. Mohammed and T. M. Wolever, Effect of carbohydrate source on post-prandial blood glucose in subjects with type 1 diabetes treated with insulin lispro, *Diabetes Research and Clinical Practice*, Vol. 65, No. 1, (2004), pp. 29–35.

[86] M. Korach-André, H. Roth, D. Barnoud, M. Pean, F. Péronnet, and X. Leverve, Glucose appearance in the peripheral circulation and liver glucose output in men after a large 13C starch meal, *The American Journal of Clinical Nutrition*, Vol. 80, No. 4, (2004), pp. 881–886.

[87] W. Brener, T. R. Hendrix, and P. R. McHugh, Regulation of the gastric emptying of glucose, *Gastroenterology*, Vol. 85, No. 1, (1983), pp. 76–82.

[88] J. Galgani, C. Aguirre, and E. Díaz, Acute effect of meal glycemic index and glycemic load on blood glucose and insulin responses in humans, *Journal of Nutrition*, Vol. 5, (2006), p. 22.

[89] K. J. Marran, B. Davey, A. Lang, and D. G. Segal, Exponential increase in postprandial blood-glucose exposure with increasing carbohydrate loads using a linear carbohydrate-to-insulin ratio, *South African Medical Journal*, Vol. 103, No. 7, (2013), pp. 461–463.

[90] A. E. Jeukendrup, A. J. Wagenmakers, J. H. Stegen, A. P. Gijsen, F. Brouns, and W. H. Saris, Carbohydrate ingestion can completely suppress endogenous glucose production during exercise, *American Journal of Physiology*, Vol. 276, No. 4 Pt 1, (1999), pp. E672–683.

[91] C. V. Gisolfi, Is the GI system built for exercise?, *News in Physiological Science*, Vol. 15, (2000), pp. 114–119.

[92] E. P. de Oliveira and R. C. Burini, The impact of physical exercise on the gastrointestinal tract, *Curent Opinion in Clinical Nutrition and Metabolic Care*, Vol. 12, No. 5, (2009), pp. 533–538.

[93] M. Samsom, L. M. Akkermans, R. J. Jebbink, H. van Isselt, G. P. vanBerge-Henegouwen, and A. J. Smout, Gastrointestinal motor mechanisms in hyperglycaemia induced delayed gastric emptying in type I diabetes mellitus, *Gut*, Vol. 40, No. 5, (1997), pp. 641–646.

[94] E. Schvarcz, M. Palmer, J. Aman, M. Horowitz, M. Stridsberg, and C. Berne, Physiological hyperglycemia slows gastric emptying in normal subjects and patients with insulin-dependent diabetes mellitus, *Gastroenterology*, Vol. 113, No. 1, (1997), pp. 60–66.

[95] C. K. Rayner and M. Horowitz, Gastrointestinal motility and glycemic control in diabetes: the chicken and the egg revisited?, *The Journal of Clinical Investigation*, Vol. 116, No. 2, (2006), pp. 299–302.

[96] G. Pehling, P. Tessari, J. E. Gerich, M. W. Haymond, F. J. Service, and R. A. Rizza, Abnormal meal carbohydrate disposition in insulin-dependent diabetes. Relative contributions of endogenous glucose production and initial splanchnic uptake and effect of intensive insulin therapy, *The Journal of Clinical Investigation*, Vol. 74, No. 3, (1984), pp. 985–991.

[97] M. G. Velchik, J. C. Reynolds, and A. Alavi, The effect of meal energy content on gastric emptying, *Journal of Nuclear Medicine*, Vol. 30, No. 6, (1989), pp. 1106–1110.

[98] J. Mourot, P. Thouvenot, C. Couet, J. M. Antoine, A. Krobicka, and G. Debry, Relationship between the rate of gastric emptying and glucose and insulin responses to starchy

foods in young healthy adults, *The American Journal of Clinical Nutrition*, Vol. 48, No. 4, (1988), pp. 1035–1040.

[99] C. Binder, T. Lauritzen, O. Faber, and S. Pramming, Insulin pharmacokinetics, *Diabetes Care*, Vol. 7, No. 2, (1984), pp. 188–199.

[100] T. Heise, C. Weyer, A. Serwas, S. Heinrichs, J. Osinga, P. Roach, J. Woodworth, U. Gudat, and L. Heinemann, Time-action profiles of novel premixed preparations of insulin lispro and NPL insulin, *Diabetes Care*, Vol. 21, No. 5, (1998), pp. 800–803.

[101] T. Sekigami, S. Shimoda, K. Nishida, Y. Matsuo, S. Ichimori, K. Ichinose, M. Shichiri, M. Sakakida, and E. Araki, Comparison between closed-loop portal and peripheral venous insulin delivery systems for an artificial endocrine pancreas, *Journal of Artificial Organs*, Vol. 7, No. 2, (2004), pp. 91–100.

[102] L. Heinemann, T. Heise, L. C. Wahl, M. E. Trautmann, J. Ampudia, A. A. Starke, and M. Berger, Prandial glycaemia after a carbohydrate-rich meal in type I diabetic patients: using the rapid acting insulin analogue [Lys(B28), Pro(B29)] human insulin, *Diabetic Medicine*, Vol. 13, No. 7, (1996), pp. 625–629.

[103] K. L. Swan, J. D. Dziura, G. M. Steil, G. R. Voskanyan, K. A. Sikes, A. T. Steffen, M. L. Martin, W. V. Tamborlane, and S. A. Weinzimer, Effect of age of infusion site and type of rapid-acting analog on pharmacodynamic parameters of insulin boluses in youth with type 1 diabetes receiving insulin pump therapy, *Diabetes Care*, Vol. 32, No. 2, (2009), pp. 240–244.

[104] S. Shimoda, K. Nishida, M. Sakakida, Y. Konno, K. Ichinose, M. Uehara, T. Nowak, and M. Shichiri, Closed-loop subcutaneous insulin infusion algorithm with a short-acting insulin analog for long-term clinical application of a wearable artificial endocrine pancreas, *Frontiers of Medical & Biological Engineering*, Vol. 8, No. 3, (1997), pp. 197–211.

[105] P. D. Home, The pharmacokinetics and pharmacodynamics of rapid-acting insulin analogues and their clinical consequences, *Diabetes, Obesity and Metabolism*, Vol. 14, No. 9, (2012), pp. 780–788.

[106] J. D. Best, S. E. Kahn, M. Ader, R. M. Watanabe, T. C. Ni, and R. N. Bergman, Role of glucose effectiveness in the determination of glucose tolerance, *Diabetes Care*, Vol. 19, No. 9, (1996), pp. 1018–1030.

[107] A. Caumo, P. Vicini, and C. Cobelli, Is the minimal model too minimal?, *Diabetologia*, Vol. 39, No. 8, (1996), pp. 997–1000.

[108] C. Cobelli, F. Bettini, A. Caumo, and M. J. Quon, Overestimation of minimal model glucose effectiveness in presence of insulin response is due to undermodeling, *American Journal of Physiology*, Vol. 275, No. 6 Pt 1, (1998), pp. E1031–1036.

[109] M. J. Quon, C. Cochran, S. I. Taylor, and R. C. Eastman, Non-insulin-mediated glucose disappearance in subjects with IDDM. Discordance between experimental results and minimal model analysis, *Diabetes*, Vol. 43, No. 7, (1994), pp. 890–896.

[110] M. R. Rickels, A. Naji, and K. L. Teff, Insulin sensitivity, glucose effectiveness, and free fatty acid dynamics after human islet transplantation for type 1 diabetes, *The Journal of Clinical Endocrinology and Metabolism*, Vol. 91, No. 6, (2006), pp. 2138–2144.

[111] J. L. Sherr, T. Ghazi, A. Wurtz, L. Rink, and K. C. Herold, Characterization of residual cell function in long-standing type 1 diabetes, *Diabetes/Metabolism Research and Reviews*, Vol. 30, No. 2, (2014), pp. 154–162.

[112] M. Kacerovsky, J. Jones, A. I. Schmid, C. Barosa, A. Lettner, G. Kacerovsky-Bielesz, J. Szendroedi, M. Chmelik, P. Nowotny, V. Chandramouli, M. Wolzt, and M. Roden, Postprandial and fasting hepatic glucose fluxes in long-standing type 1 diabetes, *Diabetes*, Vol. 60, No. 6, (2011), pp. 1752–1758.

[113] B. A. Cooperberg and P. E. Cryer, Beta-cell-mediated signaling predominates over direct alpha-cell signaling in the regulation of glucagon secretion in humans, *Diabetes Care*, Vol. 32, No. 12, (2009), pp. 2275–2280.

[114] Nadia H. J. Mohammed, Effect of carbohydrate source on postprandial blood glucose in subjects with type 1 diabetes using insulin lispro, Master's thesis, (University of Toronto, Canada, 2001).

[115] M. Garsetti, S. Vinoy, V. Lang, S. Holt, S. Loyer, and J. C. Brand-Miller, The glycemic and insulinemic index of plain sweet biscuits: relationships to in vitro starch digestibility, *Journal of the American College of Nutrition*, Vol. 24, No. 6, (2005), pp. 441–447.

[116] D. Elleri, J. M. Allen, J. Harris, K. Kumareswaran, M. Nodale, L. Leelarathna, C. L. Acerini, A. Haidar, M. E. Wilinska, N. Jackson, A. M. Umpleby, M. L. Evans, D. B. Dunger, and R. Hovorka, Absorption patterns of meals containing complex carbohydrates in type 1 diabetes, *Diabetologia*, Vol. 56, No. 5, (2013), pp. 1108–1117.

[117] T. A. van Kempen, P. R. Regmi, J. J. Matte, and R. T. Zijlstra, In vitro starch digestion kinetics, corrected for estimated gastric emptying, predict portal glucose appearance in pigs, *Journal of Nutrition*, Vol. 140, No. 7, (2010), pp. 1227–1233.

[118] H. J. Woerle, M. Albrecht, R. Linke, S. Zschau, C. Neumann, M. Nicolaus, J. E. Gerich, B. Göke, and J. Schirra, Impaired hyperglycemia-induced delay in gastric emptying in patients with type 1 diabetes deficient for islet amyloid polypeptide, *Diabetes Care*, Vol. 31, No. 12, (2008), pp. 2325–2331.

[119] S. J. Perano, C. K. Rayner, S. Kritas, M. Horowitz, K. Donaghue, C. Mpundu-Kaambwa, L. Giles, and J. J. Couper, Gastric emptying is more rapid in adolescents with type 1

diabetes and impacts on postprandial glycemia, *The Journal of Clinical Endocrinology and Metabolism*, Vol. 100, No. 6, (2015), pp. 2248–2253.

[120] M. Q. Al-Mssallem, G. S. Frost, and J. E. Brown, The metabolic effects of two meals with the same glycaemic index but different slowly available glucose parameters determined in vitro A pilot study, *Annals of Nutritional Disorders & Therapy*, Vol. 1, No. 1, (2014), pp. 1001–1005.

[121] D. J. Jenkins, H. Ghafari, T. M. Wolever, R. H. Taylor, A. L. Jenkins, H. M. Barker, H. Fielden, and A. C. Bowling, Relationship between rate of digestion of foods and postprandial glycaemia, *Diabetologia*, Vol. 22, No. 6, (1982), pp. 450–455.

[122] C. Eelderink, M. Schepers, T. Preston, R. J. Vonk, L. Oudhuis, and M. G. Priebe, Slowly and rapidly digestible starchy foods can elicit a similar glycemic response because of differential tissue glucose uptake in healthy men, *The American Journal of Clinical Nutrition*, Vol. 96, No. 5, (2012), pp. 1017–1024.

[123] G. M. Gray and F. J. Ingelfinger, Intestinal absorption of sucrose in man: Interrrelation of hydrolysis and monosaccharide product absorption, *The Journal of Clinical Investigation*, Vol. 45, No. 3, (1966), pp. 388–398.

[124] G. M. Gray and F. J. Ingelfinger, Intestinal absorption of sucrose in man: The site of hydrolysis and absorption, *The Journal of Clinical Investigation*, Vol. 44, No. 3, (1965), pp. 390–398.

[125] G. A. Bray, How bad is fructose?, *The American Journal of Clinical Nutrition*, Vol. 86, No. 4, (2007), pp. 895–896.

[126] L. Heinemann and S. Steiner, Subcutaneous injection versus subcutaneous infusion of insulin: are the rates of absorption truly the same?, *Journal of Diabetes Science and Technology*, Vol. 5, No. 5, (2011), pp. 1027–1029.

[127] L. Heinemann and D. B. Muchmore, Ultrafast-acting insulins: state of the art, *Journal of Diabetes Science and Technology*, Vol. 6, No. 4, (2012), pp. 728–742.

[128] J. W. Chen, J. S. Christiansen, and T. Lauritzen, Limitations to subcutaneous insulin administration in type 1 diabetes, *Diabetes, Obesity and Metabolism*, Vol. 5, No. 4, (2003), pp. 223–233.

[129] J. F. Wojtaszewski, J. N. Nielsen, and E. A. Richter, Invited review: effect of acute exercise on insulin signaling and action in humans, *Journal of Applied Physiology*, Vol. 93, No. 1, (2002), pp. 384–392.

[130] R. Hovorka, Closed-loop insulin delivery: from bench to clinical practice, *Nature Reviews Endocrinology*, Vol. 7, No. 7, (2011), pp. 385–395.

[131] T. Battelino, J. Š. Omladič, and M. Phillip, Closed loop insulin delivery in diabetes, *Best Practice & Research Clinical Endocrinology & Metabolism*, Vol. 29, No. 3, (2015), pp. 315–325.

[132] Y. M. Luijf, J. H. DeVries, K. Zwinderman, L. Leelarathna, M. Nodale, K. Caldwell, K. Kumareswaran, D. Elleri, J. M. Allen, M. E. Wilinska, et al., Day and night closed-loop control in adults with type 1 diabetes: a comparison of two closed-loop algorithms driving continuous subcutaneous insulin infusion versus patient self-management, *Diabetes Care*, Vol. 36, No. 12, (2013), pp. 3882–3887.

[133] P. Soru, G. De Nicolao, C. Toffanin, C. Dalla Man, C. Cobelli, and L. Magni, MPC based Artificial Pancreas: Strategies for individualization and meal compensation, *Annual Reviews in Control*, Vol. 36, No. 1, (2012), pp. 118–128.

[134] American Diabetes Association, Insulin administration, *Diabetes Care*, Vol. 27, No. suppl 1, (2004), pp. s106–s107.

[135] Y. M. Luijf, A. C. van Bon, J. B. Hoekstra, and J. H. Devries, Premeal injection of rapid-acting insulin reduces postprandial glycemic excursions in type 1 diabetes, *Diabetes Care*, Vol. 33, No. 10, (2010), pp. 2152–2155.

[136] E. Cobry, K. McFann, L. Messer, V. Gage, B. VanderWel, L. Horton, and H. P. Chase, Timing of meal insulin boluses to achieve optimal postprandial glycemic control in patients with type 1 diabetes, *Diabetes Technology & Therapeutics*, Vol. 12, No. 3, (2010), pp. 173–177.

[137] H. P. Chase, F. J. Doyle, H. Zisser, E. Renard, R. Nimri, C. Cobelli, B. A. Buckingham, D. M. Maahs, S. Anderson, L. Magni, et al., Multicenter closed-loop/hybrid meal bolus insulin delivery with type 1 diabetes, *Diabetes Technology & Therapeutics*, Vol. 16, No. 10, (2014), pp. 623–632.

[138] P. R. van Dijk, S. J. Logtenberg, K. H. Groenier, J. W. Haveman, N. Kleefstra, and H. J. Bilo, Complications of continuous intraperitoneal insulin infusion with an implantable pump, *World Journal of Diabetes*, Vol. 3, No. 8, (2012), pp. 142–148.

[139] S. J. Russell, F. H. El-Khatib, M. Sinha, K. L. Magyar, K. McKeon, L. G. Goergen, C. Balliro, M. A. Hillard, D. M. Nathan, and E. R. Damiano, Outpatient glycemic control with a bionic pancreas in type 1 diabetes, *The New England Journal of Medicine*, Vol. 371, No. 4, (2014), pp. 313–325.

[140] S. J. Russell, F. H. El-Khatib, D. M. Nathan, K. L. Magyar, J. Jiang, and E. R. Damiano, Blood glucose control in type 1 diabetes with a bihormonal bionic endocrine pancreas, *Diabetes Care*, Vol. 35, No. 11, (2012), pp. 2148–2155.

[141] V. Colon, A. Grade, G. Pulliam, C. Johnson, and R. Fass, Effect of doses of glucagon used to treat food impaction on esophageal motor function of normal subjects, *Dysphagia*, Vol. 14, No. 1, (1999), pp. 27–30.

[142] P. G. Jacobs, J. El Youssef, J. Castle, P. Bakhtiani, D. Branigan, M. Breen, D. Bauer, N. Preiser, G. Leonard, T. Stonex, and W. K. Ward, Automated control of an adaptive bihormonal, dual-sensor artificial pancreas and evaluation during inpatient studies, *IEEE Transactions on Biomedical Engineering*, Vol. 61, No. 10, (2014), pp. 2569–2581.

[143] A. Haidar, L. Legault, V. Messier, T. M. Mitre, C. Leroux, and R. Rabasa-Lhoret, Comparison of dual-hormone artificial pancreas, single-hormone artificial pancreas, and conventional insulin pump therapy for glycaemic control in patients with type 1 diabetes: an open-label randomised controlled crossover trial, *The Lancet Diabetes & Endocrinology*, Vol. 3, No. 1, (2015), pp. 17–26.

[144] A. Haidar, R. Rabasa-Lhoret, L. Legault, L. E. Lovblom, R. Rakheja, V. Messier, É D'Aoust, C. Marcelo Falappa, T. Justice, A. Orszag, et al., Single- and dual-hormone artificial pancreas for overnight glucose control in type 1 diabetes, *The Journal of Clinical Endocrinology and Metabolism*, (2015), p. jc20153003.

[145] F. J. Doyle, L. M. Huyett, J. B. Lee, H. C. Zisser, and E. Dassau, Closed-loop artificial pancreas systems: engineering the algorithms, *Diabetes Care*, Vol. 37, No. 5, (2014), pp. 1191–1197.

[146] S. A. Weinzimer, J. L. Sherr, E. Cengiz, G. Kim, J. L. Ruiz, L. Carria, G. Voskanyan, A. Roy, and W. V. Tamborlane, Effect of pramlintide on prandial glycemic excursions during closed-loop control in adolescents and young adults with type 1 diabetes, *Diabetes Care*, Vol. 35, No. 10, (2012), pp. 1994–1999.

[147] L. Hinshaw, M. Schiavon, V. Dadlani, A. Mallad, C. Dalla Man, A. Bharucha, R. Basu, J. R. Geske, R. E. Carter, C. Cobelli, A. Basu, and Y. C. Kudva, Effect of pramlintide on postprandial glucose fluxes in type 1 diabetes, *The Journal of Clinical Endocrinology and Metabolism*, (2016), p. jc20153952.

[148] T. T. Ly, A. Roy, B. Grosman, J. Shin, A. Campbell, S. Monirabbasi, B. Liang, R. von Eyben, S. Shanmugham, P. Clinton, and B. A. Buckingham, Day and night closed-loop control using the integrated medtronic hybrid closed-loop system in type 1 diabetes at diabetes camp, *Diabetes Care*, Vol. 38, No. 7, (2015), pp. 1205–1211.

[149] F. H. El-Khatib, S. J. Russell, D. M. Nathan, R. G. Sutherlin, and E. R. Damiano, A bihormonal closed-loop artificial pancreas for type 1 diabetes, *Science Translational Medicine*, Vol. 2, No. 27, (2010), p. 27ra27.

[150] L. Magni, D. M. Raimondo, C. D. Man, M. Breton, S. Patek, G. D. Nicolao, C. Cobelli, and B. P. Kovatchev, Evaluating the efficacy of closed-loop glucose regulation via

control-variability grid analysis, *Journal of Diabetes Science and Technology*, Vol. 2, No. 4, (2008), pp. 630–635.

[151] L. J. Chassin, M. E. Wilinska, and R. Hovorka, Grading system to assess clinical performance of closed-loop glucose control, *Diabetes Technology & Therapeutics*, Vol. 7, No. 1, (2005), pp. 72–82.

[152] T. M. Wolever, A. Csima, D. J. Jenkins, G. S. Wong, and R. G. Josse, The glycemic index: variation between subjects and predictive difference, *Journal of the American College of Nutrition*, Vol. 8, No. 3, (1989), pp. 235–247.

[153] S. Vega-López, L. M. Ausman, J. L. Griffith, and A. H. Lichtenstein, Interindividual variability and intra-individual reproducibility of glycemic index values for commercial white bread, *Diabetes Care*, Vol. 30, No. 6, (2007), pp. 1412–1417.

[154] R. L. Weinstein, S. L. Schwartz, R. L. Brazg, J. R. Bugler, T. A. Peyser, and G. V. McGarraugh, Accuracy of the 5-day FreeStyle Navigator continuous glucose monitoring system: comparison with frequent laboratory reference measurements, *Diabetes Care*, Vol. 30, No. 5, (2007), pp. 1125–1130.

[155] W. C. Bevier, H. Zisser, C. C. Palerm, D. A. Finan, D. E. Seborg, F. J. Doyle, A. O. Wollitzer, and L. Jovanovič, Calculating the insulin to carbohydrate ratio using the hyperinsulinaemic-euglycaemic clamp — a novel use for a proven technique, *Diabetes/Metabolism Research and Reviews*, Vol. 23, No. 6, (2007), pp. 472–478.

[156] G. Scheiner and B. A. Boyer, Characteristics of basal insulin requirements by age and gender in Type-1 diabetes patients using insulin pump therapy, *Diabetes Research and Clinical Practice*, Vol. 69, No. 1, (2005), pp. 14–21.

[157] M. Parillo, G. Annuzzi, A. A. Rivellese, L. Bozzetto, R. Alessandrini, G. Riccardi, and B. Capaldo, Effects of meals with different glycaemic index on postprandial blood glucose response in patients with Type 1 diabetes treated with continuous subcutaneous insulin infusion, *Diabetic Medicine*, Vol. 28, No. 2, (2011), pp. 227–229.

[158] L. Groele, D. Golicki, M. Blazik, and E. Pańkowska, Improving the estimation of mealtime insulin dose based on the glycaemic load of a meal in children with type 1 diabetes on insulin pump therapy: A randomized study, *Journal of Diabetes & Metabolism*, Vol. 5, No. 9, (20114).

[159] J. C. Brand-Miller, K. Stockmann, F. Atkinson, P. Petocz, and G. Denyer, Glycemic index, postprandial glycemia, and the shape of the curve in healthy subjects: analysis of a database of more than 1,000 foods, *The American Journal of Clinical Nutrition*, Vol. 89, No. 1, (2009), pp. 97–105.

[160] A. Saad, C. Dalla Man, D. K. Nandy, J. A. Levine, A. E. Bharucha, R. A. Rizza, R. Basu, R. E. Carter, C. Cobelli, Y. C. Kudva, and A. Basu, Diurnal pattern to insulin secretion

and insulin action in healthy individuals, *Diabetes*, Vol. 61, No. 11, (2012), pp. 2691–2700.

[161] L. Hinshaw, C. Dalla Man, D. K. Nandy, A. Saad, A. E. Bharucha, J. A. Levine, R. A. Rizza, R. Basu, R. E. Carter, C. Cobelli, et al., Diurnal pattern of insulin action in type 1 diabetes: implications for a closed-loop system, *Diabetes*, Vol. 62, No. 7, (2013), pp. 2223–2229.

[162] E. R. Mathiesen, P. Rubin, J. Sandahl Christiansen, P. Aaby Svendsen, T. Lauritzen, and T. Deckert, Diurnal pattern of insulin requirements in insulin-dependent diabetics, *Scandinavian Journal of Clinical and Laboratory Investigation*, Vol. 42, No. 1, (1982), pp. 63–68.

[163] F. J. Service, R. A. Rizza, L. D. Hall, R. E. Westland, P. C. O'Brien, A. H. Clemens, M. W. Haymond, and J. E. Gerich, Prandial insulin requirements in insulin-dependent diabetics: effects of size, time of day, and sequence of meals, *The Journal of Clinical Endocrinology and Metabolism*, Vol. 57, No. 5, (1983), pp. 931–936.

[164] F. K. Bishop, D. M. Maahs, G. Spiegel, D. Owen, G. J. Klingensmith, A. Bortsov, J. Thomas, and E. J. Mayer-Davis, The carbohydrate counting in adolescents with type 1 diabetes (CCAT) study, *Diabetes Spectrum*, Vol. 22, No. 1, (2009), pp. 56–62.

[165] C. E. Smart, B. R. King, P. McElduff, and C. E. Collins, In children using intensive insulin therapy, a 20-g variation in carbohydrate amount significantly impacts on post-prandial glycaemia, *Diabetic Medicine*, Vol. 29, No. 7, (2012), pp. e21–24.

[166] E. Cobry, K. McFann, L. Messer, V. Gage, B. VanderWel, L. Horton, and H. P. Chase, Timing of meal insulin boluses to achieve optimal postprandial glycemic control in patients with type 1 diabetes, *Diabetes Technology & Therapeutics*, Vol. 12, No. 3, (2010), pp. 173–177.

[167] M. Brod, T. Christensen, T. L. Thomsen, and D. M. Bushnell, The impact of non-severe hypoglycemic events on work productivity and diabetes management, *Value Health*, Vol. 14, No. 5, (2011), pp. 665–671.

[168] G. Fulcher, J. Singer, R. Castañeda, F. Fraige Filho, L. Maffei, J. Snyman, and M. Brod, The psychosocial and financial impact of non-severe hypoglycemic events on people with diabetes: two international surveys, *Journal of Medical Economics*, Vol. 17, No. 10, (2014), pp. 751–761.

[169] J. R. Castle, J. M. Engle, J. El Youssef, R. G. Massoud, K. C. Yuen, R. Kagan, and W. K. Ward, Novel use of glucagon in a closed-loop system for prevention of hypoglycemia in type 1 diabetes, *Diabetes Care*, Vol. 33, No. 6, (2010), pp. 1282–1287.

[170] S. J. Russell, F. H. El-Khatib, D. M. Nathan, and E. R. Damiano, Efficacy determinants of subcutaneous microdose glucagon during closed-loop control, *Journal of Diabetes Science and Technology*, Vol. 4, No. 6, (2010), pp. 1288–1304.

[171] T. S. Clausen, P. Kaastrup, and B. Stallknecht, Effect of insulin catheter wear-time on subcutaneous adipose tissue blood flow and insulin absorption in humans, *Diabetes Technology & Therapeutics*, Vol. 11, No. 9, (2009), pp. 575–580.

[172] Dassau E, Herrero P, Zisser H, Buckingham B, Jovanovič L, Dalla-Man C, Cobelli C, Vehí J, and Doyle F 3rd., Implications of a meal library and meal detection to glycemic control of type 1 diabetes mellitus through MPC control, *Proceedings of the 17th IFAC World Congress*, (2008), pp. 4228–4233.

[173] P. Herrero, J. Bondia, C. C. Palerm, J. Vehí, P. Georgiou, N. Oliver, and C. Toumazou, A simple robust method for estimating the glucose rate of appearance from mixed meals, *Journal of Diabetes Science and Technology*, Vol. 6, No. 1, (2012), pp. 153–162.

[174] S. Laxminarayan, J. Reifman, S. S. Edwards, H. Wolpert, and G. M. Steil, Bolus estimation — Rethinking the effect of meal fat content, *Diabetes Technology & Therapeutics*, (2015).

[175] K. A. Kelly, Gastric emptying of liquids and solids: roles of proximal and distal stomach, *American Journal of Physiology*, Vol. 239, No. 2, (1980), pp. G71–76.

[176] P. J. Collins, L. A. Houghton, N. W. Read, M. Horowitz, B. E. Chatterton, R. Heddle, and J. Dent, Role of the proximal and distal stomach in mixed solid and liquid meal emptying, *Gut*, Vol. 32, No. 6, (1991), pp. 615–619.

[177] K. M. Cunningham and N. W. Read, The effect of incorporating fat into different components of a meal on gastric emptying and postprandial blood glucose and insulin responses, *British Journal of Nutrition*, Vol. 61, No. 2, (1989), pp. 285–290.

[178] S. Salinari, A. Bertuzzi, and G. Mingrone, Intestinal transit of a glucose bolus and incretin kinetics: a mathematical model with application to the oral glucose tolerance test, *American journal of physiology. Endocrinology and metabolism*, Vol. 300, No. 6, (2011), pp. E955–965.

[179] J. Iqbal and M. M. Hussain, Intestinal lipid absorption, *American journal of physiology. Endocrinology and metabolism*, Vol. 296, No. 6, (2009), pp. E1183–1194.

[180] R. Jian, N. Vigneron, Y. Najean, and J. J. Bernier, Gastric emptying and intragastric distribution of lipids in man. A new scintigraphic method of study, *Digestive Diseases and Sciences*, Vol. 27, No. 8, (1982), pp. 705–711.

[181] A. S. Bickerton, R. Roberts, B. A. Fielding, L. Hodson, E. E. Blaak, A. J. Wagenmakers, M. Gilbert, F. Karpe, and K. N. Frayn, Preferential uptake of dietary fatty acids in adipose

tissue and muscle in the postprandial period, *Diabetes*, Vol. 56, No. 1, (2007), pp. 168–176.

[182] J. M. Miles, Y. S. Park, D. Walewicz, C. Russell-Lopez, S. Windsor, W. L. Isley, S. W. Coppack, and W. S. Harris, Systemic and forearm triglyceride metabolism: fate of lipoprotein lipase-generated glycerol and free fatty acids, *Diabetes*, Vol. 53, No. 3, (2004), pp. 521–527.

[183] C. Brøns, C. B. Jensen, H. Storgaard, N. J. Hiscock, A. White, J. S. Appel, S. Jacobsen, E. Nilsson, C. M. Larsen, A. Astrup, et al., Impact of short-term high-fat feeding on glucose and insulin metabolism in young healthy men, *The Journal of Physiology*, Vol. 587, No. Pt 10, (2009), pp. 2387–2397.

[184] G. M. Reaven, Role of insulin resistance in human disease (syndrome X): an expanded definition, *Annual Review of Medicine*, Vol. 44, (1993), pp. 121–131.

[185] J. Pihlajamäki, H. Gylling, T. A. Miettinen, and M. Laakso, Insulin resistance is associated with increased cholesterol synthesis and decreased cholesterol absorption in normoglycemic men, *The Journal of Lipid Research*, Vol. 45, No. 3, (2004), pp. 507–512.

[186] C. Baynes, A. D. Henderson, V. Anyaoku, W. Richmond, C. L. Hughes, D. G. Johnston, and R. S. Elkeles, The role of insulin insensitivity and hepatic lipase in the dyslipidaemia of type 2 diabetes, *Diabetic Medicine*, Vol. 8, No. 6, (1991), pp. 560–566.

[187] P. H. Bisschop, J. de Metz, M. T. Ackermans, E. Endert, H. Pijl, F. Kuipers, A. J. Meijer, H. P. Sauerwein, and J. A. Romijn, Dietary fat content alters insulin-mediated glucose metabolism in healthy men, *The American Journal of Clinical Nutrition*, Vol. 73, No. 3, (2001), pp. 554–559.

[188] G. Boden and L. H. Carnell, Nutritional effects of fat on carbohydrate metabolism, *Best Practice & Research Clinical Endocrinology & Metabolism*, Vol. 17, No. 3, (2003), pp. 399–410.

[189] D. S. Schalch and D. M. Kipnis, Abnormalities in carbohydrate tolerance associated with elevated plasma nonesterified fatty acids, *The Journal of Clinical Investigation*, Vol. 44, No. 12, (1965), pp. 2010–2020.

[190] G. Boden, Effects of free fatty acids (FFA) on glucose metabolism: significance for insulin resistance and type 2 diabetes, *Experimental and Clinical Endocrinology & Diabetes*, Vol. 111, No. 3, (2003), pp. 121–124.

[191] C. K. Roberts, A. L. Hevener, and R. J. Barnard, Metabolic syndrome and insulin resistance: underlying causes and modification by exercise training, *Comprehensive Physiology*, Vol. 3, No. 1, (2013), pp. 1–58.

[192] A. Garg, Insulin resistance in the pathogenesis of dyslipidemia, *Diabetes Care*, Vol. 19, No. 4, (1996), pp. 387–389.

[193] G. Collier, A. McLean, and K. O'Dea, Effect of co-ingestion of fat on the metabolic responses to slowly and rapidly absorbed carbohydrates, *Diabetologia*, Vol. 26, No. 1, (1984), pp. 50–54.

[194] R. A. DeFronzo, J. D. Tobin, and R. Andres, Glucose clamp technique: a method for quantifying insulin secretion and resistance, *American Journal of Physiology*, Vol. 237, No. 3, (1979), pp. E214–223.

[195] E. S. Kilpatrick, A. S. Rigby, and S. L. Atkin, Insulin resistance, the metabolic syndrome, and complication risk in type 1 diabetes: "double diabetes" in the Diabetes Control and Complications Trial, *Diabetes Care*, Vol. 30, No. 3, (2007), pp. 707–712.

[196] C. J. Greenbaum, Insulin resistance in type 1 diabetes, *Diabetes/Metabolism Research and Reviews*, Vol. 18, No. 3, (2002), pp. 192–200.

[197] A. M. Rosenfalck, T. Almdal, L. Viggers, S. Madsbad, and J. Hilsted, A low-fat diet improves peripheral insulin sensitivity in patients with Type 1 diabetes, *Diabetic Medicine*, Vol. 23, No. 4, (2006), pp. 384–392.

[198] I. J. Goldberg, Clinical review 124: Diabetic dyslipidemia: causes and consequences, *The Journal of Clinical Endocrinology and Metabolism*, Vol. 86, No. 3, (2001), pp. 965–971.

[199] C. M. Barbagallo, M. R. Averna, R. Citarrella, M. Rizzo, M. Amato, D. Noto, A. Pugliese, A. B. Cefalu, A. Galluzzo, and C. Giordano, Transient chylomicronemia preceding the onset of insulin-dependent diabetes in a young girl with no humoral markers of islet autoimmunity, *European Journal of Endocrinology*, Vol. 150, No. 6, (2004), pp. 831–836.

[200] S. J. Hahn, J. Park, J. H. Lee, J. K. Lee, and K. Kim, Severe hypertriglyceridemia in diabetic ketoacidosis accompanied by acute pancreatitis: Case report, *Journal of Korean Medical Science*, Vol. 25, (2010), pp. 1375–1378.

[201] S. Soejima, Y. Umeno, T. Fujita, K. Dohmen, and Y. Miyamoto, A case of diabetic ketoacidosis complicated by severe hypertriglyceridemia and acute pancreatitis, *Journal of the Japan Diabetes Society*, Vol. 43, No. 7, (2000), pp. 561–566.

[202] A. Georgopoulos, S. D. Kafonek, and I. Raikhel, Diabetic postprandial triglyceride-rich lipoproteins increase esterified cholesterol accumulation in THP-1 macrophages, *Metabolism, Clinical and Experimental*, Vol. 43, No. 9, (1994), pp. 1063–1072.

[203] B. Manuel-Y-Keenoy, C. de Vos, A. van Campenhout, M. Vinckx, P. Abrams, and C. van Campenhout, Divergent in vitro and in vivo lipid peroxidation in the postprandial phase

of patients with type I diabetes mellitus, *European Journal of Clinical Nutrition*, Vol. 62, No. 3, (2008), pp. 401–410.

[204] R. A. Heptulla, A. Stewart, S. Enocksson, F. Rife, T. Y. Ma, R. S. Sherwin, W. V. Tamborlane, and S. Caprio, In situ evidence that peripheral insulin resistance in adolescents with poorly controlled type 1 diabetes is associated with impaired suppression of lipolysis: a microdialysis study, *Pediatric Research*, Vol. 53, No. 5, (2003), pp. 830–835.

[205] P. J. Randle, P. B. Garland, C. N. Hales, and E. A. Newsholme, The glucose fatty-acid cycle. Its role in insulin sensitivity and the metabolic disturbances of diabetes mellitus, *Lancet*, Vol. 1, No. 7285, (1963), pp. 785–789.

[206] G. Boden, Fatty acids and insulin resistance, *Diabetes Care*, Vol. 19, No. 4, (1996), pp. 394–395.

[207] L. Hue and H. Taegtmeyer, The Randle cycle revisited: a new head for an old hat, *American journal of physiology. Endocrinology and metabolism*, Vol. 297, No. 3, (2009), pp. E578–591.

[208] R. R. Wolfe, Metabolic interactions between glucose and fatty acids in humans, *The American Journal of Clinical Nutrition*, Vol. 67, No. 3 Suppl, (1998), pp. 519S–526S.

[209] B. M. Wolfe, S. Klein, E. J. Peters, B. F. Schmidt, and R. R. Wolfe, Effect of elevated free fatty acids on glucose oxidation in normal humans, *Metabolism, Clinical and Experimental*, Vol. 37, No. 4, (1988), pp. 323–329.

[210] G. Boden, X. Chen, J. Ruiz, J. V. White, and L. Rossetti, Mechanisms of fatty acid-induced inhibition of glucose uptake, *The Journal of Clinical Investigation*, Vol. 93, No. 6, (1994), pp. 2438–2446.

[211] G. Boden, P. Cheung, T. P. Stein, K. Kresge, and M. Mozzoli, FFA cause hepatic insulin resistance by inhibiting insulin suppression of glycogenolysis, *American Journal of Physiology. Endocrinology and metabolism*, Vol. 283, No. 1, (2002), pp. E12–19.

[212] M. Roden, T. B. Price, G. Perseghin, K. F. Petersen, D. L. Rothman, G. W. Cline, and G. I. Shulman, Mechanism of free fatty acid-induced insulin resistance in humans, *The Journal of Clinical Investigation*, Vol. 97, No. 12, (1996), pp. 2859–2865.

[213] D. Panarotto, P. Remillard, L. Bouffard, and P. Maheux, Insulin resistance affects the regulation of lipoprotein lipase in the postprandial period and in an adipose tissue-specific manner, *European Journal of Clinical Investigation*, Vol. 32, No. 2, (2002), pp. 84–92.

[214] M. T. Pedrini, A. Niederwanger, M. Kranebitter, C. Tautermann, C. Ciardi, T. Tatarczyk, and J. R. Patsch, Postprandial lipaemia induces an acute decrease of insulin sensitivity in healthy men independently of plasma NEFA levels, *Diabetologia*, Vol. 49, No. 7, (2006), pp. 1612–1618.

[215] G. F. Lewis, N. M. O'Meara, V. G. Cabana, J. D. Blackman, W. L. Pugh, A. F. Druetzler, J. R. Lukens, G. S. Getz, and K. S. Polonsky, Postprandial triglyceride response in type 1 (insulin-dependent) diabetes mellitus is not altered by short-term deterioration in glycaemic control or level of postprandial insulin replacement, *Diabetologia*, Vol. 34, No. 4, (1991), pp. 253–259.

[216] M. Haidari, N. Leung, F. Mahbub, K. D. Uffelman, R. Kohen-Avramoglu, G. F. Lewis, and K. Adeli, Fasting and postprandial overproduction of intestinally derived lipoproteins in an animal model of insulin resistance. Evidence that chronic fructose feeding in the hamster is accompanied by enhanced intestinal de novo lipogenesis and ApoB48-containing lipoprotein overproduction, *The Journal of Biological Chemistry*, Vol. 277, No. 35, (2002), pp. 31646–31655.

[217] L. M. Federico, M. Naples, D. Taylor, and K. Adeli, Intestinal insulin resistance and aberrant production of apolipoprotein B48 lipoproteins in an animal model of insulin resistance and metabolic dyslipidemia: evidence for activation of protein tyrosine phosphatase-1B, extracellular signal-related kinase, and sterol regulatory element-binding protein-1c in the fructose-fed hamster intestine, *Diabetes*, Vol. 55, No. 5, (2006), pp. 1316–1326.

[218] A. D. Sniderman and M. Faraj, Apolipoprotein B, apolipoprotein A-I, insulin resistance and the metabolic syndrome, *Current Opinion in Lipidology*, Vol. 18, No. 6, (2007), pp. 633–637.

[219] J. Sierra-Johnson, A. Romero-Corral, V. K. Somers, F. Lopez-Jimenez, G. Walldius, A. Hamsten, M. L. Hellénius, and R. M. Fisher, ApoB/apoA-I ratio: an independent predictor of insulin resistance in US non-diabetic subjects, *European Heart Journal*, Vol. 28, No. 21, (2007), pp. 2637–2643.

[220] E. H. Johanson, P. A. Jansson, B. Gustafson, L. Lonn, U. Smith, M. R. Taskinen, and M. Axelsen, Early alterations in the postprandial VLDL1 apoB-100 and apoB-48 metabolism in men with strong heredity for type 2 diabetes, *Journal of Internal Medicine*, Vol. 255, No. 2, (2004), pp. 273–279.

[221] R. Belfort, L. Mandarino, S. Kashyap, K. Wirfel, T. Pratipanawatr, R. Berria, R. A. Defronzo, and K. Cusi, Dose-response effect of elevated plasma free fatty acid on insulin signaling, *Diabetes*, Vol. 54, No. 6, (2005), pp. 1640–1648.

[222] M. R. Burge, K. J. Hardy, and D. S. Schade, Short-term fasting is a mechanism for the development of euglycemic ketoacidosis during periods of insulin deficiency, *The Journal of Clinical Endocrinology and Metabolism*, Vol. 76, No. 5, (1993), pp. 1192–1198.

[223] S. Pampanelli, E. Torlone, C. Ialli, P. Del Sindaco, M. Ciofetta, M. Lepore, L. Bartocci, P. Brunetti, and G. B. Bolli, Improved postprandial metabolic control after subcutaneous

injection of a short-acting insulin analog in IDDM of short duration with residual pancreatic beta-cell function, *Diabetes Care*, Vol. 18, No. 11, (1995), pp. 1452–1459.

[224] A. M. Caballero-Plasencia, M. C. Muros-Navarro, J. L. Martin-Ruiz, M. Valenzuela-Barranco, M. C. de los Reyes-Garcia, R. Vilchez-Joya, F. J. Casado-Caballero, and B. Gil-Extremera, Gastroparesis of digestible and indigestible solids in patients with insulin-dependent diabetes mellitus or functional dyspepsia, *Digestive Diseases and Sciences*, Vol. 39, No. 7, (1994), pp. 1409–1415.

[225] P. Staehr, O. Hother-Nielsen, B. R. Landau, V. Chandramouli, J. J. Holst, and H. Beck-Nielsen, Effects of free fatty acids per se on glucose production, gluconeogenesis, and glycogenolysis, *Diabetes*, Vol. 52, No. 2, (2003), pp. 260–267.

[226] M. Caruso, G. D. Divertie, M. D. Jensen, and J. M. Miles, Lack of effect of hyperglycemia on lipolysis in humans, *American Journal of Physiology*, Vol. 259, No. 4 Pt 1, (1990), pp. E542–547.

[227] R. B. Heath, F. Karpe, R. W. Milne, G. C. Burdge, S. A. Wootton, and K. N. Frayn, Selective partitioning of dietary fatty acids into the VLDL TG pool in the early postprandial period, *The Journal of Lipid Research*, Vol. 44, No. 11, (2003), pp. 2065–2072.

[228] N. Mohanlal and R. R. Holman, A standardized triglyceride and carbohydrate challenge: the oral triglyceride tolerance test, *Diabetes Care*, Vol. 27, No. 1, (2004), pp. 89–94.

[229] G. M. Puga, C. Meyer, L. J. Mandarino, and C. S. Katsanos, Postprandial spillover of dietary lipid into plasma is increased with moderate amounts of ingested fat and is inversely related to adiposity in healthy older men, *Journal of Nutrition*, Vol. 142, No. 10, (2012), pp. 1806–1811.

[230] A. Stahl, J. G. Evans, S. Pattel, D. Hirsch, and H. F. Lodish, Insulin causes fatty acid transport protein translocation and enhanced fatty acid uptake in adipocytes, *Developmental Cell*, Vol. 2, No. 4, (2002), pp. 477–488.

[231] N. Ercan, M. C. Gannon, and F. Q. Nuttall, Effect of added fat on the plasma glucose and insulin response to ingested potato given in various combinations as two meals in normal individuals, *Diabetes Care*, Vol. 17, No. 12, (1994), pp. 1453–1459.

[232] J. W. Anderson, D. S. O'Neal, S. Riddell-Mason, T. L. Floore, D. W. Dillon, and P. R. Oeltgen, Postprandial serum glucose, insulin, and lipoprotein responses to high- and low-fiber diets, *Metabolism, Clinical and Experimental*, Vol. 44, No. 7, (1995), pp. 848–854.

[233] M. D. Robertson, M. Parkes, B. F. Warren, D. J. Ferguson, K. G. Jackson, D. P. Jewell, and K. N. Frayn, Mobilisation of enterocyte fat stores by oral glucose in humans, *Gut*, Vol. 52, No. 6, (2003), pp. 834–839.

[234] A. Harbis, C. Defoort, H. Narbonne, C. Juhel, M. Senft, C. Latge, B. Delenne, H. Portugal, C. Atlan-Gepner, B. Vialettes, and D. Lairon, Acute hyperinsulinism modulates plasma apolipoprotein B-48 triglyceride-rich lipoproteins in healthy subjects during the postprandial period, *Diabetes*, Vol. 50, No. 2, (2001), pp. 462–469.

[235] M. K. Hellerstein, De novo lipogenesis in humans: metabolic and regulatory aspects, *European Journal of Clinical Nutrition*, Vol. 53 Suppl 1, (1999), pp. 53–65.

[236] M. T. Timlin and E. J. Parks, Temporal pattern of de novo lipogenesis in the postprandial state in healthy men, *The American Journal of Clinical Nutrition*, Vol. 81, No. 1, (2005), pp. 35–42.

[237] H. P. Chase, S. Z. Saib, T. MacKenzie, M. M. Hansen, and S. K. Garg, Post-prandial glucose excursions following four methods of bolus insulin administration in subjects with type 1 diabetes, *Diabetic Medicine*, Vol. 19, No. 4, (2002), pp. 317–321.

[238] A. Lindholm Olinder, J. Runefors, B. Smide, and A. Kernell, Post-prandial glucose levels following three methods of insulin bolusing a study in adolescent girls and in comparison with girls without diabetes, *Practical Diabetes International*, Vol. 26, No. 3, (2009), pp. 110–115.

[239] A. De Palma, E. Giani, D. Iafusco, A. Bosetti, M. Macedoni, A. Gazzarri, D. Spiri, A. E. Scaramuzza, and G. V. Zuccotti, Lowering postprandial glycemia in children with type 1 diabetes after Italian pizza "margherita" (TyBoDi2 Study), *Diabetes Technology & Therapeutics*, Vol. 13, No. 4, (2011), pp. 483–487.

[240] L. Heinemann, Insulin pump therapy: what is the evidence for using different types of boluses for coverage of prandial insulin requirements?, *Journal of Diabetes Science and Technology*, Vol. 3, No. 6, (2009), pp. 1490–1500.

[241] M. E. Wilinska, L. J. Chassin, H. C. Schaller, L. Schaupp, T. R. Pieber, and R. Hovorka, Insulin kinetics in type-I diabetes: continuous and bolus delivery of rapid acting insulin, *IEEE Transactions on Biomedical Engineering*, Vol. 52, No. 1, (2005), pp. 3–12.

[242] R. C. Boston and P. J. Moate, NEFA minimal model parameters estimated from the oral glucose tolerance test and the meal tolerance test, *American Journal of Physiology. Regulatory, integrative and comparative physiology*, Vol. 295, No. 2, (2008), pp. 395–403.

[243] L. M. Botion and A. Green, Long-term regulation of lipolysis and hormone-sensitive lipase by insulin and glucose, *Diabetes*, Vol. 48, No. 9, (1999), pp. 1691–1697.

[244] T. Szkudelski and K. Szkudelska, Glucose as a lipolytic agent: studies on isolated rat adipocytes, *Physiological Research*, Vol. 49, No. 2, (2000), pp. 213–217.

Appendix A

Appendix

A.1 Michaelis-Menten kinetics

Michaelis-Menten kinetics is a simple and effective model to represent enzyme kinetics in term of measurable quantities relying in two simple steps: (1) substrate binding to the enzyme at rate k_1, (2) catalysis at rate k_2, *i.e.,* substrate utilization, where the former is asumed as a slow and the latter a rapid reaction. The process is usually represented as

$$E + S \rightleftharpoons ES \rightarrow E + P, \tag{A.1}$$

where E is enzyme, S is substrate and P is the product of the reaction. The expression for the rate of enzyme reaction is given by

$$V = \frac{V_{\text{max}}[S]}{K_{\text{m}} + [S]}, \tag{A.2}$$

where [S] is the substrate concentration, V_{max} is the maximum velocity achieved at maximum substrate concentration (saturation), K_{m} is the Michaelis constant that represents substrate concentration at the reaction velocity of $0.5V_{\text{max}}$.

A.2 Lehmann model

The model of gut absorption proposed by Lehmann *et al.* [43] proposes a representation of the rate of gastric emptying $G_{\text{ge}}(t)$ according to the carbohydrate intake C. Depending on whether $C \geq 10$ g or $C < 10$ g, gastric emptying $G_{\text{ge}}(t)$ is represented with two different absorption rates (see Figure A.1).

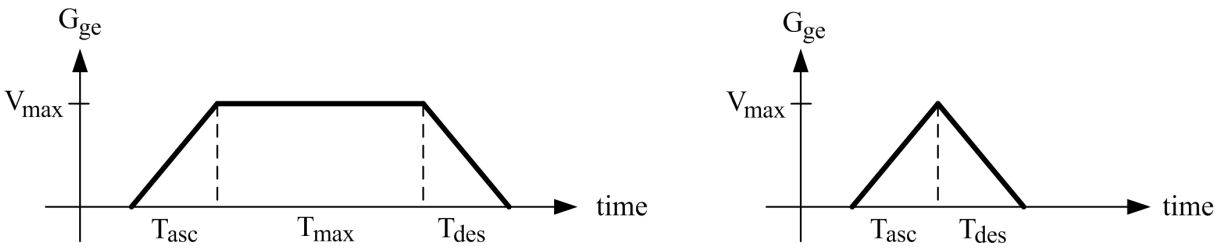

Figure A.1: Representation of the rate of gastric emptying for carbohydrate intakes $C \geq 10$ g (left) and $C < 10$ g (right) as proposed by Lehmann *et al* [43].

Provided that C (mmol) of carbohydrates are greater than the critical value C_{crit} defined as

$$C_{\text{crit}} = \frac{(T_{\text{asc}} + T_{\text{des}}) \cdot V_{\text{max}}}{2}, \tag{A.3}$$

the gastric emptying $G_{\text{ge}}(t)$ is defined by Eq. (A.4) as

$$G_{\text{ge}} = \begin{cases} \dfrac{V_{\text{max}}}{T_{\text{asc}}} \cdot t, & t < T_{\text{asc}} \\ V_{\text{max}}, & T_{\text{asc}} < t \leq T_1 \\ V_{\text{max}} - (\dfrac{V_{\text{max}}}{T_{\text{des}}}) \cdot (t - T_1), & T_1 \leq t < T_2 \\ 0, & \text{otherwise} \end{cases} \tag{A.4}$$

where $T_1 = T_{\text{asc}} + V_{\text{max}}$ and $T_2 = V_{\text{max}} + T_{\text{asc}} + T_{\text{des}}$.

A.3 Hovorka Model

In Hovorka model [49], carbohydrate absorption from monosaccharides is given by

$$U_G(t) = \frac{D_{\text{G}}\, A_{\text{G}}}{t^2_{\text{max,G}}} \cdot t\text{e}^{-t/t_{\text{max,G}}}, \tag{A.5}$$

where D_G is amount of carbohydrates digested, A_G is carbohydrate bioavailability (constant), and $t_{\text{max,G}}$ is time of maximum rate of glucose appearance in the accessible glucose compart-

ment.

SC insulin absorption of lispro insulin is modeled as a two-compartment model represented by $S_1(t)$ and $S_2(t)$ as

$$\frac{\mathrm{d}S_1(t)}{\mathrm{d}t} = u(t) - \frac{S_1(t)}{t_{\text{max,I}}}, \tag{A.6}$$

$$\frac{\mathrm{d}S_2(t)}{\mathrm{d}t} = \frac{S_1(t)}{t_{\text{max,I}}} - \frac{S_2(t)}{t_{\text{max,I}}}, \tag{A.7}$$

$$U_{\text{I}} = \frac{S_2(t)}{t_{\text{max,I}}}, \tag{A.8}$$

$$\frac{\mathrm{d}I(t)}{dt} = \frac{U_{\text{I}}(t)}{V_{\text{I}}} - k_{\text{e}}I(t), \tag{A.9}$$

where $u(t)$ is insulin administration (basal and bolus), $t_{\text{max,I}}$ is time-to-maximum insulin absorption, U_{I} is insulin absorption rate for plasma appearance and $I(t)$ is plasma insulin concentration. Additionally, the action of insulin on glucose kinetics is represented by compartments x_1, x_2 and x_3 as

$$\frac{\mathrm{d}x_1(t)}{\mathrm{d}t} = -k_{\text{a1}}x_1(t) + k_{\text{b1}}I(t), \qquad x_1(0) = \frac{k_{\text{b1}}}{k_{\text{a1}}}I_b \tag{A.10}$$

$$\frac{\mathrm{d}x_2(t)}{\mathrm{d}t} = -k_{\text{a2}}x_2(t) + k_{\text{b2}}I(t), \qquad x_2(0) = \frac{k_{\text{b2}}}{k_{\text{a2}}}I_b \tag{A.11}$$

$$\frac{\mathrm{d}x_3(t)}{\mathrm{d}t} = -k_{\text{a3}}x_3(t) + k_{\text{b3}}I(t), \qquad x_3(0) = \frac{k_{\text{b3}}}{k_{\text{a3}}}I_b \tag{A.12}$$

where each compartment represents the effect of insulin on glucose distribution/transport, glucose disposal and endogenous glucose production, respectively.

For glucose dynamics, a two-compartment glucose model given by Q_1 and Q_2 represent accessible and non-accessible glucose compartments, in addition to glucose concentration $G(t)$ as

$$\frac{\mathrm{d}Q_1(t)}{\mathrm{d}t} = -\left(\frac{F_{01}^c}{V_{\text{G}}\,G(t)} + x_1(t)\right)\cdot Q_1(t) + k_{12}Q_2(t) - F_{\text{R}} + \text{EGP} + G_{\text{ex}}(t), \tag{A.13}$$

$$\frac{\mathrm{d}Q_2(t)}{\mathrm{d}t} = x_1(t)Q_1(t) - (k_{12} + x_2(t))\cdot Q_2(t), \tag{A.14}$$

$$G(t) = \frac{Q_1(t)}{V_{\text{G}}}, \tag{A.15}$$

where Q_1 includes explicit representation of non-insulin dependent glucose flux F_{01}^c, renal glucose clearance F_{R} and EGP as

$$F_{01}^c = \begin{cases} \dfrac{F_{01} G(t)}{4.5 \text{ mmol L}^{-1}}, & \text{if } G(t) < 4.5 \text{ mmol L}^{-1} \\ 0, & \text{otherwise} \end{cases} \tag{A.16}$$

$$F_{\mathrm{R}} = \begin{cases} R_{\text{clear}}(G(t) - R_{\text{thres}}) V_{\mathrm{G}}, & \text{if } G(t) > R_{\text{thres}} \\ 0, & \text{otherwise} \end{cases} \tag{A.17}$$

$$\text{EGP} = \begin{cases} \text{EGP}_0 \cdot (1 + x_3(t)), & \text{if } G_{\mathrm{p}}(t) > k_{\mathrm{e2}} \\ 0, & \text{otherwise} \end{cases} \tag{A.18}$$

Wilinska model [241] represents SC insulin kinetics in patients with T1DM from lispro insulin as an extension of Horvoka model. It considers the differences between single-bolus and continuous insulin infusion, local insulin degradation and disappearance, and the existence of a saturation in insulin absorption rate using 4 differential equations as

$$\frac{\mathrm{d}Q_{1\mathrm{a}}(t)}{\mathrm{d}t} = kU - k_{\mathrm{a1}} Q_{1\mathrm{a}}(t) - \frac{V_{\text{MAX,LD}} \cdot Q_{1\mathrm{a}}(t)}{k_{\text{M,LD}} + Q_{1\mathrm{a}}(t)}, \tag{A.19}$$

$$\frac{\mathrm{d}Q_{1\mathrm{b}}(t)}{\mathrm{d}t} = (1-k)U - k_{\mathrm{a2}} Q_{1\mathrm{b}}(t) - \frac{V_{\text{MAX,LD}} \cdot Q_{1\mathrm{b}}(t)}{k_{\text{M,LD}} + Q_{1\mathrm{b}}(t)}, \tag{A.20}$$

$$\frac{\mathrm{d}Q_2(t)}{\mathrm{d}t} = k_{\mathrm{a1}} Q_{1\mathrm{a}}(t) - k_{\mathrm{a1}} Q_2(t), \tag{A.21}$$

$$\frac{\mathrm{d}Q_3(t)}{\mathrm{d}t} = k_{\mathrm{a1}} Q_2(t) + k_{\mathrm{a2}} Q_{1\mathrm{b}}(t) - k_{\mathrm{e}} Q_3(t), \tag{A.22}$$

where $Q_{1\mathrm{a}}(t)$ and $Q_{1\mathrm{b}}(t)$ are insulin mass as continuous infusion and bolus, respectively, $Q_2(t)$ is insulin mass in the non-accessible compartment and $Q_3(t)$ is plasma insulin mass compartment. In their model, two absorption channels for 'slow' and 'fast insulin' are considered to represent the peak in postprandial plasma insulin with no particular physiological interpretation.

A.4 Dalla Man model

In Dalla Man model [50], rate of glucose appearance from carbohydrates $\mathrm{Ra}(t)$ is modeled as a three-compartment model given by

$$\frac{\mathrm{d}Q_{\mathrm{sto1}}(t)}{\mathrm{d}t} = -k_{\mathrm{gri}}Q_{\mathrm{sto1}}(t) + D\delta(t), \tag{A.23}$$

$$\frac{\mathrm{d}Q_{\mathrm{sto2}}(t)}{\mathrm{d}t} = -k_{\mathrm{empt}}Q_{\mathrm{sto2}}(t) + k_{\mathrm{gri}}Q_{\mathrm{sto1}}(t), \tag{A.24}$$

$$\frac{\mathrm{d}Q_{\mathrm{gut}}(t)}{\mathrm{d}t} = -k_{\mathrm{abs}}Q_{\mathrm{gut}}(t) + k_{\mathrm{empt}}Q_{\mathrm{sto2}}(t), \tag{A.25}$$

$$\mathrm{Ra}(t) = \mathrm{BW}^{-1} f \cdot k_{\mathrm{abs}} \cdot Q_{\mathrm{gut}}(t), \tag{A.26}$$

where D (mg) is the input for amount of carbohydrates ingested, $Q_{\mathrm{sto1}}(t)$ and $Q_{\mathrm{sto2}}(t)$ represent solids and liquids in the stomach, respectively, $Q_{\mathrm{gut}}(t)$ is glucose in the intestinal tract, k_{empt} is fractional coefficient of transfer to the small intestine, k_{gri} is grinding coefficient and BW is body weight. Due to the nonlinear nature of gastric emptying rate, k_{empt} is modeled as a variable that depends on the total amount of glucose (solids and liquids) in the stomach by $Q_{\mathrm{sto}}(t) = Q_{\mathrm{sto1}}(t) + Q_{\mathrm{sto2}}(t)$ as

$$k_{\mathrm{empt}}(Q_{\mathrm{sto}}) = k_{\mathrm{min}} + \frac{k_{\mathrm{max}} - k_{\mathrm{min}}}{2} \cdot \left(\tanh\left(\alpha(Q_{\mathrm{sto}} - bD)\right) - \tanh\left(\beta(Q_{\mathrm{sto}}(t) - cD)\right) + 2\right), \tag{A.27}$$

where α and β are decrease and increase rates of $k_{\mathrm{empt}}(t)$, respectively, and remaining parameters being graphically illustrated in Figure A.2.

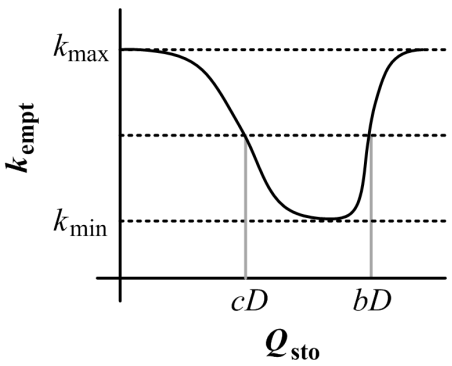

Figure A.2: Representation of the nonlinear rate of gastric emptying $k_{\mathrm{empt}}(t)$ in Dalla Man model [50].

Subcutaneous insulin kinetics is represented by

$$\frac{\mathrm{d}S_1(t)}{\mathrm{d}t} = -(k_{\mathrm{a1}} + k_{\mathrm{d}})S_1(t) + u(t), \tag{A.28}$$

$$\frac{\mathrm{d}S_2(t)}{\mathrm{d}t} = -(k_{\mathrm{a2}}S_2(t) + k_{\mathrm{d}})S_1(t), \tag{A.29}$$

$$S(t) = k_{\mathrm{a1}}S_1(t) + k_{\mathrm{a2}}S_2(t), \tag{A.30}$$

where $u(t)$ is the exogenous insulin administered, k_{d} is degradation constant, k_{a1} and k_{a2} are absorption constants and $S(t)$ is plasma insulin appearance.

The model of glucose-insulin metabolism proposed by Dalla Man *et al.* [50] consists of two compartments for plasma glucose (including rapidly equilibrating tissues) $G_{\mathrm{p}}(t)$ and slowly equilibrating tissues $G_{\mathrm{t}}(t)$ given by

$$\frac{\mathrm{d}G_{\mathrm{p}}(t)}{\mathrm{d}t} = \mathrm{EGP}(t) + \mathrm{Ra}(t) - U_{\mathrm{ii}}(t) - E(t) - k_1 G_{\mathrm{p}}(t) + k_2 G_{\mathrm{t}}(t), \quad G_{\mathrm{p}}(0) = G_{\mathrm{pb}} \tag{A.31}$$

$$\frac{\mathrm{d}G_{\mathrm{t}}(t)}{\mathrm{d}t} = -U_{\mathrm{id}}(t) + k_1 G_{\mathrm{p}}(t) - k_2 G_{\mathrm{t}}(t), \quad G_{\mathrm{t}}(0) = G_{\mathrm{tb}} \tag{A.32}$$

$$G(t) = \frac{G_{\mathrm{p}}(t)}{V_{\mathrm{G}}}, \quad G(0) = G_{\mathrm{b}} \tag{A.33}$$

with plasma glucose concentration $G(t)$ and glucose dynamics including $\mathrm{EGP}(t)$ (endogenous glucose production). The latter depends on a delayed insulin signal $I_{\mathrm{p}}(t)$ and insulin in the portal vein $I_{\mathrm{po}}(t)$ as

$$\mathrm{EGP}(t) = k_{\mathrm{p1}} - k_{\mathrm{p2}}G_{\mathrm{p}}(t) - k_{\mathrm{p3}}I_{\mathrm{p}}(t) - k_{\mathrm{p4}} \cdot I_{\mathrm{po}}(t), \tag{A.34}$$

$$\frac{\mathrm{d}I_1(t)}{\mathrm{d}t} = -k_{\mathrm{i}}\left(I_1(t) - I(t)\right) + S(t), \tag{A.35}$$

$$\frac{\mathrm{d}I_{\mathrm{p}}(t)}{\mathrm{d}t} = -k_{\mathrm{i}}\left(I_{\mathrm{p}}(t) - I_1(t)\right). \tag{A.36}$$

Moreover, renal excretion E is described by

$$E(t) = \begin{cases} k_{\mathrm{e1}}\left(G_{\mathrm{p}}(t) - k_{\mathrm{e2}}\right), & \text{if } G_{\mathrm{p}}(t) > k_{\mathrm{e2}} \\ 0, & \text{otherwise.} \end{cases} \tag{A.37}$$

Non-insulin dependent glucose utilization U_{ii} in compartment $G_{\mathrm{p}}(t)$ represents glucose uptake

by the brain and erythrocytes (constant), whereas insulin-dependent U_{id} in compartment $G_{\text{t}}(t)$ follows a nonlinear Michaelis-Menten kinetics[1], which depends on a remote-insulin compartment $X(t)$ given by

$$U_{\text{id}}(t) = \frac{V_{\text{m}}(t) \cdot G_{\text{t}}(t)}{K_{\text{m}} + G_{\text{t}}(t)}, \tag{A.38}$$

$$V_{\text{m}}(t) = V_{\text{m0}} + V_{\text{mx}} X(t), \tag{A.39}$$

$$K_{\text{m}}(t) = K_{\text{m0}} + K_{\text{mx}} X(t), \tag{A.40}$$

$$\frac{\text{d}X(t)}{\text{d}t} = -p_{2\text{U}} X(t) + p_{2\text{U}} \left(I(t) - I_{\text{b}}\right), \qquad X(0) = 0. \tag{A.41}$$

A.5 Boston model

Boston model [55] is given by

$$\frac{\text{d}R(t)}{\text{d}t} = \frac{K_c}{100} \left(G^*(t) - R(t)\right), \tag{A.42}$$

$$h(t) = \frac{1}{1 + \Phi / R(t)}, \tag{A.43}$$

$$\frac{\text{dNEFA}(t)}{\text{d}t} = S_{\text{FFA}} \left(1 - h(t)\right) - \frac{K_{\text{FFA}}}{100} \text{NEFA}(t), \tag{A.44}$$

where $R(t)$ represents an inaccessible compartment directly related to NEFA concentration, K_{c} is rate constant for glucose clearance into the remote compartment, $G(t)$ is plasma glucose concentration, $h(t)$ modulates the rate of NEFA production, NEFA(t) is NEFA concentration, Φ is a Michaelis-Menten kinetics affinity constant and G_{b} is basal plasma glucose concentration. The model includes a 'remote' glucose compartment with NEFA levels due to the effect of hyperglycemia on lipolysis with triggering BG levels given by g_{s} as given by the ancillary

[1] see Appendix A.1 for definition.

equations:

$$G^*(t) = \begin{cases} g(t) - g_s, & \text{if } g(t) > g_s \\ 0, & \text{otherwise} \end{cases} \tag{A.45}$$

$$g(t) = \begin{cases} G(t-\tau), & \text{if } t \geq \tau \\ G_b, & \text{otherwise} \end{cases} \tag{A.46}$$

where τ is the delay between BG levels and the triggering value g_s for glucose entrance into $R(t)$, which in turn affects the compartment of NEFA concentration. The identifiability of model parameters are well correlated for both OGTT and meal tolerance tests [242].

A.6 Jelic model

A model developed by Jelic *et al.* [57] proposes a representation of NEFA kinetics that focuses on prandial state where the glucose-fatty acid response is validated with an OGTT and a mixed meal. Two non-linear compartmental models for plasma NEFA and interstitial NEFA concentration in adipose tissue are given by $\text{NEFA}_{\text{PL}}(t)$ and $\text{NEFA}_{\text{INT}}(t)$, respectively, as

$$\frac{\text{dNEFA}_{\text{PL}}(t)}{\text{d}t} = \frac{1}{V_{\text{PL}}}(J_{\text{PP}} - J_{\text{FOX}} - J_{\text{HFU}}), \tag{A.47}$$

$$\frac{\text{dNEFA}_{\text{INT}}(t)}{\text{d}t} = \frac{1}{V_{\text{INT}}}(-J_{\text{PP}} - J_{\text{ATL}} - J_{\text{RST}} + J_{\text{LPL}}), \tag{A.48}$$

where plasma NEFA dynamics in Eq. (A.47) considers passive transport/diffusion of NEFA between plasma and interstitium J_{PP}, NEFA oxidation J_{FOX}, non-oxidative hepatic NEFA uptake (liver) J_{HFU} with plasma volume of distribution V_{PL}; and interstitial NEFA dynamics in Eq. (A.48) includes NEFA flux due to lipolysis J_{ATL}, re-esterification to adipose tissue J_{RST} and NEFA flux due to LPL activation J_{LPL} with interstitial volume of distribution V_{INT}. Each of these processes are respectively represented by Michaelis-Menten kinetics of the form

$$J_{\text{HFU}} = \frac{\text{HFU}_{\text{max}} \cdot \text{NEFA}_{\text{PL}}}{K_{\text{HFU}} + \text{NEFA}_{\text{PL}}}, \tag{A.49}$$

where HFU_{max} and K_{HFU} are model constants.

The time-response of insulin-sensitive pathways from plasma insulin concentration $I_{\text{PL}}(t)$ are also considered as two third-order delays for LPL, in addition to lipolysis and re-esterification

in adipose tissue AT as

$$\frac{\mathrm{d}I_{11}(t)}{\mathrm{d}t} = \frac{3}{\tau_{\mathrm{LPL}}}\left(I_{\mathrm{PL}}(t) - I_{11}(t)\right), \tag{A.50}$$

$$\frac{\mathrm{d}I_{12}(t)}{\mathrm{d}t} = \frac{3}{\tau_{\mathrm{LPL}}}\left(I_{11}(t) - I_{12}(t)\right), \tag{A.51}$$

$$\frac{\mathrm{d}I_{\mathrm{LPL}}(t)}{\mathrm{d}t} = \frac{3}{\tau_{\mathrm{LPL}}}\left(I_{12}(t) - I_{\mathrm{LPL}}(t)\right), \tag{A.52}$$

$$\frac{\mathrm{d}I_{21}(t)}{\mathrm{d}t} = \frac{3}{\tau_{\mathrm{AT}}}\left(I_{\mathrm{PL}}(t) - I_{21}(t)\right), \tag{A.53}$$

$$\frac{\mathrm{d}I_{22}(t)}{\mathrm{d}t} = \frac{3}{\tau_{\mathrm{AT}}}\left(I_{21}(t) - I_{22}(t)\right), \tag{A.54}$$

$$\frac{\mathrm{d}I_{\mathrm{AT}}(t)}{\mathrm{d}t} = \frac{3}{\tau_{\mathrm{AT}}}\left(I_{22}(t) - I_{\mathrm{AT}}(t)\right), \tag{A.55}$$

where LPL action is given in Eqs. (A.50)–(A.52), τ_{LPL} and τ_{AT} are the response delay in LPL action and adipose tissue, respectively, in Eqs. (A.53)–(A.55).

A.7 Roy model

Mixed-meal digestion and absorption is represented by three first-order differential equations [59] given by

$$\frac{\mathrm{d}N_{\mathrm{G}}(t)}{\mathrm{d}t} = x_{\mathrm{G}}G_{\mathrm{emp}}(t) - k_{\mathrm{G}}N_{\mathrm{G}}(t), \tag{A.56}$$

$$\frac{\mathrm{d}N_{\mathrm{P}}(t)}{\mathrm{d}t} = x_{\mathrm{P}}G_{\mathrm{emp}}(t) - k_{\mathrm{P}}N_{\mathrm{P}}(t), \tag{A.57}$$

$$\frac{\mathrm{d}N_{\mathrm{F}}(t)}{\mathrm{d}t} = x_{\mathrm{F}}G_{\mathrm{emp}}(t) - k_{\mathrm{F}}N_{\mathrm{F}}(t), \tag{A.58}$$

where $N_{\mathrm{G}}(t)$, $N_{\mathrm{P}}(t)$ and $N_{\mathrm{F}}(t)$ are the amounts of glucose, protein and FFA in the gut, respectively; x_{G}, x_{P} and x_{F} are the mass fraction, *i.e.,* the mass of the specific macronutrient over the total mass, of glucose, protein and FFA, respectively; and $G_{\mathrm{emp}}(t)$ is the trapezoidal gastric emptying model from Lehman *et al.* [43]. Thus, it is assumed that carbohydrate, dietary fat and protein portion of a mixed meal have the same trapezoidal gastric emptying rate, and that 60% of the dietary protein content is directly converted into glucose, whereas the dietary fat content of the mixed meal directly impacts plasma FFA appearance.

The compartmental representation in Roy model includes plasma free fatty acids concentration F, and two 'remote' compartments for insulin effect on fatty acid uptake as Y—similar to X in the minimal model—and another compartment Z for glucose uptake dynamics affected by FFA concentration. A mutual interaction between glucose and fatty acid metabolism includes the impairing effect of FFA on glucose uptake (the Randle cycle) and the effect of hyperglycemia on lipolysis [243], which affects plasma FFA dynamics as previously found in experiments with rats [244]. The compartmental model consists of the differential equations

$$\frac{\mathrm{d}I(t)}{\mathrm{d}t} = -n\left(I(t) - I_{\mathrm{b}}\right) + p_5 u_1(t), \tag{A.59}$$

$$\frac{\mathrm{d}X(t)}{\mathrm{d}t} = -p_2\left(X(t) - X_{\mathrm{b}}\right) + p_3\left(I(t) - I_{\mathrm{b}}\right), \tag{A.60}$$

$$\frac{\mathrm{d}G(t)}{\mathrm{d}t} = -p_1\left(G(t) - G_{\mathrm{b}}\right) - p_4\left(X(t)G(t) - X_{\mathrm{b}}G_{\mathrm{b}}\right) + p_6\left(G(t)Z(t) - G_{\mathrm{b}}Z_{\mathrm{b}}\right) + \frac{u_2(t)}{V_{\mathrm{G}}}, \tag{A.61}$$

$$\frac{\mathrm{d}Y(t)}{\mathrm{d}t} = -p_{\mathrm{F2}}\left(Y(t) - Y_{\mathrm{b}}\right) + p_{\mathrm{F3}}\left(I(t) - I_{\mathrm{b}}\right), \tag{A.62}$$

$$\frac{\mathrm{d}F(t)}{\mathrm{d}t} = -p_7\left(F(t) - F_{\mathrm{b}}\right) - p_8\left(Y(t)F(t) - Y_{\mathrm{b}}F_{\mathrm{b}}\right) + p_9\left(F(t)G(t) - F_{\mathrm{b}}G_{\mathrm{b}}\right) + \frac{u_3(t)}{V_{\mathrm{F}}}, \tag{A.63}$$

$$\frac{\mathrm{d}Z(t)}{\mathrm{d}t} = -p_{10}\left(Z(t) - Z_{\mathrm{b}}\right) + p_{11}\left(F(t) - F_{\mathrm{b}}\right), \tag{A.64}$$

where parameters p_1, p_4, G_{b}, V_{G} and $u_2(t)$ have the same representation as the original minimal model. The physiological representation of fat metabolism includes the impairing effect of FFA on glucose uptake by $p_6 G(t)Z(t)$ in Eq. (A.61), combined insulin-independent FFA uptake by adipose tissue and periphery by $p_7 F(t)$ in Eq. (A.63), and lipolysis due to hyperglycemia by $p_9 F(t)G(t)$. Description of each parameter of Roy model is as follows:

Table A.1: Parameters of FFA dynamics in Roy model [58].

p_6	Impairing action of plasma FFA on glucose uptake.
$Y(t)$	Remote insulin dynamics that represent lipolysis/lipogenesis.
p_{F2}	Rate of disappearance of insulin from compartment Y.
p_{F3}	Rate of plasma insulin appearance into compartment Y.
$F(t)$	Plasma FFA concentration.
F_{b}	Basal FFA concentration.
V_{F}	FFA distribution space.
$u_3(t)$	Dietary FFA absorption / external lipid infusion.
p_7	Insulin-independent uptake of FFA by AT (storage) and periphery.
p_8	Combined rate of insulin-dependent plasma FFA disappearance.
p_9	Lipolytic effect dependent of plasma glucose concentration $G(t)$.
$Z(t)$	Remote FFA dynamics.
p_{10}	Rate of FFA appearance from the remote FFA compartment.
p_{11}	Rate of FFA disappearance from the remote FFA compartment.